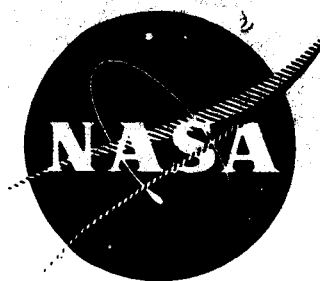


NASA CR-72254

AEROJET 3386



SNAP-8 PERFORMANCE POTENTIAL STUDY FINAL REPORT

prepared for

NATIONAL AERONAUTICS AND SPACE ADMINISTRATION
LEWIS RESEARCH CENTER

CONTRACT NASW 1296

GPO PRICE \$ _____

CFSTI PRICE(S) \$ _____

Hard copy (HC) 3.00

Microfiche (MF) 1.65

ff 653 July 65

FACILITY FORM 602

N67-29172

(ACCESSION NUMBER)

304
(PAGES)

CR-72254
(NASA CR OR TMX OR AD NUMBER)

(THRU)

1
(CODE)

22
(CATEGORY)



VON KARMAN CENTER
AEROJET-GENERAL CORPORATION
AZUSA, CALIFORNIA

NASA CR-72254
Aerojet Report No. 3386

Final Report ,
SNAP-8 PERFORMANCE POTENTIAL STUDY 4

Prepared For
NATIONAL AERONAUTICS AND SPACE ADMINISTRATION

/ April 1967 /

25 Contract NASW-1296 27

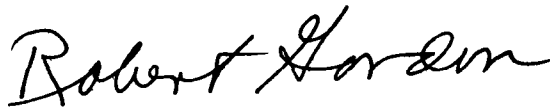
TECHNICAL MANAGEMENT
NASA LEWIS RESEARCH CENTER
CLEVELAND, OHIO
SNAP-8 PROJECT OFFICE
C.J. DAYE

/ VON KARMAN CENTER.
/ AEROJET-GENERAL CORPORATION
Azusa, California 2

CONTRACT FULFILLMENT STATEMENT

This final report is submitted in partial fulfillment of National Aeronautics and Space Administration Contract NASW-1296, and covers the period from 27 July 1965 through 31 December 1966.

Approved:

A handwritten signature in cursive script, reading "Robert Gordon".

Robert Gordon, Manager
Power Systems Division
Von Karman Center

ABSTRACT*

The SNAP-8 Performance Potential Study is an evaluation of the performance of the developmental SNAP-8 electrical generating system (EGS). The objective of the study is to assess the improvement in overall efficiency, weight, radiator area, and power output that can be realized by specified modifications of the system or its components. This report, the final report of the study, describes the work performed and the results obtained. The performance characteristics and weight compilation of the current SNAP-8 EGS are presented and compared with similar data for six improved systems incorporating various modifications.

The study also included an investigation of the SNAP-8 power system integrated with a direct-broadcast TV satellite vehicle in synchronous orbit. Finally, an assessment was made of the potential for increasing the operating life of the SNAP-8 system from 10,000 to 20,000 hours. The results of these studies also are given in the report.

* NASA STAR Category 03.

CONTENTS

	<u>Page</u>
Abbreviations _____	ix
Symbols _____	xi
I. SUMMARY _____	1
A. Objectives and Guidelines of the Performance Potential Study _____	1
B. Study Plan _____	2
C. Summary Results _____	4
D. Conclusions of the Study _____	9
II. INTRODUCTION _____	11
A. SNAP-8 and its Development _____	11
III. FUNDAMENTAL DATA APPLICABLE TO ALL SYSTEMS STUDIED _____	13
A. Basic Configuration _____	13
B. Reactor and Shield _____	14
C. Radiator _____	14
D. Structural Concepts _____	21
E. System Performance Analysis _____	23
IV. BASELINE SYSTEM - EGS-0 _____	25
A. Selection of Operating Condition for Analysis _____	25
B. Performance and Weight of EGS-0 _____	26
V. BASIS FOR PERFORMANCE IMPROVEMENT _____	29
A. Improvement in Overall Efficiency _____	29
B. Weight Reduction _____	31
C. Component Modifications and Substitutions _____	31
D. Improvement by System Modifications _____	50
VI. PERFORMANCE OF IMPROVED SYSTEMS _____	59
A. EGS-1 _____	59
B. EGS-2 _____	60

CONTENTS (cont.)

	<u>Page</u>
C. EGS-3 _____	61
D. EGS-4 _____	62
E. EGS-5 _____	63
F. EGS-6 _____	64
VII. INTEGRATION OF THE SNAP-8 EGS WITH A TV SATELLITE: AN ILLUSTRATIVE APPLICATION STUDY _____	66
A. Introduction _____	66
B. Vehicle Conceptual Design _____	69
C. Subsystem Characteristics _____	74
D. Power Increase and Redundancy _____	80
E. Potential of SNAP-8 EGS for 20,000-Hour Operating Life _____	80
References _____	R-1
	<u>Table</u>
Summary Description of Systems Studied _____	1
Comparative Performance Summary _____	2
EGS Weight Summary _____	3
Assessment of 20,000-Hour Life-Limiting Components _____	4
Advanced Reactor Characteristics _____	5
Summary of Vapor-Chamber Fin Radiator Design Data _____	6
HRL Radiator Design Parameters _____	7
HRL Radiator Weight Breakdown _____	8
L/C Radiator Design Parameters _____	9
L/C Radiator Weight Breakdown _____	10
PCS Component Weight Reduction Summary _____	11
Comparison of Energy Distribution for 5800- and 4800-rpm NaK PMA's _____	12
Parameters for Custom Designed NaK PMA's _____	13
Summary of MPMA Parameters and Parasitic Losses _____	14
Comparison of Losses for Present SNAP-8 (200°C) and High-Temperature (400°C) Alternators _____	15

CONTENTS (cont.)

	<u>Table</u>
Mercury Boiler Modification Summary _____	16
Capacitive Reactance (kvar) for Alternator Load Power Factor Correction _____	17
Weight Summary - TV Satellite Vehicle (pounds) _____	18
Summary of SNAP-8 Performance and Specification Data _____	19
Summary of Typical Data for Station Keeping/Attitude Control of TV Satellite _____	20
Effect of Power Increase and Redundancy on TV Satellite Vehicle _____	21
	<u>Figure</u>
SNAP-8 4-Loop System Schematic _____	1
SNAP-8 Electrical Generating System Configuration _____	2
Heat Rejection Loop Radiator Characteristics _____	3
Lubricant-Coolant Radiator Characteristics _____	4
600-kwt SNAP-8 Reactor and Shield _____	5
Relative Location of Heat Rejection Loop and Lubricant- Coolant Loop Radiators _____	6
Development of Radiator Tube Patterns _____	7
Tube-Fin Configuration _____	8
Fin Effectiveness Function _____	9
Heat Rejection Loop Radiator Map _____	10
Vapor-Chamber Fin Configuration _____	11
Comparison Between Vapor-Chamber Fin and Bumper-Fin Capabilities _____	12
Lubricant-Coolant Radiator Map for One- and Two-Pass Flow _____	13
Radiator Structure Elements _____	14
PCS Structural and Component Arrangement _____	15
EGS-0 Summary Performance Chart _____	16
EGS-0 Performance With Reactor Outlet Temperature at Lower Limit _____	17
Power Distribution Diagram for EGS-0 _____	18
Pressure Rise and Input Power vs Flow Rate for 5800 RPM NaK PMA _____	19

CONTENTS (cont.)

	<u>Figure</u>
Pressure Rise and Input Power vs Flow Rate for 4800 rpm NaK PMA _____	20
Input Power and Head Rise vs Flow Rate for NaK PMA's Custom Designed for Lower Loop Impedance _____	21
Mercury PMA Suction Characteristics _____	22
Mercury Pump on Turbine Shaft _____	23
Mercury Pump on Alternator Shaft _____	24
Flow Diagram of Mercury Loop Incorporating Jet Pumps _____	25
SNAP-8 Alternator Characteristics _____	26
Comparison of Induction and Homopolar Alternators _____	27
SCR Speed-Control Schematic _____	28
SCR Speed-Control Envelope _____	29
Boiler Pressure Stability Characteristics _____	30
Ratio of Primary NaK Flow Rate to Mercury Flow Rate vs Turbine Inlet Pressure _____	31
Effect of Vehicle Load Variation on Alternator Load Power Factor _____	32
Speed Control Power Factor vs Vehicle Load _____	33
Turbine Aerodynamic Efficiency as a Function of Inlet and Exit Pressures _____	34
System Characteristics as a Function at Turbine Inlet and Exit Pressures _____	35
Effect of NaK Radiator ΔT and Turbine Exit Pressure on Radiator Area _____	36
EGS-1 Summary Performance Chart _____	37
EGS-2 Summary Performance Chart _____	38
EGS-3 Summary Performance Chart _____	39
EGS-4 Summary Performance Chart _____	40
EGS-5 Summary Performance Chart _____	41
EGS-6 Summary Performance Chart _____	42
Diagram of TV Satellite in Synchronous Orbit _____	43
Saturn V Vehicle (Left) and Enlarged View of SNAP-8 TV-Satellite Vehicle (Right) _____	44
Conceptual Design of SNAP-8 TV-Satellite Vehicle _____	45

CONTENTS (cont.)

	<u>Figure</u>
Electrical Power Distribution _____	46
Power Conditioning System Diagram _____	47
TV Subsystem Water Cooling Circuit _____	48
Attitude Control System Diagram _____	49

APPENDIX A - METEOROID PROTECTION CRITERIA

APPENDIX B - ELECTRICAL GENERATING SYSTEM WEIGHTS

APPENDIX C - ANALYSIS OF TURBINE EFFICIENCY AS AFFECTED BY
PRESSURE RATIO AND NUMBER OF STAGES

ABBREVIATIONS

AA	Alternator Assembly
AGC	Aerojet-General Corporation
AI	Atomics International
EGS	Electrical Generating System
FRA	Flight Radiator Assembly
Hg	Mercury
HRL	Heat Rejection Loop
KVA	Kilovolt-ampere
KVAR	Kilovolt-ampere reactive
LiH	Lithium Hydride
LCA	Low Temperature Control Assembly
L/C	Lubricant/Coolant
Hg PMA	Mercury Pump Motor Assembly
NaK	Sodium-Potassium Alloy
NaK PMA	NaK Pump Motor Assembly
NPSH	Net Positive Suction Head
NS	Nuclear System
PCS	Power Conversion System
PLR	Parasitic Load Resistor
PM	Permanent Magnet
PMA	Pump Motor Assembly
SCAN	System Cycle Analysis-Computer Program
SC	Speed Control
SCR	Silicon-Controlled Rectifier
TA	Turbine Assembly
TAA	Turbine Alternator Assembly
TRA	Transformer-Reactor Assembly
VLB	Vehicle Load Breaker
VR	Voltage Regulator

SYMBOLS

<u>Symbol</u>		<u>Unit</u>
y	Flow path coordinate	ft
T _y	Temperature along the flow path	°R
T ₂	Temperature at base of radiator fin	°R
n	Number of radiator tubes	--
w	Radiator flow rate	lb/hr
c _{pL}	Specific heat of radiator fluid	$\frac{\text{Btu}}{\text{lb-}^\circ\text{R}}$
d	Diameter of radiator tube	ft
t _w	Wall thickness of radiator tube	ft
t _a	Micrometeoroid armor thickness	ft
t _f	Radiator fin thickness	ft
K _w	Thermal conductivity of radiator tube	$\frac{\text{Btu}}{\text{hr-ft-}^\circ\text{R}}$
K _F	Thermal conductivity of radiator fin and armor	$\frac{\text{Btu}}{\text{hr-ft-}^\circ\text{R}}$
D ₁	Diameter of radiator at inlet manifold plane	ft
α	Half-angle of radiator cone	--
σ	Stefan-Boltzmann constant	$\frac{\text{Btu}}{\text{hr-ft}^2\text{-}^\circ\text{R}^4}$
ε	Emissivity of radiator fin	--
h	Film coefficient within radiator tube	$\frac{\text{Btu}}{\text{hr-ft}^2\text{-}^\circ\text{R}}$
U	$\frac{1}{\frac{1}{h} + \frac{t_w}{K_w}}$	$\frac{\text{Btu}}{\text{hr-ft}^2\text{-}^\circ\text{R}}$

SYMBOLS (cont.)

<u>Symbol</u>		<u>Unit</u>
λ	$\sqrt{\frac{4U}{K_F t_a}}$	1/ft
ω	Fin effectiveness - defined by curves of Figure 9	--
I	Environment radiation absorbed by radiator fins	$\frac{\text{Btu}}{\text{hr-ft}^2}$

I. SUMMARY

A study of the performance potential of the SNAP-8 Electrical Generating System (EGS) was performed by the Aerojet-General Corporation under contract to the National Aeronautics and Space Administration (NASA). The purpose of the study was to evaluate the performance that can be attained by specified system and component modifications and to compare the computed performance to that of the development SNAP-8 power system as thus far demonstrated by test. This report, the final report of the study, documents the work performed and the results obtained.

The SNAP-8 EGS is a 35 kwe nuclear Rankine-cycle power system designed for space applications. Mercury is used as the two-phase working fluid. SNAP-8 has been under development since 1960 jointly sponsored by NASA and the Atomic Energy Commission (AEC). It was initially designed for unmanned space missions and for a continuous operating life of 10,000 hours. In the past year its design requirements have been revised to accommodate the needs of manned applications as well.

A. OBJECTIVES AND GUIDELINES OF THE PERFORMANCE POTENTIAL STUDY

Broadly, the objectives of the study are as follows:

1. To evaluate the performance improvement potential of the SNAP-8 EGS. In this context of the study, performance includes overall efficiency, weight, radiator area, and power growth.
2. To investigate the integration of the SNAP-8 EGS in an unmanned flight vehicle. For this purpose, a direct-broadcast TV satellite was chosen as the mission model.
3. To assess the potential for increasing the operating life of SNAP-8 from 10,000 to 20,000 hours.

In pursuing these objectives the following study guidelines were established in order to maximize the utility of the study results.

1. The existing SNAP-8 four-loop system with organic-lubricated ball bearings and low-temperature electrical machinery was maintained. The SNAP-8 four-loop system is illustrated in a simplified schematic diagram (Figure 1).

2. The nominal maximum system temperature of 1300°F was used throughout the study.

3. Maximum reactor output was kept at 600 kw thermal, consistent with existing reactor design.

4. The power system configuration was based on the use of a Saturn-class launch vehicle and an unmanned mission.

5. Radiator properties were calculated on the basis of a 300 nautical-mile orbit with maximum sun and earth incident radiation and with the recent meteoroid flux and penetration data furnished by NASA, Lewis Research Center (LeRC).

6. Power system requirements such as nuclear radiation levels, output power characteristics, and launch environmental structural loads conform to NASA SNAP-8 Specifications, Series 417.

B. STUDY PLAN

1. Baseline System

The first task of the study was the characterization of the baseline system, the existing developmental SNAP-8. The baseline EGS* (designated EGS-0) was defined by compiling available test data, supplementing this with detailed design data, and then developing a representative flight configuration of the complete power system.

- a. The configuration was selected for an unmanned low-orbital mission and on the basis of compatibility with the Saturn S-IVB upper

* The term EGS designates the complete power system, including the nuclear systems (reactor and shield), the power conversion system (PCS), and the radiator assembly.

stage. A conical shape with a 9.75 degree cone half-angle and a 56-ft length was adopted. There is a separation distance of 50 ft between the reactor center line and the electronic payload located adjacent to the S-IVB mounting plane. The configuration is sketched in Figure 2.

b. Reactor and shield data were based on the existing Atomics-International (AI) design, designated S8DS (Reference 1). The shield size was adjusted so that it would conform to the selected configuration.

2. Improved Systems

Six improved SNAP-8 systems (designated EGS-1 through -6) were synthesized by means of a steady-state analysis and a detailed weight breakdown; the six improved systems incorporate various modifications from the baseline EGS, and are based on the configuration described above. In all cases there were no changes in the nominal maximum system temperature of 1300°F. The purpose in examining six different systems was partly to isolate the effects of the various changes and partly to develop interim results before all of the modifications were completely analyzed. The results of the first three improved systems were reported in the mid-term report of the study (Reference 2). The chief features of the improved systems are summarized in Table 1.

3. Application Study

A study of the integration of the SNAP-8 EGS with a direct-broadcast TV satellite was conducted to evaluate the effect of the mission on the EGS and the effect of the EGS on the mission, to identify critical interfaces and integration problems, and to develop a conceptual vehicle design and general performance information. The EGS-4 power system was selected for the vehicle integration analysis.

4. Assessment of 20,000-hour Life Potential of SNAP-8

A brief analysis was made to assess the life-limiting components of the SNAP-8 PCS; i.e., identify potential failure modes and probable solutions required to extend the operating life of the power system from 10,000 to 20,000 hours.

C. SUMMARY RESULTS

1. Performance Improvement

The major power system performance parameters are tabulated in Table 2 for the baseline system and the six improved systems. The data indicate relatively small incremental improvements in each system compared to its immediate predecessor; however, when the change in the later systems is compared to the baseline system, the improvement in performance is large. The overall change in performance may be seen from the following:

	<u>EGS-0</u> <u>Baseline</u>	<u>EGS-5</u> <u>40 kwe</u>	<u>EGS-6</u> <u>Max kwe</u>
Overall Efficiency, %	7.0	10.9	11.9
Weight, lb	11,000	8,700	9,960
Radiator Area, ft ²	1,433	888	1,440
Output Power, kwe	36	40	71

a. It is of interest to examine the factors contributing to the improvement in efficiency. Considering efficiency as the product of Rankine cycle efficiency, turbine efficiency, alternator efficiency, and parasitic efficiency* we find that the change in overall efficiency of 7% to 10.9% is attributable to the following changes in the subordinate efficiencies.

	<u>EGS-0</u>	<u>EGS-5</u>
Cycle efficiency	.24	.26
Turbine efficiency	.54	.59
Alternator efficiency	.86	.90
Parasitic efficiency	.65	.79

Cycle efficiency is increased by raising turbine inlet pressure from 240 to 350 psia; turbine efficiency is increased by the aerodynamic design improvements of the turbine; alternator efficiency is increased by using capacitors to correct the load power factor from .65 to 1.0; parasitic

* Parasitic efficiency is defined as the ratio of net power available to the vehicle to gross alternator output power.

efficiency is increased by many small changes, the most important of which are reduction of NaK pumping power and electrical control losses.

Overall efficiency is not important per se, but is significant as a means of obtaining other performance gains. Reduction in radiator area is accomplished primarily through efficiency improvement, thereby requiring less heat to be rejected by the radiator. Weight is related to efficiency through radiator area since the radiator is an important weight contributor. Power growth potential is dependent upon efficiency since the reactor is presently designed for 600 kw.

b. Looking at the weight values reported in Table 2, when the total weight for EGS-0 (11,000 lb) is compared with the weight for EGS-5 (8,700 lb), a weight reduction of 2,300 lb is noted. A breakout of this weight reduction by major subsystems is derived from Table 3, as follows:

	<u>Net Change</u>	<u>EGS-0</u>	<u>EGS-5</u>
Nuclear system	110 lb	2340 lb	2230 lb
Radiator Assembly	610 lb	2440 lb	1830 lb
PCS	1590 lb	6230 lb	4640 lb

The nuclear system weight reduction is due to minor adjustments in shield thickness in conformance to reactor thermal power. The weight reduction indicated for the radiators is due to reductions in the required heat rejection and a small increase in the effective radiating temperature. The weight reduction in the PCS is due largely to a change in the structural concept. Excluding the structure, the net change in PCS weight is 485 lb which represents a decrease of approximately 12%. Hence, the weight reduction of the PCS, obtained by a weight analysis of all the components, except the structure, is seen to be less than the weight reduction in the radiator due to efficiency improvements.

c. Note in Table 2 the radiator area reduction from 1430 sq ft for EGS-0 to 890 sq ft for EGS-5. The reduction in area has been achieved by reducing total heat rejection from 460 to 316 kw for the combined heat rejection loop (HRL) and lubricant/coolant (L/C) radiators, by increasing the NaK outlet temperature of the HRL radiator from 488 to 510°F, and by transferring approximately 2 kw from the L/C radiator to the HRL radiator where the effective

heat transfer is much higher. The latter change is accomplished by cooling the NaK pump motor assemblies at 500°F by means of the HRL NaK. Throughout the study, the configuration and dimensional properties of the two radiators were maintained constant. No attempt was made to optimize radiator design for the particular conditions pertaining to each system. The radiator characteristics for the HRL and L/C radiators are summarized in Figures 3 and 4.

d. The power growth potential represented by EGS-6 in Table 2 also is highly significant. Comparing EGS-6 with EGS-0 a doubling of net power output is seen for virtually the same radiator area and weight (if the structure weight reduction is excluded). In order to realize the indicated power growth, it is necessary to enlarge the fluid flow passages of the present SNAP-8 turbine, boiler and condenser by about 20% and to design the NaK pump motor assemblies to new flow and pressure rise requirements. These changes, of course, necessitate dimensional design modifications of PCS components but do not entail major development effort. No modification is required to the alternator, mercury PMA, L/C PMA, or space seals.

e. In the latter phase of the performance improvement analysis, several other component changes were explored. Among these was an evaluation of a mercury jet pump to replace the motor-driven mercury pump. This is a promising concept because all of the losses associated with the jet pump are returned to the system in the form of sensible heat imparted to the mercury stream. The jet pump system was not incorporated in the final system synthesis, however, because of (a) extensive development required, and (b) its possible impact on startup procedures. The latter required a more extensive analysis than the present study permitted. Other changes which have been analyzed but not adopted are a high-temperature (600 to 700°F) alternator, an induction alternator, a mercury pump direct-driven by the turbine or alternator, and a vapor-chamber fin radiator. In general, it was found that the gains attainable by these modifications were small in relation to the attendant development problems.

2. SNAP-8/TV Satellite Integration Study

The integration of SNAP-8 in a direct-broadcast TV satellite was evaluated by developing a conceptual vehicle design and general performance characteristics, and by analyzing environmental factors, power system/payload interfaces, heat rejection and attitude control requirements. The study was based on the EGS-4 system defined in the performance improvement task. A net power of 35 kwe to the payload was assumed (leaving a 5 kw margin for power degradation or other contingencies). The vehicle was designed to be dimensionally compatible with the Saturn S-IVB upper stage. The radiator areas were adjusted for lower incident radiation to the vehicle from the earth, compatible with a 22,300 mile synchronous orbit.

The vehicle data generated in the study are summarized below:

Vehicle length	59 ft
Configuration:	
Upper 31 ft	Conical, 35° incl. angle
Lower 24 ft	Cylindrical, 21.7 ft dia
Launch weight	17,100 lb
Orbiting weight	15,000 lb
Antenna dia	34 ft (deployed)
Available radiator surface area	1900 sq ft

Nuclear radiation levels and satellite pointing accuracy were selected primarily to provide a basis for estimating weights, and establishing an overall height (on the launch vehicle) of the satellite-power system assembly. In addition, to eliminate the necessity of considering a radiation scattering analysis, it was assumed that the parabolic antenna would be entirely within the shield cone angle. On this basis, the results are judged to be conservative; it is possible that the total weight of the assembly (and its overall height) could be reduced a little by detailed configuration and radiation studies.

The vehicle weights were calculated for a 10,000-hour operating life without redundancy of either power system or TV system. On that basis, the

launch weight given above is about twice the capability of the present Saturn IB and less than 30% of the Saturn V capability. It was of interest, therefore, to estimate what additional launch weight could provide in increased power and reliability (through redundancy). The following table gives a rough extrapolation of the basic vehicle data to illustrate possible growth potential within the Saturn V lift capability.

<u>SNAP-8 Composition</u>	<u>EGS-4</u>	<u>EGS-6</u>	<u>2 x EGS-6</u>
Power output, kwe	35	70	140
Launch weight, lb			
Without redundancy	17,000	20,000	40,000
With redundancy*	22,000	26,000	52,000
Vehicle length, ft	59	62	68
Radiator area, sq ft	1250	2100	4200
Antenna dia., ft	34	27	22

* includes inactive PCS, radiator tubes, and klystron tubes

No objectionable interface problems were uncovered in the study. The shield was sized to limit the radiation dose at the payload to 10^{11} nvt and 10^6 rad (c) gamma, values which the power system electronic components are designed to withstand. If necessary, the payload radiation dose can be reduced one order of magnitude by increasing shield weight about 1000 lb. Thermal management is accounted for by (1) providing a separate radiator and circulation system for the TV system, (2) by separating the TV system from the hot portions of the power system, and (3) by investing 100 lb in a thermal insulation diaphragm between the PCS and the TV system. Attitude control and station keeping requirements are met by a reactive thrust system. For simplicity, the thrust system was based on the use of monopropellant hydrazine pressurized by nitrogen. A weight saving of about 400 lb for 10,000 hours life could be realized by selecting a higher performance bi-propellant thrust system.

One element of the power system contributing to attitude disturbance of the vehicle is the angular momentum of the rotating masses

(both solid and liquid) in the PCS. Analysis indicated that this is not a large factor in total attitude control (it might require 100 lb of mono-propellant for a 10,000 hour mission), but the study also indicated that the angular momentum of the power system could be internally balanced. By orienting all solid rotating components parallel to the major axis of the vehicle so that the lesser components counteract the largest one (the turbine-alternator assembly), and by further counteracting the remaining unbalanced momentum by the primary NaK piping, it was concluded that a virtual balance could be achieved by the addition of about 30 ft of piping at a weight penalty of 60 lb.

In summary, no serious integration or interface problems were found in this application study. However, it is evident that higher power and longer life are important avenues for further evaluation.

3. Assessment of 20,000-hour Life Potential of SNAP-8

To assess the potential for extended life of the SNAP-8 system, the components of the PCS were examined to identify, if possible, those components which are life-limiting. Since failure modes have not been identified for the majority of components, the present study is necessarily speculative and qualitative. With this qualification, the assessment summarized in Table 4 was made of the components judged most subject to wear-out failure in less than 20,000 hours.

Examination of the list of failure modes and probable solutions in Table 4 on the basis of present knowledge establishes that there is no evidence that components, etc., which have demonstrated 10,000 hours of life cannot attain 20,000 hours life, with or without some minor modification. Neither does it appear that a severe penalty in weight and performance must be paid as the price for attaining longer life. However, the identification of true-failure mode and mean-time-to-failure is essential to a quantitative assessment of operating life potential.

D. CONCLUSIONS OF THE STUDY

The findings of the study lead to the following general conclusions:

1. Large gains in SNAP-8 system performance appear attainable without sweeping redesign of the system or components and without advance in the state of the art. No estimation has been made, however, of the effort (in cost and time) required to effect redesign where indicated and verify through test programs.

2. The integration of the SNAP-8 power system in an unmanned TV satellite appears feasible. All interfaces between the power system and TV payload and all integration aspects studied between the subsystems and the launch vehicle appear susceptible to straight forward engineering solutions. The study indicates, however, that the consideration of using a nuclear power system with such a satellite will require consideration of Saturn class boosters.

3. The extension of SNAP-8 operating life from 10,000 to 20,000 hours appears feasible. No fundamental barriers to preclude attainment of the longer life were found, based on presently-available information. Moreover, it appears that achievement of the 20,000-hour life need have only a small impact on weight and performance.

II. INTRODUCTION

The SNAP-8 Performance Potential Study serves an important function, supplemental to the SNAP-8 Development Program, in providing a basis for projecting the performance of the system beyond the immediate development limitations. In evaluating the competitive merits of candidate power systems, attainable flight system performance becomes an important criteria. Performance comparisons between a SNAP-8 EGS based on ground test developmental components and a competitive power system based on paper designs of advanced technology are not realistic. The intent of this study, therefore, is to examine and document a projection of SNAP-8 EGS performance that is the logical extension of the current development effort, and thereby provide a useful aid to mission planners.

A. SNAP-8 AND ITS DEVELOPMENT

The SNAP-8 is a turboelectric, nuclear, space power system using a mercury Rankine cycle. The system is comprised of three major subsystems: (1) a nuclear system consisting of a reactor, reactor controls, and shielding; (2) a flight radiator assembly consisting of radiator heat exchangers required to remove heat from the liquid cooling loops; and (3) the PCS, consisting of turbine-alternator assembly (TAA), boiler, condenser, mercury and NaK pump-motor assemblies (PMA's) and necessary controls, piping, and structure. The SNAP-8 nuclear system is being developed by Atomics International Division of North American Aviation, Inc. under contract to the AEC. The PCS and the integration of the PCS with the nuclear system is the responsibility of Aerojet-General Corporation, Von Karman Center, under contract to NASA. Development of the radiator assembly is not a part of the current program.

The EGS is designed to operate continuously for 10,000 hours in space after a remote automatic startup. The net electrical output of the SNAP-8 system is 35 kw.

Figure 1 shows schematically the functional arrangement of the four-loop SNAP-8 system. Since both the third and fourth loops must reject heat to space, there are two distinct radiating elements in the flight radiator

assembly. The first element rejects the heat from the NaK HRL of the PCS at temperatures in the range of 500 to 700°F. The second element rejects heat from the organic lubricating loop at temperatures in the range of 200 to 250°F.

The early development phase of SNAP-8, wherein the major components were designed and tested, has been completed. Reference 3 describes the current status of the program.

III. FUNDAMENTAL DATA APPLICABLE TO ALL SYSTEMS STUDIED

This section is concerned with certain basic information which had to be defined before the systems to be studied could be analyzed. In some cases, the information set forth below is based on source material in conformance to the study ground rules. In other cases, the data were arbitrarily chosen in order to afford a reasonable basis for comparison of performance of the various systems. In all cases, the data are identified in the context of the systems to which they apply, and sources of information are identified.

A. BASIC CONFIGURATION

One of the first tasks of the study was to establish a suitable configuration applicable to all of the SNAP-8 EGS's to be examined. This was necessary because some aspects of performance, notably weight, are dependent upon the configuration. The selected configuration was based on the following criteria:

1. A flight vehicle for an unmanned mission. This implies the use of a shadow shield of minimum dimension but of sufficient thickness to provide the necessary radiation environment for the more sensitive payload components.
2. Use of a Saturn-class launch vehicle; i.e., a vehicle which will use the S-IVB upper stage.
3. Sufficient surface area to provide for rejection of the necessary heat by means of radiators mounted on the surface of the vehicle.

The configuration selected on the basis of these criteria is shown in Figure 2. It is a simple conical shape with an included angle of 19.5 degrees and an overall length of 56 ft. Allowing a reasonable space above the mounting ring for an electronic payload, there is a separation distance of 50 ft between the center of the reactor and the top of the payload which provides a basis for calculating shield thickness. Due to the second order effect of variations in reactor power, shield thickness and, therefore, shield weight vary only slightly from one system to another. The surface of the selected configuration is sufficient to accommodate the radiator area of all

of the systems studied. For systems requiring less radiator area, the base of the radiator will be located closer to the small end of the cone. Consequently, there is a variable space between the base of the radiator and the S-IVB mounting ring which must be occupied by a suitable structure. This additional structure is not included in the weights of the SNAP-8 power systems.

B. REACTOR AND SHIELD

The baseline performance data for reactor and shield used throughout the study are based on information published or otherwise made available by Atomics International. For the baseline system EGS-0 and for improved systems EGS-1, -2, and -3, the reactor and shield characteristics are based on AI's development nuclear system (designated S8DS) as defined in References 1 and 4. The reactor and shield configuration are shown in Figure 5. For improved systems EGS-4, -5 and -6, the reactor properties used are for an "advanced" reactor concept as defined in Table 5 which reflects recent design studies by Atomics International. In each case the design reactor thermal power is 600 kw. Shield design data applicable to both the development reactor and the advanced reactor are based on Reference 4 which illustrates the variation in shield thickness and weight as a function of payload diameter, separation distance and reactor power.

C. RADIATOR

1. Configuration

a. Shape

The configuration adopted for this study is a cone frustrum based on a 53.4-inch reactor shield base diameter, a 260-inch vehicle base diameter, and a separation distance of 50 ft between the reactor shield and the base. This cone frustrum has a 9.75° half-angle. Making due allowance for a transition between the reactor shield and the radiators, the HRL and L/C radiators are arranged on the surface of this cone, extending downward from the 55.5-inch diameter plane.

b. Relative Location of HRL and L/C Radiators

For the purposes of this study, the HRL radiator was placed nearest the reactor and the L/C radiator was placed immediately below

the HRL radiator nearer the base of the cone (see Figure 6). This relative orientation provides an orderly transition from high to low temperature as follows: the 1100 to 1300°F reactor circuit is near the apex of the cone; the 490 to 660°F HRL radiator is immediately below the reactor shield surrounding the PCS; and the 210 to 243°F L/C radiator is near the base of the cone. Such an arrangement is desirable for earth orbiting applications where a manned or unmanned payload compartment may very likely adjoin the base of the L/C radiator. It also is recognized that for ground based operation on the moon or on a planet a different arrangement could be advantageous.

c. Tube Patterns

For the purposes of this study, simple tube patterns were selected wherein circumferential inlet and exit manifolds are connected by a parallel-flow arrangement of tubes on the elements of the cone. Figure 7A illustrates the development of the HRL radiator tube pattern. In order to improve the characteristically poor film coefficient of the L/C fluid, a slightly different tube pattern development was considered for the L/C radiator (Figure 7B). The effect of this arrangement, using multiple passes for each flow path, is to increase the flow rate per tube thereby increasing the Reynolds number and film coefficient.

d. Manifolds

Each manifold consists of an entrance tube which carries the flow into a T-section where the flow splits and passes in opposite directions around the tapered circumferential manifold ring. In order to preserve equal pressure drop for all flow paths through the radiator, it is necessary to stagger the location of the radiator inlet and output in the manner illustrated in Figure 7A. Equal pressure drop is achieved in both manifolds using a slightly greater tube diameter for the manifold at the large end of the radiator since greater distances are traversed at the large end. Each of the manifold segments tapers to one-half of the diameter at the T-section.

e. Direction of Flow

For the purpose of this study, radiator flow entered through the manifold at the small end of the radiator and exited through the

manifold at the large end of the radiator. The merits of reversing this procedure were not investigated.

f. Bumper-Fin Configuration

The bumper-fin configuration adopted for this study is shown in Figure 8. Use of the thermal radiation fin as a meteoroid bumper permits reduction of armor on the back and sides of the tube to one-quarter of the nominal armor thickness. This tube-fin configuration was used for both HRL and L/C radiators.

g. Micrometeoroid Armor Criteria

The micrometeoroid armor criteria are based on data furnished by NASA, LeRC which update the criteria set forth in Reference 5. The updated criteria are presented in Appendix A. A probability of survival for both radiators of 0.9 for 10,000 hours was used. One-hundred square feet of vulnerable area was assigned to the PCS components within the radiator. The vulnerable area of the radiators was assumed to be equal to the projected area of the tubes and manifolds, multiplied by $\pi/2$.

2. Radiator Model

The model used for radiator analysis is based on the tube-fin configuration and parameters shown in Figure 8. Considering the back side of the radiator tube (away from the radiator fin) to be a convection-heated fin, leads to the following expression for heat transfer between T_y and T_2 :

$$\frac{dT}{dy} = - \frac{n}{\dot{w} c_{pL}} \left[\frac{T_y - T_2}{\frac{\pi}{2} U d + \frac{\lambda}{2} K_F t_a \tanh \frac{\pi}{4} \lambda d + \frac{t_a}{\frac{K_F}{2} (d + t_a)}} \right]$$

The heat transfer from T_2 (identified in Figure 8) to the space environment is determined by

$$\frac{dT_y}{dy} = - \frac{\pi}{w c_{pL}} (D_1 + 2y \sin \alpha) V \epsilon T_2^4 \Omega$$

where Ω , fin effectiveness, is given in Figure 9 and the parameter definitions are identified in the nomenclature list at the front of this report. Radiator designs for the study were obtained by simultaneous integration of these two equations by an IBM 7094 computer program.

An environmental thermal radiation absorption of 0.67 Btu/hr sq in. was used for all but one of the HRL radiator calculations. This value corresponds to an absorptivity of 0.4, an emissivity of 0.9, and a 300-mile orbit altitude. The remaining HRL radiator calculation, using a value of 0.395 Btu/hr sq in., represents a synchronous orbit. Representative HRL radiator characteristics were calculated over a heat rejection range of 200 to 500 kw. Lubricant-coolant radiator heat rejection rates covered the range from 14 to 21 kw. All radiator calculations were for a cone half-angle of 9.75° .

3. Radiator Options; Weight vs Area

a. HRL Bumper-Tube-Fin

The HRL radiator results presented in Figure 10 reveal that the designer has considerable freedom, depending on the number of tubes selected, to achieve either low radiator weight or low radiator area - but not both. There is clearly no optimum radiator design in the context of this study since for some applications weight is more dear than area while in other applications the reverse is true. Once the number of tubes has been selected, there is a fin thickness which gives the lowest possible combination of weight and area. This most favorable correspondence of tube number and fin thickness has been identified and all of the results of Figure 10 are optimum in this regard.

Radiator pressure drop increases as the number of tubes, and hence parallel flow paths, is reduced. Consequently, for any tube diameter selection there is a point where further reduction in the number of tubes causes

an objectionably large pressure loss. At this point, the option of trading increased area for decreased weight can be exercised only if tube diameter is increased. Conversely, as a larger number of tubes is selected in an effort to reduce radiator area, at the expense of increased weight, the designer has the option of reducing tube diameter. However, one soon reaches the point where, with a tube diameter of 0.25 in., further reductions increase the possibility of fabrication difficulties. With an allowable HRL radiator pressure drop of 20 to 30 psi, the 0.25 in. tube diameter is generally acceptable. If radiator weights corresponding to higher pressure loss values are desired, an increased tube diameter is necessary.

The radiator map of Figure 10 reveals that such parameters as sq ft/kw and lb/kw are not discrete values as sometimes listed. Actually, the designer has the choice of a range of values for any heat rejection value. Representative ranges of these parameters for the systems studied are tabulated below. Values correspond to the variation obtained by varying the tube number in the range between 50 and 200.

<u>System</u>	<u>HRL Radiator</u>		
	<u>Heat Rejection (kw)</u>	<u>sq ft/kw (Range)</u>	<u>lb/kw (Range)</u>
EGS-0	439	2.3 - 3.0	3.7 - 1.5
EGS-1	392	2.3 - 2.9	3.7 - 1.5
EGS-2	352	2.3 - 2.9	3.7 - 1.5
EGS-3	506	2.3 - 3.0	3.7 - 1.5
EGS-4	322	2.3 - 2.9	3.7 - 1.5
EGS-5	304	2.3 - 2.9	3.7 - 1.5
EGS-6	499	2.3 - 3.0	3.7 - 1.5

b. HRL Vapor-Chamber Fin

A comparative evaluation of the vapor-chamber fin radiator concept applied to a nonredundant, nonmanrated SNAP-8 EGS was made as part of this study. The vapor-chamber fin concept has received some attention recently as a way of increasing radiator effectiveness over that of the typical tube-and-fin radiator concept. All vapor-chamber fin radiator design data were furnished by NASA-LeRC.

The vapor-chamber fin concept proposes to reduce radiator area and weight by providing an essentially isothermal fin between the fluid-carrying tubes. It does this by replacing the single solid fin of a conventional radiator, which transfers heat by conduction, with a double-wall fin which forms a hollow chamber. Inside this chamber is a heat transport fluid. This fluid is boiled off the outer tube surface and condensed on the fin surface. This results in a radiating fin of constant temperature and, consequently, high effectiveness.

Condensate is returned to the boiling surface by means of capillary pumping which is essentially insensitive to gravity. A sketch of the basic vapor-chamber fin geometry used in this study is shown in Figure 11. In a space system like SNAP-8, where meteoroid impact must be considered, the vapor chamber can be compartmented into a large number of sealed segments, minimizing the effects of meteoroid puncture.

The weight and area of the vapor-chamber fin radiator were compared to those of the bumper-tube fin radiator at conditions representative of the SNAP-8 HRL. Data for the vapor-chamber fin radiator, furnished by NASA-LeRC, are reproduced in Table 6. The performance of the two types of radiators is compared in Figure 12; weight is plotted against area. The curves indicate that each configuration has its region of superiority. While a somewhat smaller area is available when the vapor-chamber fin is used, this superiority is accompanied by relatively heavy radiator weight. The bumper-fin configuration has a definite weight advantage for radiators somewhat larger in area. For the purpose of this study, the bumper-fin configuration has been retained. The comparison shows, however, that the vapor-chamber fin configuration does have advantages that should be kept in mind for certain applications where minimum area is of utmost importance.

c. L/C Bumper-Fin Radiator

The high viscosity of the L/C fluid makes effective heat transfer difficult. In order to avoid excess radiator area and weight, special attention must be given to flow velocity within the tube. One way of increasing flow velocity is to decrease tube diameter. It was with this in mind that a tube diameter (OD) of 0.1875 in. was selected for the radiator maps of Figures 13A

and 13B. A second way of increasing flow velocity is to reduce the number of parallel flow paths by placing some tubes in series (multiple pass). The radiator map of Figure 13B shows the performance improvement obtained by letting each flow path contain two radiator tubes in series (two pass). Figure 7A shows an arrangement with three passes in each flow path. Although this arrangement triples the flow rate per tube, it creates a noticeable increase in pressure drop. As a result, the data shown in Figure 13B, representing an arrangement with two passes per flow path, have been used in this study.

Representative two-pass parameter value ranges, obtained by varying the tube number between 60 and 240, are tabulated below.

<u>System</u>	<u>L/C Radiator Heat Rejection (kw)</u>	<u>sq ft/kw (Range)</u>	<u>lb/kw (Range)</u>
EGS-0	21.2	16.4 - 19.8	18.8 - 9.5
EGS-1	21.2	16.4 - 19.8	18.8 - 9.5
EGS-2	13.9	16.4 - 19.4	22.4 - 10.9
EGS-3	17.4	16.4 - 20.1	20.8 - 10.1
EGS-4	12.2	16.4 - 19.4	22.4 - 10.7
EGS-5	12.1	16.4 - 19.4	22.4 - 10.9
EGS-6	15.0	16.4 - 20.1	20.8 - 10.1

4. Performance Potential Program Radiator Summary

Tables 7 through 10 summarize the dimensions and weight breakdowns of the HRL and L/C radiators.

The summarized HRL values are based on a 125-tube radiator design with an 0.030-in. fin thickness. As mentioned earlier, in the absence of a specific application, there is no optimum radiator design. The radiator weights in the summary tables can be decreased by using fewer tubes, but this increases radiator area. Conversely, the radiator area can be reduced by adding tubes, but this increases radiator weight. The 120-tube design selection is an arbitrary one which gives a reasonably representative radiator. The freedom to exchange area for weight, and vice versa, (illustrated in Figure 10) should always be kept in mind, however.

In viewing Tables 7 and 8, it should be observed that EGS-0 through -3 are based on a NaK temperature drop of 172°F while EGS-4 through -6 are based on a temperature drop of 150°F.

Similarly, the summarized L/C radiator values in Tables 9 and 10 are based on a 120-tube design with an 0.030-in. fin thickness and two passes per flow path. This also is an arbitrary but representative selection.

D. STRUCTURAL CONCEPTS

In the absence of an established flight-structure design for the SNAP-8 PCS some judgments were necessary to establish a reasonable basis for structural concepts and weights. Therefore, evaluation of structural concepts was performed during this study; however, a detailed structural design or precise weight determination is beyond the scope of this study. For the baseline system EGS-0, structural weight was based on previous SNAP-8 structural studies.

The structural concepts used in estimating the structural weights given in this report are strongly influenced by the general arrangement discussed in Section III,A. When the study was initiated, the SNAP-8 structural concept used a rigid truss-type frame capable of supporting all of the PCS components and the nuclear system. This design concept does not provide any support to the radiator nor assume any support from it. After some estimates were made regarding the structural strength of the conical radiator, additional stiffening of the radiator structure was provided by means of longitudinal half-sections and circumferential "Z" rings below the base of the frame, extending down the conical envelope to the base of the radiator assembly. It was calculated that this combined structure, comprised of the radiator with the added stiffeners and the rigid frame supporting the PCS and the nuclear system, is capable of withstanding the launch acceleration loads in conformance to the SNAP-8 environmental specification (Reference 6).

For the improved systems, starting with EGS-1, alternate structural concepts were examined in order to develop a concept that was somewhat closer to optimum. Preliminary calculations indicated that the tube-in-fin radiator design in the conical configuration was, in itself, an efficient structure. By the use of relatively lightweight stiffeners, it was possible to use this structure to support not only itself but the PCS and the nuclear system as well. The addition of rings and stringers to this component results in a much lighter structure than would be possible using a rigid frame. Calculations

have shown that the rings and stringers illustrated in Figure 14 are satisfactory. No attempt was made to optimize these reinforcing elements.

Using the stiffened radiator as the primary structural member, the concept shown in Figure 15 was developed. In this design the nuclear system, which is a compact rigid assembly, is directly supported by the radiator through a mounting ring attaching the base of the shield to the top of the radiator. The PCS components, supported by the radiator through tension members, are packaged as sub-assemblies to provide for a relatively small number of focal points for supports. In order to reduce the number of tension members required, the PCS components have been grouped into four assemblies: (1) PNL PMA, expansion reservoir, and PLR when used in PNL; (2) turbine, alternator, and condenser assembly; (3) boiler; and (4) MPMA, HRL NaK PMA, L/C PMA and mercury injection system (MIS). Tension members might be either cables or rods; the following discussion uses the term cable for convenience.

The primary loop NaK PMA and associated components are fixed directly to the nuclear shield assembly. The turbine-alternator assembly (TAA) is currently designed so that the axis of its trunnion mountings passes through its center of mass. This feature has been preserved in this study. Four cables are attached to each side of the turbine mounting. Consequently, the eight cables supporting the TAA at its center of mass extend to the radiator where they are fastened so as to diffuse their loads through the radiator skin and stringers. Cable orientation is to be selected so as to hold the TAA against all anticipated loading. During steady-state conditions, or at any instantaneous time during launch, orbit, or startup, they provide positive, fixed support. The cables are preloaded to keep them in tension during maximum flight acceleration conditions. It was calculated that 5/16-in. diameter cables would be more than adequate to carry the load. The boiler is supported at two points with the cables so arranged and preloaded as to account for the spring rate of the boiler helix. The mercury NaK, and L/C pumps and their associated components are supported at their combined mass center in a manner comparable in principle to that of the TAA support.

Exact cable orientation, preloading and final selection of cable couplings and attachment points were not determined in this study. Preliminary

calculations were made only to establish the feasibility of the concept. By using this structural design, a weight saving of 1100 lb was estimated. This structural concept was used for all of the improved systems, EGS-1 through -6.

Structural continuity between the HRL and L/C radiators is necessary in order to transfer the loads to the payload structure which in turn is supported by the payload mounting ring of the Saturn IVB stage. In order to establish structural weight requirements, it was necessary to consider the design of the structural joint at each of the above interfaces. Figure 14 shows a typical joint used in estimating the weight of the radiator structural supports.

E. SYSTEM PERFORMANCE ANALYSIS

Analysis of the SNAP-8 EGS requires iterative calculations which are best handled by a computer. A digital computer program was written for the SNAP-8 development program for steady-state performance analysis. This program, described in Reference 7, was given the code name of SCAN (System Cycle ANalysis). The program incorporates a set of "M" functional equations containing "n" variables which describe the steady-state performance of the SNAP-8 EGS. When n-m independent variables are assigned fixed values, and a complete set of values (initial guesses) are given for the unknown variables, the computer program uses a variation of the Newton-Rapheson method for iterating the variables until a power balance is achieved. In addition to the variables mentioned above, the SCAN program requires the following input; piping characteristics, component performance characteristics, mercury thermodynamic properties, and selected state-points. Component characteristics are defined by curve-fitting actual test data wherever possible. With these inputs, the computer calculates final values of the unknown variables which will match the variables assigned fixed values that are supplied as part of the input. In the process, the computer also calculates trim-orifice pressure drops for each loop to achieve a balance between the head rise of the pump and the pressure losses throughout the loop. The computer output includes a system diagram with all significant temperatures, pressures, flow rates and input and output power;

a list of the values of all of the n variables; and a list of other important calculated values, such as overall efficiency, alternator efficiency, and alternator kva output.

In the present study, the computer program was modified to the extent of replacing, adding, or deleting equations as necessary to define the system being analyzed. The number of equations used ranged from 53 to 56 and the number of variables from 70 to 72. Typically, the systems were analyzed with either the net output power or the reactor input power fixed. Other parameters that were fixed inputs to the computer are the turbine efficiency, the turbine inlet pressure, the turbine exit pressure, and the reactor coolant outlet temperature.

IV. BASELINE SYSTEM - EGS-0

Characteristics of the baseline electrical generating system (EGS-0) were established primarily by the experimental data on SNAP-8 PCS components that were available as of September 1965. Where component experimental data were not available, the prevailing detailed design calculations and drawings were used. Properties of the nuclear system, structure and radiators were identified as described in the previous section. On the basis of this information, a steady-state performance analysis and a detailed weight compilation of EGS-0 were made; data used to evaluate the changes incorporated in the improved systems.

A. SELECTION OF OPERATING CONDITION FOR ANALYSIS

To completely analyze the performance of the power system, it is necessary to consider many different conditions which might be encountered in a typical space mission; e.g., variations in (1) the incident heat input to the radiators (sun or shade), (2) the electrical load demanded by the vehicle (100 to 0%), and (3) the gravity field (0 to 1 g or greater). In the present study, one operating condition only is of interest, since the object is to compare the effects of internal power system improvements. The conditions chosen for comparison of all of the SNAP-8 systems characterized in the study are zero gravity, 100% vehicle load, and maximum sun and earth incident heat input to the radiators in a 300 nautical mile orbit. In general, these are the conditions which yield the lowest available electrical power for a given SNAP-8 system.

One other condition which deserves special mention is the variation in temperature of the NaK leaving the reactor. This temperature is continuously measured and maintained by the reactor controller within the limits of 1280 and 1330°F. This variation in temperature slightly influences the performance of the EGS because it affects conditions in the boiler. Since it was not obvious which temperature extreme would yield the lowest available output power, the performance of EGS-0 at both temperature conditions was analyzed. It was found that slightly lower output power (0.8 kw) was obtained when the reactor outlet temperature is at its upper limit of 1330°F. Consequently, this condition was selected as a basis for comparing the performance of all of the systems evaluated in this study.

B. PERFORMANCE AND WEIGHT OF EGS-0

The results of the performance analysis of EGS-0 operating at the upper temperature limit of the reactor coolant are summarized in Figure 16. This summary performance chart gives all significant steady-state operating data for the system presented in a standardized format. At the top of Figure 16 significant temperatures, pressures and flow rates for each loop are identified on a schematic diagram. Below the diagram, descriptive features defining the makeup of the system are tabulated. This list will help to distinguish modifications incorporated into the improved systems described in later sections of this report. Also tabulated below the schematic diagram are the overall performance parameters of the EGS. On the left side of the diagram, the alternator power distribution and the thermal power (in kw) dissipated by the L/C radiator are tabulated. On the right side of the chart is a line diagram of system configuration showing axial height of the radiators applicable to the system. This chart format was used for each of the systems analyzed to facilitate comparison.

Regarding the pressure values identified on the schematic diagram, a word of explanation is in order. For the NaK loops, the pressures given represent the total loop pressure drop. In EGS-0 (and in some of the improved systems), the NaK PMA generates a higher pressure rise than the loop requires. In that case, the excess ΔP is dissipated by a trimming orifice located at the pump discharge port not shown on the diagram. For the mercury loop, where various pressures around the loop are identified, the pressure at the pump discharge is that produced by the pump upstream of a flow control valve (not shown). In all of the systems analyzed, the mercury pump discharge pressure is higher than that required to meet the loop ΔP requirements. This is seen in the diagram by comparing the pressure at the pump exit with that at the boiler inlet.

The overall efficiency of EGS-0 (Figure 16) is 7.0% and the net power output is 36.0 kwe. The rated power output of the SNAP-8 EGS is 35 kwe. EGS-0 meets this requirement with a one kilowatt margin for performance degradation over 10,000 hours of operation. It was planned that the system analysis

would be normalized at 40 kw net power, thereby providing 5 kw for performance degradation (this being an arbitrary, but generous number). However, in analyzing EGS-0 the system would not produce the desired 40 kwe net output without exceeding one, or more, of the component design limitations. The EGS-0 power output of 36.0 is limited by a mercury flow rate of 12,000 lb/hr at the assumed turbine inlet pressure and temperature and fluid flow area.

The total weight of EGS-0 is given in the performance summary of Figure 16 as 11,003 lb. This value includes the weight of all PCS components, the nuclear system, the radiators, and supporting structure. A detailed tabulation of weights is given in Appendix B of this report.

The performance of EGS-0 at the lower temperature limit of the reactor coolant is summarized in Figure 17. It is seen that the net power output increases to 36.8 kwe and that mercury flow rate and turbine inlet pressure increase a small amount. These changes are due to reduction in mercury pressure drop through the boiler associated with the change in boiler NaK-side temperature levels.

V. BASIS FOR PERFORMANCE IMPROVEMENT

Performance improvement in the context of this study is defined as weight reduction, radiator area reduction, available power increase, and overall efficiency increase.

Total radiator area is an important factor in applying any power system to a space vehicle since the size of the booster payload envelope may limit the amount of surface area available for this purpose. Therefore, ways of reducing radiator area were investigated. Not only increased overall efficiency reduces radiator area, but the temperatures at which the energy is radiated has a direct effect on area. Radiating temperatures also were evaluated in the course of this study.

Weight reduction is not directly related to overall efficiency but results from reduced radiator area due to improved overall efficiency. If the saving in structure is not included, it can be stated that a greater weight reduction was achieved by increasing overall efficiency than was obtained by reducing PCS component weights.

In the cases where the reactor output power is fixed at 600 kwt, as in EGS-3 and -6, the net power output is directly related to the overall system efficiency. In all other systems, from EGS 2 and up, the net power output was fixed at 40 kwe. The reactor power required for these systems is inversely related to the overall system efficiency.

A. IMPROVEMENT IN OVERALL EFFICIENCY

In order to identify what kinds of modifications offer the greatest gain in efficiency, an assessment of the power distribution throughout the SNAP-8 system was made. By examining the power losses occurring in the several loops and components of EGS 0, it is possible to develop a logical plan for improving efficiency. Figure 18 depicts the distribution of power in EGS-0 as it is being transformed from thermal to electrical power by the boiler, turbine, and alternator. Overall efficiency is the ratio of the net electrical output

to reactor thermal input $\left(\frac{36.0}{512} = 7.0 \right)$. The overall efficiency can be defined as $\eta_o = \eta_c \eta_t \eta_a \eta_p$, where η_c is the Rankine cycle efficiency and is equal to the ratio of the energy available to the turbine divided by the total thermal energy in the fluid. In Figure 16, $\eta_c = \frac{120}{510} = .235$. η_t equals the total turbine efficiency equal to $\left(\eta_t = \frac{64.9}{120} = .541 \right)$. η_a equals alternator efficiency $\left(\eta_a = \frac{55.8}{64.9} = .860 \right)$. η_p equals parasitic efficiency defined as the net electrical output divided by the gross electrical output of the alternator $\left(\eta_p = \frac{36.0}{55.8} = .645 \right)$. It is logical to start first on 0.235 (η_c) since this is the lowest value. This value, however, is the most difficult to increase since, for this study, the reactor outlet temperature must remain constant due to the characteristics of the reactor fuel elements. The only way to increase this value is to increase the pressure ratio; refer to Section V,D for a more detailed discussion.

The next efficiency value is 0.541 (η_t) which is the turbine efficiency. This value is determined by the turbine pressure ratio, number of stages, blade velocity to nozzle velocity ratio, and the size and shapes of the flow passages (see Section V,C,1).

The alternator efficiency of 0.860 (η_a) is determined by the alternator design and the alternator-load power factor. Power factor and alternator design are discussed in Section V,C 4.

The parasitic load determined the value of $\eta_p = 0.645$. This value can be increased by reducing pump power required, increasing the efficiency of the electrical controls, and increasing the efficiency of the pump and motors used in the system.

In this study, all four efficiencies which define the overall system efficiency were improved. This increased overall efficiency results in several improvements; reduced radiator area, reduced weight, increased power output, and reduced power input for a specified output.

B. WEIGHT REDUCTION

Part of the effort directed toward the evaluation of EGS-1 consisted of a weight reduction study of PCS components. Each component of the PCS was critically reviewed by examining detail drawings to identify parts which could be lightened without affecting component function or reliability. Much of the weight reduction was effected by replacing heavy bolted flanges with welded pipe connections. In some cases, component housings were thinned but only where it was determined that stresses were far below allowable levels. Table 11 summarizes the amount and nature of the weight reductions estimated for the major components. The revised weights shown in Table 11 were used in compiling the detailed weight tables for EGS-1 presented in Appendix B. They also were used as a basis for the weight breakdown of the later systems, after making adjustments to account for subsequent component modifications.

Referring to Table 11, a reduction of 1545 lb in PCS dry weight may be noted. Of this total, the largest single increment is 1100 lb attributable to a major change in the structural design concept. The remaining 445-lb reduction for all of the other PCS components amounts to about 12% of the original weight of the PCS less the structure. This is a relatively small reduction, reflecting the rather cautious approach of the weight study. Some additional weight savings may be observed by comparing the detailed weight tables for EGS-0 and EGS-1 in Appendix B. The primary loop NaK inventory is reduced 57 lb as a by-product of the boiler weight analysis described in Reference 8; a reduction in radiator weight of 88 lb is due to a reduction in heat rejected. This effect becomes increasingly important in the later systems, amounting to over 600 lb in EGS-5.

C. COMPONENT MODIFICATIONS AND SUBSTITUTIONS

The principal technique employed to evaluate the performance improvement potential of the SNAP-8 EGS was that of examining the performance of individual components. Each of the major components of the PCS was reviewed. Design modifications (or, in some cases, entirely different designs) which might increase efficiency or decrease parasitic losses were analyzed to estimate individual performance gain. Modified or substituted components were then incorporated analytically in one or more of the systems to determine their effect on EGS performance. Some of the component modifications were eliminated after

analysis indicated that gains were too small or development effort was too great to justify further consideration. The following paragraphs discuss the nature and effect of the modifications and their application in the various improved systems.

1. Turbine

The turbine was reviewed to evaluate the effect of design improvements on the turbine aerodynamic efficiency. The SNAP-8 turbine assembly is a four-stage, axial flow, impulse-type turbine designed to operate at 12,000 rpm. Labyrinth seals are used to minimize interstage leakage. A thrust balance piston on the first-stage rotor is used to neutralize axial thrust so that bearing loads are reduced, thereby increasing bearing life. Mercury vapor flowing past the thrust-balance piston is vented directly to the exhaust. On the basis of test data, the aerodynamic efficiency of this design was determined to be 57% when the mercury vapor contained 2% by weight of liquid carryover. This efficiency does not include bearing and seal-to-space losses which have been established as 3.3 kw.

Analysis indicated that performance can be improved by incorporating the following design modifications:

- a. Reduce the diameter and clearances, and improve the labyrinth and concentricity of the thrust balancing piston; provides a reduction in the bypass flow through the piston.
- b. Reduce the present blade-tip clearances; can be reduced from the present 0.040 to 0.020 in. on the basis of thermal expansion data.
- c. Reduce the nozzle-vane tip clearances; sufficient reduction eliminates leakage path common to all four stages.
- d. Reduce trailing edge thickness of rotor blades; can be reduced from 0.014 down to 0.006 in.

These changes were estimated to increase aerodynamic efficiency by 7.4 percentage points to 64.4% with 2% liquid carryover (Reference 9). This value was used in the system analysis for EGS-1, -2, and -3.

In EGS-5 and -6, the turbine inlet pressure was increased from 240 to 350 psia. Appendix C shows the equations used and the assumptions made in correcting the stage efficiencies to account for higher partial admission

losses due to the change in absolute pressures and pressure ratios. A turbine efficiency of 62.5%, obtained by this process, was used in EGS-5 and -6.

A more recent analysis, described in Reference 10, indicates that the attainment of an efficiency of 62% would be more probable with the above-listed modifications. Therefore, in EGS-4, which also has a turbine inlet pressure of 350 psia, an efficiency of 61% was used to evaluate the performance of that system. In all systems, it was assumed that the flow passages were adjusted to match the mercury flow rates calculated in the system performance analysis.

2. NaK Pump Motor Assemblies (NaK PMA)

This component was reviewed to determine the feasibility of reducing its required input power. This is an important contributor to the parasitic power of the EGS since the same assembly is used in both the PNL and HRL. The present SNAP-8 NaK PMA is driven by a 5800-rpm induction motor; its characteristics are given in Figure 19. This type of NaK PMA was used in EGS-0, -1, and -3 where there is the requirement for relatively high-head-rise and flow characteristics.

For systems with lower flow rates and lower head-rise requirements, such as in EGS-2 and -4, it was found that the PMA could be modified in a simple way to reduce the power required. The modification consisted of rewinding the motors to produce a 10-pole motor instead of the present 8-pole motor; reduces the synchronous speed from 6000 to 4800 rpm. The operating speed for this design would be 4800 rpm if a synchronous motor is used or 4650 rpm if an induction motor is employed.

Analysis of the reduced-speed NaK PMA was conducted to establish the new H-Q characteristic and to determine the power input requirements. The H-Q and power input of the 4800-rpm synchronous NaK PMA are given in Figure 20. It is assumed here that a 3% increase in impeller diameter will give the same characteristics at 4650 rpm as given for the 4800-rpm assembly. The greatest gain in pump motor efficiency is obtained from the reduction of hydrodynamic losses associated with the NaK-flooded motor rotor and the reduced hydraulic power imparted to the pumped NaK. Table 12 gives a comparison of the losses and input power with those of the 5800 rpm NaK PMA.

A third class of NaK PMA was developed analytically for EGS-5 and -6 by custom designing the assembly to match the NaK flow rate and reduced

loop ΔP requirements. Allowances were made for impeller efficiency, hydraulic losses and motor electrical losses to obtain input power. Figure 21 shows the head rise and input power vs NaK flow rate obtained by this method. This figure implies that a specific PMA must be designed for each flow rate. The specific design requirements are shown in Table 13. The head rise requirements given in this table reflect modifications in pipe size and components to reduce loop hydraulic impedance.

In addition to varying the head and power input characteristics of the NaK PMA, the method of cooling the assembly was reviewed. The motors for the SNAP-8 PMA's were designed to operate at 600°F but are cooled by L/C fluids so that they operate at 325°F. Recent tests made on a NaK PMA operating at motor temperatures of 600°F has shown that 500°F HRL NaK can be used as coolant for these assemblies. The input power reduces slightly at the high motor temperature for increased electrical losses due to higher winding resistance. The advantage of cooling these motors with HRL NaK is in a reduction of radiator area. There is a net reduction of approximately 15 sq ft for each kw transferred from the L/C radiator to the HRL radiator. NaK cooling of the NaK PMA's was used in EGS-2 through EGS-6.

3. Mercury Pump

The present SNAP-8 mercury PMA characteristics have been found to be satisfactory for all systems considered in this study as long as the system state-points are such as to provide adequate suction pressure to the pump. This PMA employs a liquid-to-liquid jet pump to increase the inlet pressure to the centrifugal impeller. The NPSH requirements of the mercury pump are, therefore, determined by the jet-pump requirements, shown in Figure 22. Two independent parameters influence the NPSH available: the turbine exhaust pressure, and the HRL radiator NaK ΔT . All of the systems synthesized in the study provide sufficient NPSH for operation of the mercury PMA. However, if for some applications a reduction in turbine exit pressure was desired, the pump HPSH requirement could be reduced by relatively simple design changes.

The SNAP-8 MPMA also includes a motor scavenger impeller which absorbs 0.65 kw shaft power. The study indicated that this part could be eliminated, thereby reducing the motor input power by 0.74 kw (based on a motor efficiency of 87.8%). This modification was adopted in EGS-4, -5, and -6.

The mercury pump power demand could be reduced further by mounting the mercury pump impeller on the turbine or alternator shaft. The effect of this modification was investigated for three different impeller locations. The impeller was located on the outboard end of the turbine, between the turbine and the mercury space seal, and on the outboard end of the alternator shaft.

a. Turbine Mounted Mercury Pump

This arrangement (shown in Figure 23) makes it possible to eliminate the seal-to-space associated with the present MPMA. However, there are several disadvantages associated with this design concept which would require considerable development effort to overcome. The two main disadvantages are the large overhang which causes difficulty in controlling running clearances due to the thermal gradients in the frame structure and the flow of mercury vapor at 155 psia from the first turbine wheel cavity into the pump impeller back vanes. The vapor flow causes an estimated temperature rise to 900°F at the back vanes which increases corrosion and erosion rates.

b. Alternator-Mounted Mercury Pump

This arrangement (shown in Figure 24) eliminates the losses associated with the electric motor drive of the present MPMA. The seal-to-space is retained in this design so that the reduction in parasitic power is not as great as noted in the above paragraph. Because this design concept is similar to the present MPMA design, it is the easiest to accomplish and, therefore, represents the recommended approach to mounting the pump impeller on the TAA. Table 14 compares the parasitic losses associated with these modifications.

c. Mercury Pump at Turbine Exhaust End of Turbine Shaft

A third configuration was studied to evaluate the feasibility of integrating the mercury pump on the turbine shaft between the turbine and the space seal. The primary purpose of the study was to evaluate the effect, if any, on turbine overhang. Toward that end, the dimensional requirements of the mercury pump centrifugal stage and the turbine housing and shaft necessary to accommodate the pump were studied. It was found that it is mechanically possible to install the pump on the turbine shaft by increasing the turbine overhang about one inch. To do this while maintaining a satisfactory shaft critical speed, it is necessary to increase the shaft diameter by about 0.1 inch, and to

select a larger bearing (55 mm instead of 40 mm). However, the feasibility of such a design is difficult to assess. There are two uncertainties in the design: (1) a shaft surface speed of about 90 fps at the pump inlet which will cause prerotation of the mercury entering the pump, and (2) heat conduction to the mercury space seal. In view of these uncertainties, this design concept was not incorporated in the systems being studied.

In summary, the investigation of mercury pumps mounted on the turbine or alternator shaft yielded the following results:

(1) An appreciable reduction in parasitic power may be realized by that approach. Table 14 shows about 1.8 kw lower losses for either of the outboard pump configurations. (The net gain is this value less the 0.74 kw realized by eliminating the motor scavenger as described in paragraph C,3 above.) The inboard arrangement of the pump could, in principle, reduce losses by as much as 1 kw.

(2) All of the configurations require component design and development work to resolve uncertainties which prevent accurate prediction of performance by analysis alone.

(3) Use of any TAA-mounted mercury pump in SNAP-8 imposes severe restraints on system configuration and operation. Configuration is influenced by the pump suction pressure requirements and the effect of orientation of the turbine, the condenser and the pump on the available suction pressure when operating in a gravity environment. System startup and shutdown operations are limited by the fact that the pump cannot be operated independently of the turbine. In view of the above observations, none of the TAA-mounted pump concepts were incorporated in the improved system studies.

d. Mercury Jet Pump

Mercury jet pumps, using saturated mercury vapor as the drive fluid, do not produce enough head rise to make their use feasible. However, if saturated liquid mercury is used as the drive fluid, sufficient head rise can be attained so that two jet pumps in series could operate in the SNAP-8

Rankine-cycle loop as boiler feed pumps. This concept is shown schematically with typical steady-state operating data in Figure 25.

The saturated-liquid drive fluid enters the mixing section through the central nozzle while the pumped fluid enters through an annular-nozzle. Condensation of the vapor in the drive fluid takes place in the mixing section, and conservation of momentum is the basis for the mixing process. The pumped fluid must be sufficiently subcooled so that it can absorb the heat of condensation of the vapor present in the drive fluid. Thus, at the end of the mixing section, all the fluid is in the liquid phase. A diffuser then converts most of the kinetic energy to pressure.

The efficiency (mechanical work divided by thermal input) is low. However, all of the thermal input is useful to the Rankine cycle since the heat that is not converted to mechanical work is returned to the boiler.

A gain in system efficiency is derived from the elimination of the power required to drive the present MPMA. This amounts to a potential reduction in parasitic power of 3.5 kw.

The total heat input to the mercury in a typical SNAP-8 EGS (e.g., EGS-2) with mercury PMA is:

$$\begin{aligned} Q_{cp} &= \dot{w} (h_{out} - h_{in}) \text{ boiler} \\ &= 9765 (162.8 - 17.8) = 1.415 \times 10^6 \text{ Btu/hr} \end{aligned}$$

This compares with an equivalent jet-pump system where the heat input is:

$$\begin{aligned} Q_{jp} &= \dot{w} (h_{out} - h_{in}) \text{ boiler} + 0.5 \dot{w} (h_{out} - h_{in}) \text{ heater} \\ &= 9765 (162.8 - 22.3) + 4882 (35.5 - 22.3) = 1.436 \times 10^6 \text{ Btu/hr} \end{aligned}$$

Based on the accuracy of this analysis, there is no essential difference in heat input to the system.

In order to take advantage of this concept, it would be necessary to develop mercury jet pumps to establish flow and pressure control requirements and also to determine suitable startup procedures for this type of pump. Preliminary evaluation of the effect of decreasing the driving fluid temperature by 50°F (this change is equivalent to the reactor dead band) indicates that the discharge pressure of the jet pump would decrease by approximately 16%. Therefore, it is necessary to provide a control device for the jet pump to avoid power excursions due to normal off-design operating conditions. Because of anticipated development problems, the mercury jet-pump concept was not incorporated in any of the systems analyzed.

4. Alternator

The alternator used in the SNAP-8 PCS is of the homopolar type producing 400 cps at 12,000 rpm. The alternator was reviewed for the purpose of determining the feasibility of weight reduction and possible performance improvement by modification or replacement by another type. One modification considered was operation at HRL temperatures so that the electrical losses could be rejected by the HRL radiator. The use of an induction alternator may result in increased alternator efficiency and also a saving in weight. The SNAP-8 alternator and modifications that were studied in this program are discussed below:

a. SNAP-8 Alternator

The overall efficiency of the present SNAP-8 homopolar alternator is shown in Figure 26. Since the test data available for this alternator did not provide efficiency data at power levels of 70 to 80 kwe at unity power factor, the efficiency at these conditions was estimated by using the following relation:

$$\eta_{AH} = \frac{kwe}{kwe + \left(\frac{kva}{80}\right)^2 \left(\frac{60}{\eta_o} - 60\right) + 2.0}$$

where η_o = the alternator efficiency at 60 kwe gross power and 0.75 power factor and kva is the kva value for the power factor and gross kwe output at which the efficiency is to be evaluated.

This method was used to estimate the efficiency of the alternator in EGS-3 and -6. It should be noted that the alternator design rating of 83 kva is slightly exceeded in these systems. EGS-3 requires 85 kva capability at 0.92 power factor and EGS-6 requires 86 kva at a power factor of 1.0. If the vehicle load were to drop to 0 in EGS-6, the kva load on the alternator would increase since the net power factor decreases in the leading direction as more power is shunted to the PLR. This may be corrected by reducing the amount of capacitive reactance in the circuit and/or adding inductive reactance in the PLR circuit. Re-evaluation of the allowable temperature of the ML insulation and the effect of temperature on the life and reliability of this insulation may permit operation of this component at the power output levels of EGS-3 and -6. This temperature limit, the power factor variation with vehicle load, and voltage control limits, must be evaluated in more detail in future specific application studies.

b. Induction Alternator

An evaluation was made of a capacitor-excited induction generator. This evaluation was prompted by the fact that the lobed rotor unidirectional flux principle of the homopolar alternator results in less than 50% utilization of the output voltage capability normally achieved in machinery of this size. Since the magnetic circuit of the induction generator would be utilized 100% of the time, instead of the 50% utilization of the homopolar alternator, a significant weight reduction is possible.

Other potential advantages of the induction generator are to be expected in the elimination of the field coil and heavy magnetic yoke that are basic to the homopolar alternator, and the reduced losses from windage and bearings with the lighter and smaller rotor. An electrical efficiency approaching 95% is attainable as a consequence of these reduced electrical and mechanical losses.

The induction alternator, which features a single stator output winding, substitutes capacitor excitation for the voltage regulator-exciter now used. This preliminary concept would be an open loop regulation

system using magnetic saturation of the rotor iron to stabilize the output voltage. For a constant power output such as the SNAP-8 system, it appears that the voltage can be held within $\pm 3.0\%$ with a $\pm 1.0\%$ speed variation. Additional work is required to evaluate the problems of voltage buildup and short-circuit protection.

For the induction alternator to function properly in the SNAP-8 system, the capacitor-exciter must furnish a leading power factor under all conditions, or else the alternator will collapse electrically. The design point for this evaluation assumes that the worst alternator load has a 0.75 lagging power factor. In order to correct this to a 0.75 leading power factor and, thereby, provide an ample design margin, a capacitor with an estimated weight of 50 lb would be needed to furnish the required capacitive reactance.

The electrical efficiency of the induction alternator was estimated at 95% with 0.75 leading power factor; however, the acceptance test data for the homopolar alternator, from which Figure 26 was plotted, shows an overall efficiency of 90.7% at 55 kw and a unity power factor. Correcting this value by deducting the 2.0 kw loss for bearings and slingers gives an electrical efficiency of 93.8%.

It was assumed, in keeping with the replaceable component concept, that the induction alternator would bolt to the TA as does the present alternator, and would contain its own bearings, slingers, and cooling jacket. Preliminary design established rotor, stator, and end-turn dimensions for both a four-pole 12,000 rpm and a two-pole 24,000 rpm machine. An allowance of 10 in. for bearings, slingers, end turns, and mounting flange was added to the rotor stack length to obtain overall lengths. Diameters were determined by adding 1 in. to the stator diameter to allow for structure and cooling jackets. With volumes established, weights were estimated by ratioing to the homopolar alternator weight and volume.

In making a weight comparison between the two machines, the induction alternator is charged with the capacitor-exciter unit weighing 50 lb. The dimensions and weights of the two machines are compared on Figure 27.

From this evaluation, it appears that the electrical efficiency of the two machines is comparable. On a weight basis, the induction alternator is estimated to be approximately 175 lb lighter than the present SNAP-8 alternator, or 110 lb lighter than the weight-reduced alternator. Additional analysis of speed control and electrical system problems would be needed if the induction alternator were to replace the present SNAP-8 alternator. The induction alternator was not used in the systems synthesized in this study.

c. High-Temperature Alternator

The possibility of using a high-temperature (400°C) alternator was evaluated as a means of reducing radiator area. The high-temperature alternator would be cooled by HRL NaK, decreasing the heat rejected by the L/C radiator.

This investigation showed that the alternator efficiency decreased as the temperature of the winding increased due to increased resistivity of the conductors.

The effect of high-temperature operation on performance at 1.0 power factor is summarized in Table 15, showing a drop in alternator efficiency of approximately 2 percentage points. Somewhat greater losses result at lower power factor.

The effect of substituting this high-temperature alternator for the L/C cooled alternator on system performance was analyzed. System efficiency decreased by 0.26 percentage points. This causes the HRL radiator to increase by 20 sq ft due to the reduced cycle efficiency. An additional 12 sq ft was required to cool the alternator with HRL NaK so that 39 sq ft were added to the HRL radiator while 64.5 sq ft were removed from the L/C radiator. This results in a net reduction in total radiator area of 32.5 sq ft. These numbers are based on the assumption that the heat flow to the L/C cooled and lubricated high-temperature alternator bearings is negligible. Any heat flow to these parts would further reduce the savings in radiator area obtained by using a NaK-cooled alternator.

Because of the small reduction in radiator area, the loss in efficiency, and the effort required to develop it, the high-temperature alternator was not used in the systems synthesized in this study.

5. Speed Control

The SNAP-8 speed control is a closed-loop system that senses the alternator output frequency, and controls the speed of the turbine by varying the

load in the parasitic load resistor. The PLR load is controlled by means of saturable reactors. The speed is regulated to $\pm 1\%$. With this system, a minimum load of 1.5 kw is delivered to the PLR when the control is in the "off" mode of operation (i.e., at 100% vehicle load). In addition, internal losses in the saturable reactor are approximately 800 watts. The saturable reactor assembly weighs about 190 lb.

A silicon-controlled rectifier (SCR) type of speed control was evaluated as a design alternative with the expectation of reducing the parasitic load on the alternator. The SCR system is capable of cutting off the power to the PLR to virtually zero when it is in the "off" mode, eliminating the need for 1.5 kw residual parasitic load. In addition, the SCR circuit described below has an internal power loss of only 330 watts. A net reduction in parasitic power of 1.97 kw is therefore attainable by adoption of the SCR speed control design.

A simplified schematic diagram of the SCR speed-control system is shown in Figure 28; its approximate dimensions are given in Figure 29. Parallel SCR's and diodes are shown in each phase for increased reliability since each SCR and diode can carry the current required. The current-carrying capability is a function of the temperature of the SCR. Westinghouse Type 2N 3888 SCR's and Type 1N 3291 silicon-rectifier diodes were selected as typical components for this control. The maximum allowable case temperatures are 118°C (244°F) and 182°C (357°F) for the SCR and diodes, respectively, which allows the assembly to be cooled by the L/C fluid. With an average current of 22 amp, the loss per diode and SCR is 25 and 30 watts, respectively. Consequently, the total heat load to the L/C loop for the 6 diodes and 6 SCR's is 330 watts.

The estimated weight of the SCR speed control is 40 lb. An additional 50 lb for local shielding was included in the weight estimates for EGS-2 through -6 in which the SCR control system was used. This weight of shielding, consisting of tungsten and lithium hydride, is sufficient to reduce the radiation dose at the SCR's by one order of magnitude to 10^5 rads gamma and 10^{10} nvt neutrons. It is not at all certain that this supplemental shielding is necessary; however, since the SCR's are somewhat more sensitive to radiation than the diodes and the other electronic components, the shielding was added as a precaution.

6. Boiler

The SNAP-8 boiler is a single-pass counter-flow design in which seven parallel tubes containing mercury are enclosed in a single tube containing NaK. The characteristic temperature profile of this type of boiler is such that the mercury and NaK temperatures approach the same value at a point where initial mercury boiling occurs, about 10% along the tube from the mercury inlet end. This location has been referred to as the "pinch-point". The NaK-mercury temperature difference at the pinch-point (ΔT_p) is an important parameter affecting system performance. This is discussed in the following paragraph. In subsequent paragraphs, other boiler performance characteristics and their treatment in the system studies are described.

a. Boiler Pressure Stability

Boiler pressure stability, expressed as the ratio of pressure fluctuation to the absolute pressure at the boiler mercury outlet, is shown in Figure 30 as a function of ΔT_p . The curves are based on boiler test data and show that pressure oscillations increase as ΔT_p decreases. The pressure oscillations occur at a frequency of 0.2 to 0.5 cps, low enough that the turbine output power will fluctuate correspondingly at approximately the same amplitude (in %).

From the data on which Figure 30 is based, a minimum ΔT_p of 250°F was chosen as the limiting criterion for boiler operation; on this basis, the boiler pressure fluctuation will not exceed +3%. In applying this criterion to the system performance calculations in the present study, a ΔT_p of 75°F was used because all of the systems were computed for the upper temperature limit (1330°F) of the reactor coolant. If the lower temperature limit (1280°F) were used, the ΔT_p would be 25°F since the temperatures in the primary NaK loop would be uniformly 50°F lower, while the temperatures in the mercury loop would be substantially unchanged. This approach assures that the systems compared in the study are capable of operating stably at the lower temperature condition of the reactor coolant.

Variations in turbine output power, caused by boiler pressure fluctuations, were accounted for in the EGS performance analysis by the following method: The system power was balanced at the nominal turbine inlet pressure (240 psia for EGS-0). When the turbine inlet pressure is at the minimum point in its oscillation, the turbine will produce 3% less power. This increment of power is allocated to the PIR at nominal operating pressure so that the speed control will have sufficient margin to maintain full speed at the low point in the pressure cycle. The power increment budgeted to the PIR for boiler stability in the several systems is: 3 kw in EGS-0 and -1; 2 kw in EGS-2, -4, and -5, assuming improved boiler performance and lower mercury flow rates; and 3.0 and 3.3 kw, respectively, in EGS-3 and -6 which were increased because of higher mercury flow rates.

b. Pressure Drop

In conducting the study on each of the systems described, the pressure drop of both the NaK and mercury flow paths of the boiler was varied as described below.

(1) Mercury Pressure Drop

The equations used to express the boiler mercury pressure drop were changed to conform to the characteristics of the boiler selected for the system. In evaluating the EGS-0 system, the following mercury pressure-drop equation was used:

$$\Delta P = (27.3 + 0.7 \Delta T_p) (\dot{W}_{Hg}/11,500)^2$$

For EGS-1 and -2

$$\Delta P = 56 (\dot{W}_{Hg}/12,000)^{1.8} + 0.37 \Delta T_p$$

For EGS-3

$$\Delta P = 56 (\dot{W}_{Hg}/15,430)^{1.8} + 0.25 \Delta T_p$$

For EGS-4 and -5

$$\Delta P = 56 (\dot{W}_{Hg}/13,700)^{1.8} + 0.25 \Delta T_p$$

For EGS-6

$$\Delta P = 51 \text{ psi}$$

In each of these equations \dot{W}_{Hg} is the mercury flow rate in lb/hr, and ΔT_p is the ΔT at the mercury pinch-point. Pinch point is defined as the difference in temperature between the mercury and the NaK at the point in the boiler where boiling starts.

The equation given for mercury ΔP for EGS-0 was obtained from the tube-in-tube boiler design analysis while the equation for mercury ΔP used in EGS-1 and -2 was obtained empirically from test data on the tube-in-tube boiler, and, therefore, represented the actual measured mercury pressure drops for the 7-tube mercury boiler. In EGS-3, a higher mercury flow rate compatible with 600 kw input from the reactor made it necessary to increase the number of mercury tubes to nine. The \dot{W} term in the ΔP equation was normalized for nine tubes at the same mercury flow per tube and the ΔT_p coefficient was reduced on the assumption of a potential improvement in boiler plug design. In EGS-4 and -5, the turbine inlet pressure was increased from 240 to 350 psia. This change resulted in modification of the mercury Δp equation to account for the effect of the change in mercury vapor density on the pressure drop. For EGS-6, it was assumed that a boiler with 51 pounds ΔP could be designed when the mercury flow rate is 14,000 lb/hr.

(2) NaK Pressure Drop

In EGS-0, the boiler NaK-tube ID was 4.0 inches while the EGS-1 and -2 boiler was reduced in NaK-tube ID so that maximum weight reduction could be achieved. The reduced NaK-tube ID is 3.375 inches which increases the boiler NaK ΔP from 1.5 to 8.1 psi at 48,100 lb/hr. The reduced NaK flow rates for EGS-1 and -2 result in NaK ΔP of 5.6 and 4.3 psi, respectively. The NaK tube for the EGS-3 boiler was increased to give the same NaK velocities as in the original boiler; the NaK ΔP in this boiler is 1.55 psi at 49,000 lb/hr.

Since the state points were changed for the remaining systems, it was necessary to consider the effect of these state-point changes on boiler design requirements. In all boilers used in this study, a constant ΔT_p value of 75°F was used for the upper temperature limit of the reactor dead-band system operating condition..

As turbine inlet pressure increases, the mercury boiling temperature at the point where boiling commences also increases. Since the reactor outlet temperature is constant, and a constant value of $75^{\circ} \Delta T_p$ is required, the NaK flow rate in the primary loop must increase as the turbine inlet pressure increases. Figure 31 shows the ratio of primary NaK flow rate to mercury flow rate as a function of turbine inlet pressure. Because of this relation, the NaK tube diameter of the boilers for the remaining systems was increased to reduce the NaK pressure drop. For EGS-4 and -5, the ID of the EGS-0 boiler was used; for EGS-6, the ID was increased to maintain the same NaK velocity as in the EGS-0 boiler. Table 16 lists the physical characteristics of the boilers used in the various systems.

c. Boiler Materials

The present SNAP-8 boiler uses 316 stainless steel for the NaK tube and 9Cr-1Mo steel tubes for the mercury. At present, there is considerable effort being expended on the development of material for the mercury tubes which has higher strength and corrosion resistance at operating temperature. The performance potential study has been based on the assumption that suitable materials will be available for use in boilers where the pressures have been increased to meet the state-point requirements for EGS-4, -5, and -6.

7. Electrical System

The alternator efficiency is a function of the power factor of the total alternator load and the gross power output, as shown in Figure 26. The total alternator load is made up of the following: vehicle load, primary NaK PMA, mercury PMA, HRL NaK PMA, L/C PMA, SCR speed control, voltage control, PLR stability allowance, and reactor controls.

By adding the kvar values and the kw values of each load, the total kva load on the alternator is obtained by taking the square root of the sum of the squares of kvar and kw. The gross kw divided by the kva then gives the alternator load power factor. The amount of power factor correction is, therefore, a function of the vector sum of all the loads on the alternator.

When the load to the vehicle is reduced by shifting the difference in vehicle load to the PLR, the alternator load power factor changes. This is due to the difference in power factor at the point of use. In the PLR, the power factor is essentially 1.0 while the power factor of the vehicle load is 0.75 lagging. Since the PCS control system operates on the basis of constant alternator output power, decreasing the vehicle load requires energy dissipation in the PLR. Because of the difference in power factor between the vehicle load and the PLR power factor, the power factor of the total alternator load increases as the vehicle load decreases. In the first four systems, the load power factor was 0.75 and the alternator voltage control was assumed to be limited to lagging power factors up to 1.0. For these systems, it was considered necessary to limit the power factor at maximum vehicle load so that the alternator load power factor would not become leading. The top curve in Figure 32 shows the variation of alternator-load power factor as a function of vehicle load for an electrical system using a saturable-reactor speed control having power factor characteristics shown in Figure 33, with maximum power factor correction. It can be seen from this figure that the maximum alternator power factor at 100% vehicle load is 0.91, which becomes 1.0 when the vehicle load is zero. This curve is based on 40-kw maximum vehicle load and 42.3 kvar capacitive reactance. If synchronous pump motors are used, only 23.9 kvar capacitive reactance is required, since 18.4 kvar of inductive reactance is removed from the alternator load by using these motors. The middle curve in Figure 32 shows the effect of the synchronous motors on alternator power factor with no capacitive reactance added to the system. The lower curve shows the variation of the alternator-load power factor with induction motors on the pumps, and no capacitive reactance added as in the EGS-0 and -1 systems. Similar alternator-load power factor variation occurs with changing vehicle load when an SCR-type speed control is used; its power factor characteristics also are shown in Figure 33. Thus, the alternator load power factor varies to some extent regardless of the type of speed control used.

With the exception of EGS-0 and -1, all systems use L/C-cooled capacitors to obtain power factor corrections. The capacitors reject approximately 100 watts of heat to the L/C loop coolant.

During the course of the performance potential study, it was learned that the alternator voltage control would operate down to 0.92 leading power factor at a gross output of 60 kwe. The leading power factor limit is determined by the voltage regulator characteristics which result in increasing output voltage when the power factor decreases in the leading direction. The lagging power factor is limited by the temperature rise of the alternator windings and is, therefore, a function of the gross kw output of the alternator. At 55 kwe, which is representative of those systems that produce 40 kwe net power, the lowest alternator-load power factor is 0.66 lagging. This limit is established by the maximum temperature rise of the alternator windings commensurate with insulation life and reliability. The vehicle-load power factor also was increased from 0.75 lagging to 0.85 lagging which reduces the effect of changing vehicle load on the net alternator power factor. As a result of these input changes, the system performance of EGS-4, -5, and -6 have been evaluated at a net alternator power factor of 1.0 at full vehicle load.

Table 17 gives the capacitive reactance required for each EGS where the power factor of the alternator has been corrected. As a representative example, a 42.3 kvar condenser assembly will weigh approximately 25 lb and have dimensions of 8 x 8 x 9 inches, if made up as a single assembly. There is an advantage, however, in making the power factor corrections at each load. For example, if the power factor of the individual pump motors is corrected locally, this will either reduce the startup battery and inverter requirements, or provide better motor startup torque. Also, by correcting the power factor of each individual load, at the load, the net power factor of the alternator will not be affected as much by the changing vehicle load. These considerations should be evaluated in more detail for any specific application.

8. Components Not Modified

In this section, the components are noted which were reviewed for possible performance improvement but not modified. Modifications here imply a change in performance characteristics and do not include changes made

in a component which may be required for changes in flow rate. Components which have not been changed in characteristics are: mercury condenser; alternator; mercury PMA; startup components, such as batteries and inverter; electrical components, such as voltage control, sequencer, vehicle load switch, power transmission cable, and PLR; valves, such as the mercury flow-control valve, NaK temperature-control valve, auxiliary NaK startup-loop shutoff valve, and L/C loop shutoff valves; mercury injection system; expansion reservoirs; and L/C PMA. In EGS-3 and -6, the mercury condenser was changed in size only to accommodate the increased mercury flow rates. The number of mercury tubes was increased from 73 to 85 tubes.

The alternator was found to have sufficient power output capability when the load power factor was increased for most of the systems; possible exceptions were EGS-3 and -6. The differences in individual alternators tested indicated a maximum kva range of 83 to 89 before the end-turn temperatures exceeded the 200°C limitation imposed by the ML organic insulation used in this component.

The mercury PMA was found to have ample head rise for all systems studied even when turbine inlet pressures of 400 psia are used. However, the motor scavenger slinger was removed for EGS-4, -5, and -6 to reduce the pump motor input power requirement.

Startup components, such as batteries and the inverter, were not changed. The performance potential study was limited to improvements in steady-state performance of the SNAP-8 EG systems so that startup procedures and improvements were not included in this study.

The voltage control, start programmer, vehicle load switch, power buss, and the PLR were considered satisfactory for all systems studied. There are some conditions of operation which may make it desirable to improve the voltage control so that the output voltage of the alternator will remain within specified limits over a greater leading power-factor range. However, the amount of power factor correction, and the manner in which it is applied, may make this unnecessary. The location of the PLR was changed from the primary NaK loop to the HR NaK loop in EGS-4, -5, and -6. This change reduces the operating temperature of the resistance elements and increases the reliability

and life of this component. The penalty for this is 4 to 7 sq ft of additional HRL NaK radiator area.

The valves used in the SNAP-8 PCS are retained for all of the systems analyzed for performance in this study.

The MIS concept has been retained and the only changes made were in capacity. The mercury inventory of the various EG systems changes so that the MIS reservoir must be changed.

Expansion reservoirs for the NaK and L/C loops will vary in capacity requirements in proportion to the respective loop inventory variations. The basic design concept for these components was not changed but the weights of these components were changed in accordance with the loop inventories for each of the EG systems studied.

The L/C PMA was considered satisfactory for all systems studied.

D. IMPROVEMENT BY SYSTEM MODIFICATIONS

In addition to changes in component characteristics, the effect of state-point changes in the mercury loop and other system changes on overall system performance was evaluated for application to EGS-4, -5, and -6. The Rankine-cycle efficiency and, therefore, the overall system efficiency increases with turbine pressure ratio increase. The purpose of this part of the study was to determine whether any worthwhile performance improvement could be realized by operating at new turbine inlet and exit pressures (but without changing the maximum system temperature of 1300°F nominal at the reactor outlet). A secondary and related purpose of the analysis was concerned with reducing radiator area by increasing effective radiating temperature. This was evaluated by calculating radiator area for different values of temperature drop through the radiator at several state-points. In summary, it was found that SNAP-8 performance could be improved by adjusting the turbine inlet pressure, but this is feasible only in conjunction with other improvements; i.e., component

modifications previously discussed. The state-points selected for use in EGS-4, -5, and -6 are compared with those used in EGS-0 as follows:

	<u>EGS-4, -5, -6</u>	<u>EGS-0</u>
Turbine inlet pressure, psia	350	240
Turbine exit pressure, psia	14.5	14.5
Radiator NaK ΔT , $^{\circ}F$	150	172

1. Scope of the Statepoint Analysis

The statepoint analysis comprised a series of steady-state computer runs in which turbine inlet and exit pressures and HRL radiator temperature drop were varied independently. Over 40 computer runs were made to show the effect of these variables on SNAP-8 system performance. Most of the runs were made with output power fixed at 40 kwe. However, a few runs were also made with input (reactor) power fixed at 600 kwt to determine whether the same state-points would be satisfactory at the higher power condition. Turbine inlet pressure was varied from 250 to 450 psia, exit pressure from 8.5 to 32.5 psia and HRL radiator ΔT from 100 to 200 $^{\circ}F$. Other considerations accounted for in the analysis regarding component characteristics are described in the following paragraphs.

a. Treatment of Turbine Efficiency

Since turbine efficiency is influenced by the pressure ratio across the turbine and since the pressure ratio varied from 8 to 53 over the range of pressures covered, it was necessary to develop a turbine efficiency/pressure ratio function for use in the analysis. At the higher pressure ratios, turbine efficiency is reduced as a result of reduced arc of admission in the first two stages and increased disk losses at higher stage pressures. The turbine efficiency characteristic developed for the statepoint analysis is shown in Figure 34. These values are also used in the system performance analysis for EGS-4, -5, and -6. Appendix C describes in detail the development of this relationship.

b. HRL Radiator Temperature Conditions

The temperature of the NaK entering the HRL radiator varies as the turbine exit pressure increases. At higher turbine exit pressures the condensing temperature is higher, corresponding to mercury saturation conditions. The temperature of the NaK leaving the condenser is related to the condensing temperature. For purposes of this analysis, a drop of 10°F between the mercury condensing temperature and the NaK temperature entering the radiator was assumed. Therefore, increasing the turbine exit pressure automatically increases the effective radiator temperature, thereby reducing radiator area. The relationship between turbine exit pressure and NaK temperature entering the radiator was as follows:

<u>Turbine Exit Pressure</u> psia	<u>Radiator Inlet Temperature</u> $^{\circ}\text{F}$
8.5	607
14.5	660
20.5	696
26.5	724
32.5	748

The temperature drop across the radiator was varied independently for each condition of turbine exit pressure to explore optimum radiator area for each exit pressure.

c. Other Component Characteristics Used in the State-point Analysis

(1) Lube/Coolant radiator temperature were held constant at 243°F in and 210°F out.

(2) Temperature leaving the reactor was maintained at 1330°F . The temperature entering the boiler is only one or two degrees less, allowing for a small heat loss from the pipe.

(3) The boiler pressure drop was defined by the following equation which was later used for EGS-4 and -5 as well:

$$\Delta P = 56 (\dot{W}_{\text{Hg}}/13,700)^{1.8} + 0.25 \Delta T_p$$

(4) The pinch-point temperature difference in the boiler was maintained at 75°F . This means that as turbine inlet pressure increased, mercury boiling pressure increased, and hence the mercury temperature in the boiler at the pinch-point. This, in turn, required an increase in the NaK temperature in the boiler at the pinch-point. Since the temperature entering the boiler was essentially constant, the temperature drop of NaK in the boiler then decreased, and the NaK flow rate increased in order to transfer the required heat rate. Hence the NaK flow rate in the primary loop was sensitive to the turbine inlet pressure and, in fact, limited the maximum turbine inlet pressure which could be considered.

(5) For the two NaK PMA's it was found necessary to "customize" the pumps and to reduce loop pressure drop in order to meet the wide variation in flow rates in the PNL and HRL. The NaK PMA characteristics used were very similar but not identical to those shown in Figure 21. Loop pressure drop data are discussed further in paragraph 2.b.(3), below.

d. In general, the systems characterized in the statepoint analysis approximate, but do not match precisely, the conditions that were later defined in characterizing EGS-4. However, the purpose of the analysis was not to characterize any particular system but to provide a basis for evaluating the effects of the selected independent variables.

2. Results of State-Point Analysis

a. Discussion of Results

The results of the state-point analysis are shown in Figures 35 and 36. Figure 35 shows the variation of reactor input power, total radiator area, parasitic load, Rankine-cycle efficiency, and overall system efficiency with turbine inlet pressure for a constant net output of 40 kwe, radiator NaK ΔT of 150°F , and L/C radiator ΔT of 33°F .

The total radiator area curves include both the HRL radiator and L/C radiator areas. The results indicate that minimum radiator area occurs at a turbine inlet pressure of 400 psia, the minimum radiator area is reached at a turbine exhaust pressure of 26.5 psia; however, exhaust pressures of 20.5 and 32.5 psia also result in very near the minimum total radiator area.

The curves of parasitic power in Figure 35 rise sharply as turbine inlet pressure increases above 400 psia. This is due to increasing power demand by the primary NaK PMA corresponding to increasing NaK flow rates. NaK flow must increase as turbine inlet pressure rises in order to maintain a 75°F pinch-point ΔT in the boiler. For example, at 350 psia turbine inlet pressure and 14.5 psia exit pressure, the primary NaK flow is 44,100 lb/hr; at 450 and 14.5 psia turbine pressures, the NaK flow is 68,400 lb/hr. This effect also is illustrated in Figure 31. Flow rates in the mercury loop and heat rejection loop are virtually unchanged over this same range of conditions. At the higher turbine exit pressures, the increase in parasitic power is more pronounced because flow rates in all loops are higher, reflecting lower overall efficiencies.

The Rankine-cycle efficiency curves are a direct result of the increased available energy due to the higher turbine pressure ratios. Overall system efficiencies tend to follow the trend in Rankine-cycle efficiencies until the parasitic load increases at the higher turbine inlet pressures causes a drop. For a turbine exhaust pressure of 14.5 psia, the overall system efficiency is nearly constant at turbine inlet pressures ranging from 350 to 450 psia.

Another independent parameter in determining system performance, and particularly the HRL radiator area, is the NaK ΔT in the radiator. Values of NaK ΔT considered were 100, 125, 150, and 175°F . Decreasing the NaK ΔT increases the average HRL radiator temperature and thus decreases its size. Figure 36 shows the effect of NaK radiator ΔT on total radiator area. Included in this curve is a line defining the region of NPSH difficulties. As the ΔT of the radiator decreases, the amount of subcooling of the mercury decreases which reduces the NPSH available at the MPMA. To avoid NPSH problems, it is necessary to operate at turbine exhaust pressures and NaK radiator ΔT values which are in the region below the marginal NPSH line.

The total radiator area appears to be a linear function of NaK radiator ΔT at constant turbine back pressure until NaK ΔT values of 125°F are reached. Below this value, the HRL NaK flow rates increase sufficiently to make the HRPMA pumping power requirements start increasing the mercury

flow rates to supply the necessary additional pumping power. This results in a leveling off of radiator area reduction for values of NaK radiator ΔT of 100°F or less.

For a turbine back pressure of 14.5 psia, the minimum radiator NaK ΔT is 150°F which is established by NPSH considerations. This results in a total radiator area of about 990 sq ft. For 20.5 and 26.5 psia turbine exhaust pressures, a reduction in total radiator area results from the higher radiator inlet temperatures and the NPSH limitation allows the radiator NaK ΔT to be reduced to 100°F . This combination results in a total radiator area of about 900 sq ft or a total reduction of about 9.1 percent.

b. Component Effects

(1) Mercury Pump NPSH

The NPSH requirement of the present MPMA limits the turbine exit pressure to 14.5 psia in zero gravity when the HRL radiator NaK ΔT is 150°F . The pump NPSH performance could be improved by modifying the jet pump design, probably enough to permit operation at 8.5 psia turbine exit pressure. However, to operate at this condition would require an increase in radiator area. This approach to system design might be of interest in some applications where radiator area is not a restraint.

(2) Turbine

At the selected state-point of 350 psia inlet and 14.5 psia exit pressure, the overall turbine pressure ratio is 24.2. This results in an average stage-pressure ratio of 2.22 which produces a nozzle exit Mach number of 1.06. For this Mach number it is considered feasible to retain the four-stage design with converging nozzles so that turbine overhang does not need to be increased to allow for nozzle divergence. Details of the turbine design parameters and the resulting turbine efficiency vs pressure ratio and number of turbine stages are given in Appendix C. It was concluded from this analysis that when the turbine is designed for the operating conditions selected, the turbine efficiency does not change greatly. It should be noted that each EGS

study assumed that the turbine flow areas were modified to accommodate the mercury flow rate defined by the system analysis. This is necessary to meet the pressures shown for the respective systems.

(3) NaK PMA Limits

(a) Primary Loop

The NaK flow rate and the primary NaK loop pressure drop determine the primary NaK-loop pumping requirements. In the state-point analysis, it was anticipated that the primary NaK loop ΔP would become very high as turbine inlet pressure increased. Consequently, this loop was modified to reduce its impedance. The NaK lines were enlarged to 2.25 in. OD, the boiler NaK tube was enlarged to 4 in. ID and the low ΔP advanced reactor was used. Even with these changes, the 5800-rpm SNAP-8 NaK PMA limited the turbine inlet pressures because of insufficient head rise. The turbine inlet pressures at which the NaK PMA became limiting is shown in Figure 35. This data applies to a system designed to produce 40 kwe net output power. It was estimated that at 600 kwt input power, the NaK PMA would limit the turbine inlet pressure to 270 psia with a 14.5 psia turbine exhaust pressure.

(b) Heat Rejection Loop

In this loop, the pump limit occurs at low rather than high turbine inlet pressure and at high values of exhaust pressure. This is true because the heat rejection requirements increase at the low turbine inlet pressures as system efficiency falls off. However, the HRL loop conditions are not as critical as those in the primary loop. The HRL PMA was not limiting at turbine pressure conditions of interest in the state-point study.

In summary, it becomes apparent that the state-point limits for the NaK PMA's are variable, depending on the loop design. When the limit is close to the desired state-point, a slight modification in component or piping pressure drop may be sufficient to permit the use of an existing NaK PMA.

c. Basis for Selection of New State-Points

The results sought from this analysis were twofold: an increase in overall efficiency and a reduction in total radiator area. An examination of Figure 35 shows that an increase in turbine inlet pressure (above the 240 psia used in EGS-0 through -3) is advantageous up to about 400 psia. Since the curves are relatively flat between 350 and 400 psia, and since the higher inlet pressure is less attractive at maximum power (EGS-6) conditions, a value of 350 psia was selected.

In choosing turbine exit pressure, Figure 35 shows that it is not possible to optimize for both overall efficiency and radiator area. However, there is no advantage in choosing an exit pressure above 20.5 psia. At the other end of the range, an exit pressure of 8.5 psia causes a rather large penalty in radiator area (~ 100 sq ft greater than 14.5 psia). This leaves a choice of exhaust pressures between 14.5 and 20.5 psia. Since there is only a four percent reduction in radiator area by going to 20.5 psia, 14.5 psia was selected because it results in a higher net power output for EGS-6.

The selection of the radiator ΔT was based on Figure 36. This figure shows that 150°F is the lowest ΔT value which could be selected at 14.5 psia turbine exit pressure without jeopardizing mercury pump suction pressure.

3. NaK PMA's Cooled by HRL NaK

Apart from the state-point analysis, another kind of system modification was made in order to reduce the L/C radiator area requirements. This modification consisted of using HRL NaK to cool the NaK PMA's in EGS-2 through -6. The amount of heat rejected by the NaK PMA's to the cooling circuit is estimated to be 46% of the electrical input. The net reduction of total radiator area (HRL + L/C) amounts to about 15 sq ft/kw transferred from the L/C radiator to the HRL radiator. The use of HRL NaK to cool these components is discussed in Section V,C,2.

The feasibility of cooling these components with liquid mercury also was investigated. Since the subcooled liquid mercury temperature is very near the condenser inlet NaK temperature this could be done. However, cooling of both NaK PMA's is required during startup and shutdown when mercury flow is not available. Therefore, this method of cooling the NaK PMA's was not used.

VI. PERFORMANCE OF IMPROVED SYSTEMS

This section of the report describes briefly the modifications incorporated in each of the six improved SNAP-8 systems and summarizes the impact of the modifications on system performance. The results of the analysis of each system are presented in a summary performance chart similar to that given in Figure 16 for the baseline system. It will be seen that each EGS incorporates a few changes from its predecessor; by this technique, the relative importance of the different modifications can be assessed. However, the net output power of the system increased to only 38.1 kw, a gain of 2.1 kw. It was still not possible to obtain the desired 40 kw net output because the system was limited by the alternator design limit of 90 kva. The gain in turbine efficiency is reflected in lower loop flow rates and in higher overall efficiency. These advantages result in slightly lower pumping losses, and in considerably lower HRL radiator area. Specific weight decreases from 306 to 243 lb/kwe as a consequence of the PCS component weight reductions, the lower radiator area, and a small increase in net output power.

In summary, some progress is seen in EGS-1 in improving weight, efficiency and radiator area. But it is clear that additional modifications are needed if the system is to be capable of any significant growth in output power.

A. EGS-1

EGS-1 incorporates only two improvements over EGS-0. The first is the replacement of the turbine with a new turbine of higher efficiency and adjusted flow areas that are compatible with the reduced mercury flow rate. The second is that it includes weight-reduced components which resulted from the weight reduction study made as part of this program. This system was analysed to determine the effect of these changes on system performance. The results of this analysis are summarized in Figure 37 which may be compared to the corresponding summary for EGS-0 that is shown in Figure 16. A detailed weight breakdown is presented in Appendix B.

The turbine modifications increased the aerodynamic efficiency to 64.4% from 57.0%. (The modifications are described in Section V,C, above.)

B. EGS-2

This system incorporates additional modifications whose purpose was to increase alternator efficiency, reduce parasitic loads, and reduce radiator area. The following changes from EGS-1 were made:

1. The effective alternator power factor was raised to 0.90 by means of capacitors. This effectively increases alternator efficiency from 0.86 to 0.89.
2. Both NaK PMA's were modified to operate at 4800 rpm using synchronous motors rather than at 5800 rpm with induction motors. This change reduces parasitic power by 3.6 kw. The synchronous motors afford a slight advantage in reducing the size of the capacitors for power factor correction. In the later systems they were abandoned in favor of lower speed induction motors which provide equivalent gain in reducing parasitic power.
3. The speed control design was changed from a magnetic-amplifier saturable reactor type to a silicon controlled rectifier (SCR) type. This substitution reduces parasitic power by 2.0 kw.
4. The boiler stability allowance to the PLR was reduced from 3 to 2 kw, thereby further reducing parasitic power by 1 kw.
5. The NaK PMA's were cooled by HRL NaK at 500°F. This modification reduces the radiator area by 39 sq ft by shifting 2.6 kw of heat from the low temperature radiator to the HRL radiator.

The effect of these modifications on overall system performance is seen by comparing the EGS-2 Summary Performance Chart, Figure 38, with the similar chart for EGS-1. The overall efficiency has increased from 8.2% to 9.6%. Loop flow rates and alternator kva are lowered so that there is no difficulty in reaching 40 kwe net output. Parasitic power is reduced 6.5 kw to 13.0 kw, indicating at least that much potential increase in net power over EGS-1. Radiator area is decreased by more than 200 sq ft. EGS weight drops 376 lb primarily due to reduction in radiator area. A detailed weight breakdown for EGS-2 is given in Appendix B.

Altogether EGS-2 shows significant improvement over the baseline SNAP-8 system in all performance aspects. Moreover, this improvement has been attained by relatively simple changes in components. The system, as calculated to yield 40 kwe net output, exhibits a potential for producing considerably greater power. This feature is evaluated as the next step in the study.

C. EGS-3

In this system, the power growth potential of SNAP-8 was evaluated. This was done by fixing the reactor input power at its maximum rating of 600 kw, and computing the net output power. EGS-3 incorporates the component improvements previously identified and used in the analysis of EGS-2. In addition, it was necessary to scale-up the flow areas of many of the components, since the flow rates in both of the NaK loops and in the mercury loop increase approximately in proportion to the reactor power. This kind of dimensional adjustment can be made without exceeding the limits of fundamental operating parameters, such as flow velocities, demonstrated by test. Changes of this type assumed in analyzing EGS-3 are outlined below:

1. The turbine flow passages were enlarged about 12% over the current SNAP-8 design. This degree of change requires an increase of nozzle and blade height of approximately 1/16 in., or for the first two stages an increase in the admission arc of from 38 to 43%.
2. The boiler flow passages for both mercury and NaK were enlarged by increasing the number of mercury tubes from 7 to 9 and by restoring the 4.0 in. ID of the NaK tube (It had been reduced to 3.25 in. in EGS-1 and -2).
3. The condenser was enlarged by increasing the number of mercury tubes from 73 to 85. The NaK shell was enlarged proportionately to accommodate the larger number of tubes.
4. The NaK PMA's operating at 5800 rpm, like those used in EGS-0, were required for this system. The loop pressure drops were too high to justify use of the lower-speed pumps incorporated in EGS-2.

5. The NaK loop piping was enlarged from 2.0 to 2.25 in.

The results of the EGS-3 analysis are given in the summary performance chart, Figure 39. The net output power has been increased to 60.1 kw at an overall efficiency of 10.0%. Efficiency increased slightly over that for EGS-2 because parasitic losses, though higher, do not increase in proportion to the gross turbine output. Although the system weight is increased over EGS-2, it is lower than that of the baseline system, and specific weight drops sharply to 166 lb/kwe. A detailed weight table is presented in Appendix B. Most important, the analysis shows that the output power of SNAP-8 can be nearly doubled by making a few cautious improvements and by scaling-up certain components of the baseline system. No change was made in the mercury PMA, the L/C PMA, and the NaK PMA's. The alternator also was unchanged although, at 85 kva, it is operating slightly above its design rating (83 kva).

D. EGS-4

This system evaluates additional component and system improvements at 40 kw output power. The most important feature of EGS-4 is an increase in turbine inlet pressure to 350 psia, reflecting the state-point analysis described in section V,D, above. This change was made to increase Rankine cycle efficiency. In one respect (the assumed turbine efficiency) EGS-4 is more conservative than the previously described systems. The turbine efficiency was pegged at 61%, as compared to 64.4% in EGS-1 and -2. This value reflects an adjustment downward due to higher turbine inlet pressure, as described in Appendix C, and a further correction based on a more cautious estimate of the improvement realizable with the design changes previously outlined. Other modifications characterizing EGS-4 are listed in the performance summary chart, Figure 40.

An examination of Figure 40 reveals that the performance of EGS-4 is somewhat better than that of EGS-2 despite a reduction in turbine efficiency. Overall efficiency is 10.3%, compared to 9.6% for EGS-2, due principally to the effect of higher turbine inlet pressure. Parasitic power is reduced about 0.7 kw due to removal of the motor scavenger pump in the mercury PMA. Radiator area and total weight are lower because of increased efficiency. A detailed weight breakdown is given in Appendix B.

E. EGS-5

This system incorporates all of the modifications evaluated in the study which were judged to be feasible. The performance computed for EGS-5, therefore, is considered to approach the ultimate performance potential of the SNAP-8 system at 40 kw net output. Specifically, EGS-5 differs from EGS-4 in the following respects: The turbine aerodynamic efficiency was increased in the primary and heat rejection NaK loops, and the NaK PMA's were sized to match reduced loop pressure drop and flow rates.

The turbine aerodynamic efficiency was increased to 62.5%. This value corresponds to the 64.4% used in EGS-1 and -2 after adjusting for 350 psia turbine inlet pressure (as described in Appendix C). In this manner, a better comparison with the earlier systems is obtained, and EGS-5 comes closer to representing optimum SNAP-8 performance. Turbine flow area was assumed to match the flow rate required for this turbine as determined by the system analysis at an inlet pressure of 350 psia.

In order to reduce the parasitic power required by the NaK PMA's, these components were "rubberized", i.e., sealed to match the pressure drop and flow rate required in each loop. Hydraulic impedance of the primary loop was greatly reduced in EGS-4 by using the advanced reactor, a modified mercury boiler, removing the PLR from this loop, and increasing the NaK piping size. Table 13 shows the NaK ΔP allowances made for the PNL and HRL in EGS-5 as a function of loop flow rate. The NaK PMA's are based on the same design concept as the SNAP-8 development NaK PMA's. Figure 21 shows the characteristics of the NaK PMA's custom designed for the respective NaK loop ΔP and flow rate.

The EGS-5 system described above was then analyzed to determine component operating conditions and system performance. Figure 41 is the resulting summary performance chart for this system based on a net power output of 40 kwe. Parasitic power is seen to be 10.7 kw, 9 kw lower than that of EGS-0. The overall efficiency of 10.9% represents a 55% increase over EGS-0.

The weight for this system is approximately 2300 lb lighter than EGS-0, and the radiator area is less than 900 sq ft. The weight saving is largely due to the change in PCS structural concept, use of weight-reduced components, and the reduced radiator size. Appendix B gives the detailed weight breakdown for EGS-5.

F. EGS-6

This system takes advantage of all of the improvements used in EGS-5. The system analysis was performed to establish the maximum net power output that could be obtained with a 600-kwt reactor input, and in that respect is comparable to EGS-3. The following paragraphs describe the design changes necessary to accommodate the higher loop flow rates which are the consequence of 600 kw input.

1. To reduce the parasitic power required by the NaK PMA's used in this EGS, the hydraulic impedance of both NaK loops was reduced as much as possible. In the primary NaK loop, the boiler NaK tube size, and the NaK pipe size were increased. In the HRL, the radiator NaK tubes were increased by 0.030 inches in diameter, the NaK piping was increased, and the condenser NaK flow area was increased. These changes were calculated to give the ΔP values listed in Table 13 at flow rates compatible with the EGS-6 power level. As in EGS-5, the NaK PMA's were assumed to be custom designed to match the loop pressure drop and flow rates required by the system.

2. The mercury boiler used in EGS-6 was increased in size to meet the increased NaK and mercury flows. The number of mercury tubes was increased from 7 to 9 and the NaK tube surrounding these tubes was increased to 4.55 in ID. With these changes, the boiler NaK-side ΔP was estimated to be 1.8 psi at 70,000 lb/hr flow rate.

3. The mercury condenser was enlarged by increasing the number of mercury tubes from 73 to 85 and increasing the NaK flow area to reduce the NaK ΔP in this component. The scaling of the number of tubes was made on the basis of constant mercury flow-rate per tube. The NaK flow area was increased to yield a pressure drop of 5 psi at 50,000 lb/hr flow rate.

The results of the EGS-6 performance analysis are presented in Figure 42. A net electrical output of 71.1 kwe is shown for this system at an overall system efficiency of 11.9%. The alternator gross output of 86.1 kva slightly exceeds the design rating of the present SNAP-8 design.

The weight breakdown for this system, given in Appendix B, shows that the weight of this system is about 1000 lb lighter than EGS-0. Also, the EGS-6 radiator area of 1440 sq ft is only 7 sq ft greater than that of EGS-0, while the net power output is 35.1 kwe greater. This demonstrates the advantages of the modifications made to the system as a result of this study.

VII. INTEGRATION OF THE SNAP-8 EGS WITH A TV SATELLITE: AN ILLUSTRATIVE APPLICATION STUDY

A. INTRODUCTION

The performance of improved SNAP-8 power systems having been evaluated, as described in the preceding sections of this report, it was of interest to study a typical application of the power system in an unmanned space mission. A direct-broadcast TV satellite in synchronous orbit was selected as the mission model, and the EGS-4 power system was chosen as the improved power system model. Mission and space vehicle data were not generated in the present study but were taken from available sources as cited herein. Design and performance data for the TV system and orbital station-keeping requirements were obtained primarily from Space-General Corporation, based on a study of unmanned applications of SNAP-8 conducted under NASA Contract NASw-1069 (Reference 11). Supplemental information on antenna and transmitter characteristics was obtained from TRW Systems and from EIMAC Division of Varian. The assistance of these organizations is gratefully acknowledged.

1. Scope

The purpose of this study is to define and examine the major power system/TV spacecraft interfaces and to project overall characteristics of a conceptual vehicle design. For this purpose, a conceptual design layout was developed to define the vehicle shape, component arrangement and weight distribution, and to identify major power system/payload interfaces. The configuration selected in the study is based on use of a Saturn-class launch vehicle (i.e., one using an S-IVB upper stage). The study does not aim to optimize the configuration, but simply to define a feasible arrangement. Thermal management of the power and TV systems were analyzed, interface problems identified, and characteristics of the major spacecraft subsystems are discussed. In concluding the study, power system redundancy and increased power output were examined briefly. The potential for increasing the operating life of SNAP-8 from 10,000 to 20,000 hours also was evaluated.

2. Application Study Guidelines

The general guidelines followed in developing the initial conceptual design are as follows:

Saturn-class launch vehicle with S-IVB upper stage.

Twenty-four hour equatorial orbit (22,300 mi altitude)

Unmanned vehicle.

10,000-hour continuous operating life.

No redundancy of power system or payload.

35 kwe net power to payload; 10 kw radiated by antenna.

Antenna inside shield-cone.

0.1° satellite pointing accuracy assumed.

Radiation levels in payload assumed the same as current

SNAP-8 417-1 Specification.

3. Overall Satellite Performance Summary

The findings of the study indicate that if one is willing to consider Saturn class launch vehicles, the use of the SNAP-8 kwe EGS (or probably any nuclear power system) with a TV satellite is feasible. The study indicates a total satellite launch weight of not more than 17,000 pounds would be attainable with a non-redundant power system. The overall height above the SIVB-payload interface is reasonable compared with the current Apollo-LEM assembly and other proposed nose-cone configurations. However, it should be noted that the impact of these surfaces and heights on the launch situation (aerodynamics, c.g., etc.) were not analyzed. The launch weight exceeds the capacity of the current Saturn IB launch vehicle, but is within the capability of various proposed upgraded IB versions. If one of these becomes available, the use of the Saturn V vehicle would be required. Such an eventuality would no doubt cause a considerable alteration of present TV satellite concepts. The satellite vehicle in earth orbit is illustrated diagrammatically in Figure 43. The general configuration

of the TV satellite conceived here and its relationship to the Saturn V launch vehicle is shown in Figure 44.

The broadcast area of the TV satellite could be extended significantly by increasing the available electrical power to 70 kw. This could be done by using EGS-6, as described in the preceding sections of this report. A weight increase of 3000 lb would result from the use of this system without redundancy.

4. Conclusions

a. SNAP-8 Integration

The application of SNAP-8 to an unmanned direct-broadcast TV satellite is feasible. No extraordinary interface or integration problems are evident. Payload equipment can be adequately protected from the thermal and radiation environment associated with the SNAP-8 system by thermal barriers and appropriate shielding to yield maximum reliability and life. Gyroscopic disturbing forces induced by rotating machinery and fluid loops are readily counterbalanced by discrete component orientation and pipe geometry that impose no undue constraint on the power system. The overall height of the satellite on the launch vehicle is reasonable.

b. Reliability, Redundancy and Increased Life

Reliability and life are related and important aspects of any SNAP-8 application. Both could be enhanced by employing redundancy of the power system and/or the TV system. The study shows that the weight increase associated with selective addition of redundant subsystems can be relatively small and well within the Saturn V payload capability. For example, to provide one redundant PCS and klystron transmitter would increase the basic vehicle weight from 17,000 to 22,000 lb. To extend operational life of the satellite to 20,000 hours requires the addition of approximately 2000 lb for the reactive thrust system, increasing gross vehicle weight to 24,000 lb. The mode of redundancy (i.e., whether active or standby) is a topic requiring further study.

c. Increase in Power Rating

The study shows that an increase in power rating would be desirable to increase TV coverage area of the vehicle. Coverage is approximately proportional to radiated beam power. The beam power could be increased by uprating SNAP-8 from 35 to 70 kw (using EGS-6 instead of EGS-4), or by using multiple SNAP-8 systems operating in parallel. The present payload capability of Saturn V permits the use of multiple SNAP-8 systems for this purpose within the height and radiator surface limitations of the launch vehicle.

d. Balancing of PCS Gyroscopic Moments

The study shows that the angular momentum of the rotating components and fluids of the PCS can be balanced so as to produce virtually zero net gyroscopic moment on the vehicle without undue constraint on the power system.

B. VEHICLE CONCEPTUAL DESIGN

1. Configuration and Location of Subsystems

Preliminary layouts of several vehicle arrangements were evaluated which covered the following tradeoffs: fore and aft location of the reactor and shield, retractable and fixed antenna, and length of vehicle vs cone angle. After consideration of these alternatives, the configuration and arrangement shown in Figure 44 was selected. An overall length of 59.3 ft was chosen to be compatible with the S-IVB stage, based on information contained in Reference 12, "The Saturn V Payload Planner's Guide. This length is only a little greater than the Apollo-LEM length of 53 ft and, when mounted on the Saturn V launch vehicle, is well below the height limit of the launch tower. The 34-ft diameter antenna is located as far from the reactor and shield as is feasible so as to minimize the shield cone angle while keeping the antenna within the shadow of the shield. The resultant cone angle of 35° was thereby established. The reason for shielding the antenna is to protect the solid-state electronic components, located just forward of the antenna, from scattered radiation. A detailed analysis of radiation dose levels might show that shielding of the antenna is unnecessary. In that event, the shield weight could be reduced, saving perhaps a few hundred pounds.

The radiators for rejecting heat from SNAP-8, and the TV system form the vehicle outer structural shell. The high-temperature (HRL) radiator occupies the conical surface of the vehicle. The SNAP-8 L/C radiator and the TV radiator are mounted on the cylindrical surface of the vehicle. This arrangement of the radiators minimizes thermal management problems by separating the high-temperature radiator and PCS components from the lower temperature L/C and TV radiator and the TV electrical components. A jettisonable adapter structure is required at the aft end of the vehicle to connect the radiator assembly with the S-IVB stage. In addition, jettisonable shrouds must be provided over the reactor and shield to protect them during launch, and over the radiators to prevent freezing of heat transfer fluids during injection into orbit. Additional features of the configuration and general arrangement are shown in the conceptual design layout, Figure 45, and are discussed below.

a. A collapsible parabolic antenna with an extended diameter of 34 ft is shown in the conceptual design. The 34-ft diameter was estimated as a representative size compatible with 10-kw of radiated power, a 2° beam width and good quality direct TV reception on one channel. The antenna is provided with petals which will fold within the 21-ft diameter vehicle envelope during launch. The surrounding structure is jettisoned at the parting surfaces shown, to permit deployment of the folded antenna.

b. All TV systems and electronic components are located in proximity to the transmitting antenna to minimize power losses and provide lowest radiation and temperature environment.

c. The station keeping and attitude control propellant tanks have been centrally located and as near to the center of mass as feasible. The twelve attitude control thrusters are shown mounted outside the radiator shell on a 24-ft diameter. Four station keeping thrusters are located so that they will thrust through the center of mass. The center of mass varies a negligible amount as propellant is consumed by the reactive thrust system.

d. The SNAP-8 PCS components are located within the forward conical section and partially surrounded by the HRL radiator. A thermal barrier isolates the HRL from other systems as shown in the conceptual design.

e. A total surface area of 840 sq ft in the conical section and 1050 sq ft in the cylindrical section is available as radiator surface. This amounts to 643 sq ft more than the estimated radiator area requirements. The vehicle surface is determined by the cone angle and length which were selected on the basis of payload radiation dose criteria. With the component arrangement shown, an additional volume of at least 5000 cu ft is available for additional payload.

f. The system tube-and-fin radiators are utilized as the main vehicle structure; circumferential "Z" rings and longitudinal streamers provide stiffening of the radiators against buckling. The structure needed to support the TV system utilizes the structural ring at the base of the cylindrical radiator shell. Structural support also is provided for propellant tankage in the conical section of the vehicle. A 260-in. diameter jettisonable structure adapts the vehicle radiator structure to the S-IVB stage. This section of structure surrounds the collapsed antenna and is jettisoned upon separation from the S-IVB stage.

2. Interfaces and Integration Features

Integration of SNAP-8 with other systems of an unmanned TV satellite was investigated to identify major considerations necessary in evolving the conceptual design of a vehicle. It is not the intent of this study to resolve all interface problems, rather to identify those of major importance, indicate their influence on system design and performance, and suggest potential areas for further study.

a. Thermal Environment

The high-temperature environment associated with SNAP-8 creates the necessity to thermally isolate electronic equipment, power conditioning equipment, low-temperature coolants (such as water and L/C fluid), as well as attitude control propellant, from the high temperatures of the SNAP-8 system. This is accomplished by providing a thermal barrier between the HRL radiator and the L/C radiator, and installing all of the major SNAP-8 hardware in the forward

conical section as shown in Figure 45. Thus, interchange of heat from the HRL to the L/C and TV radiators is minimized. Further, all other components except the L/C circuit, are located on the payload side of the thermal barrier so that they are not adversely affected by high-temperature radiator surfaces. Thermal insulation is employed on SNAP-8 components that operate at temperatures significantly different from the HRL radiator.

To withstand the low-temperature environment which will exist for several days during orbital transfer maneuvers, the vehicle is provided with a light-weight jettisonable shroud. In addition, propellant and coolant tanks are insulated to prevent freezing.

Rejection of waste heat from the TV power conditioning, receiving and transmitting equipment is accomplished by a cooling circuit, independent of the SNAP-8 cooling loops. The TV cooling circuit uses water as coolant, and includes a separate motor-driven pump and radiator. It has been assumed that of the 35 kwe supplied, 25 kw will be rejected to space by the water cooling loop. This implies a certain efficiency of the TV subsystem. If the TV subsystem is not this efficient, this cooling load would be higher. This will affect the size of the cooling system and the amount of pumping power required, but will not affect the overall integration problem being studied. The TV heat rejection requirements and characteristics are discussed in paragraph C,2,b.

b. Radiation Environment

The TV equipment and the LCS are located in the aft end of the vehicle where the total integrated radiation dose for 10,000 hours is:

Fast neutrons	10^{11} nvt
Gammas	10^6 rads

These radiation levels are those established for the SNAP-8 electrical components as set forth in Reference 13. The suitability of these levels for other equipment in the vehicle was not evaluated. The radiation shield is sized to limit the radiation dose to the levels indicated at the separation distance defined by the vehicle configuration. The TV antenna, when unfolded during operation, lies within the shadow of the shield in order to prevent radiation scatter which would increase the dose received by the electronic equipment.

If the above-noted radiation levels prove to be excessive, they can be reduced by increasing shield thickness at the expense of additional weight. A reduction in dose at the payload, in both neutrons and gamma radiation, of one order of magnitude would require approximately 1000 lb of additional shield weight. A reduction in dose of two orders of magnitude would require an additional 4000 lb of shield weight.

3. Weight Estimate

The weight estimate for the power system was taken from the weights developed for EGS-4. Those weights were adjusted for the increased shield cone angle and for reduced radiator area. The latter results from operation of the radiators in synchronous orbit with attendant reduction in the incident thermal radiation from the earth. The weight estimates for the TV system were obtained from the sources previously cited, in particular, Reference 11. The weights for the attitude control system were generated in the study as described in paragraph C,3 below. The gross launch weight of the vehicle was estimated at 17,000 lb for a nonredundant 35-kw power system and a 10,000-hour attitude control system. After jettisoning structure and shrouds, the flight weight of the vehicle is a little less than 15,000 lb. A summary weight breakdown for the vehicle is presented in Table 18.

Of launch vehicles now being developed, only Saturn V has the capability of placing this vehicle in synchronous orbit. The Saturn V payload capability in synchronous orbit is estimated to be 62,000 lb. The next largest available booster, Saturn IB, has a capability of only about 8000 lb.

If other launch vehicles, such as the Saturn IB, were upgraded to increase payload capability, satellite launch weight may become a significant constraint. If this were the case, there are several possibilities for reducing launch weight by detailed weight optimization studies. To mention a few examples:

- a. A low-freezing-point heat rejection fluid, such as sodium-potassium-cesium alloy might permit elimination of the shroud over the radiators.

b. Shield weight might be reduced by reducing the shadow cone angle if analysis showed radiation scatter from the antenna to be negligible.

c. Radiator weight could be reduced by increasing radiator area as indicated in Section III,C,3 of this report.

d. The reaction control system weight might be optimized by selecting higher performance propellants or by allowing the vehicle to drift out-of-plane and compensating for the drift by attitude control corrections. (Attitude control adjustments generally require less propellant than station-keeping maneuvers.)

Optimization studies like these are beyond the scope of the present study, but there is no question that significant weight savings could be realized if launch weight were the major criterion for vehicle design for a particular mission.

C. SUBSYSTEM CHARACTERISTICS

1. SNAP-8 EGS

The power system performance characteristics used in the vehicle integration study were taken from the data for EGS-4 which are presented in Section VI,D of this report. Power output ratings of EGS-4 conform to the requirements of the SNAP-8 development program as set forth in Reference 13. Of primary concern in the application study are the power ratings of 35 kwe output; 120/208 volts, ac, at 400 cps; and 0.85 power factor at the payload. Radiator areas have been adjusted downward to account for the very low incident thermal radiation from earth in a 22,300 mile orbit. Weight of the power system was revised to account for a larger shield, and lower radiator areas. A summary of SNAP-8 performance and specification data applicable to the TV vehicle study are given in Table 19.

2. TV Subsystem

a. Transmitter and Receiver

Characteristic design and performance data for the TV system was taken from the study performed by Space-General Corporation (Reference 11). This source information indicated that with 35 kw available power a parabolic antenna of approximately 34 ft in diameter was required to provide good quality direct TV reception on one channel over an area of up to one-half million square miles. Hence, this antenna size was taken as sufficiently representative for the purposes of this study. An antenna this size must be collapsible to fit within the vehicle envelope during launch. The outer seven feet of radius of the antenna is made up of petals which can fold upon each other in a manner similar to the photoflash reflector of some cameras. Devices of this type have been built and tested up to 32 ft in diameter for solar collectors.

For this study, use of a magnetically-focused klystron transmitter-amplifier was assumed. Typically, this type of transmitter, rated at 10 kw rf output would weigh about 280 lb, would have an efficiency of 33%, and would require active cooling to carry off waste heat. A water cooling system for the klystron was assumed.

Design and selection of the TV receiver, receiver antenna and associated equipment, appear to fall well within present state-of-the-art hardware and presents no significant problems. For this reason, the specific details of the receiver circuitry have not been investigated. The receiving antenna as shown in Figure 45 is mounted on the parabolic reflector of the transmitting antenna to permit full view of earth transmitting stations over a wide area outside of the TV broadcast area.

b. Power Conditioning and Heat Rejection

Typical distribution of the power supplied to the TV system is shown in Figure 46. Approximately 83 percent of the 35 kw is transformed to 12,500 volts for the beam circuit of the klystron transmitter. In

addition, the klystron requires 33 volt dc power for the focusing magnet and 5.5 volt ac power for the cathode heater. A diagram of a typical power conditioning system showing a suggested circuitry for the high-voltage conversion is shown in Figure 47. Overall efficiency of the high-voltage power conditioning system was established at 87 per cent, based on individual component efficiencies shown in Figure 47.

It was necessary to examine the requirements for cooling the TV system in order to evaluate possible interfaces with the power system and to complete the conceptual design of the vehicle. Of the 35 kw supplied by the SNAP-8 EGS, about 70% must be rejected to space. The major cooling loads are the power conditioner and the klystron transmitter. The power conditioner operates with an efficiency of 87% on virtually all of the 35 kw supplied; this means that 13% of the power, or 4.5 kw must be removed by a cooling circuit at temperatures not exceeding 200°F. The klystron tube receives 29.8 kw from the power conditioner and operates at an estimated efficiency of 33%; therefore, it must be cooled at the rate of 19.8 kw. Indications are that the klystron tube can stand somewhat higher temperatures than the solid-state electronic components. For this study, a maximum coolant temperature of 270°F for the klystron tube was used after checking with various sources of information. The remainder of the payload equipment shown in the block diagram, Figure 46, requires cooling of approximately 400 watts at a maximum temperature of 200°F.

Various alternative schemes for cooling the TV system were briefly considered, such as integration with the SNAP-8 L/C loop, and passive cooling of some of the smaller components. In the end, no significant advantage in radiator area or in pumping power could be found in these alternatives over a separate active cooling circuit for the TV system. It was convenient, however, to cool the SNAP-8 low-temperature control assembly (LCA) by means of the TV cooling circuit, since the environmental requirements and the environmental requirements and locations of the LCA are nearly identical to those of the payload components.

The TV system cooling circuit, shown schematically in Figure 48, uses water as the coolant and has a separate motor-driven pump. Selection of water as the coolant was primarily based on available information on the klystron transmitter, which indicated that water is compatible where other fluids may or may not be. Operation of the klystron at temperatures higher than the other electronic systems permits some reduction in overall radiator area. To take advantage of this, parallel radiator circuits are used as shown in the diagram. The total radiator area required for the water loop is 370 sq ft.

3. Station Keeping and Attitude Control

a. General Requirements

Station keeping and attitude control requirements were based on the Space-General Corporation report, Reference 11. Translational corrections of the vehicle are necessary to compensate for injection errors and sun-moon gravitational effects. The largest factor to be accounted for is an out-of-plane correction based on a $1^\circ/\text{yr}$ inclination due to the sun-moon gravitational effects. A value of 240,000 lb-sec total impulse was estimated to be required for station keeping for 10,000 hours.

Concerning attitude control, the use of gravity-gradient torque to maintain orientation with the earth was considered. This method has been successfully employed for some satellites; e.g., MIDAS. It was calculated that for a 15,000 lb vehicle, 50-ft long, in a synchronous orbit, the gravity-gradient torques resulting from a 0.1 degree misalignment is about 10^{-7} ft-lb; this magnitude is insignificant. In Reference 11, it was concluded that to maintain the vehicle completely immobile with respect to the earth would be impractical. The attitude of the vehicle can be controlled by applying corrective thrust in any of 3 axes whenever the vehicle reaches the allowable limit of attitude error. In this manner, the thrust forces applied in short bursts produce controlled oscillation of the satellite. The total impulse required for attitude control was estimated at 8600 lb-sec based on vehicle moments of inertia of 9×10^4 lb-sec-ft² about the lateral axis and 9×10^3 about the longitudinal axis.

b. Selection of Thrust System and Propellant

After various propulsion devices were examined briefly, a monopropellant hydrazine system was selected for use in this study. The hydrazine (N_2H_4) requirements for 10,000 hours of operation were estimated as follows:

	<u>Total Impulse</u> <u>(lb-sec)</u>	<u>Propellant Weight</u> <u>(lb)</u>
Station Keeping	240,000	1100
Attitude Control	8,600	39

A twelve-thruster attitude control system and a four-thruster station keeping system are shown schematically in Figure 49. The attitude control thrusters operate in pairs on a 24-ft diameter to apply a turning moment to the vehicle. Each thruster produces 0.5 lb thrust and must operate for 0.02 sec every 20 minutes to maintain the vehicle within 0.1 degree of the nominal attitude. The four station-keeping thrusters impart translational motion to the vehicle and, therefore, must thrust through the vehicle center of mass. These thrusters produce a 20-lb thrust force to impart velocity changes to correct "in-plane" and "out-of-plane" drift. Typical design data for the reactive thrust system are summarized in Table 20.

Prior to selecting monopropellant hydrazine for the reactive thrust system, a number of other chemical and heated-gas systems were considered. N_2H_4 was about 400 lb heavier than a bi-propellant $N_2O_4 - N_2H_4$ system but was chosen because it is simpler and presumably more reliable.

Other types of propulsion systems also were examined briefly. Plasma, arc jet and resistojet thrusters are attractive in that they operate at higher specific impulse. However, for good performance they must operate at temperatures above $3500^{\circ}F$ and require storage of hydrogen or other cryogenic fluids. Because of the reliability implications of high-temperature operation and cryogenic storage, these propulsion methods were discarded in the current study.

c. Internal and External Disturbances

Internal and external disturbances may cause satellite drift or rotation. One possible source of disturbance is the angular momentum of the SNAP-8 rotating machinery and fluids. The largest single component tending to produce a disturbing torque on the vehicle is the TAA which has an angular momentum of 89 ft-lb-sec. This angular momentum will produce a disturbing torque of 0.0065 ft-lb on the vehicle as a result of precession at the rate of 1 revolution every 24 hours. This moment will cause the vehicle to rotate 0.1 degree in approximately 4.5 minutes. Approximately 100 lb of mono-propellant N_2H_4 , operating continuously, would be required to compensate for this torque. The possibility of countering this effect was examined.

The angular momentum of all other rotating components and the boiler were estimated as follows:

PN PMA	2.9
HR PMA	2.9
MPMA	2.1
L/C PMA	0.2
Boiler	<u>7.7</u>
Total	15.8 ft-lb-sec

In the conceptual design layout, Figure 45, these components and the TAA were mounted with their axis of rotation parallel to the longitudinal axis of the vehicle in such a way as to counteract the angular moment of the TAA. A net unbalanced angular momentum of 73 ft-lb-sec resulted. It was determined that this unbalanced force could be nullified by routing the primary NaK piping through two 9-ft diameter turns. The angular momentum of other fluid loops is easily balanced without undue constraint on pipe routing.

The unbalanced torques produced during startup of SNAP-8 also were examined. As the worst case, the disturbances caused by acceleration of the TAA during starting with no counter-balancing forces was determined.

This disturbing torque was found to cause an angular velocity of the vehicle of 0.1 rpm which requires a negligible amount of propellant for correction of vehicle position.

Micrometeoroid impingement disturbances on the vehicle also were estimated. Considering the largest particle which radiator armor is designed to protect against, a momentum of 5.8×10^{-3} lb-sec was calculated. This requires an equal thrust impulse to counteract, and is seen to be negligible. A relatively large meteoroid of ten grams mass would have a momentum of 45 lb-sec. This would require about 0.2 lb of propellant to counteract.

D. POWER INCREASE AND REDUNDANCY

Since the Saturn V booster has the capability of lifting much more than 17,000 lb, it is of interest to examine the advantage that increased launch weight might offer in vehicle performance, life, and reliability. Vehicle performance (i.e., broadcast area and quality) could be enhanced by increasing available power. SNAP-8 power output can be essentially doubled by using EGS-6 instead of EGS-4, with a relatively small weight increase. Redundancy can be used to increase reliability, or life (or both, if more than one redundant system is employed). Another approach to increasing life of the SNAP-8 EGS is discussed in paragraph E, below. Table 21 summarizes the effect of power increase and redundancy on vehicle size, weight, and performance. In general, the table indicates that a large potential for growth exists within the capability of Saturn V. Redundancy concepts, vehicle weight and configuration trade-offs, overall reliability, and operating life warrant much more study in the context of a direct-broadcast TV satellite mission.

E. POTENTIAL OF SNAP-8 EGS FOR 20,000-HOUR OPERATING LIFE

The importance of increased operating life for space power systems has been stressed in numerous mission studies concerning SNAP-8 and other power systems for both manned and unmanned missions. The present SNAP-8 design life

is a minimum of 10,000 hours. An assessment of the potential for SNAP-8 for increased life, from 10,000 to 20,000 hours, was established as one of the objectives of the present study. This increase by a factor of two was selected on the basis that it was consistent with trends in planning of long duration missions. The present study attempts to identify the most probable life-limiting factors of the power system. The assessment is necessarily qualitative because failure modes for most of the components have not yet been identified by continuing development tests.

1. Assessment of Possible Failure Modes

To assess the potential for extended life of SNAP-8, possible wearout failure modes of the components of the PCS were examined to identify those characteristics which are life-limiting. In the following paragraphs, the components judged to be subject to wearout failure in less than 20,000 hours are discussed.

- a. Boiler

Based on present developmental experience with mercury boilers, the most likely failure mode of this component is by corrosion of the mercury containment tubes. Mercury corrosion of boiler tubes has been experienced to date. The reference boiler tube material has been 9Cr-1Mo steel. A program is now in progress to develop boiler fabrication techniques using tantalum as the mercury containment material. It has been known that tantalum (and other refractory metals) has far lower solubilities in mercury than 9Cr-1Mo. When the new boiler design and fabrication procedures have been determined, it is expected that refractory, or refractory-lined boiler tubes will be more than sufficient to meet the 10,000-hour life requirement. Therefore, to extend life to 20,000 hours should involve a relatively small, if any, additional impact on the SNAP-8 system. Since the refractory metals have much higher density than ordinary steels, an increase in metal thickness to extend life from 10,000

to 20,000 hours would probably involve some weight penalty. A maximum weight increase of 100 lb was estimated.

b. Condenser

The SNAP-8 condenser is subject to the same sort of attack by mercury but to a lesser degree than the boiler. To date, condenser corrosion has not been found to be a problem. Should subsequent testing show that the condenser mean-time-to-failure is less than 20,000 hours, the probable solution to the problem would be to change the material to a refractory metal. To accomplish this a maximum weight increase of 30 lb was estimated.

c. Rolling Contact Bearings

Precision ball bearings lubricated by polyphenyl ether (MIX-4P3E) are used in the TAA and in the MPMA. Analysis has indicated that the fatigue life of these bearings is well in excess of 20,000 hours. Wear-out failures of the bearings in less than 20,000 hours may be experienced. If, and when, such failures are identified, the probable solutions to the problem are:

(1) Reduce bearing load. To reduce bearing load, it is necessary to invest some weight in redesign of components to accommodate larger bearing sizes. A weight penalty of up to 100 lb is estimated for this solution.

(2) Select a better lubricant. To improve the lubricant, an experimental program is necessary to assure that a potentially better lubricant, such as high-grade mineral oil, has the capability to withstand the radiation and temperature environment of SNAP-8. If the use of mineral oil was found unsatisfactory due to the radiation environment, it might involve a weight penalty to provide additional shielding for the lubricant. At this point even a rough estimate of penalties which must be imposed on the PCS is not possible.

d. Dynamic Seals

Cavitation erosion has been experienced in the turbine dynamic seal which limits to very low values the rate of leakage of mercury to space. Cavitation damage to the visco pump element was observed after about 800 hours of testing. This problem was subsequently resolved by choice of a harder material and dimensional changes which stabilize the mercury vapor-liquid interface within the seal assembly. Subsequent testing has shown that these changes have corrected the immediate problem.

A similar type of failure might occur in attempting to extend life to 20,000 hours. The experience cited above is typical of the method usually employed to resolve life-limiting design problems, and indicates such problems are susceptible to straightforward engineering solutions.

e. Alternator and Motor Windings

Although no failures have been identified to date, there is a possibility that the organic insulation protecting the windings of the alternator and the mercury pump motor might deteriorate after long periods of operation. If this should occur, the most probable solution would be to change the insulation material, perhaps to use an inorganic material like that used in the NaK pump motor. A small weight increase might be associated with this type of modification.

f. Batteries

Battery life under SNAP-8 environmental conditions is not precisely known. Long battery life may or may not be needed for unmanned applications but for manned applications, where restart is required, the battery must last as long as the rest of the power system. One possible solution for a battery failure is a controlled environment which will protect the battery from temperatures above 100°F. This solution may involve a penalty of one or two kw for refrigeration. A second possible solution is derating of the battery. Assuming that the battery does not completely fail but produces

less than the required power, the addition of more batteries at lower power density would provide the necessary power. This solution might entail a weight penalty of 150 lb for an unmanned mission; greater weight penalty would be associated with a manned mission. A third possible solution is development of a new battery which will withstand the environment. This latter would not penalize SNAP-8 performance or weight. Since much effort currently is being devoted to development of new kinds of batteries this solution for the 1970 decade is not unlikely.

2. Failure Modes Considered to Have Greater Than 20,000 Hour Life

The following types of failures were not listed as life-limiting in paragraph 1 above because they are not expected to cause system shutdown or excessive performance degradation in 20,000 hours of operation.

a. Turbine blade erosion. Stationary power plant experience with mercury turbines operating under more severe conditions for longer periods, indicates that the SNAP-8 turbine should not sustain significant blade erosion in 20,000 hours.

b. Pump impeller cavitation. No cavitation damage to mercury or NaK pump impellers or to the mercury jet-pump nozzle has been observed in several thousand hours of testing. If some cavitation damage does occur, it is not expected to cause system shutdown although it could cause system performance degradation.

REFERENCES

1. "SNAP-8 Progress Report for August - October 1965," Atomics International Report No. NAA-SR-11692, dated 29 December 1965.
2. C. J. Daye, "SNAP-8 Performance Potential Study, midterm topical report to NASA Lewis Research Center - SNAP-8 Project Office, Aerojet Report No. 3173, dated March 1966.
3. "SNAP-8 Electrical Generating System Development Program Progress Report for July - September 1966," Aerojet Report No. 3297, dated November 1966.
4. "SNAP-8 Nuclear Systems for Unmanned and Manned Applications," Atomics International Report No. NAA-SR-10859, dated 15 May 1965.
5. "Specifications for SNAP-8 Meteoroid Protection for Space Systems," Specification No. 417-5 Revision A, NASA Lewis Research Center, dated 25 May 1964.
6. "Specifications for SNAP-8 Meteoroid Protection for Space Systems," Specification No. 417-2 Revision A, NASA Lewis Research Center, dated 25 May 1964.
7. A. B. Burgess (Aerojet-General Nucleonics), "SCAN, A Computer Code for SNAP-8 System Analysis with Influence Coefficient Calculation Option," Technical Memorandum No. 4921:66-375, dated 8 November 1966.
8. R. L. Lessley, "Weight Reduction of SNAP-8 Boiler (Phase A-II of Performance Potential Program)," Aerojet-General Technical Memorandum No. 4921:66-392, dated 22 February 1966.
9. M. G. Cherry, "SNAP-8 Turbine Performance Potential Study, Steps I and II," Aerojet-General Technical Memorandum No. 4932:66-432, dated 27 July 1966.
10. M. G. Cherry, "Design Calculations for the Improved Performance SNAP-8 Turbine," Aerojet-General Technical Memorandum No. 4932:66-437, dated 19 August 1966.
11. "SNAP-8 Unmanned Applications Study," NASA Contract NASw-1069 by Space Operations Division of Space-General Corporation, Report No. SGC 778FR-1, dated February 1965.
12. L. O. Shute, "SATURN V Payload Planners Guide," Missile and Space Systems Division, Douglas Aircraft Co., Inc., Report No. SM-47274, dated November 1965.
13. "Specifications for SNAP-8 Meteoroid Protection for Space Systems," Specification No. 417-1 Revision A, NASA Lewis Research Center, dated 25 May 1964.

TABLE 1
SUMMARY DESCRIPTION OF SYSTEMS STUDIES

	Baseline <u>EGS-0</u>	<u>EGS-1</u>	<u>EGS-2</u>	<u>Improved</u>			
				<u>EGS-3</u>	<u>EGS-4</u>	<u>EGS-5</u>	<u>EGS-6</u>
Output Power	36	38	40	Max*	40	40	Max*
Turbine Aerodynamic Efficiency	57	64.4	64.4	64.4	61	62.5	62.5
PCS Weight Reduced		X	X	X	X	X	X
Power Factor Corrected			X	X	X	X	X
Solid State Speed Control			X	X	X	X	X
500°F NaK PMA Cooling			X	X	X	X	X
HRL Radiator Outlet Temperature Increased					X	X	X
Turbine Inlet Pressure Increased					X	X	X
Hg PMA Scavenger Removed					X	X	X
"Advanced" Reactor					X	X	X
NaK Loop Impedance Reduced						X	X

* With 600 kwt reactor input.

TABLE 2

COMPARATIVE PERFORMANCE SUMMARY

	<u>EGS-0</u>	<u>-1</u>	<u>-2</u>	<u>-3</u>	<u>-4</u>	<u>-5</u>	<u>-6</u>
Net Reactor Input (kwt)	512	467	419	600	387	368	600
Net Elect. Output (kwe)	36.0	38.1	40.0	60.1	40.0	40.0	71.1
Overall Efficiency (%)	7.0	8.2	9.6	10.0	10.3	10.9	11.9
Weight (lb)	11000	9270	8900	9970	8770	8700	9960
Specific Weight (lb/kwe)	306	243	222	166	219	217	140
Radiator Area (ft ²)	1433	1308	1079	1541	935	888	1440
Specific Rad. Area (ft ² /kwe)	39.8	34.4	27.0	25.7	23.4	22.2	20.2

TABLE 3

EGS WEIGHT SUMMARY

		Wet Weight (lb)						
		<u>EGS-0</u>	<u>-1</u>	<u>-2</u>	<u>-3</u>	<u>-4</u>	<u>-5</u>	<u>-6</u>
Reactor and Shield		2340	2300	2270	2390	2233	2228	2358
Power Conversion System		6226	4624	4540	4876	4642	4641	5013
Radiator Assembly		<u>2436</u>	<u>2348</u>	<u>2086</u>	<u>2707</u>	<u>1892</u>	<u>1830</u>	<u>2588</u>
Total		11,002	9272	8896	9973	8767	8699	9959

	Inventory Weight (lb)						
	<u>EGS-0</u>	<u>-1</u>	<u>-2</u>	<u>-3</u>	<u>-4</u>	<u>-5</u>	<u>-6</u>
Sodium-Potassium	502	437	430	541	475	471	610
Mercury	189	189	189	205	189	189	205
Polyphenyl Ether	123	123	115	127	114	114	127
	<u> </u>	<u> </u>	<u> </u>	<u> </u>	<u> </u>	<u> </u>	<u> </u>
Total	814	749	734	873	778	774	942

TABLE 4

ASSESSMENT OF 20,000-HOUR LIFE-LIMITING COMPONENTS

<u>Component</u>	<u>Possible Failure Mode</u>	<u>Probable Solution</u>	<u>Estimated Effect</u>
Boiler	Corrosion by Hg	Material change to Ta	+ 100 lb
Condenser	Corrosion by Hg	Material change to Ta	+ 30 lb
Bearings TAA (MPMA)	Ball bearing wear	1. Reduced bearing load 2. Better lubricant	+ 100 lb
Dynamic Seals	Cavitation erosion	1. Material change 2. Configuration change	--
Alternator and Motor Windings	Insulation breakdown	Material change	
Battery	Chemical breakdown	1. Environmental control (temp.) 2. Derating 3. Battery development	1-2 kw power loss + 150 lb

TABLE 5

ADVANCED REACTOR CHARACTERISTICS

Lengths (in.):	Inlet Plenum	3.50
	Lower Grid	0.65
	Fuel Elements	17.37
	Upper Grid	0.85
	Outlet Plenum	1.50
Diameters (in.):	Forward Plane of Upper Grid	21.1
	Mid-Plane of Reactor	24.4
	Plane 1 in. Forward of Forward Plane of Lower Grid Plate	27.6
	Core	9.2
Minimum Coolant Temperature Drop (°F):		100
Pressure Drop (at 600 kw, 13.6 lb/sec NaK Flow):		
	<u>With Above Diameters</u>	<u>With 0.87 in. Added to Above Diameters</u>
Core Pressure Drop (psi)	4.8	0.8
Inlet-to-Outlet Pressure Drop, AGC Connections (psi)	6.5	2.5

NOTES:

- (1) Diameters include 1/2 in. radial clearance when drums are in the outward position.
- (2) The reactor assembly tapers outward from the 21.1 in. dia to the 27.6 in. dia, and then tapers back inwards to the shield interface.
- (3) The actuator drive extends approximately 10 in. beyond the outlet plenum. It is totally contained within the reactor cone angle.
- (4) The weight of the advanced reactor corresponding to the 632 lb listed in the PP Phase A-II weight compilation is 600 lb.

TABLE 6

SUMMARY OF VAPOR-CHAMBER FIN RADIATOR DESIGN DATA

Input: heat rejected 377 kw
 NaK ΔT 660°F - 488°F
 armor ratio 0.25
 vapor chamber survival ratio 0.90
 surface emissivity 0.90

cylindrical radiator, radiating outside only - diameter 9 feet

No.	Number of Tubes	Outer Surface Area, One Chamber (in. ²)	Total No. of Chambers	Tube ID (in.)	Radiator Length (ft)	Radiator Area (ft ²)	Radiator ^{1,2} Weight (lb)
1	150	80	1225	.181	27.9	788	1766
2	150	40	2447	.181	27.8	785	1653
3	125	80	1257	.194	28.0	790	1666
4	125	40	2514	.194	28.0	790	1553
5	100	80	1295	.211	28.2	796	1572
6	100	40	2587	.211	28.2	796	1457
7	80	80	1330	.230	28.5	804	1500
8	80	40	2656	.230	28.5	804	1381
9	50	80	1400	.276	29.2	825	1403
10	50	40	2800	.276	29.2	825	1289

1. Weight includes tubes and armor, fins, headers, ducts, and armor, and also includes the fluid inventory (NaK).
2. 400-500 lb of stiffening structure is required with the tube and fin to support the PCS, and the reactor-shield combination. The vapor chamber fin radiator may require less additional structure due to its better structural rigidity.

TABLE 7

HRL RADIATOR DESIGN PARAMETERS

for cone half-angle of 9.75 degrees, thermal emissivity of 0.9, solar absorbtivity of 0.4

	EGS-0	EGS-1	EGS-2	EGS-3	EGS-4	EGS-5	EGS-6
Heat Rejection (kw)	439	392	352	507	322	304	499
Flow Rate (lb/hr)	41,100	36,700	33,000	47,400	34,600	32,600	53,600
Inlet Temperature (°F)	660	660	660	660	660	660	660
Exit Temperature (°F)	488	488	488	488	510	510	510
Area (ft ²)	1071	946	842	1257	727	682	1173
Dry Weight (lb)	1099	993	904	1251	802	762	1183
Inventory (lb)	110	102	96	122	88	85	115
Wet Weight (lb)	1209	1095	1000	1373	890	847	1298
ΔP (psi)	13.5	10.2	7.9	19.2	7.8	6.7	22.9
Ft^2/kw	2.44	2.41	2.39	2.48	2.26	2.24	2.35
Number of Tubes	125	125	125	125	125	125	125
Tube Diameter, OD (in.)	.250	.250	.250	.250	.250	.250	.250
Tube Wall (in.)	.020	.020	.020	.020	.020	.020	.020
Fin Thickness (in.)	.030	.030	.030	.030	.030	.030	.030
Manifold Dia. (OD) Max. (in.)	2	2	2	2	2	2	2
Manifold Wall (in.)	.035	.035	.035	.035	.035	.035	.035
Armor Thickness (in.)	.171	.170	.168	.173	.167	.166	.172
Radiator Slant Height (in.)	400	369	342	443	310	297	424
Radiator Diameter (ft)							
Small End	4.6	4.6	4.6	4.6	4.6	4.6	4.6
Large End	15.9	15.1	14.3	17.1	13.3	13.0	16.6
Axial Length (ft)	32.9	30.3	28.1	36.4	25.4	24.4	34.8

Report No. 3386

TABLE 8

HRL RADIATOR WEIGHT BREAKDOWN

	<u>EGS-0</u>	<u>EGS-1</u>	<u>EGS-2</u>	<u>EGS-3</u>	<u>EGS-4</u>	<u>EGS-5</u>	<u>EGS-6</u>
Heat Rejection (kw)	439	392	352	506	322	304	499
Tube Weight	202	187	173	224	157	150	215
Tube Armor	401	366	335	451	300	287	429
Fins	442	390	347	518	300	281	484
Inlet Manifold	8	8	8	8	8	8	8
Inlet Manifold Armor	2	2	2	2	2	2	2
Exit Manifold	36	33	32	39	29	28	37
Exit Manifold Armor	8	7	7	9	6	6	8
Total Dry Weight (lb)	1099	993	904	1251	802	762	1183
Tube Inventory	50	46	43	56	39	37	53
Inlet Manifold Inventory	9	9	9	9	9	9	9
Exit Manifold Inventory	51	47	44	57	40	39	53
Total Inventory (lb)	110	102	96	122	88	85	115
Total Wet Weight (lb)	1209	1095	1000	1373	890	847	1298

TABLE 9

I/C RADIATOR DESIGN PARAMETERS

for cone half-angle of 9.75 degrees, thermal emissivity of 0.9, solar absorptivity of 0.4

	<u>EGS-0</u>	<u>EGS-1</u>	<u>EGS-2</u>	<u>EGS-3</u>	<u>EGS-4</u>	<u>EGS-5</u>	<u>EGS-6</u>
Heat Rejection (kw)	21.2	21.2	13.9	16.1	12.2	12.1	15.0
Flow Rate (lb/hr)	6090	6110	4000	4630	3510	3480	4320
Inlet Temperature, (°F)	243	243	243	243	243	243	243
Exit Temperature, (°F)	210	210	210	210	210	210	210
Area, (ft ²)	362	362	237	284	208	206	267
Dry Weight, (lb)	281	281	202	230	183	182	218
Inventory, (lb)	56	56	50	60	50	50	60
Wet Weight (lb)	337	337	252	290	233	232	278
ΔP , (psi)	8.8	8.8	4.0	5.7	3.5	3.5	4.9
Ft ² /kw	17.1	17.1	17.1	17.6	17.0	17.0	17.8
Number of Tubes	120	120	120	120	120	120	120
Tube Diameter (OD), (in.)	.187	.187	.187	.187	.187	.187	.187
Tube Wall, (in.)	.020	.020	.020	.020	.020	.020	.020
Fin Thickness, (in.)	.030	.030	.030	.030	.030	.030	.030
Manifold Dia. (OD) Max., (in.)	1.50	1.50	1.50	1.50	1.50	1.50	1.50
Manifold Wall, (in.)	.035	.035	.035	.035	.035	.035	.035
Armor Thickness (in.)	.141	.141	.140	.141	.140	.140	.141
Radiator Diameter (ft)							
Small End	15.9	15.1	14.3	17.1	13.3	13.0	16.6
Large End	18.1	17.4	15.9	18.7	14.9	14.6	18.2
Axial Length, (ft)	6.7	7.0	4.9	5.0	4.6	4.7	4.8

TABLE 10
L/C RADIATOR WEIGHT BREAKDOWN

	<u>EGS-0</u>	<u>EGS-1</u>	<u>EGS-2</u>	<u>EGS-3</u>	<u>EGS-4</u>	<u>EGS-5</u>	<u>EGS-6</u>
Heat Rejection (kw)	21.2	21.2	13.9	16.1	12.2	12.1	15.0
Tubes	30.5	30.5	21.5	21.3	18.9	18.7	19.9
Tube Armor	50.5	50.5	35.5	35.3	31.1	30.9	32.8
Fins	149.4	149.4	97.9	117.5	85.9	85.2	108.2
Inlet Manifold	19.8	19.8	18.7	22.8	18.7	18.7	22.8
Inlet Manifold Armor	3.6	3.6	3.3	4.1	3.3	3.3	4.1
Exit Manifold	23.0	23.0	21.0	24.9	21.0	21.0	25.2
Exit Manifold Armor	4.1	4.1	3.8	4.5	3.8	3.8	4.5
Total Dry Weight (lb)	280.9	280.9	201.7	230.4	182.7	181.6	217.5
Tube Inventory	7.1	7.1	5.1	5.0	5.1	5.1	5.4
Inlet Manifold Inventory	22.6	22.6	21.3	26.0	21.3	21.3	26.0
Exit Manifold Inventory	26.3	26.3	24.0	28.5	24.0	24.0	28.8
Total Inventory (lb)	56.0	56.0	50.4	59.7	50.4	50.4	60.4
Total Wet Weight (lb)	336.9	336.9	252.1	290.1	233.1	232.0	277.9

TABLE 11

PCS COMPONENT WEIGHT REDUCTION SUMMARY

<u>Component</u>	<u>Baseline SNAP-8 Component Dry Weight (lb)</u>	<u>Improved SNAP-8 Component Dry Weight (lb)</u>	<u>Weight Saving (lb)</u>	<u>Remarks</u>
Alternator assembly	446	380	66	Titanium ends and lightening parts
Turbine assembly	256	223	33	Eliminate bolted flanges and lightening parts
Mercury PMA	150	85	65	Lighten parts
NaK PMA primary	225	170	55	Lighten parts
NaK PMA (HRL)	225	170	55	Lighten parts
L/C PMA	28	20	8	Lighten parts
Mercury boiler	377	258	119	Reduce NaK tube wall and diameter
Auxiliary NaK-NaK heat exchanger	20	12	8	Reduce size of heat exchanger to meet requirements
PNL NaK expansion reservoir	134	98	36	Scaled to NaK inventory
PCS structure	1600	500	1100	Replace truss structure with tension cables and support NS on reinforced radiators
Totals ⁽¹⁾	3461	1916	1545	

⁽¹⁾ Note: This is not the total EGS weight, but only the weight of the items changed, as listed.

TABLE 12

COMPARISON OF ENERGY DISTRIBUTION FOR 5800- AND 4800-RPM NaK PMA'S

	<u>5800 rpm</u>	<u>4800 rpm*</u>
<u>Pump</u>		
Head rise (ft)	115	78.3
Flowrate (gpm)	100	82.5
Hydraulic power (kw)	1.59	.89
Impeller input power (kw)	2.24	1.25
<u>Hydrodynamic Losses (kw)</u>		
Cylinder (motor rotor)	.410	.340
Thrust bearing disk	.350	.199
Bearing pads	.095	.079
Rotor nut	.105	.059
Auxiliary coolant pump	.105	.060
	<u>1.065</u>	<u>.737</u>
 <u>Motor</u>		
	<u>8-Pole Induction</u>	<u>10-Pole Synchronous</u>
Required power	3.31	1.987
Stator iron loss	.112	.112
Stator copper loss	.123	.074
Rotor can loss	.154	.099
NaK eddy loss	.351	.225
Stray load	.060	.040
Required Input (kw)	<u>4.110</u>	<u>2.537</u>

* Mechanical parts identical to parts for 5800-rpm PMA.

TABLE 13

PARAMETERS FOR CUSTOM DESIGNED NaK PMA'S*

		NaK Flow Rate $\div 10^4$					
		<u>3</u>	<u>4</u>	<u>5</u>	<u>6</u>	<u>7</u>	<u>8</u>
Primary NaK Loop	Pipe OD (in.)	1.875	2.0	2.125	2.25	2.375	2.5
	Line ΔP (psi)	4.1	6.0	6.9	8.1	8.8	9.4
	Reactor ΔP (psi)	1.6	2.5	3.0	3.8	4.4	5.1
	Boiler ΔP (psi)	1.8	1.8	1.8	1.8	1.8	1.8
	Loop ΔP (psi)	7.5	10.3	11.7	13.7	15.0	16.3
	Hyd Power (kw)	0.27	0.49	0.70	0.98	1.13	1.55
	PMA Input (kw)	1.63	1.94	2.25	2.74	3.13	4.00
	$\eta\%$	16.5	25.2	31.1	35.7	36.1	38.8
Heat Rejection Loop	Radiator ΔP (psi)	7.5	10.0	11.0	12.0		
	Line ΔP (psi)	2.3	3.4	4.0	4.5		
	Cond ΔP (psi)	2.3	4.0	5.0	6.0		
	PLR ΔP (psi)	0.3	0.5	0.7	0.9		
	Loop ΔP (psi)	12.4	17.9	20.7	23.4		
	Hyd Power (kw)	0.40	0.77	1.11	1.50		
	PMA Input (kw)	1.82	2.34	2.98	3.90		
	$\eta\%$	21.9	32.7	37.2	38.5		

* Used in analysis of EGS-5 and EGS-6.

TABLE 14

SUMMARY OF MPMA PARAMETERS AND PARASITIC LOSSES

	<u>Existing MPMA</u>	<u>Turbine Mounted Pump</u>	<u>Alternator Mounted Pump</u>
<u>Operating Conditions (EGS-2)</u>			
Speed (rpm)	7800	12,000	12,000
Flow Rate (gpm)	1.45	1.45	1.45
Head (ft)	89.4	89.4	89.4
Impeller Discharge Pressure (psia)	514	514	514
Jet Pump Discharge Pressure (psia)	70	70	70
Jet Pump Suction Pressure (psia)	13	13	13
Pump Efficiency (%)	25.8	25.8	25.8
<u>Parasitic Losses (watts)</u>			
Hydraulic Power	317	317	317
Pumping Losses	913	913	913
Motor Viscous & Mechanical Losses	1640	---	---
Motor Electrical Losses	428	---	---
Additional Loss of Duplex Bearing	----	200	200
Visco Seal Loss	----	---	15
Turbine Bearings & Slinger Losses	1664	1664	1664
Total Pump-Related Parasitic Loss (watts)	4962	3094	3109
Net Reduction in Parasitic Losses (watts) (compared to existing MPMA)	0	1868	1853

Table 14

TABLE 15COMPARISON OF LOSSES FOR PRESENT SNAP-8 (200°C) AND
HIGH-TEMPERATURE (400°C) ALTERNATORS

Output (kw)	51.1	51.1	54.4	54.4
PF	1.0	1.0	1.0	1.0
Temp (°C)	200	400	200	400
Losses (watts)				
Stator I ² R	660	1610	750	1830
Stator Iron	2110	2110	2110	2110
Field				
Field I ² R	240	585	260	635
Pole Face	690	690	690	690
Seals & Brgs.	1960	1960	1960	1960
Total Losses	5660	6955	5770	7225
Input (kw)	56.76	58.06	60.17	61.63
Efficiency (%)	90.0	88.0	90.4	88.3

TABLE 16

MERCURY BOILER MODIFICATION SUMMARY

<u>EGS</u>	<u>No. of Hg Tubes</u>	<u>Hg Inventory (lb)</u>	<u>NaK Tube ID (in.)</u>	<u>NaK Tube Wall (in.)</u>	<u>NaK Inventory (lb)</u>	<u>Dry Weight (lb)</u>
-0	7	17	4.0	.125	107	377
-1	7	17	3.25	.049	56	258
-2	7	17	3.25	.049	56	258
-3	9	22	4.0	.060	72	343
-4	7	17	4.0	.060	107	280
-5	7	17	4.0	.060	107	280
-6	9	22	4.55	.060	138	356

TABLE 17

CAPACITIVE REACTANCE (kvar) FOR ALTERNATOR LOAD POWER FACTOR CORRECTION

<u>EGS</u>	<u>Alternator Load pf</u>	<u>kvar</u>
-0	.64	0
-1	.64	0
-2	.90	24*
-3	.92	46
-4	1.0	48
-5	1.0	47
-6	1.0	71

* This EGS uses synchronous pump motors operating at 1.0 pf which reduces the amount of leading kvar required to obtain the 0.9 alternator load power factor.

TABLE 18
 WEIGHT SUMMARY - TV SATELLITE VEHICLE
 (pounds)

<u>POWER SYSTEM</u> (Including fluid inventories)		10,010
Reactor Assembly	758	
Shield	2430	
Power Conversion System (including structure)	4702	
Radiator Assembly	1155	
HRL	940	
L/C	215	
Radiator Stiffeners and Adapter	715	
Thermal Insulation	250	
<u>TV SYSTEM</u>		2,360
Antenna	400	
Power Conditioning	300	
Klystron Transmitter	280	
Uplink Receiver	50	
Water Cooling System (Dry)	70	
Support Structure	300	
Radiator	330	
Radiator Stiffeners and Adapter	500	
Coolant Inventory	130	
<u>REACTIVE THRUST SYSTEM (MONOPROPELLANT)</u>		2,030
Propellant and Gas	1150	
Tankage	310	
Nozzles, Plumbing & Controls	35	
Support Structure	535	
ORBITING WEIGHT		14,400
<u>JETTISONABLE GROUP</u>		2,240
Nose Shroud	200	
Thermal Shield	900	
Adaptor Structure & Shroud	1140	
LAUNCH WEIGHT		16,640

Table 18

TABLE 19

SUMMARY OF SNAP-8 PERFORMANCE AND SPECIFICATION DATA

Net Electrical Output (kwe)	35
Voltage (AC volts)	120/208
Frequency (cps)	400 \pm 4
Voltage Regulation (from 3.5 to 35 kw)	\pm 5%
Load Power Factor	0.85 lagging
Phase	3-phase, 4-wire
Harmonic Content	8% RMS line-to-line with balanced linear 100% load at 1.0 pf
Rated Life of EGS (hr)	10,000 continuous
Radiation Environment (in area of PCS)	
Fast neutron	5×10^{12} nvt, integrated dose for 10^4 hours
Gamma	5×10^7 rads (C), integrated dose for 10^4 hours
Operational Gravity Environment	Zero gravity
* Radiator Area (ft ²)	
HRL	706
L/C	173

* EGS-4 data adjusted for synchronous orbit

TABLE 20

SUMMARY OF TYPICAL DATA FOR
STATION KEEPING/ATTITUDE CONTROL
OF TV SATELLITE

<u>PROPELLANT SYSTEM</u>	<u>STATION KEEPING</u>	<u>ATTITUDE CONTROL</u>
Type Propellant	Monopropellant, Hydrazine	
Total Impulse (lb-sec)	240,000	8600
Specific Impulse (sec)	220	220
Propellant Weight (lb)	1090	39
Tank Weight (lb)	200	10
Tank Volume (ft ³)	19	0.7
Operating Pressure (psia)	225	225
Expulsion Method	Bellows	Bellows
 <u>GAS PRESSURIZATION SYSTEM</u>		
Type Gas	Nitrogen	Nitrogen
Initial Pressure (psia)	3000	3000
Gas Weight (lb)	21	0.8
Tank Weight (lb)	100	-
 <u>THRUST CHAMBER</u>		
No. Required	4	12
Chamber Pressure (psia)	175	175
Gas Temperature (°F)	1500	1500
Thrust Per Chamber (lb)	20	0.5
Minimum Pulse Bit (lb-sec)	0.20	0.005
Area Ratio	40/1	40/1
Propellant Flow (lb/sec/chamber)	0.091	0.0023
Miscellaneous Weight (lb)	25	10
(Valves, piping, etc.)		

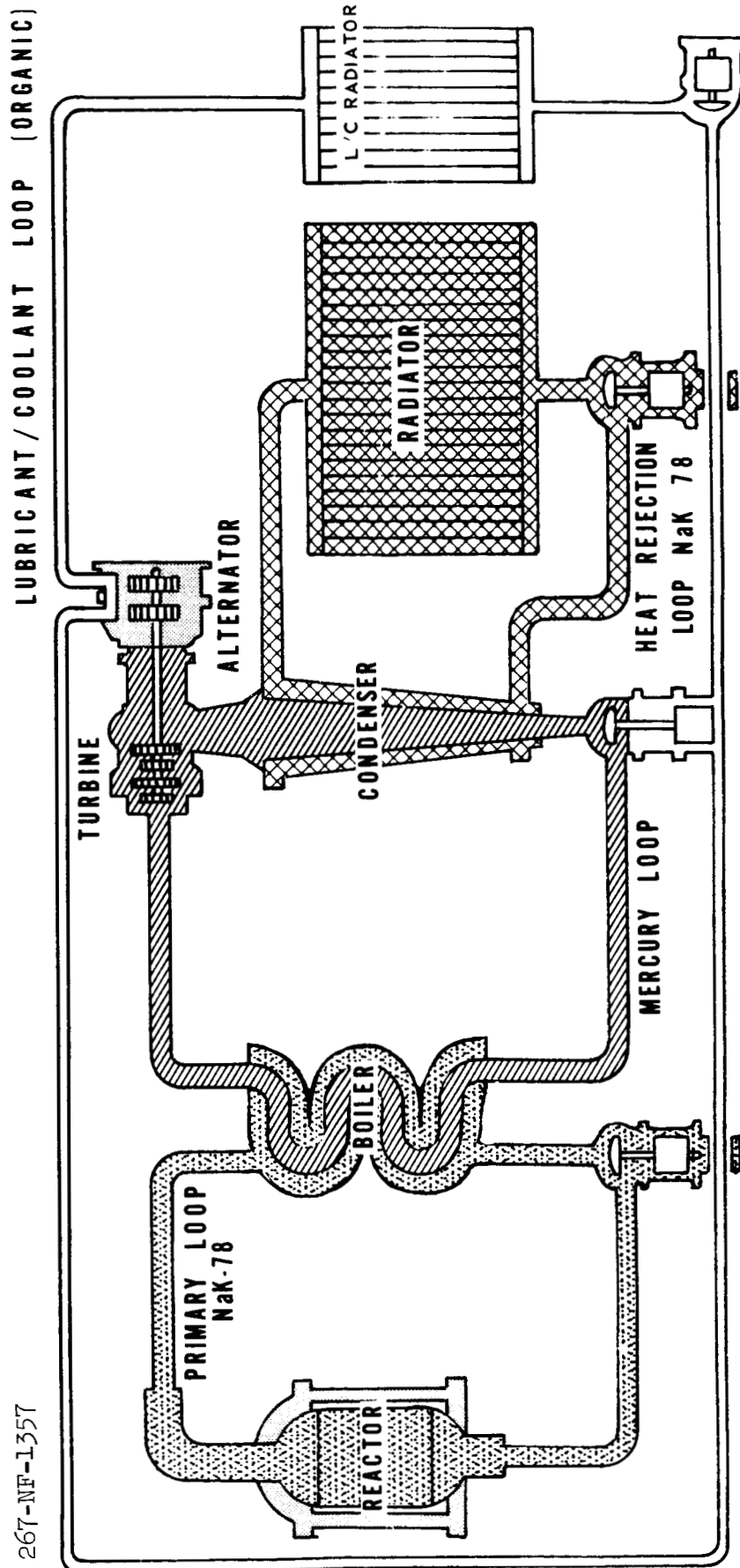
Table 20

TABLE 21

EFFECT OF POWER INCREASE AND REDUNDANCY
ON TV SATELLITE VEHICLE

	<u>Available Power (kw)</u>		
	<u>35</u> <u>(EGS-4)</u>	<u>70</u> <u>(EGS-6)</u>	<u>140</u> <u>2(EGS-6)</u>
<u>Launch Weight (lb)</u> , (for 10,000 hours)			
No redundancy	17,000	20,000	40,000
With redundancy*	22,000	26,000	52,000
<u>Required Radiator Area</u> (ft ²)	1,250	2,100	4,200
<u>Available Vehicle Surface Area</u> (ft ²)	1,900	2,100	4,200
<u>Vehicle Length</u> (ft)	59.3	62	68
<u>Antenna Diameter</u> (ft)	34	27	22

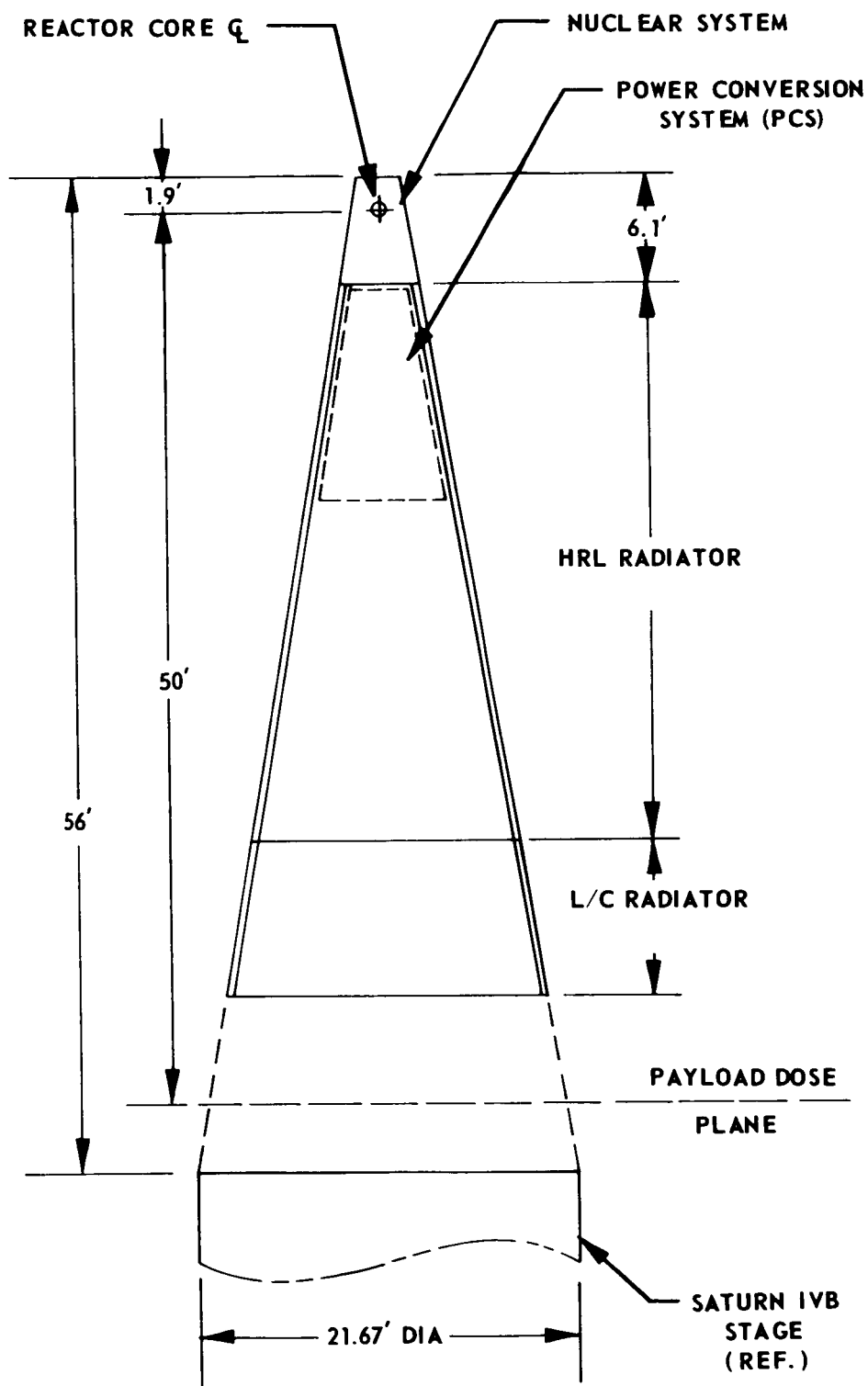
*Includes one redundant PCS, set of radiator tubes and armor and klystron tube



SNAP-8 4-Loop System Schematic

Figure 1

167-581

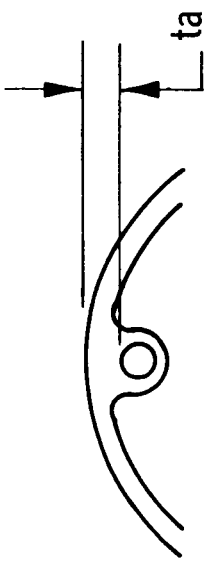


CONE HALF-ANGLE = 9.75°

SNAP-8 Electrical Generating System Configuration

Figure 2

167-DV-1201



125 TUBES

TUBE SIZE .250 OD x .020 IN. S.S.

FIN THICKNESS - .030 IN. ALUMINUM

ARMOR THICKNESS t_a .170 IN. ALUMINUM

MANIFOLD 2.0 OD MAX TAPERED x .035 IN. S.S.

TEMPERATURE:

660° - 488F	EGS-0, 1, 2, 3
660° - 510F	EGS-4, 5, 6

AREA PER KW

2.4 - 2.5	FT^2/KWT	EGS-0, 1, 2, 3
2.2 - 2.3	FT^2/KWT	EGS-4, 5, 6

SPECIFIC WEIGHT: ~ 2.7 LB/KWT

Heat Rejection Loop Radiator Characteristics

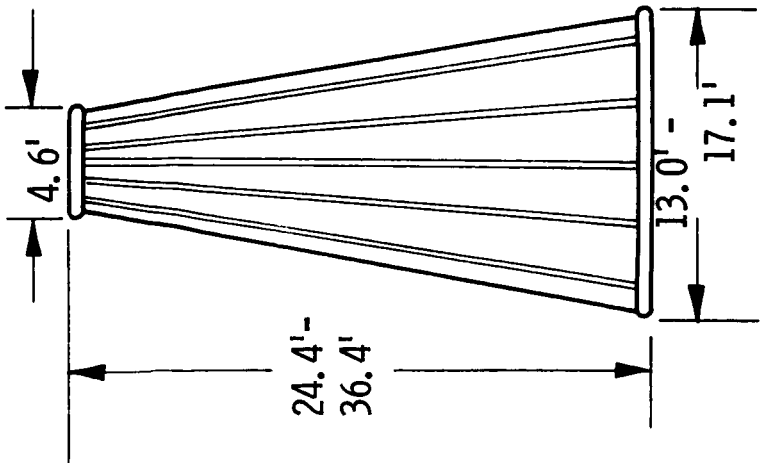


Figure 3

167-DV-1202

120 TUBES - 3 PASS

TUBE SIZE .187 OD x .020 IN. S.S.

FIN THICKNESS - .030 IN. ALUMINUM

ARMOR THICKNESS .140 IN. ALUMINUM

MANIFOLD 1.50 OD TAPERED x .035 IN. S.S.

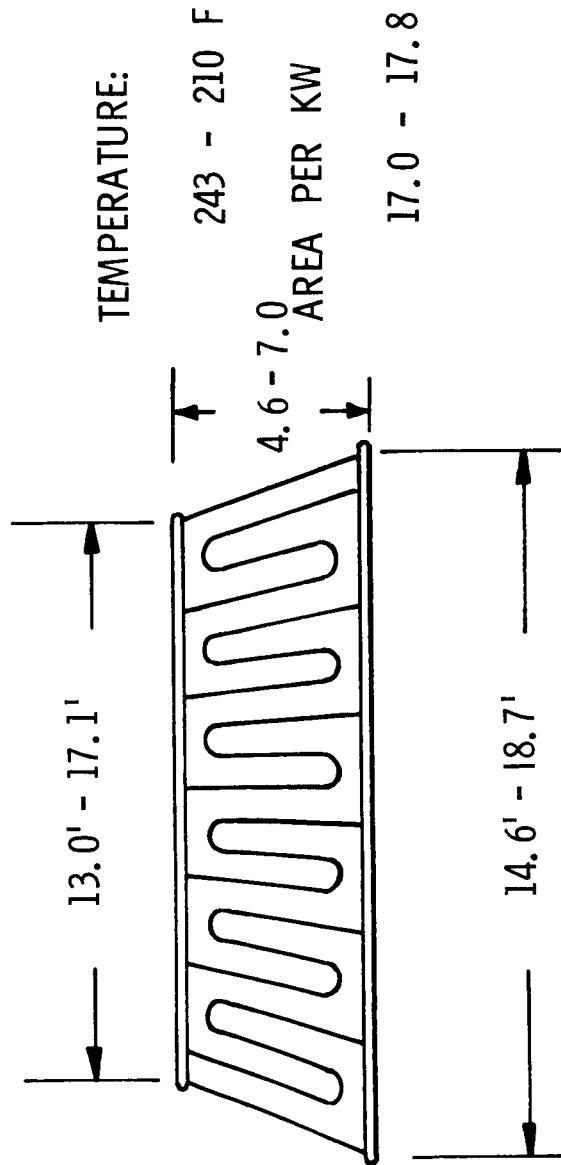
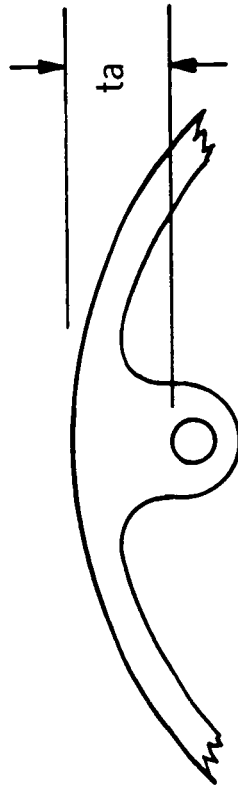
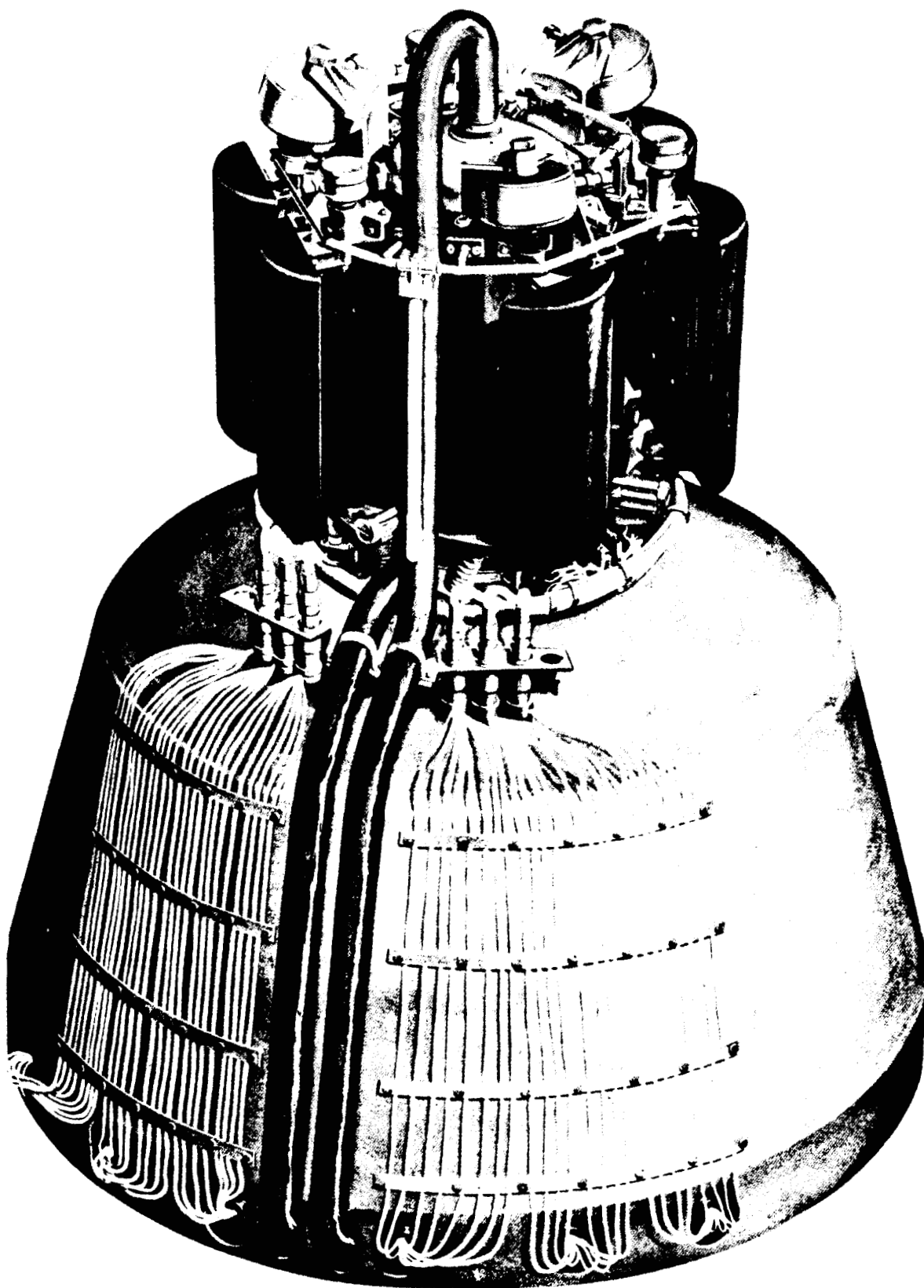


Figure 4

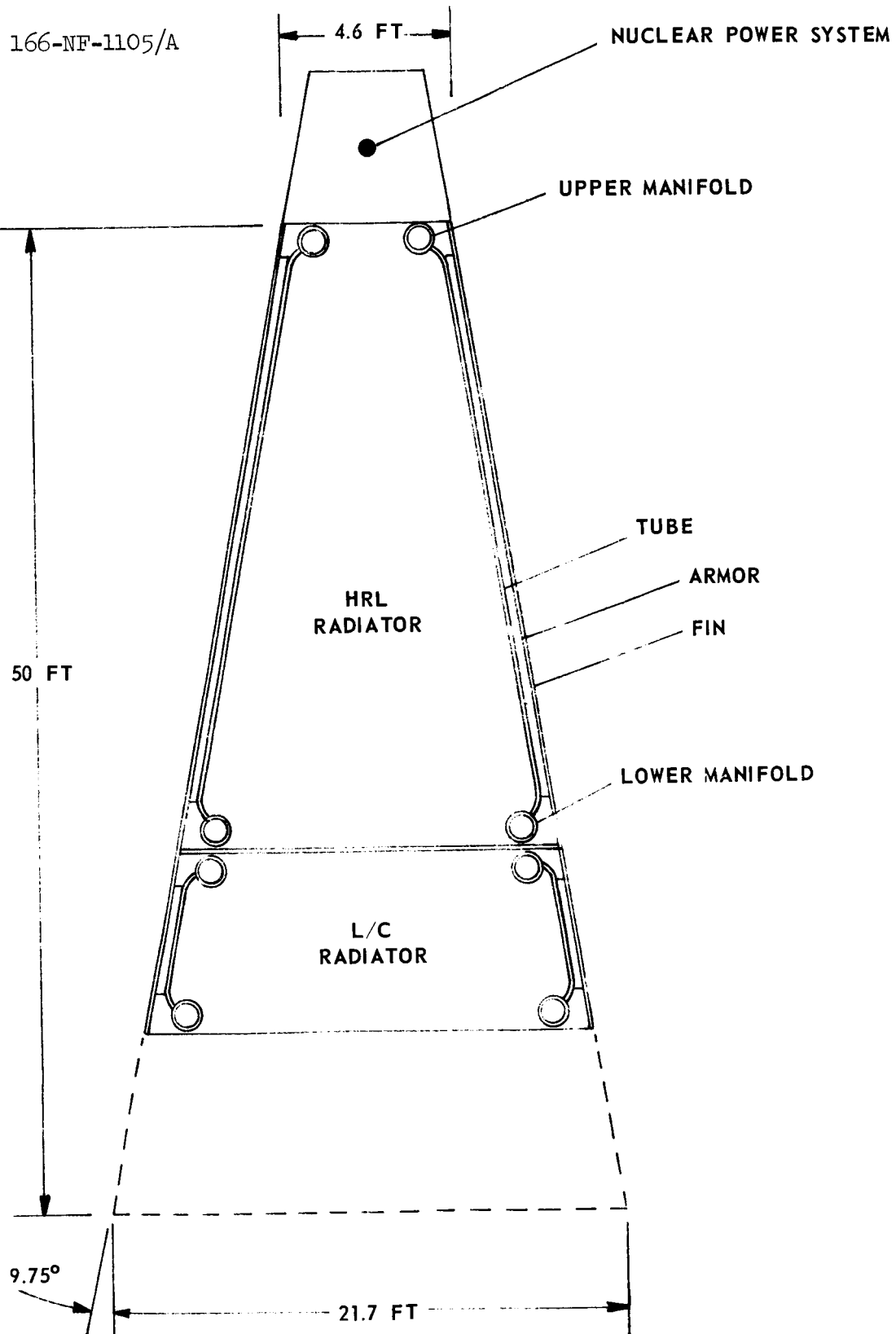
SPECIFIC WEIGHT ~ 19 LB/KWT

Lubricant-Coolant Radiator Characteristics

1166-286



600-KWT SNAP-8 Reactor and Shield



Relative Location of Heat Rejection Loop
and Lubricant-Coolant Loop Radiators

Figure 6

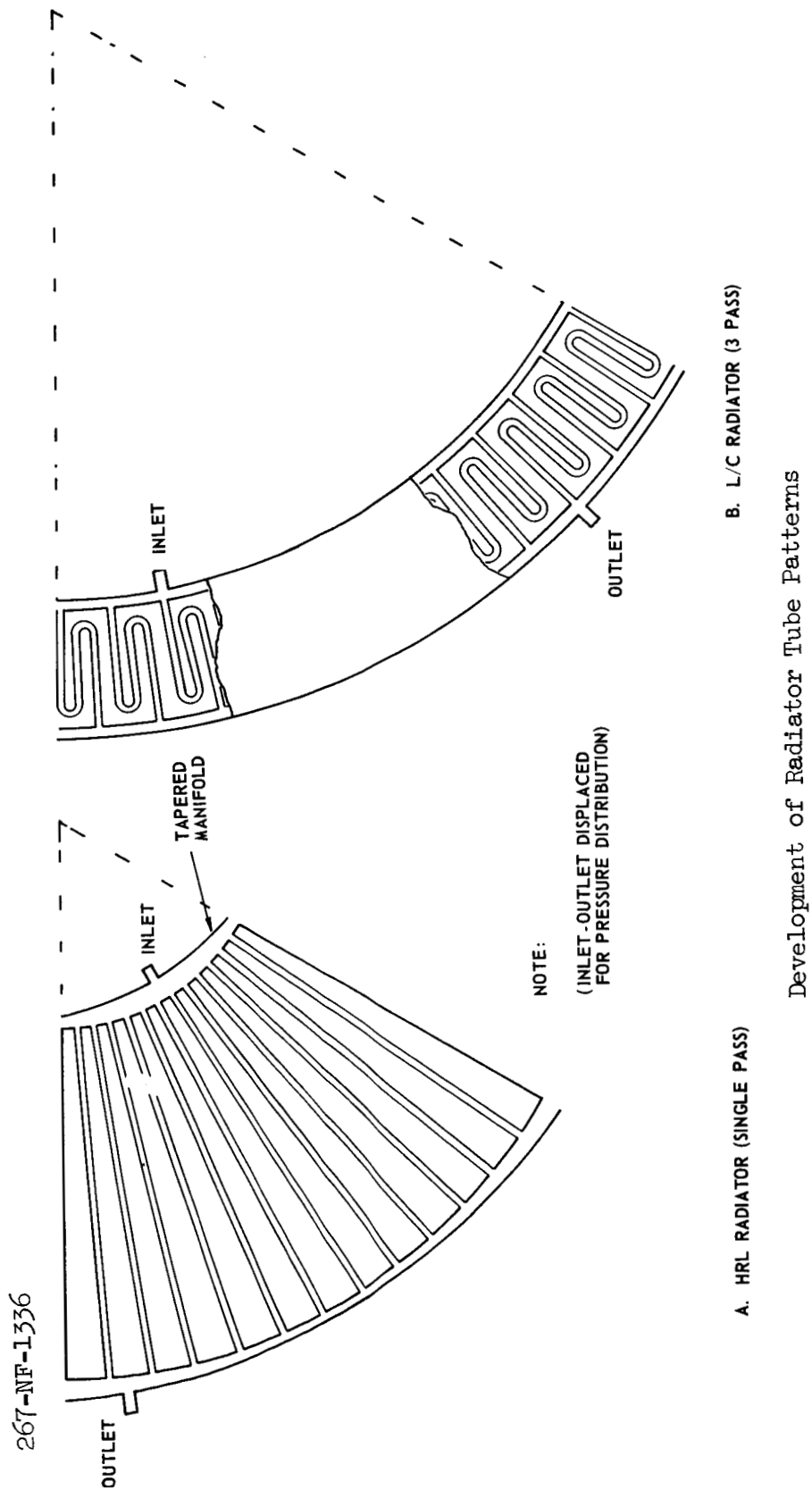
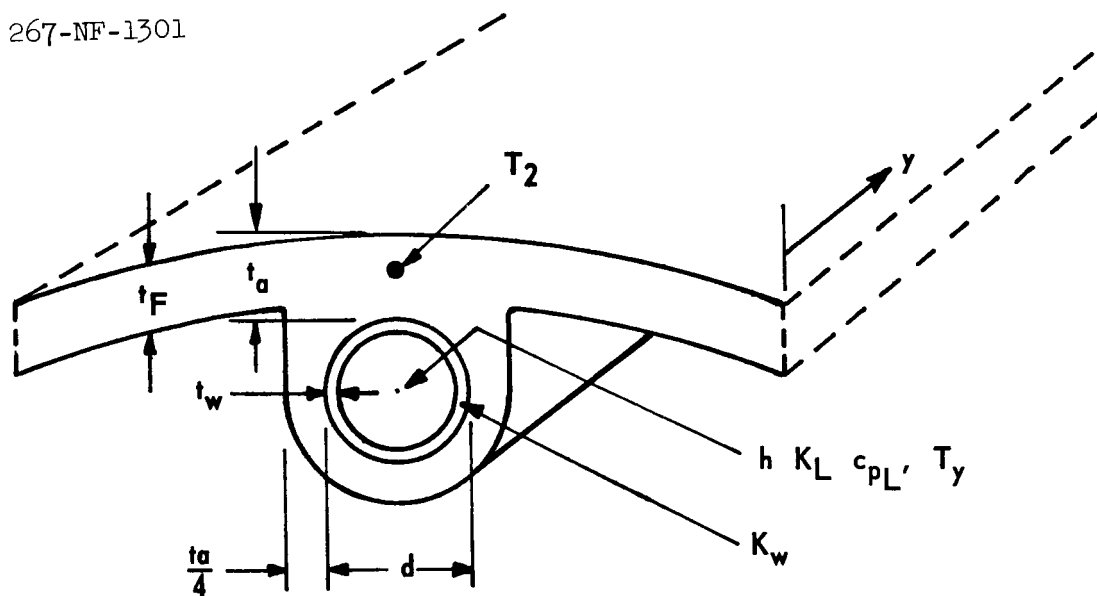


Figure 7

267-NF-1301



Tube-Fin Configuration

Figure 8

267-NF-1302

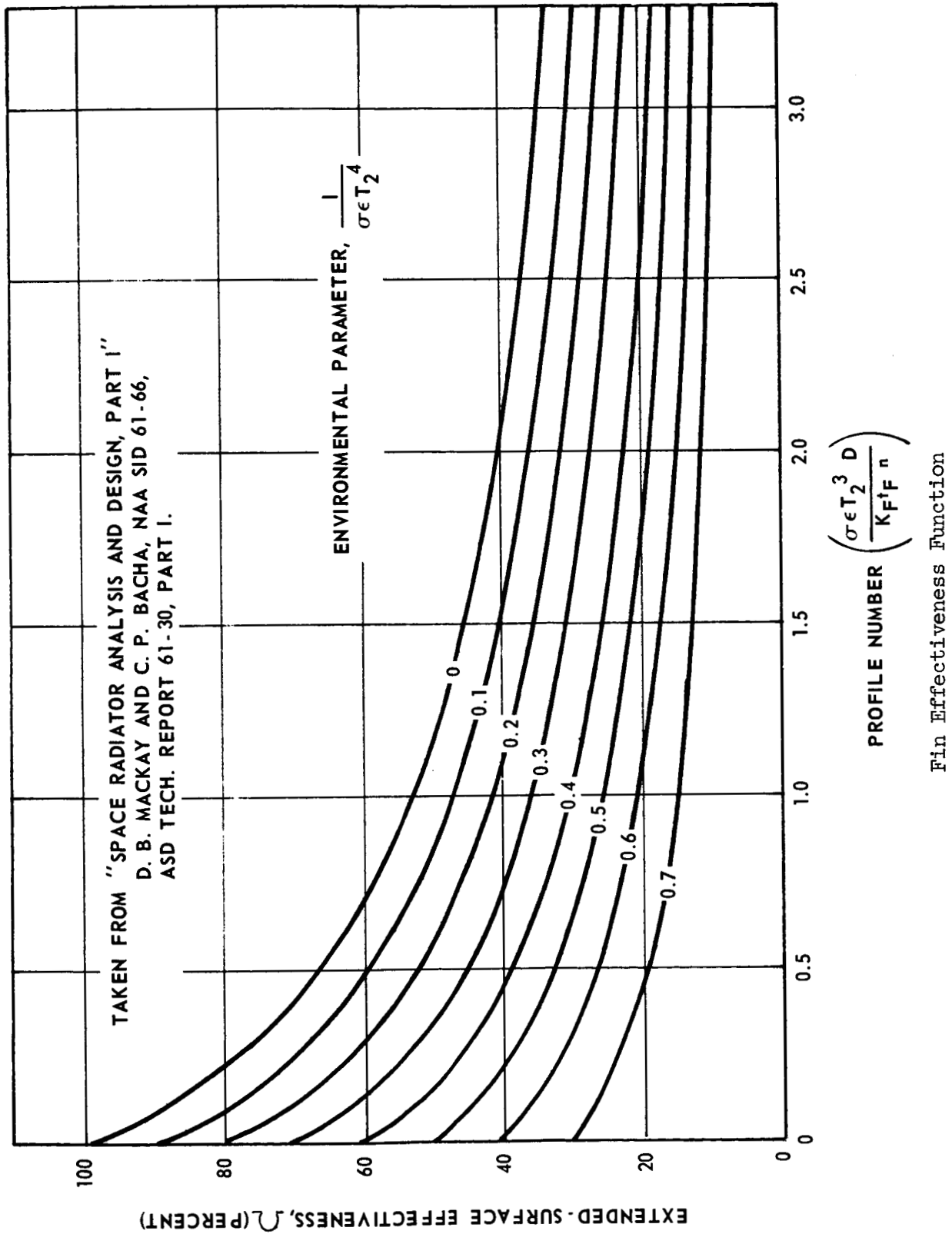


Figure 9

267-NF-1303

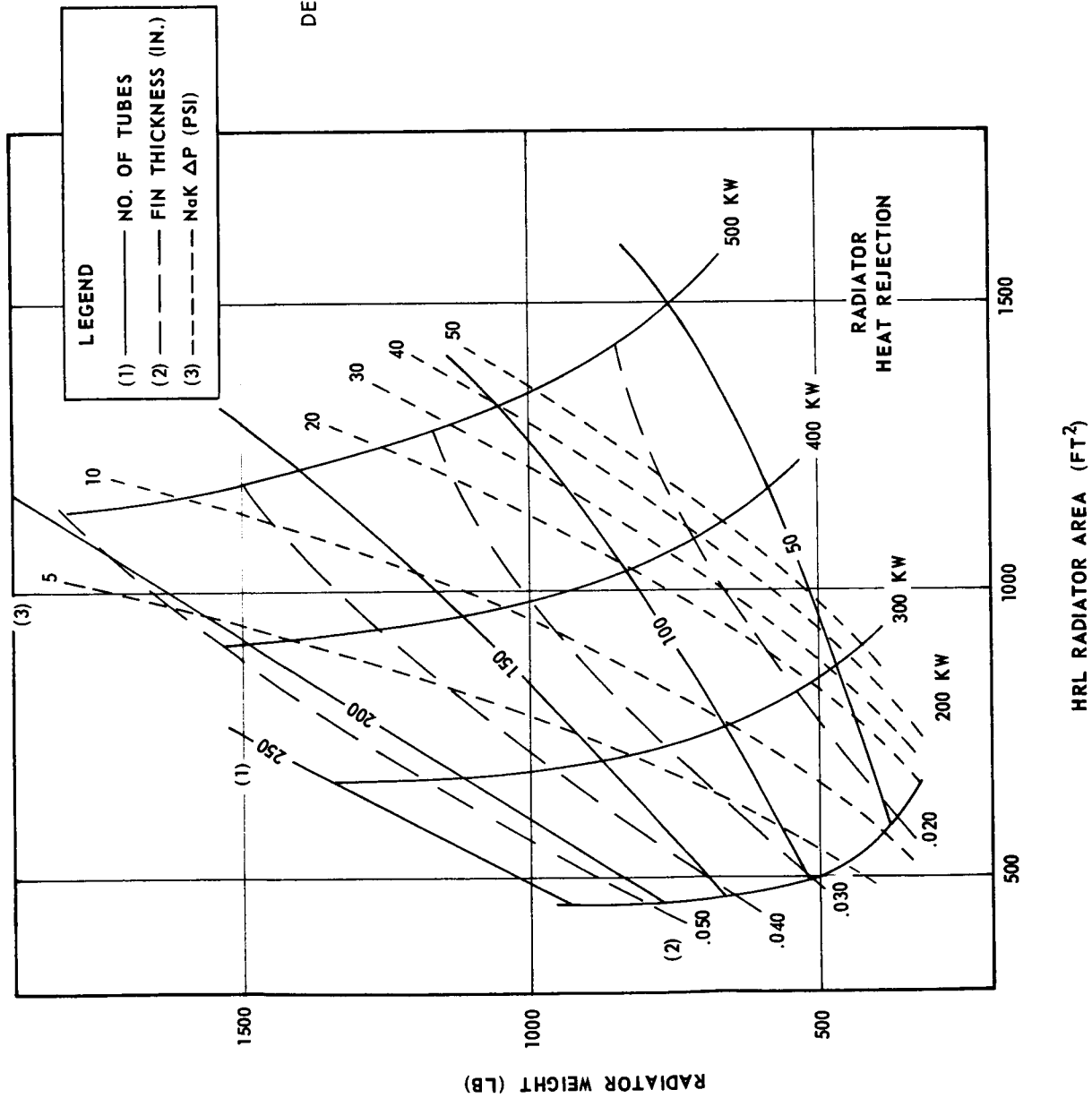
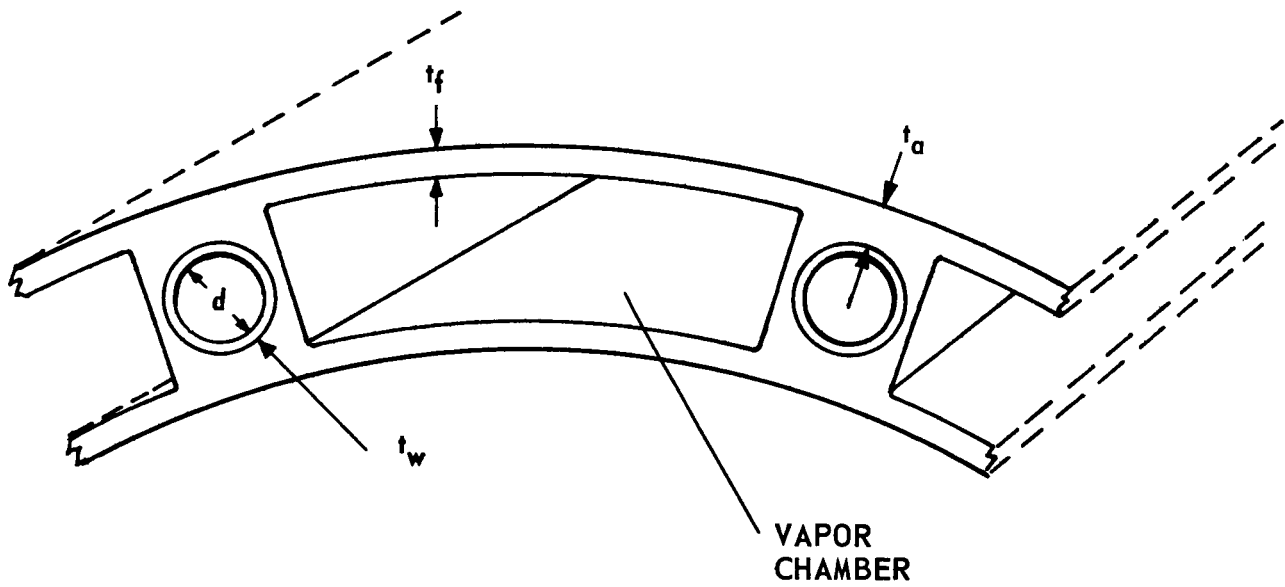


Figure 10

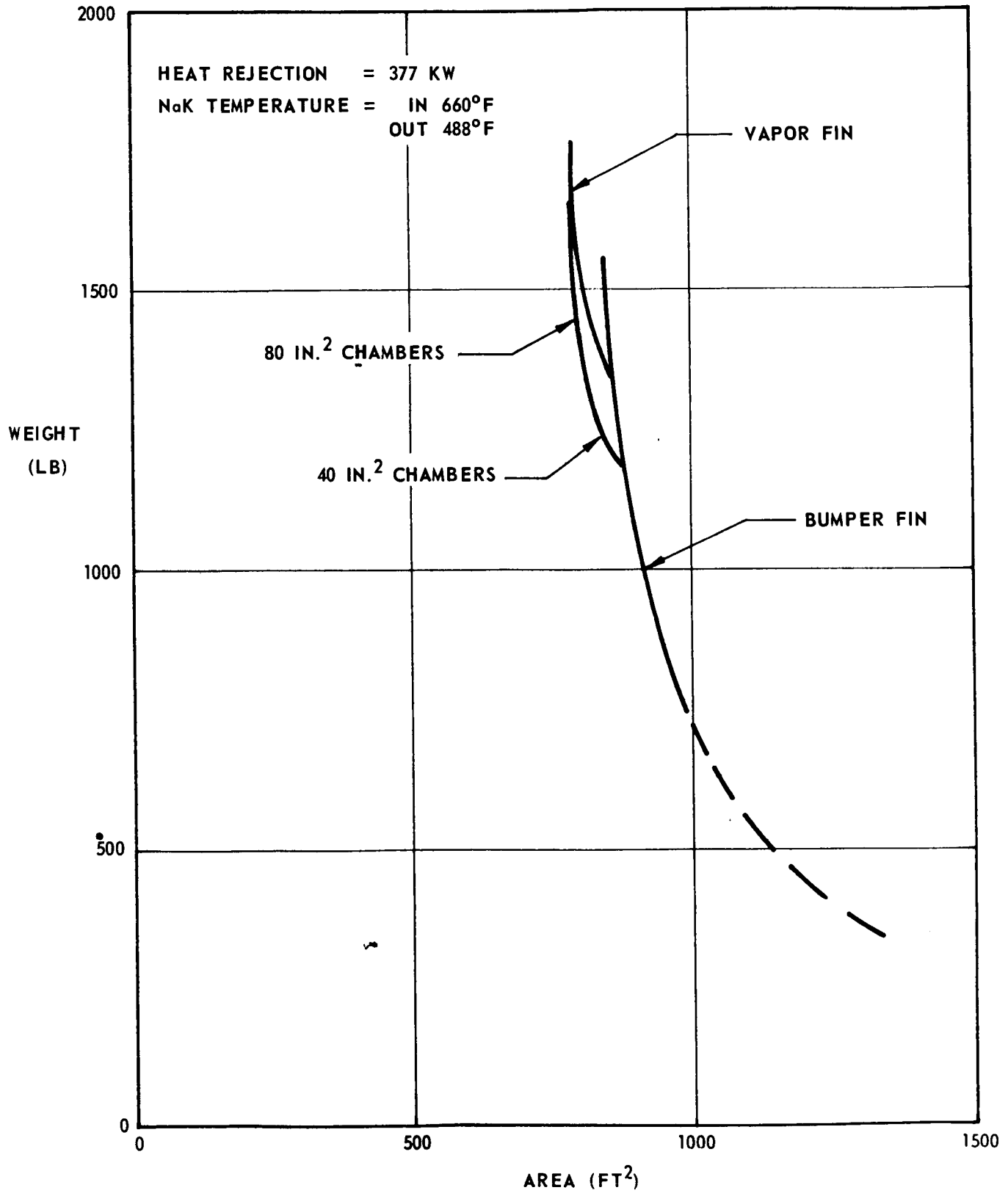
Heat Rejection Loop Radiator Map

267-NF-1304



Vapor-Chamber Fin Configuration

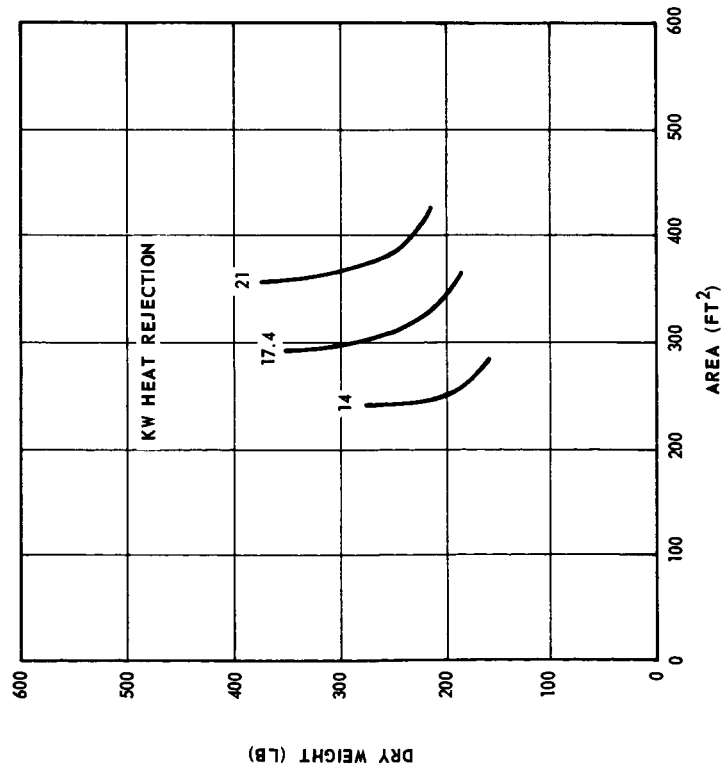
267-NF-1305



Comparison Between Vapor-Chamber
Fin and Bumper-Fin Capabilities

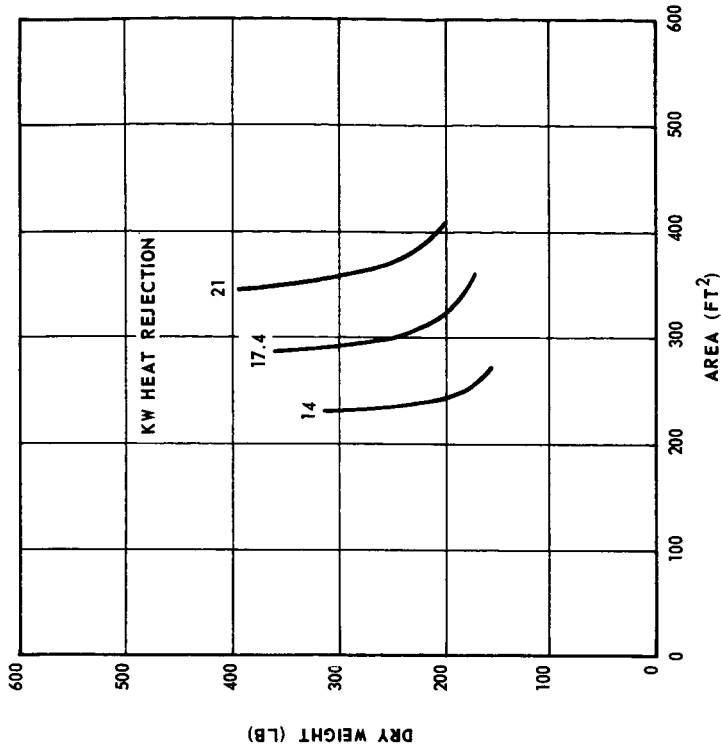
Figure 12

267-NF-1306



NOTE: CONE HALF ANGLE = 9.75 DEG
INVENTORY WT = 55 TO 60 LB
TUBE DIA. = 0.1875 OD

A. ONE PASS FOR EACH FLOW PATH



B. TWO PASSES FOR EACH FLOW PATH

Lubricant-Coolant Radiator Map
for One- and Two-Pass Flow

Figure 13

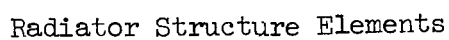
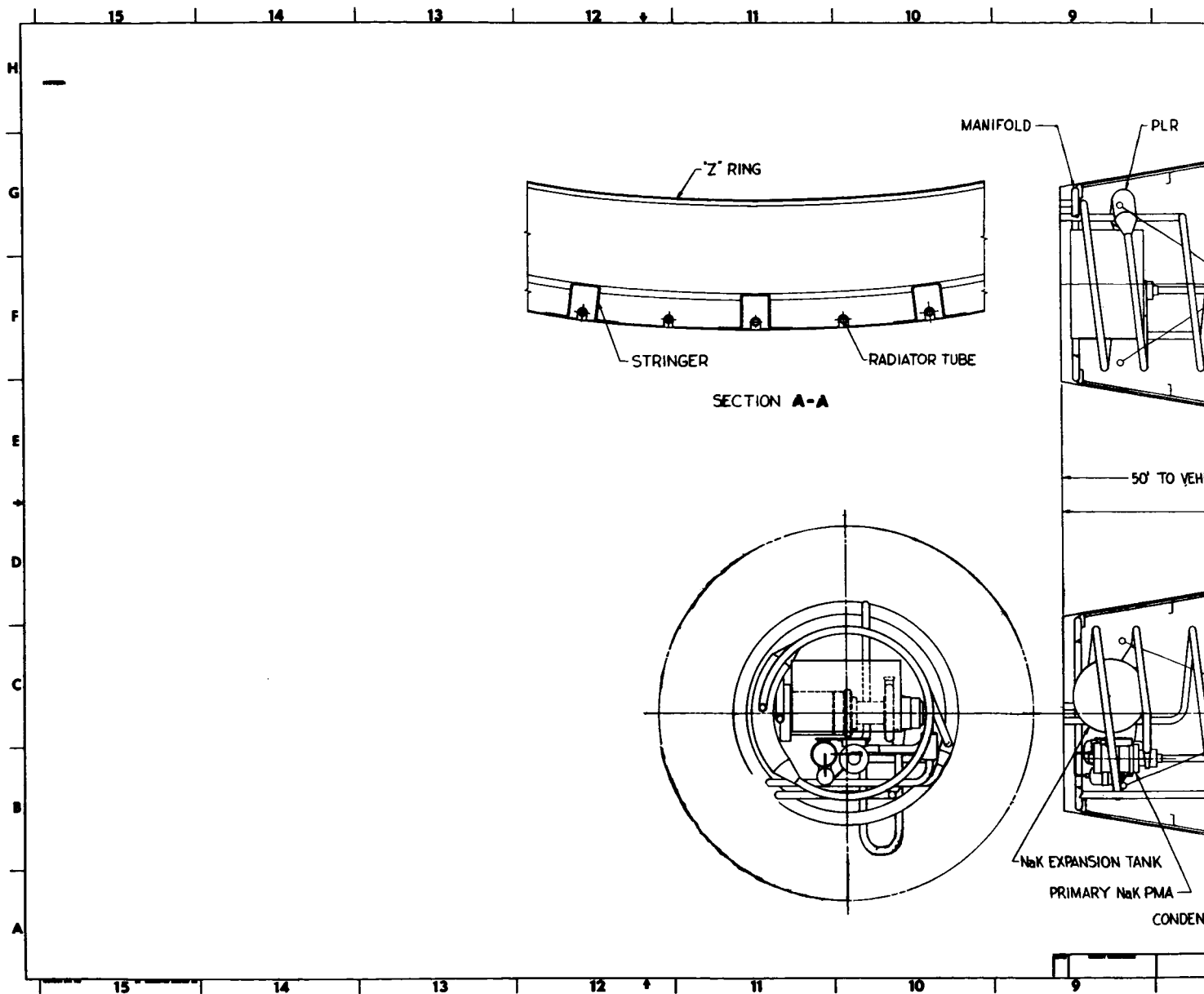
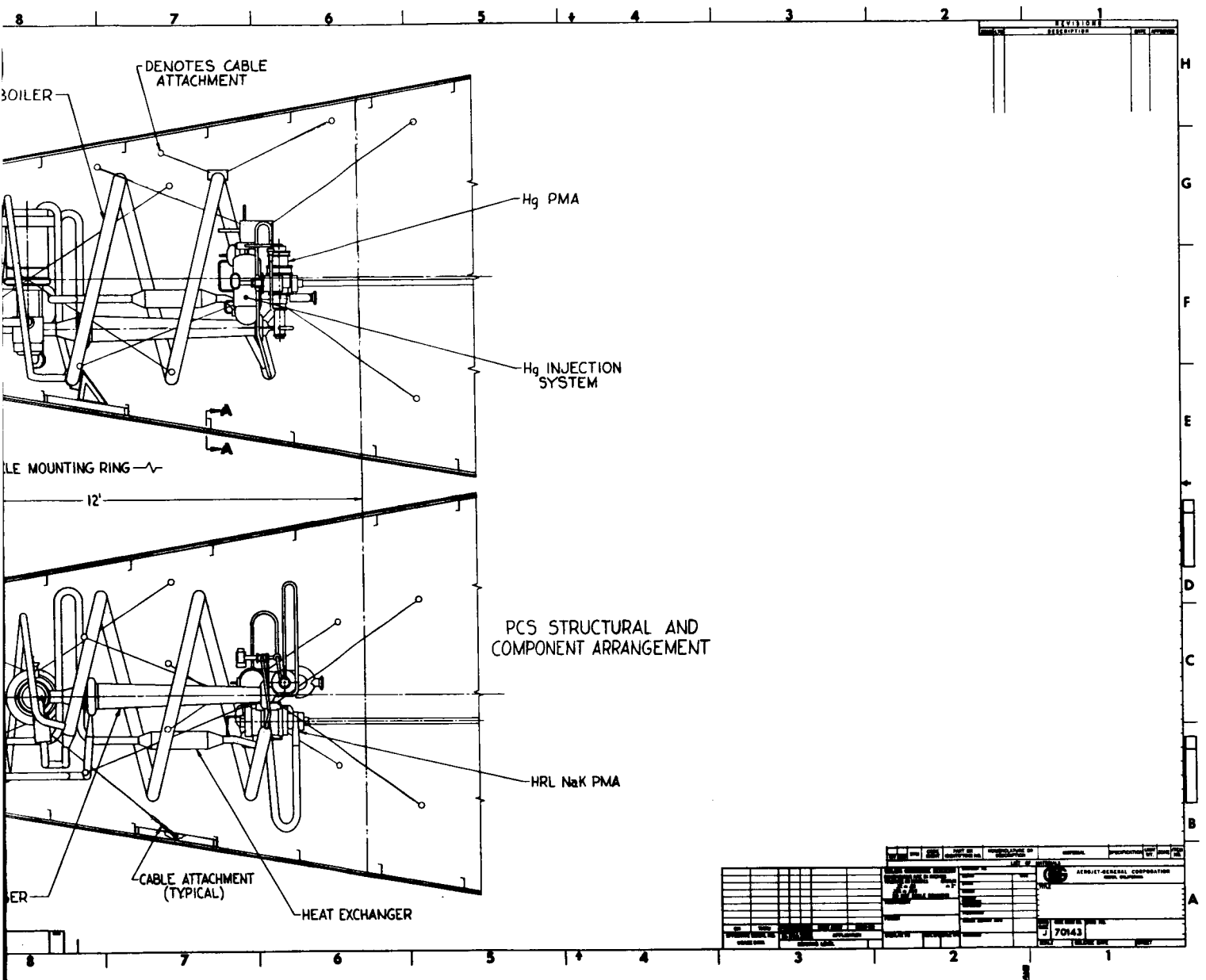


Figure 14

366-NF-1138/A



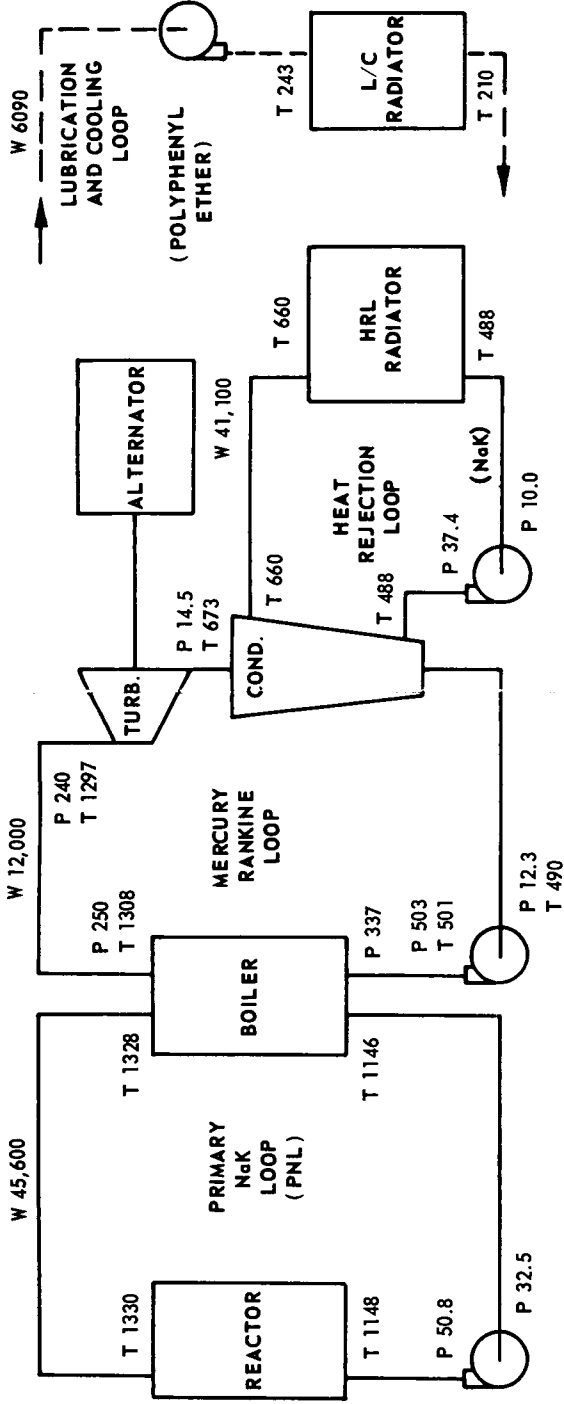
15-1



PCS Structural and Component Arrangement

267-NF-1309

ALTERNATOR POWER DISTRIBUTION	
SHAFT POWER	64.9 KW
EFFICIENCY	86.0 %
GROSS OUTPUT POWER	55.8 KW
LOAD P. F.	0.64
OUTPUT KVA	87.5
PARASITIC LOAD	
PNL PMA	4.60
Hg PMA	3.55
HRL PMA	4.81
L/C PMA	1.37
PLR	4.50
VOLTAGE CONTROL	0.20
SPEED CONTROL	0.80
NET OUTPUT POWER	36.0 KW



DESCRIPTIVE FEATURES

TURBINE AERODYNAMIC EFFICIENCY - 57 %
TURBINE INLET PRESSURE - 240 PSIA
TURBINE EXHAUST PRESSURE - 14.5 PSIA
TURBINE FLOW AREAS SIZED FOR 12,000 LBS/HR AND 240 PSIA INLET PRESSURE
NaK LOOP PRESSURE DROPS BASED ON CURRENT COMPONENTS AND 50 FT OF 2" OD LINES
NaK PMA's: 5800 RPM INDUCTION MOTORS, BOTH NaK LOOPS
NaK PMA's COOLED BY L/C FLUID
Hg PMA WITH MOTOR SCAVENGER
TUBE-IN-TUBE BOILER (7 Hg TUBES)
TUBE-IN-SHELL CONDENSER (73 Hg TUBES)
S8DS REACTOR
PARASITIC LOAD RESISTOR (PLR) IN PNL
ALTERNATOR POWER FACTOR UNCORRECTED, BASED ON 0.75 PF VEHICLE LOAD
SATURABLE REACTOR-MAGNETIC AMPLIFIER SPEED CONTROL
RADIATOR NaK $\Delta T = 172^{\circ}F$

PERFORMANCE SUMMARY

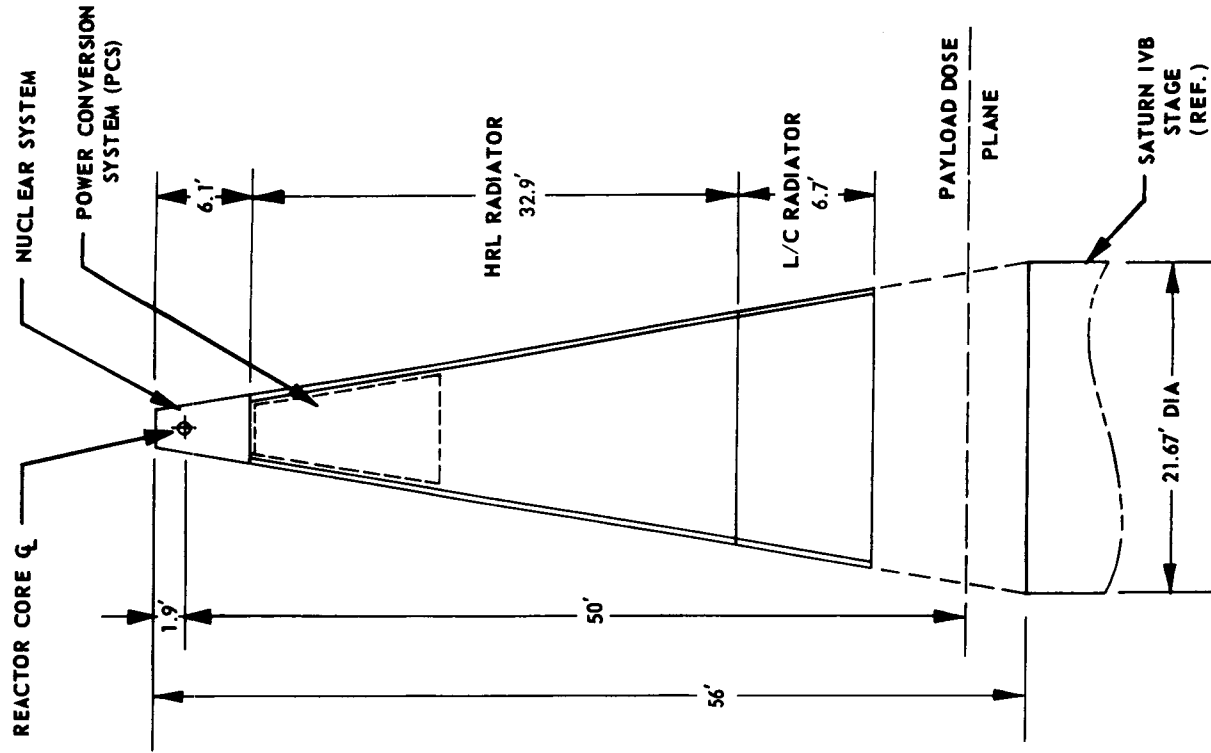
NET REACTOR INPUT TO PCS 512 KWT
NET ELECTRICAL OUTPUT 36.0 KWE
OVERALL SYSTEM EFFICIENCY 7.0 %
EGS WEIGHT 11,002 LBS
SPECIFIC WEIGHT 306 LBS/KWE
HRL RADIATOR AREA 1071 FT²
HEAT REJECTED 439 KWT
L/C RADIATOR AREA 362 FT²
HEAT REJECTED 21.2 KWT
TOTAL RADIATOR AREA 1433 FT²
SPECIFIC RADIATOR AREA 39.8 FT²/KWE

LEGEND

W = FLOW RATE, LB/HR
T = TEMPERATURE, °F
P = PRESSURE, PSIA

16-1

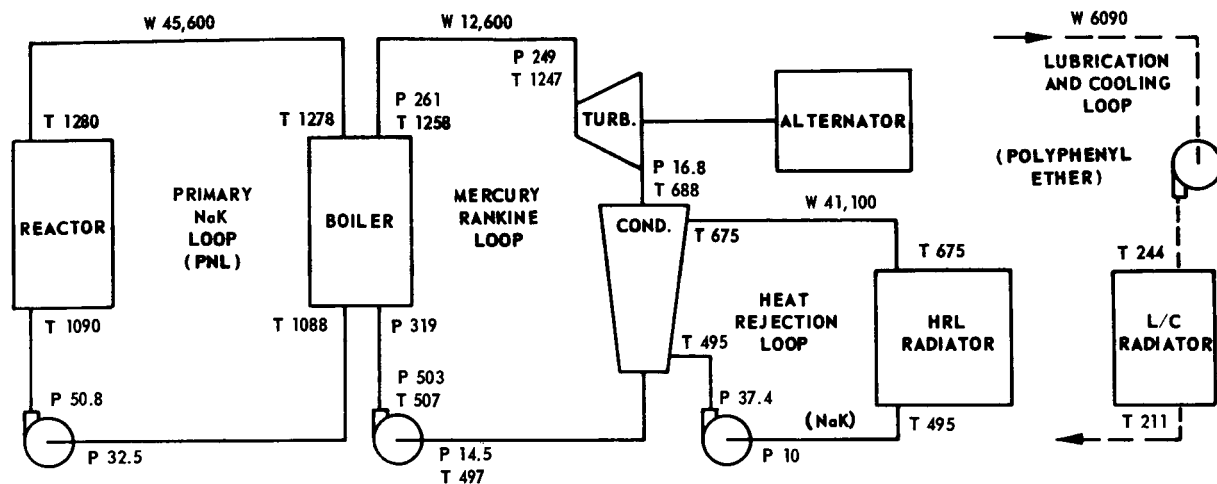
EGS-O SUMMARY PERFORMANCE CHART



CONE HALF-ANGLE = 9.75°

Figure 16 -8

267-NF-1310



PERFORMANCE SUMMARY

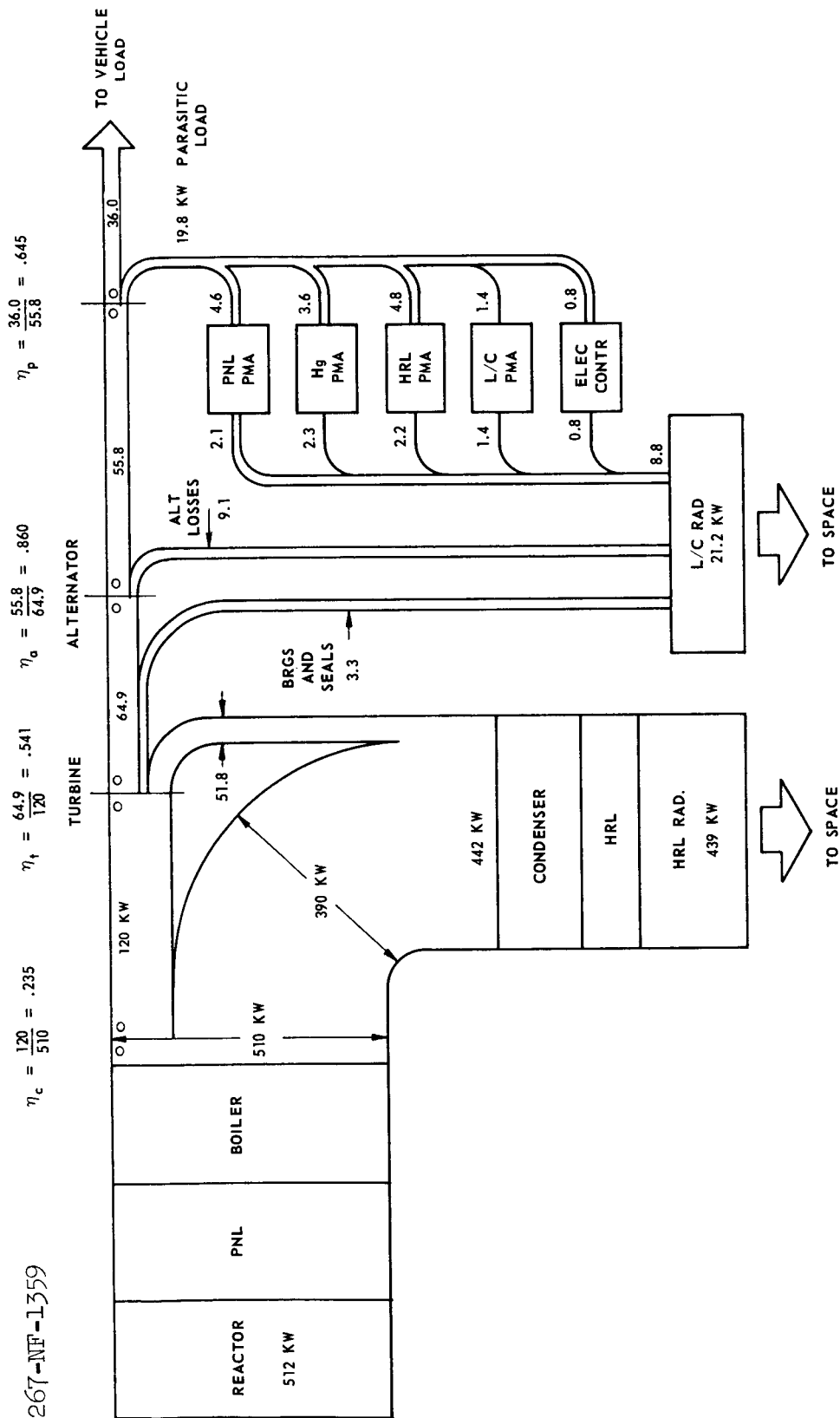
NET REACTOR INPUT TO PCS	534 KWT
NET ELECTRICAL OUTPUT	36.8 KWE
OVERALL SYSTEM EFFICIENCY	6.9 %
GROSS ELECTRICAL OUTPUT	57.0 KWE
PARASITIC ELECTRICAL LOAD	19.9 KWE
HRL RADIATOR	
AREA	1071 FT ²
HEAT REJECTED	459 KW
L/C RADIATOR	
AREA	362 FT ²
HEAT REJECTED	21.3 KW

LEGEND

W = FLOW RATE, LB/HR
 T = TEMPERATURE, °F
 P = PRESSURE, PSIA

EGS-0 PERFORMANCE WITH REACTOR OUTLET TEMPERATURE AT LOWER LIMIT

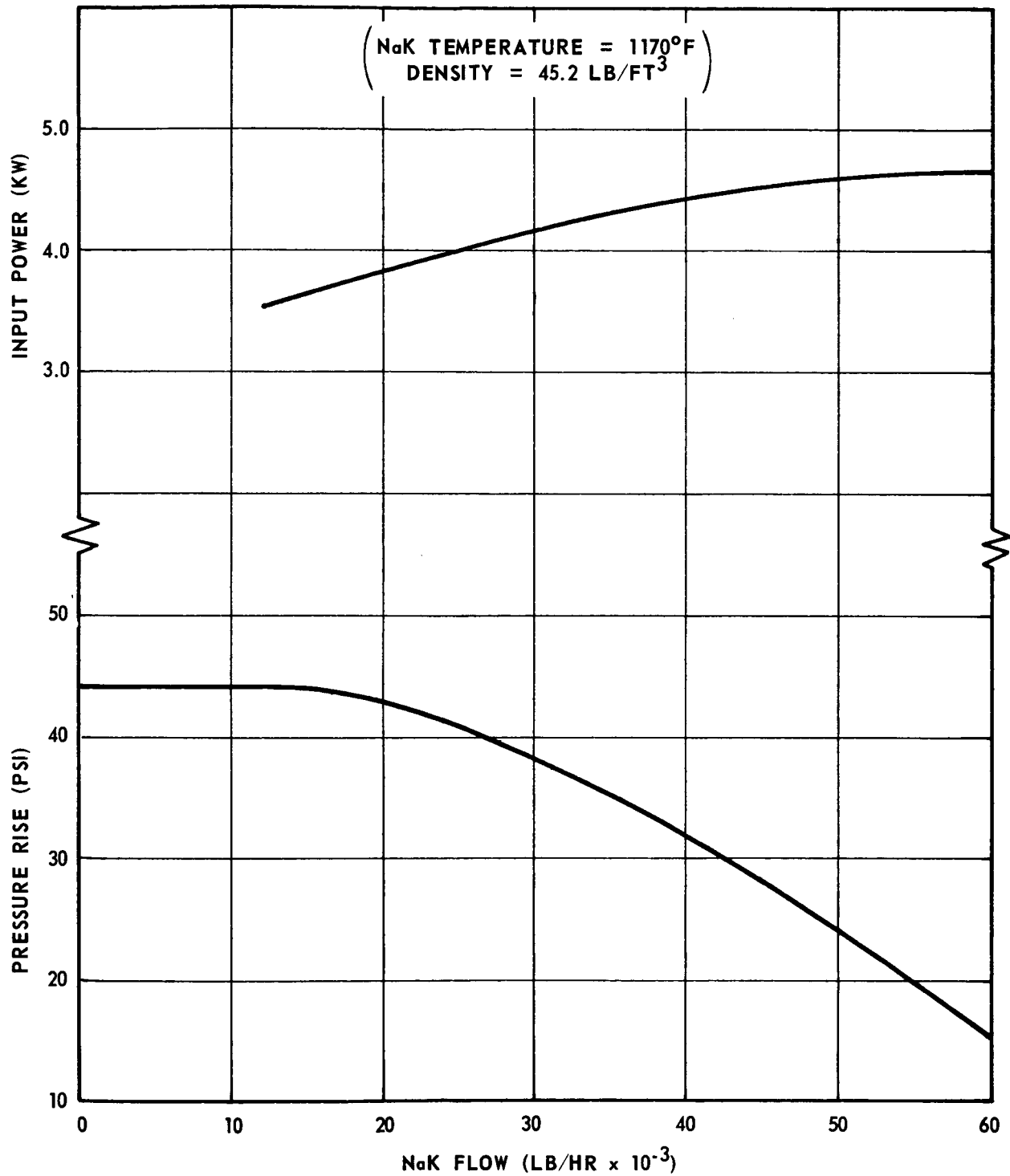
Figure 17



Power Distribution Diagram for EGS-O

Figure 18

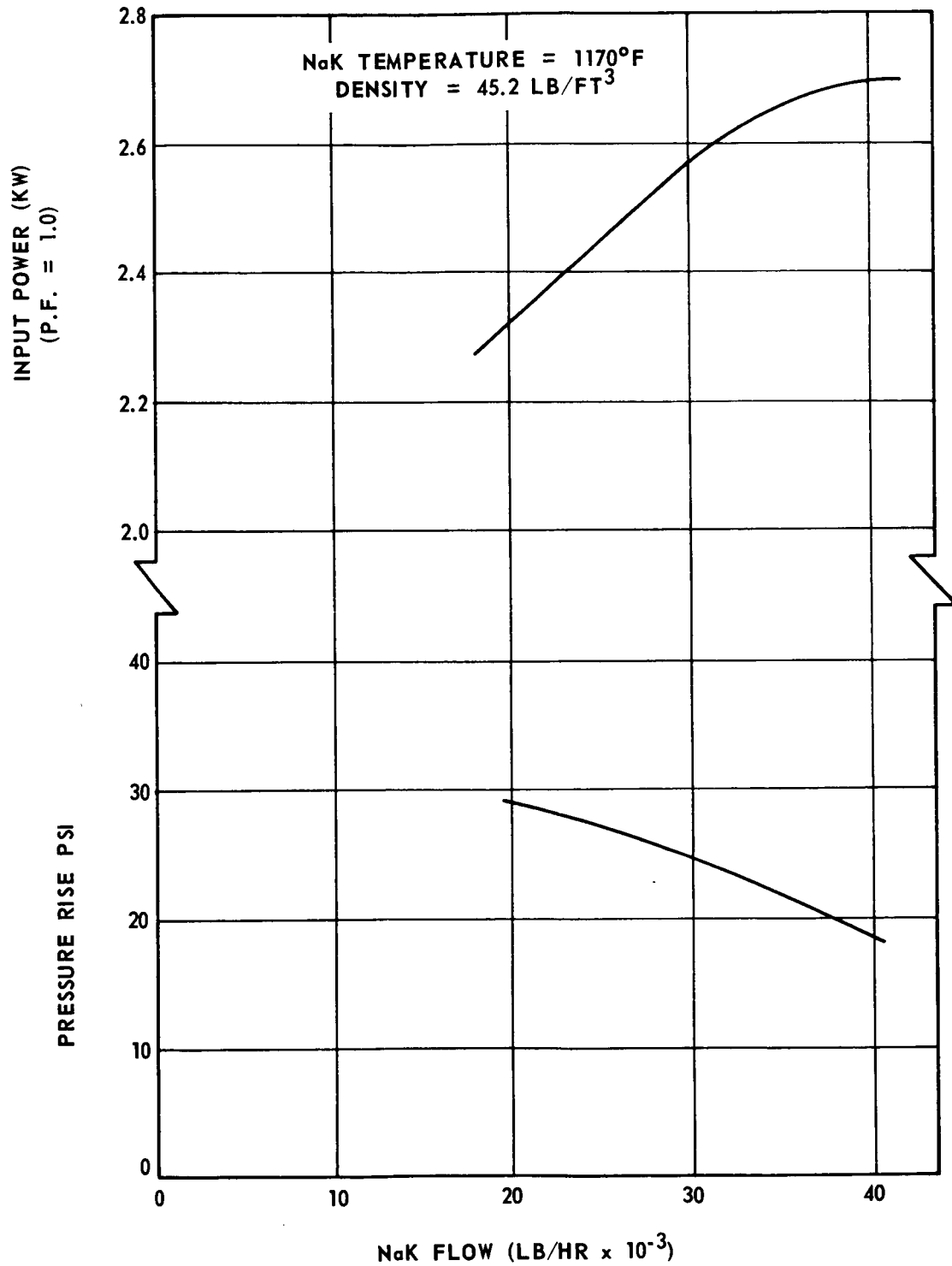
267-NF-1308



Pressure Rise and Input Power vs Flow Rate for
5800 rpm NaK PMA

Figure 19

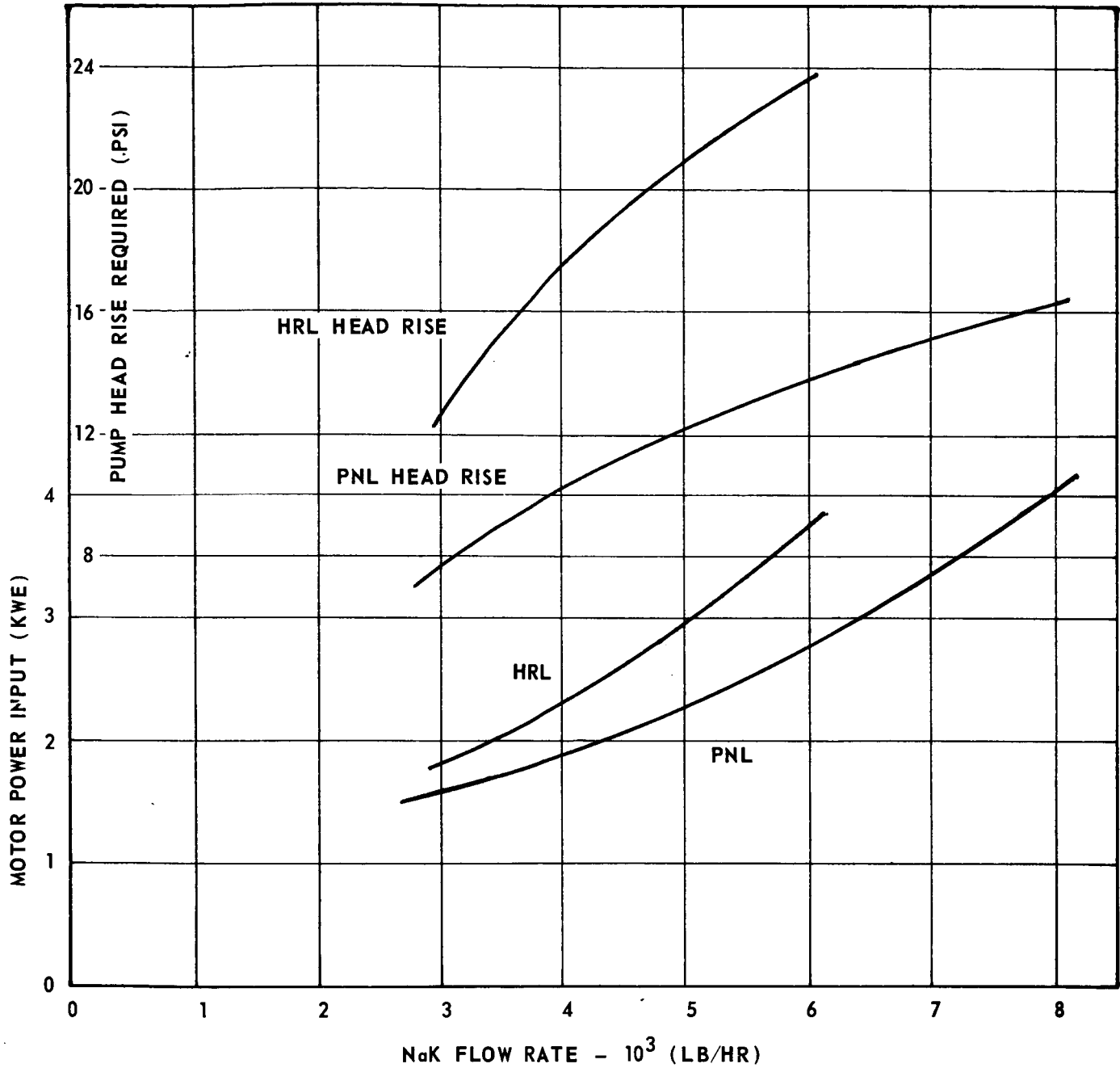
267-NF-1311



Pressure Rise and Input Power vs Flow Rate for
4800 rpm NaK PMA

Figure 20

267-NF-1312

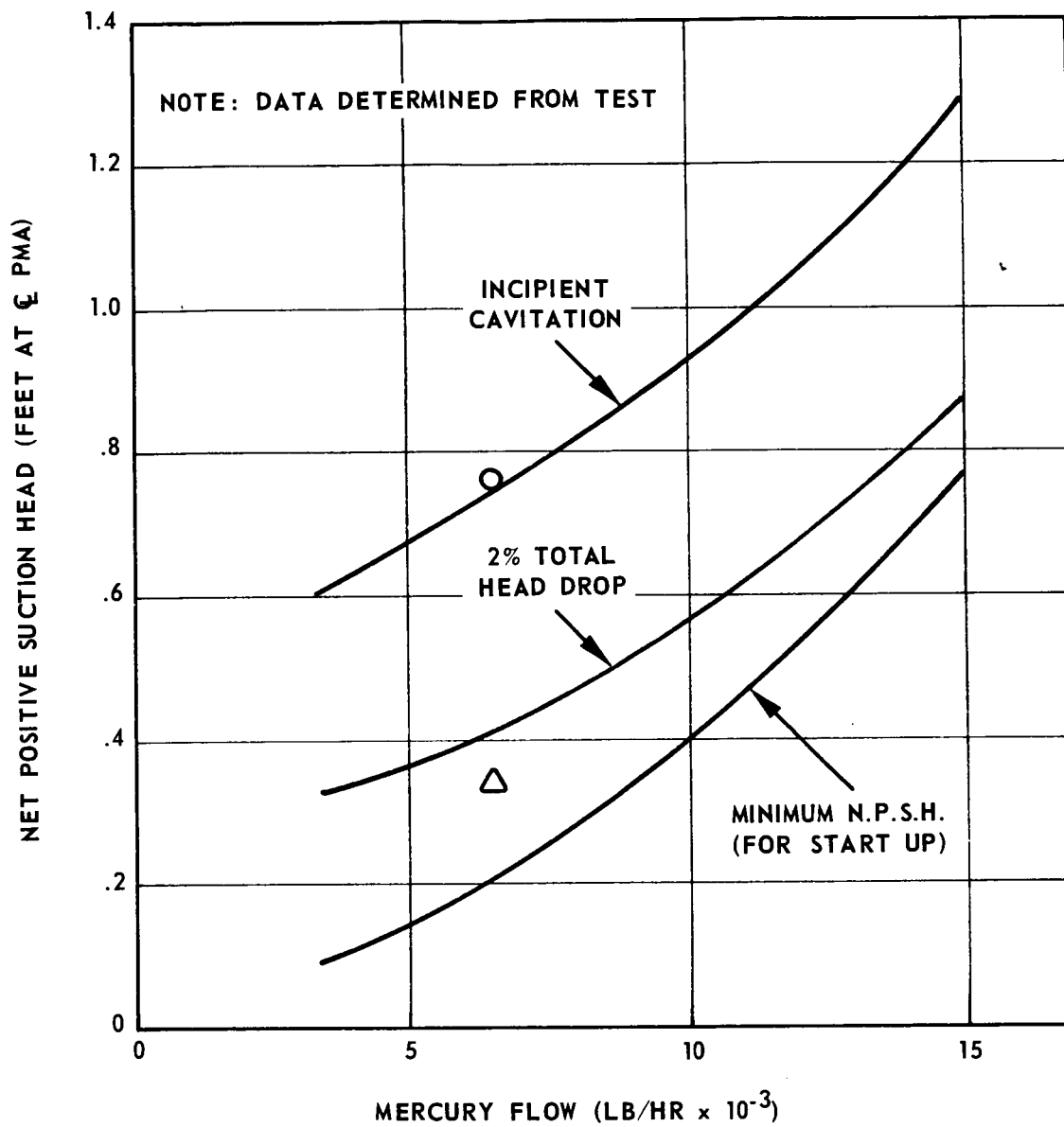


- NOTES: 1. PUMP DESIGN PARAMETERS VARIED TO MEET HEAD RISE REQUIREMENT AT EACH FLOW.
2. PMA CONCEPT USED IN SNAP-8 NaK PMA IS RETAINED.
3. HEAD RISE REQUIRED BASED ON CHANGING COMPONENT AND PIPING P VS FLOW RATE.

Input Power and Head Rise vs Flow Rate for NaK PMA's
Custom Designed for Lower Loop Impedance

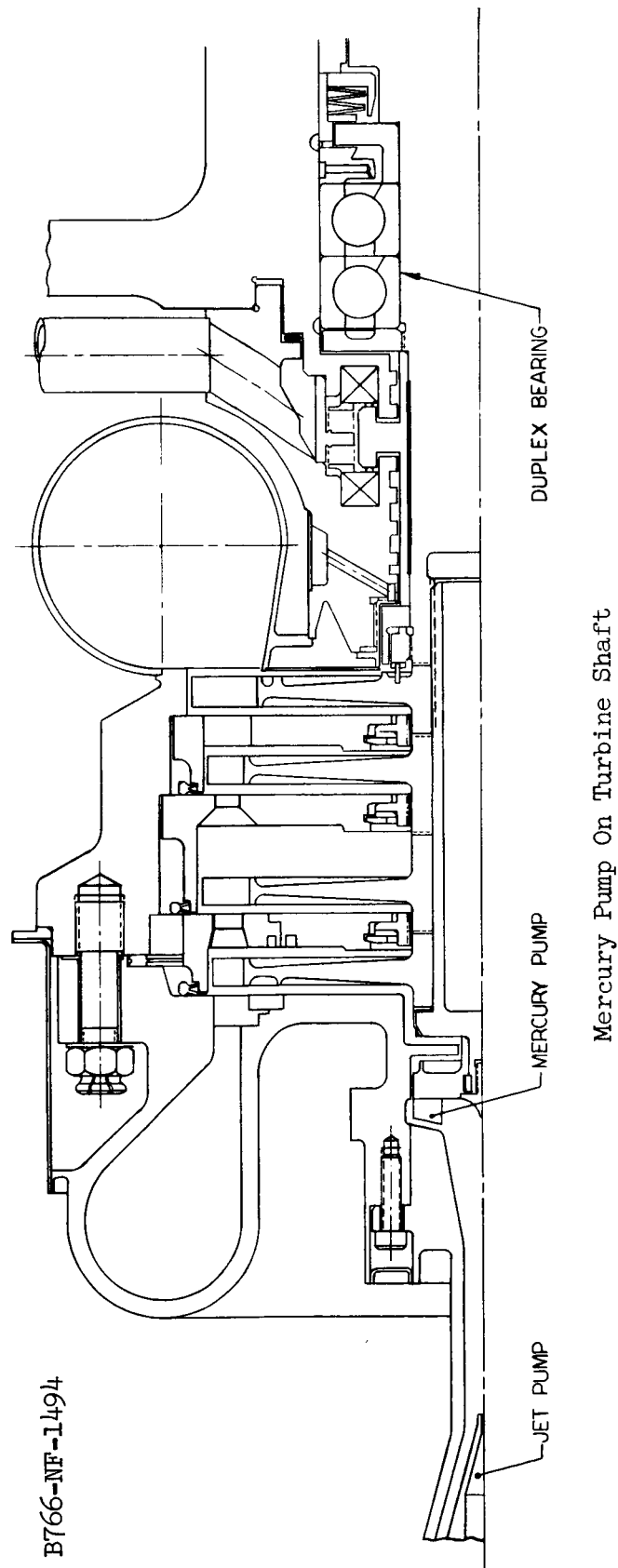
Figure 21

267-NF-1313



Mercury PMA Suction Characteristics

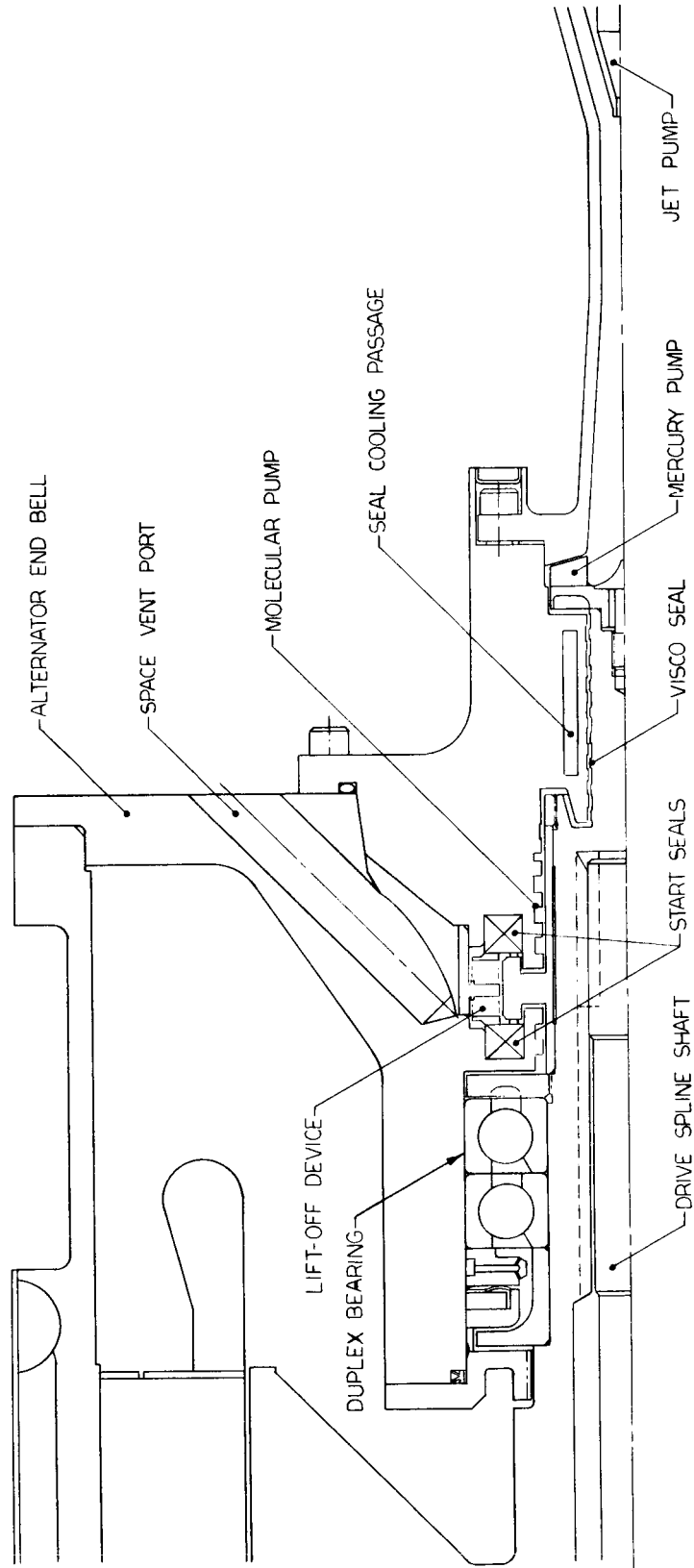
Figure 22



B766-NF-1494

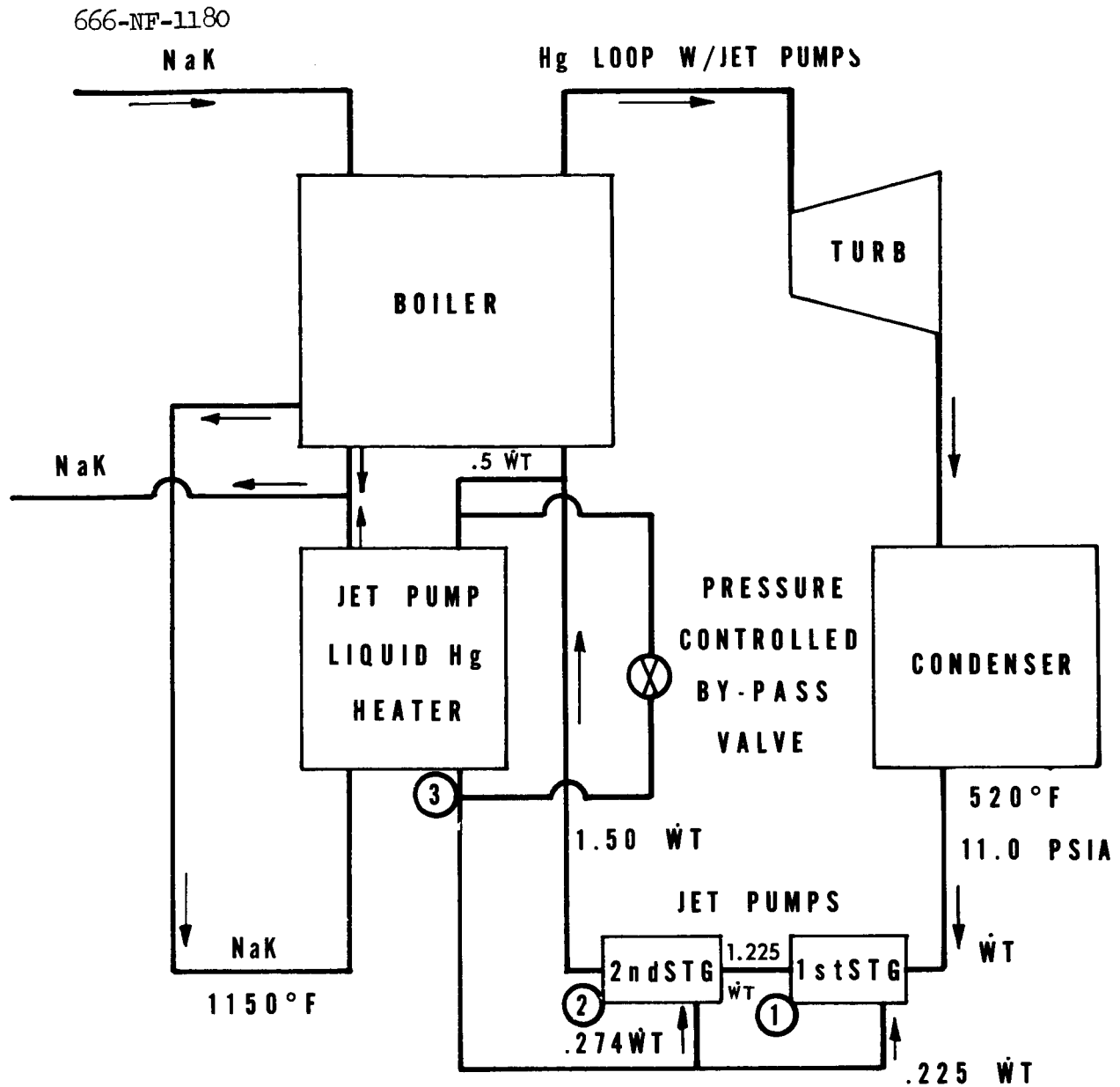
Figure 23

B766-NF-1493



Mercury Pump on Alternator Shaft

Figure 24



$$P_1 = 200 \text{ PSIA}$$

$$T_1 = 615^\circ\text{F}$$

} 1st STAGE DISCHARGE CONDITIONS

$$P_2 = 380 \text{ PSIA}$$

$$T_2 = 703^\circ\text{F}$$

} 2nd STAGE DISCHARGE CONDITIONS

$$P_3 = 350 \text{ PSIA}$$

$$T_3 = 1120^\circ\text{F}$$

} Hg CONDITIONS AT HEATER OUTLET

Flow Diagram of Mercury
Loop Incorporating Jet Pumps

Figure 25

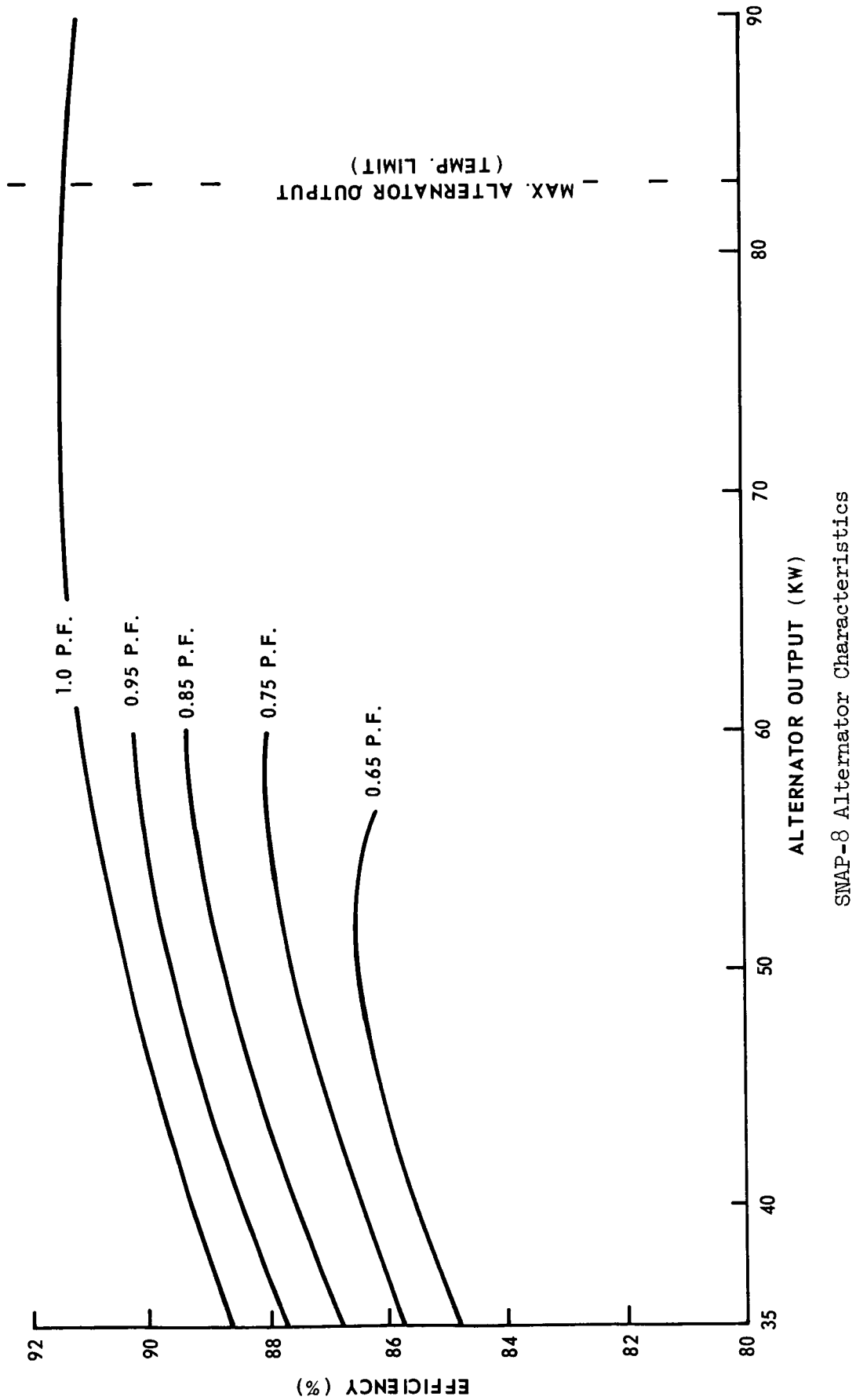
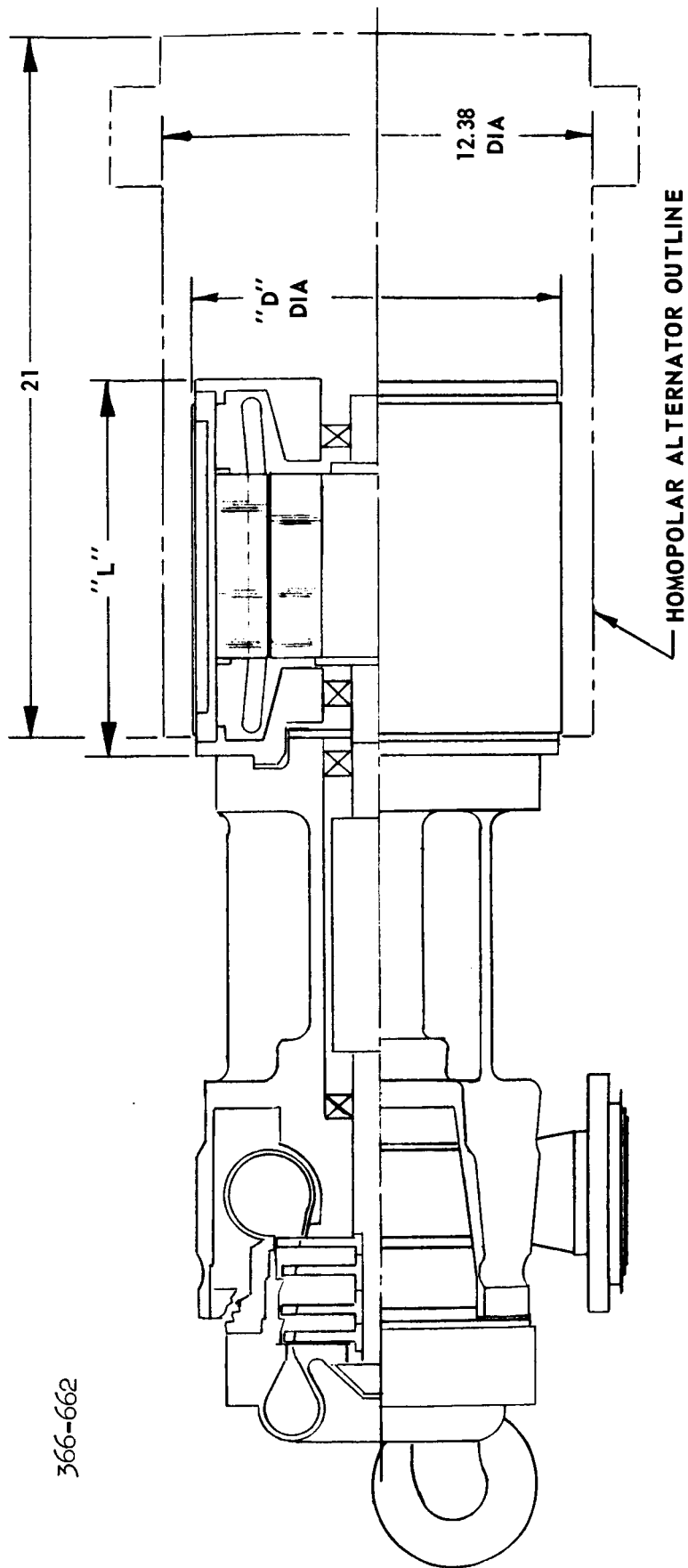


Figure 26



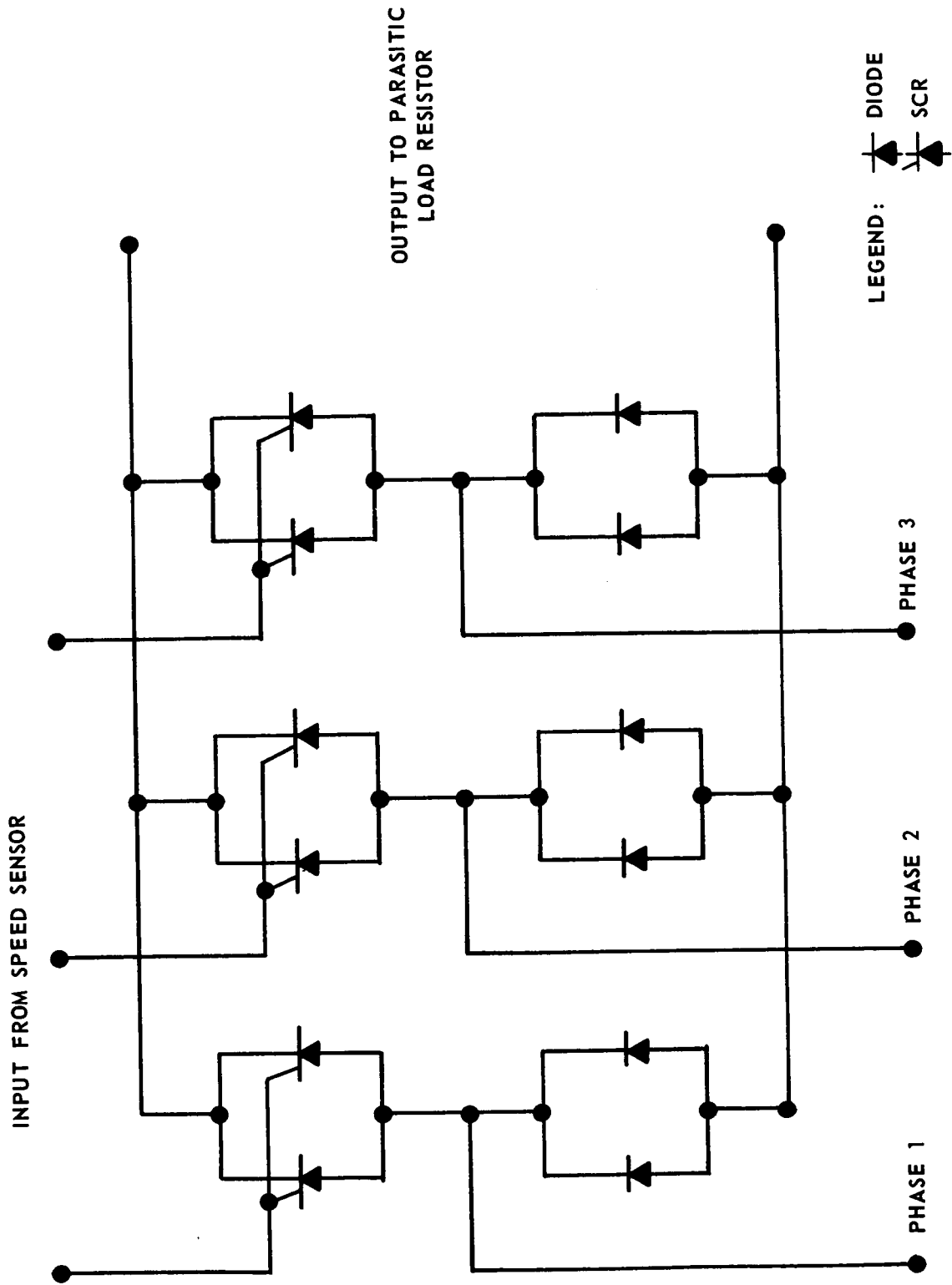
SUMMARY

INDUCTION ALTERNATOR		HOMOPOLAR ALTERNATOR	
	12,000 RPM	24,000 RPM	TOTAL WEIGHT - 445 LB
DIMENSION "L" (INCHES)	15	13	
DIAMETER "D" (INCHES)	10.25	95	
WEIGHT			
INDUCTION ALTERNATOR	220 LB	165 LB	
CAPACITOR - EXCITER	50 LB	50 LB	
TOTAL	270 LB	215 LB	

Comparison of Induction and Homopolar Alternators

Figure 27

267-NF-1315



SCR Speed-Control Schematic

Figure 28

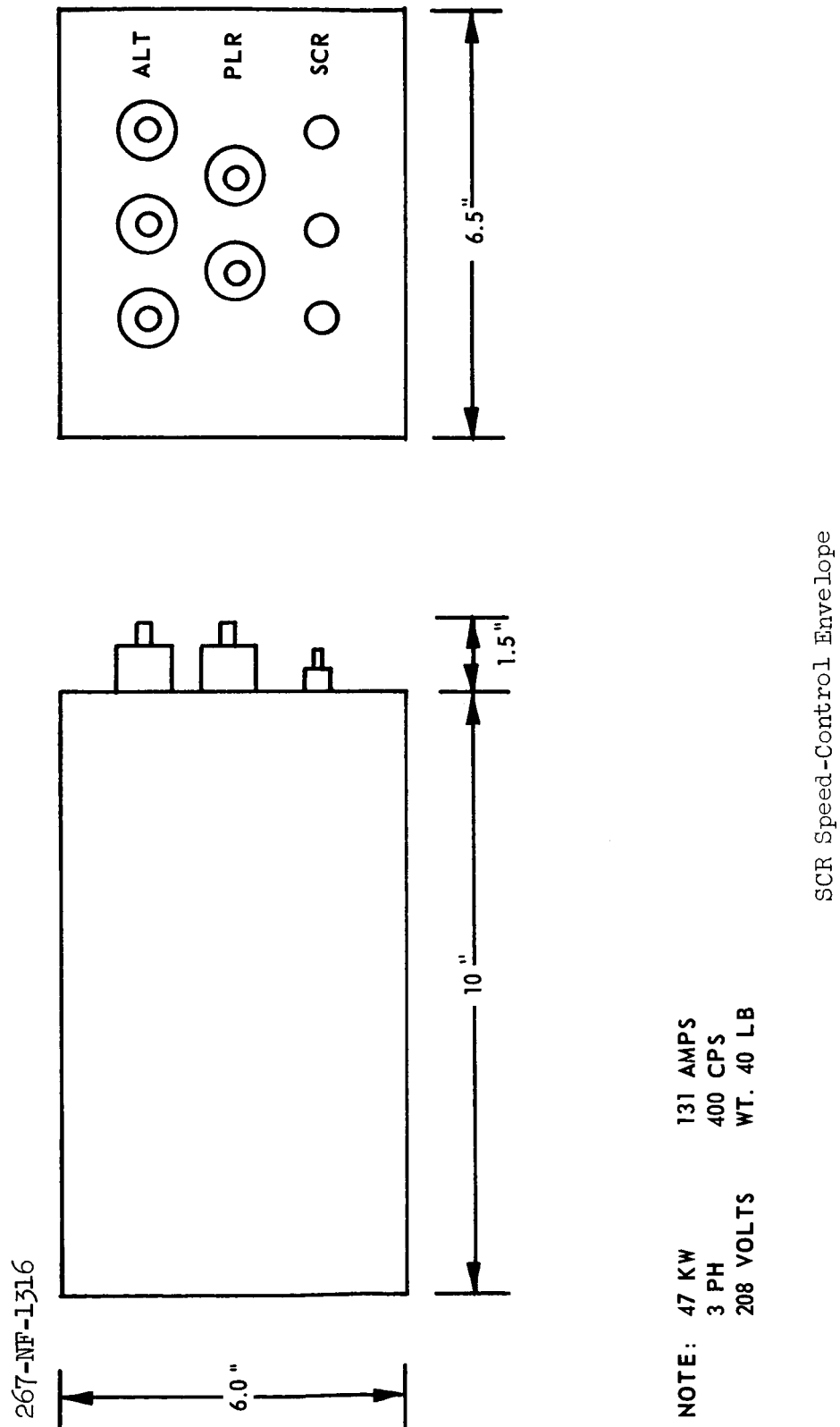


Figure 29

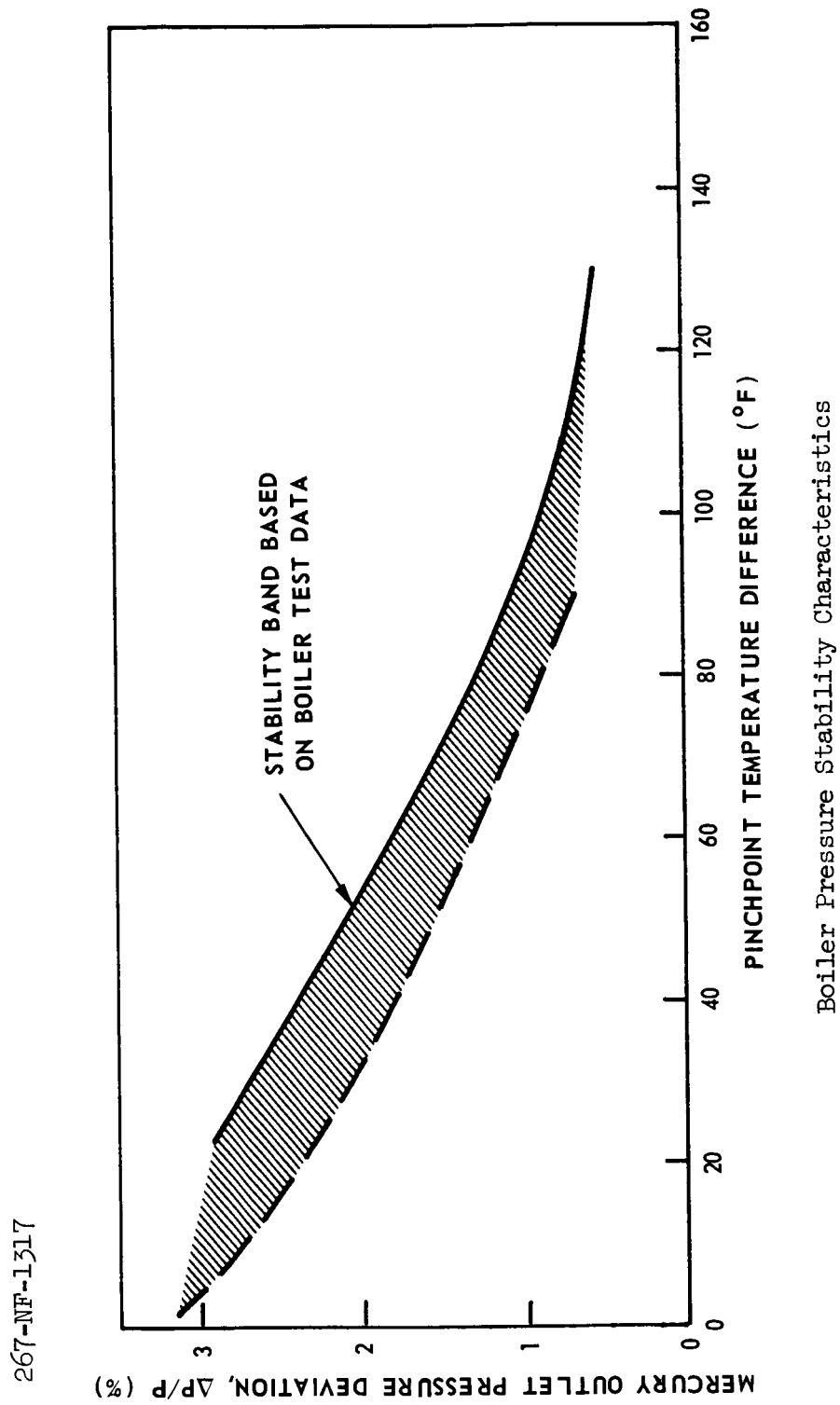
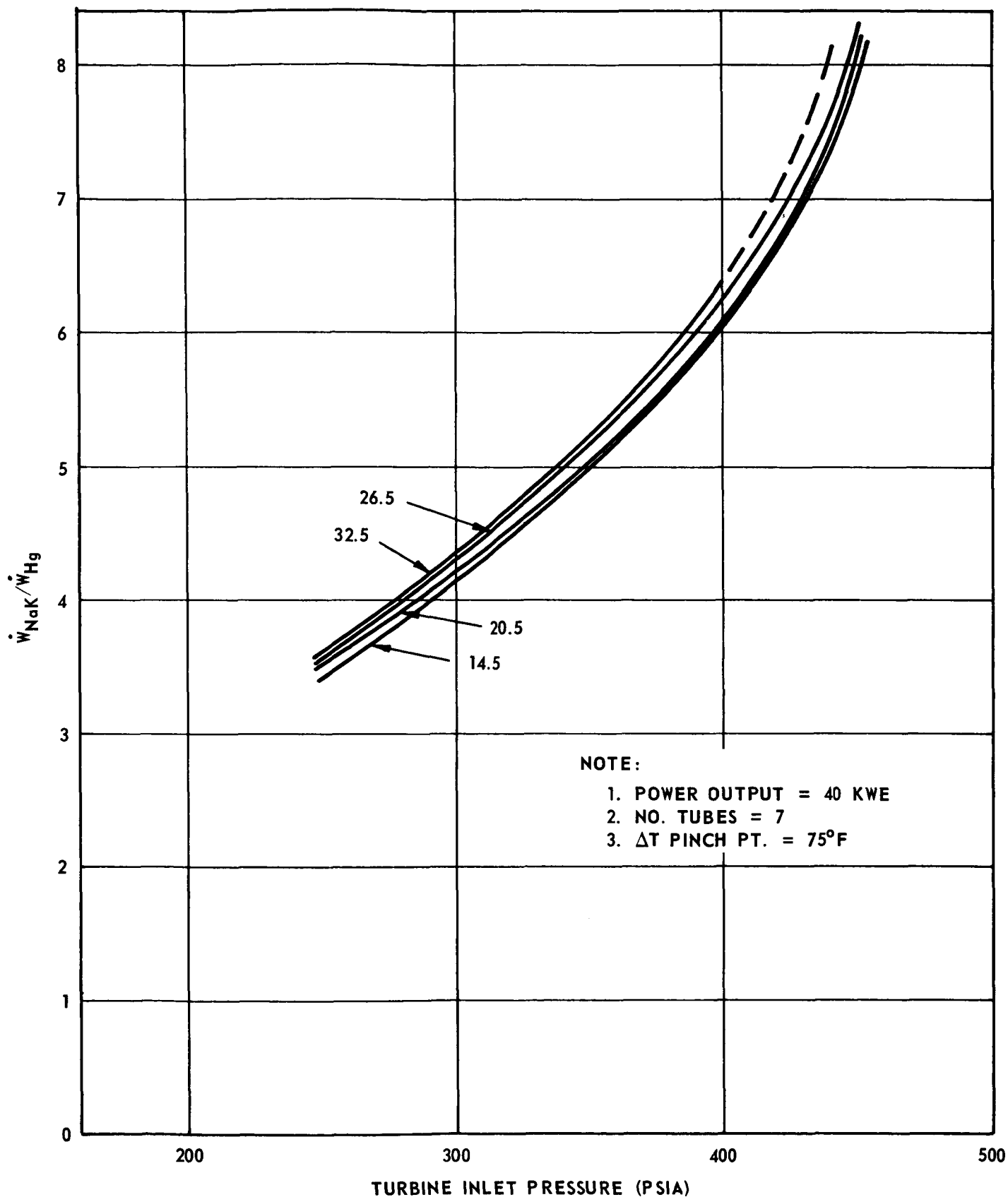


Figure 30

267-NF-1318



Ratio Primary NaK Flow Rate to Mercury Flow
Rate vs Turbine Inlet Pressure

Figure 31

267-NF-1319

NOTE: LOAD POWER FACTOR = 0.75

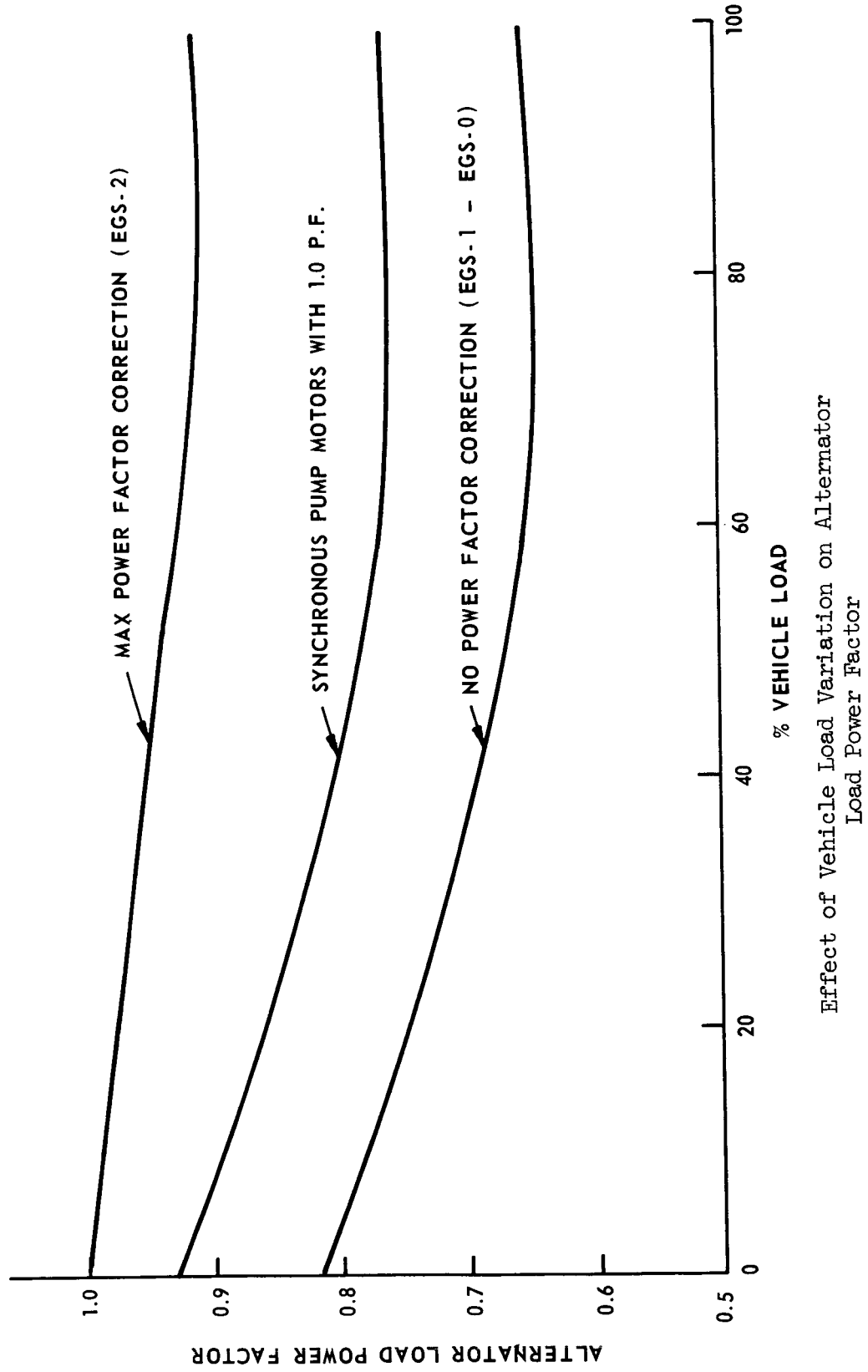
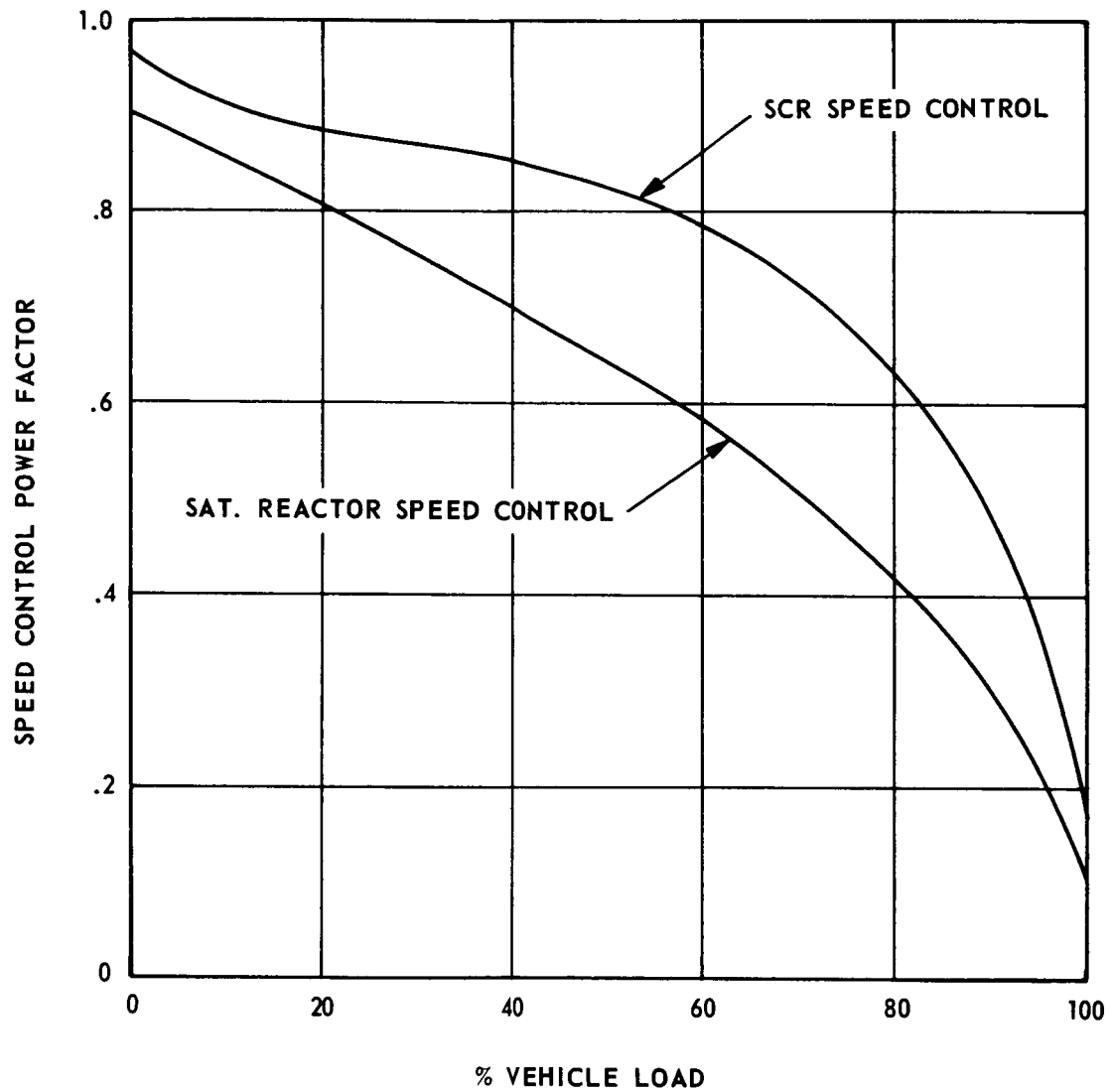


Figure 32

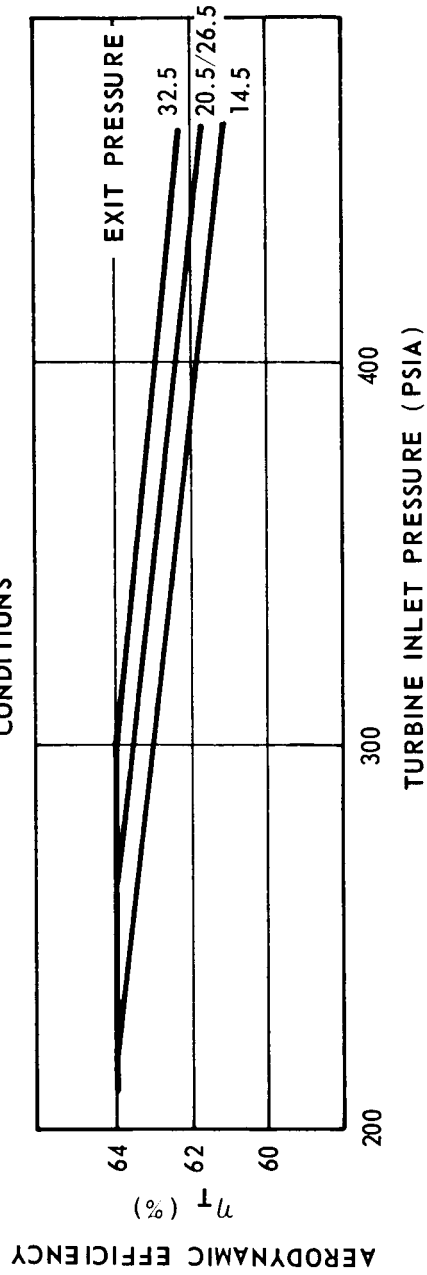
267-NF-1320



Speed Control Power Factor vs Vehicle Load

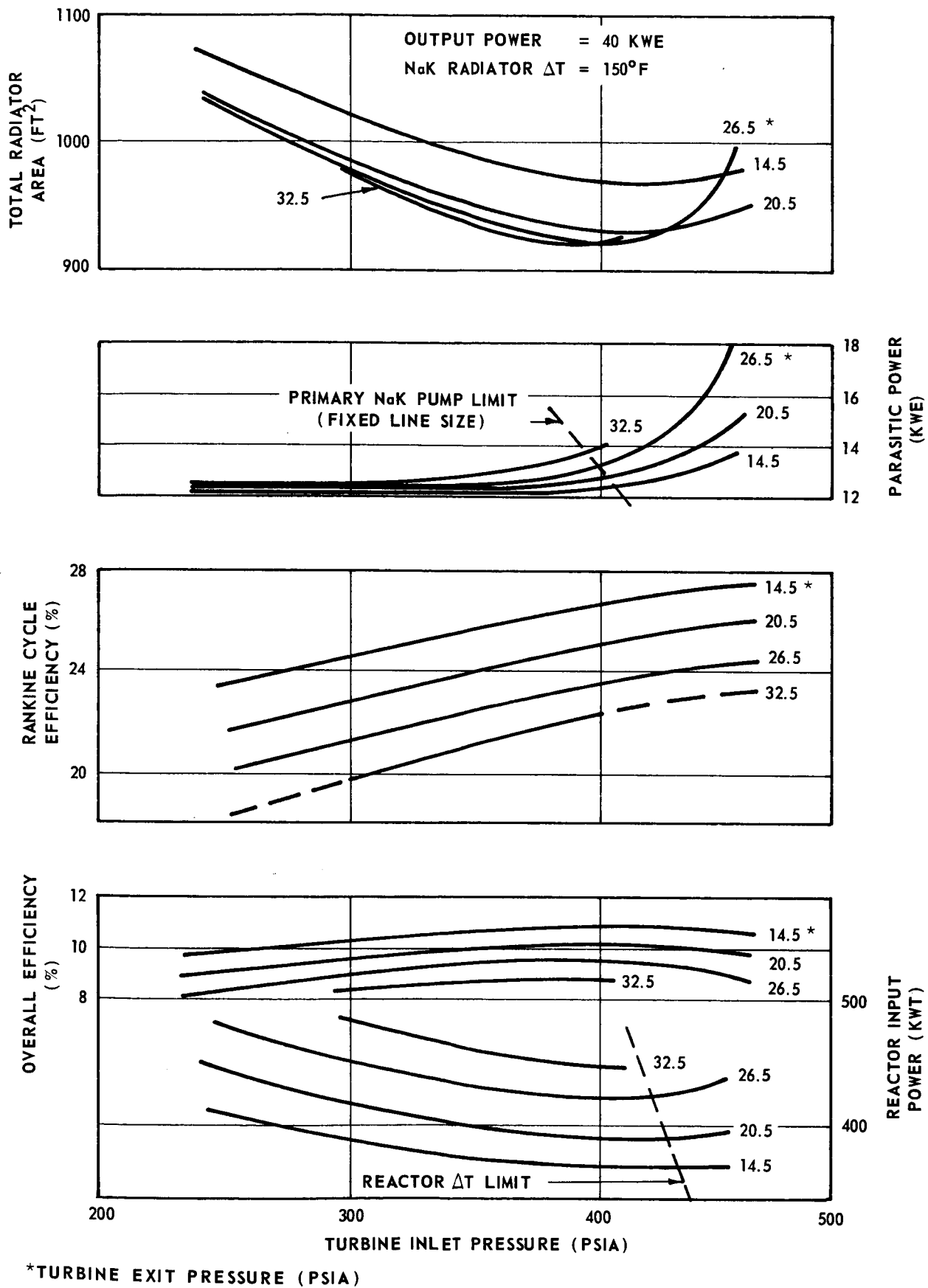
267-NF-1321

NOTE: TURBINE DESIGN PARAMETERS
VARIABLE WITH OPERATING
CONDITIONS



Turbine Aerodynamic Efficiency as a Function of
Inlet and Exit Pressures

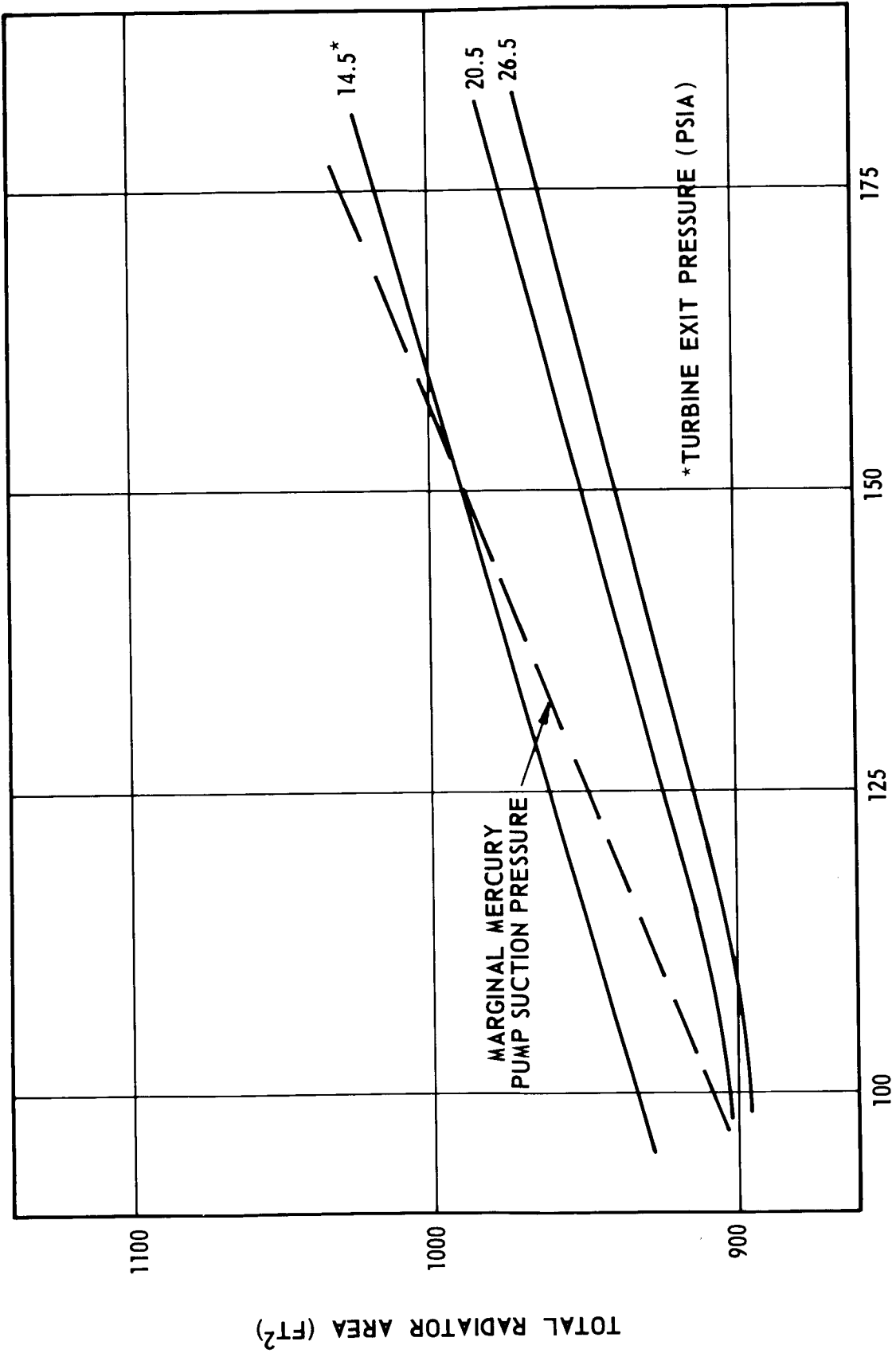
Figure 34



System Characteristics as a Function of Turbine Inlet and Exit Pressures

Figure 35

167-DV-1223

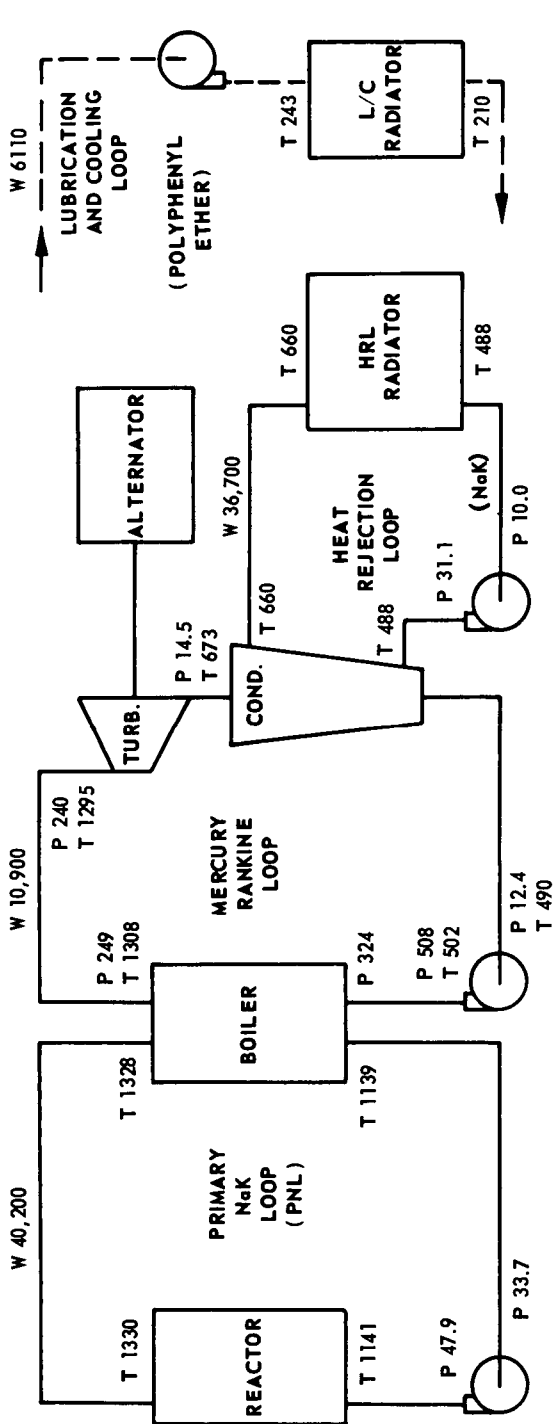


NaK RADIATOR ΔT - °F
Effect of NaK Radiator ΔT and Turbine
Exit Pressure on Radiator Area

Figure 36

267-NF-1323

ALTERNATOR POWER DISTRIBUTION	
SHAFT POWER	67.0 KW
EFFICIENCY	86.1 %
GROSS OUTPUT POWER	57.6 KW
LOAD P. F.	0.64
OUTPUT KVA	90.0
PARASITIC LOAD	TOTAL 19.5 KW
PNL PMA	4.45
Hg PMA	3.53
HRL PMA	4.67
L/C PMA	1.37
PLR	4.50
VOLTAGE CONTROL	0.20
SPEED CONTROL	0.80
NET OUTPUT POWER	38.1 KW



PERFORMANCE SUMMARY

NET REACTOR INPUT TO PCS	467 KWT
NET ELECTRICAL OUTPUT	38.1 KWE
OVERALL SYSTEM EFFICIENCY	8.2 %
EGS WEIGHT	9272 LB
SPECIFIC WEIGHT	243 LB/KWE
HRL RADIATOR AREA	946 FT ²
HEAT REJECTED L/C RADIATOR AREA	392 KWT
HEAT REJECTED TOTAL RADIATOR AREA	362 FT ²
SPECIFIC RADIATOR AREA	21.2 KWT
	1308 FT ²
	34.4 FT ² /KWE

DESCRIPTIVE FEATURES.
(DEPARTURES FROM EGS-O)

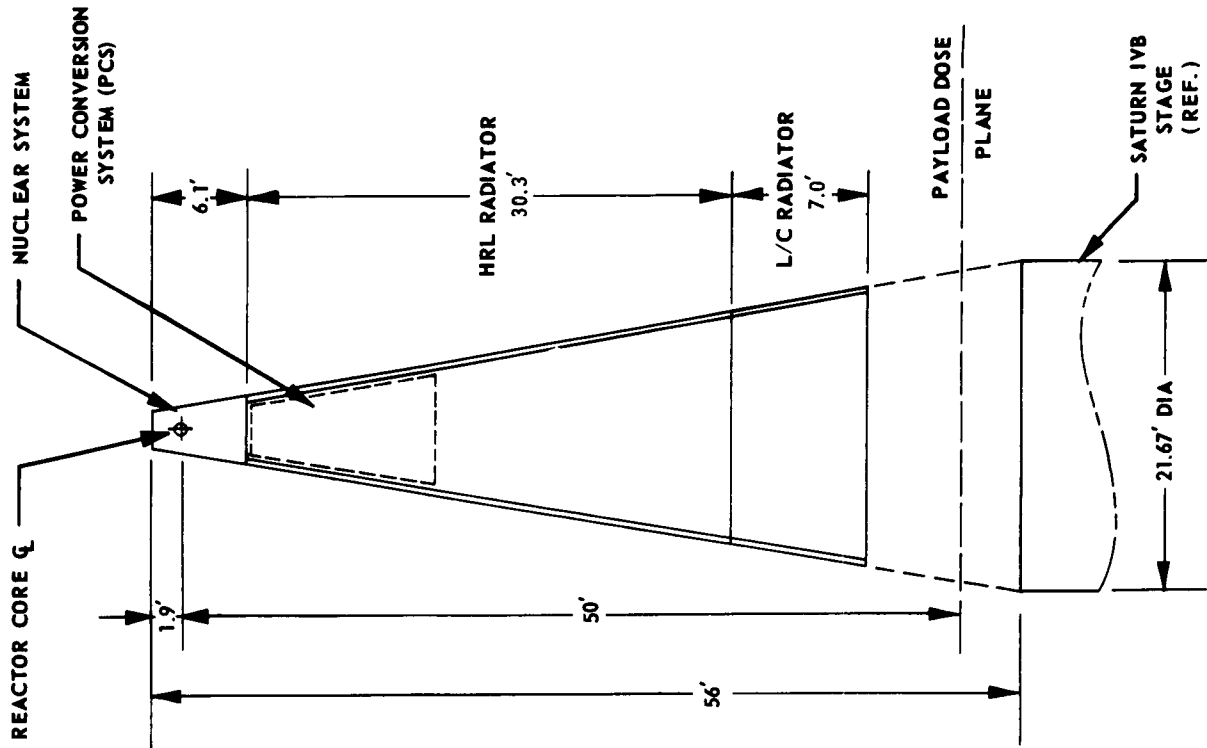
TURBINE AERODYNAMIC EFFICIENCY - 64.4 %
TURBINE FLOW AREAS ADJUSTED FOR \dot{w}

HEAT RADIATED BY L/C RADIATOR, KW

TURBINE BEARINGS & SEALS	3.3
ALTERNATOR ELECTRICAL LOSSES	7.3
BEARINGS & SEALS	2.0
L/C PMA	1.4
Hg PMA	2.3
SPEED CONTROL	0.8
PNL PMA	2.0
HRL PMA	2.1
	21.2

LEGEND

W = FLOW RATE, LB/HR
T = TEMPERATURE, °F
P = PRESSURE, PSIA



CONE HALF-ANGLE = 9.75°

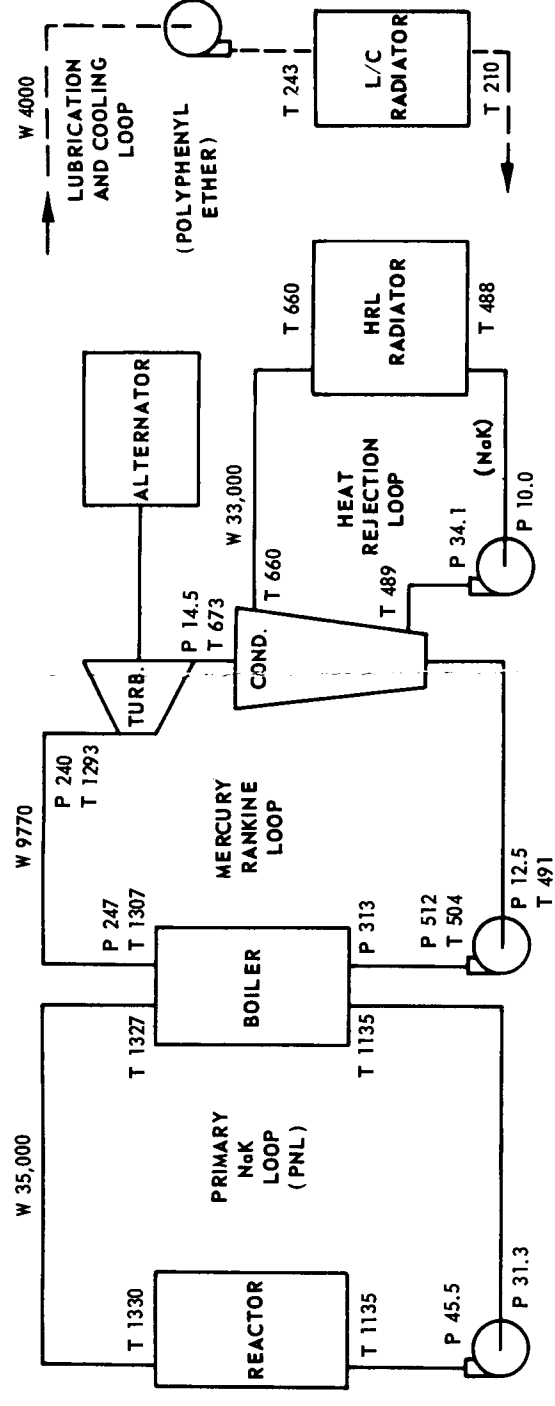
EGS-1 Summary Performance Chart

37-1

Figure 37 -2

ALTERNATOR POWER DISTRIBUTION

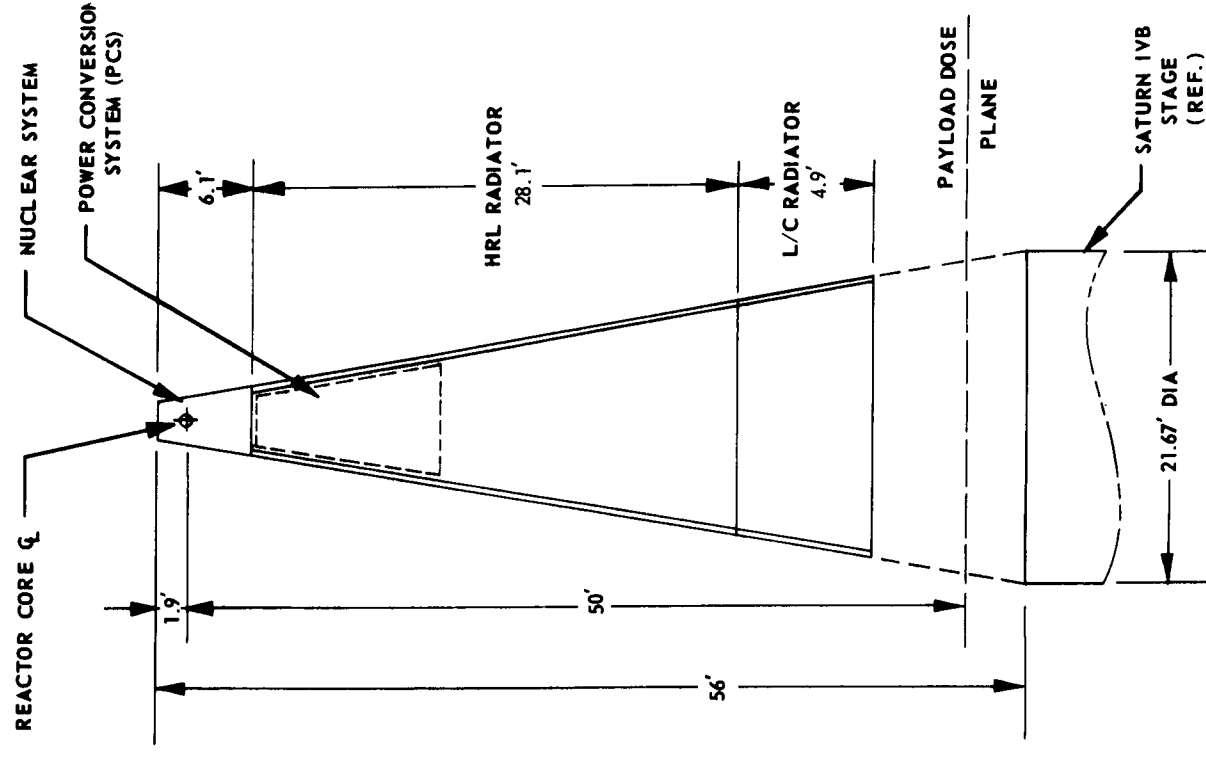
SHAFT POWER		59.4 KW
EFFICIENCY		89.2 %
GROSS OUTPUT POWER		53.0 KW
LOAD P. F.	0.90	
OUTPUT KVA	58.8	
PARASITIC LOAD	TOTAL	13.0 KW
PNL PMA	2.65	
Hg PMA	3.51	
HRL PMA	2.89	
L/C PMA	1.29	
PLR	2.00	
VOLTAGE CONTROL	0.20	
SPEED CONTROL	0.33	
CAPACITOR	0.10	
NET OUTPUT POWER		40.0 KW

DESCRIPTIVE FEATURES
(DEPARTURES FROM EGS-O)

HEAT RADIATED BY L/C RADIATOR, KW	
TURBINE BEARINGS & SEALS	3.30
ALTERNATOR	
ELECTRICAL LOSSES	4.42
BEARINGS & SEALS	2.00
L/C PMA	1.29
H _g PMA	2.27
VOLTAGE CONTROL	0.20
SPEED CONTROL	0.33
CAPACITOR	0.10
	<hr/> 13.91

PERFORMANCE SUMMARY

TURBINE AERODYNAMIC EFFICIENCY - 64.4 %	NET REACTOR INPUT TO PCS	419 KWT
TURBINE FLOW AREAS ADJUSTED FOR w	NET ELECTRICAL OUTPUT	40 KWE
NaK PMA's MODIFIED TO 4800 RPM SYNCHRONOUS MOTORS	OVERALL SYSTEM EFFICIENCY	9.6 %
NaK PMA's COOLED BY HRL NaK	EGS WEIGHT	8896 LBS
ALTERNATOR POWER FACTOR CORRECTED BY CAPACITORS	SPECIFIC WEIGHT	222 LB/KWE
SPEED CONTROL - SILICON CONTROL RECTIFIER (SCR) TYPE	HRL RADIATOR	
	AREA	842 FT ²
	HEAT REJECTED	352 KWT
	L/C RADIATOR	
	AREA	237 FT ²
	HEAT REJECTED	13.9 KWT
	TOTAL RADIATOR AREA	1079 FT ²
	SPECIFIC RADIATOR AREA	27.0 FT ² /KWE



LEGEND

W = FLOW RATE, LB/HR
T = TEMPERATURE, °F
P = PRESSURE, PSIA

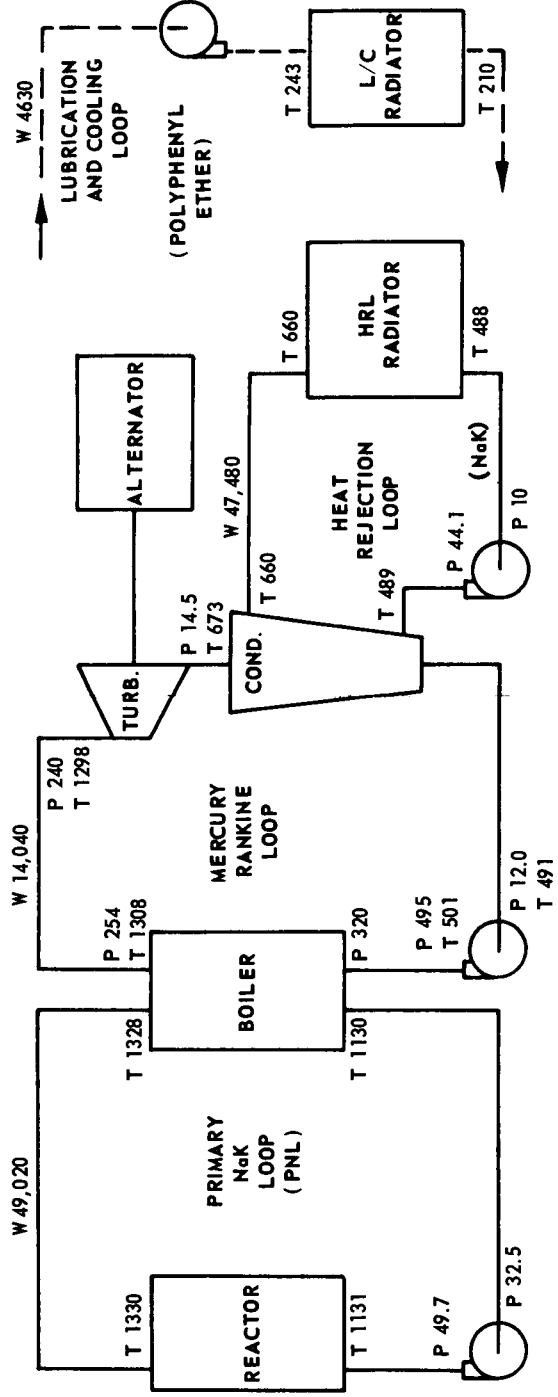
CONE HALF-ANGLE = 9.75°

EGS-2 Summary Performance Chart

267-NF-1325

ALTERNATOR POWER DISTRIBUTION

SHAFT POWER	86.9 KW
EFFICIENCY	90.1 %
GROSS OUTPUT POWER	78.3 KW
LOAD P. F.	0.92
OUTPUT KVA	85.1
PARASITIC LOAD	TOTAL 18.2 KW
PNL PMA	4.69
Hg PMA	3.59
HRL PMA	4.99
L/C PMA	1.31
PLR	3.00
VOLTAGE CONTROL	0.20
SPEED CONTROL	0.33
CAPACITOR	0.10
NET OUTPUT POWER	60.1 KW



HEAT RADIATED BY L/C RADIATOR, KW

TURBINE BEARINGS & SEALS	3.3
ALTERNATOR	
ELECTRICAL LOSSES	6.6
BEARINGS & SEALS	2.0
L/C PMA	1.3
Hg PMA	2.3
SPEED CONTROL	0.3
VOLTAGE CONTROL	0.2
CAPACITOR	0.1
	16.1

LEGEND

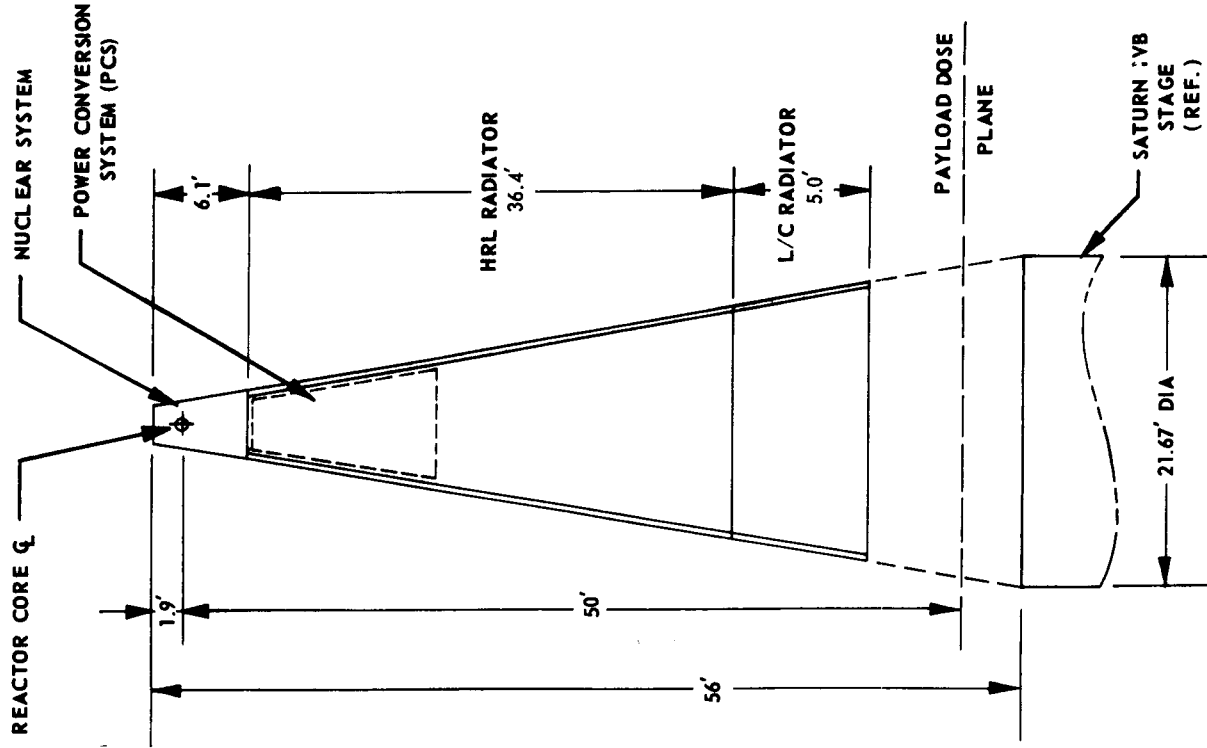
W = FLOW RATE, LB/HR
T = TEMPERATURE, °F
P = PRESSURE, PSIA

DESCRIPTIVE FEATURES
(DEPARTURES FROM EGS-O)

TURBINE AERODYNAMIC EFFICIENCY - 64.4 %
TURBINE FLOW AREAS ADJUSTED FOR \dot{w}
REDUCED ΔP IN PNL AND HRL
NaK PMA's COOLED BY HRL NaK
BOILER SCALED TO HIGHER \dot{w} (9 Hg TUBES)
CONDENSER SCALED TO HIGHER \dot{w} (85 Hg TUBES)
ALTERNATOR POWER FACTOR CORRECTED BY CAPACITORS
SPEED CONTROL SCR TYPE

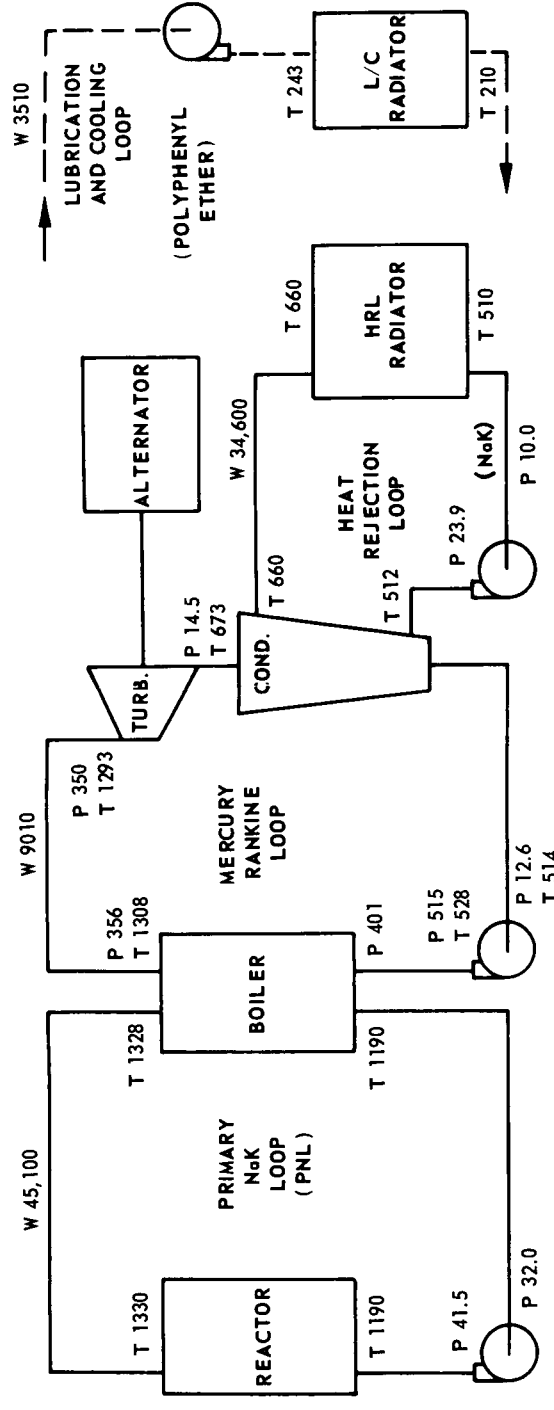
PERFORMANCE SUMMARY

NET REACTOR INPUT TO PCS	600 KWT
NET ELECTRICAL OUTPUT	60.1 KWE
OVERALL SYSTEM EFFICIENCY	10.0 %
EGS WEIGHT	9973 LB
SPECIFIC WEIGHT	166 LB/KWE
HRL RADIATOR	
AREA	1257 FT ²
HEAT REJECTED	507 KWT
L/C RADIATOR	
AREA	284 FT ²
HEAT REJECTED	16.1 KWT
TOTAL RADIATOR AREA	1541 FT ²
SPECIFIC RADIATOR AREA	25.7 FT ² /KWE

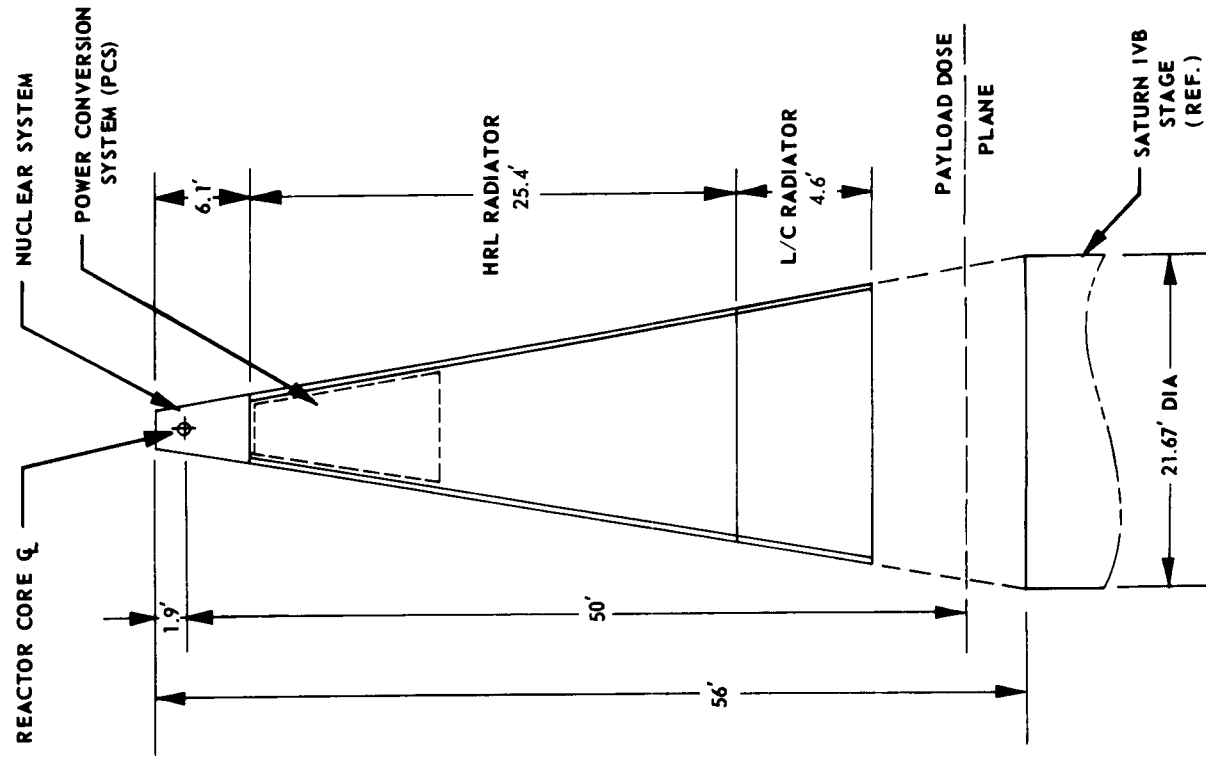


CONE HALF-ANGLE = 9.75°

<u>ALTERNATOR POWER DISTRIBUTION</u>	
SHAFT POWER	57.7 KW
EFFICIENCY	90.5 %
GROSS OUTPUT POWER	52.3 KW
LOAD P. F.	1.0
OUTPUT KVA	52.3
PARASITIC LOAD	TOTAL 12.3 KW
PNL PMA	2.70
Hg PMA	2.76
HRL PMA	2.90
L/C PMA	1.27
PLR	2.00
VOLTAGE CONTROL	0.20
SPEED CONTROL	0.33
CAPACITOR	0.10
NET OUTPUT POWER	40.0 KW



<u>HEAT RADIATED BY L/C RADIATOR, KW</u>		<u>DESCRIPTIVE FEATURES</u> <u>(DEPARTURES FROM EGS-O)</u>	<u>PERFORMANCE SUMMARY</u>
TURBINE BEARINGS & SEALS	3.3	TURBINE AERODYNAMIC EFFICIENCY - 61%	NET REACTOR INPUT TO PCS
ALTERNATOR		TURBINE INLET PRESSURE - 350 PSIA	NET ELECTRICAL OUTPUT
ELECTRICAL LOSSES	3.44	TURBINE FLOW AREAS ADJUSTED FOR \dot{w} AND INLET PRESSURE	OVERALL CYCLE EFFICIENCY
BEARINGS & SEALS	2.0		EGS WEIGHT
L/C PMA	1.27	NaK PMA's MODIFIED TO 4650 RPM INDUCTION MOTOR	SPECIFIC WEIGHT
Hg PMA	1.52	NaK PMA's COOLED BY HRL NaK	HRL RADIATOR
SPEED CONTROL	0.33	ADVANCED REACTOR	AREA
LTCA	0.20	Hg PMA MOTOR SCAVENGER REMOVED	HEAT REJECTED
CAPACITOR	0.10	PARASITIC LOAD RESISTOR IN HR LOOP	L/C RADIATOR
		ALTERNATOR PF CORRECTED BY CAPACITORS	AREA
	12.16	SPEED CONTROL SCR TYPE	HEAT REJECTED
		RADIATOR NaK $\Delta T = 150^{\circ}F$	TOTAL RADIATOR AREA
			SPECIFIC RADIATOR AREA



LEGEND

W = FLOW RATE, LB/HR
 T = TEMPERATURE, °F
 P = PRESSURE, PSIA

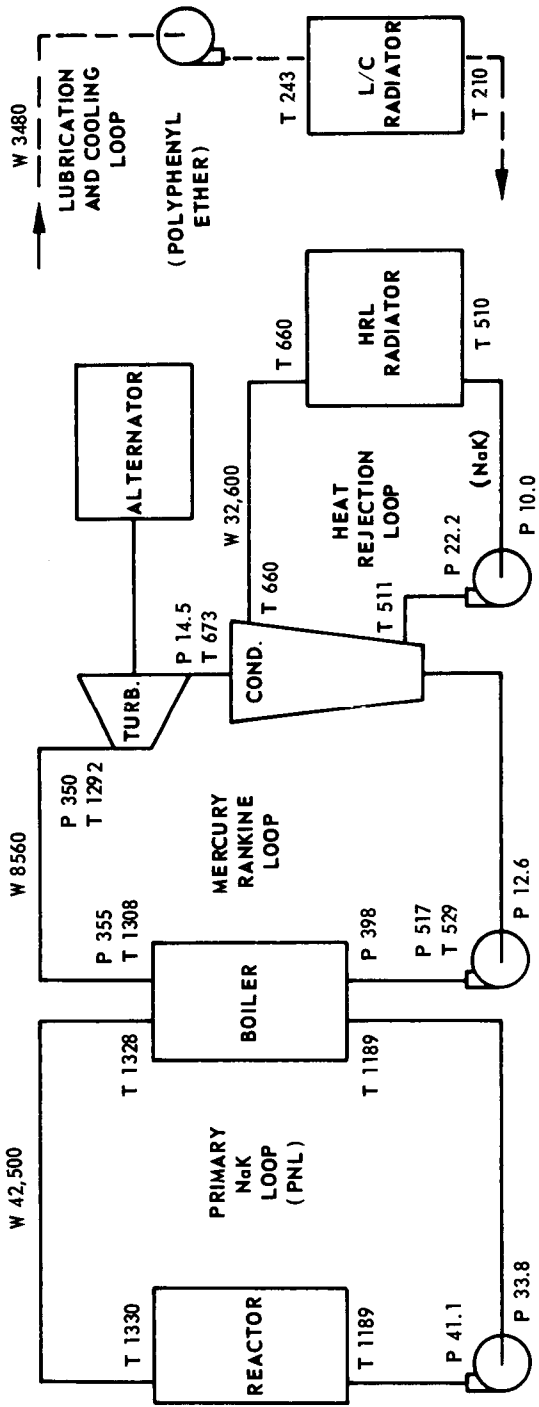
CONE HALF-ANGLE = 9.75°

EGS-4 Summary Performance Chart

Figure 40-2

267-NF-1328

ALTERNATOR POWER DISTRIBUTION		
SHAFT POWER	56.1 KW	
EFFICIENCY	90.4 %	
GROSS OUTPUT POWER	50.7 KW	
LOAD P. F.	1.0	
OUTPUT KVA	50.7	
PARASITIC LOAD		TOTAL 10.7 KW
PNL PMA	1.97	
Hg PMA	2.76	
HRL PMA	2.11	
L/C PMA	1.27	
PLR	1.95	
VOLTAGE CONTROL	0.20	
SPEED CONTROL	0.33	
CAPACITOR	0.10	
NET OUTPUT POWER		40.0 KW



DESCRIPTIVE FEATURES
(DEPARTURES FROM EGS-O)

TURBINE AERODYNAMIC EFFICIENCY - 62.5%
TURBINE INLET PRESSURE - 350 PSIA
TURBINE FLOW AREAS ADJUSTED FOR \dot{w} AND INLET PRESSURE
REDUCED ΔP IN PNL AND HRL
NaK PMA's CUSTOM DESIGNED FOR LOOP ΔP AND \dot{w}
NaK PMA's COOLED BY HRL NaK
Hg PMA MOTOR SCAVENGER REMOVED
ADVANCED REACTOR
PARASITIC LOAD RESISTOR IN HR LOOP
ALTERNATOR POWER FACTOR CORRECTED BY CAPACITORS
SPEED CONTROL - SCR TYPE
RADIATOR NaK $\Delta T = 150^\circ F$

PERFORMANCE SUMMARY

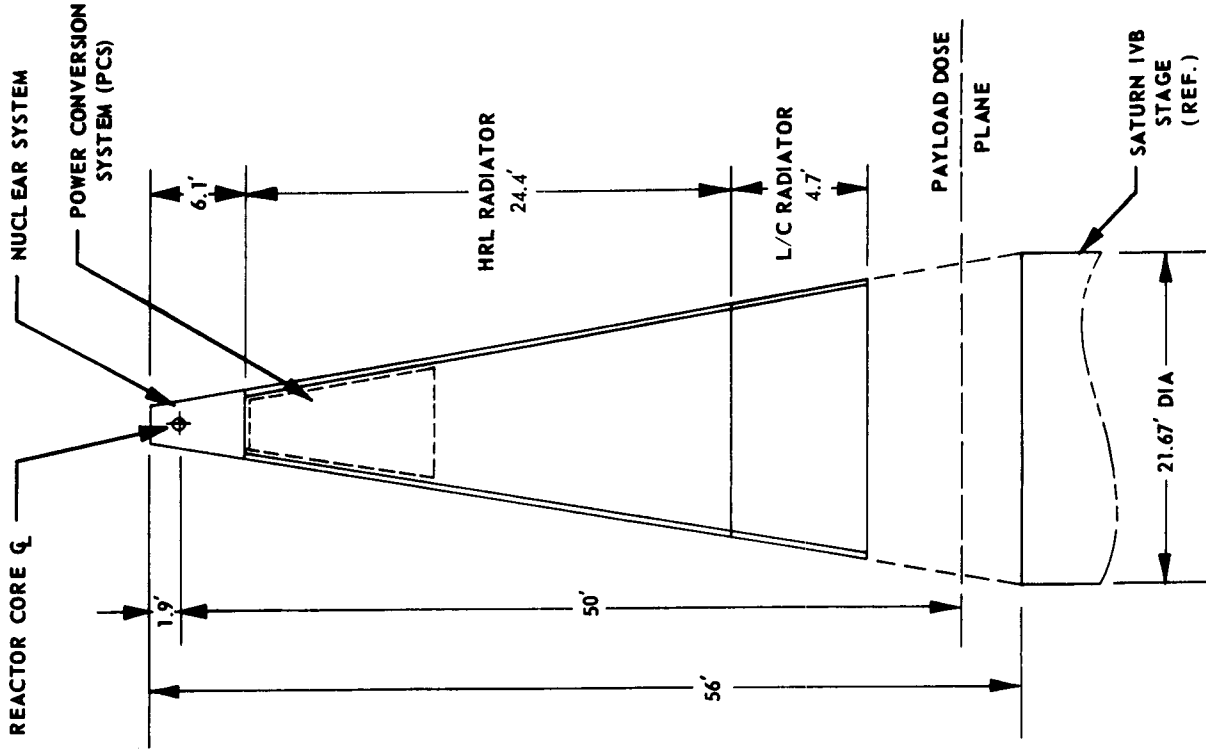
NET REACTOR INPUT TO PCS 368 KWT
NET ELECTRICAL OUTPUT 40 KWE
OVERALL CYCLE EFFICIENCY 10.9 %
EGS WEIGHT 8699 LB
SPECIFIC WEIGHT 217 LB/KWE
HRL RADIATOR
AREA 682 FT²
HEAT REJECTED 304 KWT
L/C RADIATOR
AREA 206 FT²
HEAT REJECTED 12.1 KWT
TOTAL RADIATOR AREA 888 FT²
SPECIFIC RADIATOR AREA 22.2 FT²/KWE

HEAT RADIATED BY L/C RADIATOR, KW

TURBINE BEARINGS & SEALS	3.30
ALTERNATOR	
ELECTRICAL LOSSES	3.39
BEARINGS & SEALS	2.00
L/C PMA	1.27
Hg PMA	1.52
SPEED CONTROL	0.33
LTCA	0.20
CAPACITOR	0.10
	12.11

LEGEND

W = FLOW RATE, LB/HR
T = TEMPERATURE, °F
P = PRESSURE, PSIA

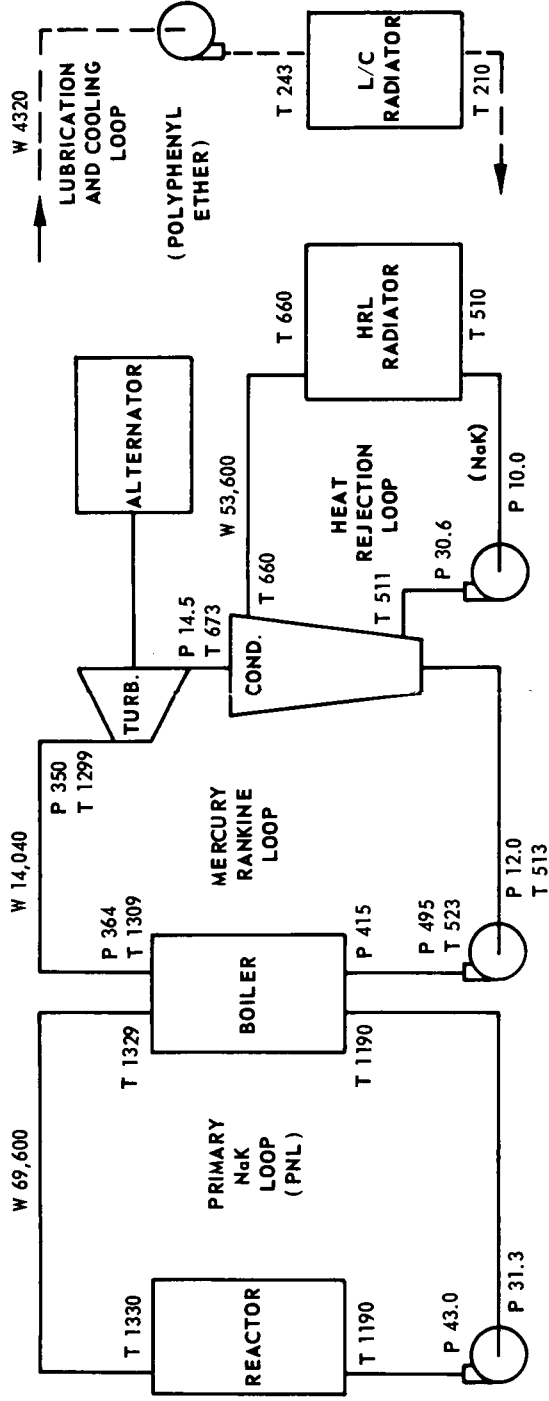


CONE HALF-ANGLE = 9.75°

EGS-5 Summary Performance Chart

267-NF-1329

ALTERNATOR POWER DISTRIBUTION	
SHAFT POWER	94.3 KW
EFFICIENCY	91.3 %
GROSS OUTPUT POWER	86.1 KW
LOAD P. F.	1.0
OUTPUT KVA	86.1
PARASITIC LOAD	TOTAL 15.0 KW
PNL PMA	3.28
Hg PMA	2.85
HRL PMA	3.61
L/C PMA	1.30
PLR	3.31
VOLTAGE CONTROL	0.20
SPEED CONTROL	0.33
CAPACITOR	0.10
NET OUTPUT POWER	71.1 KW



HEAT RADIATED BY L/C RADIATOR, KW	
TURBINE BEARINGS & SEALS	3.30
ALTERNATOR	6.20
ELECTRICAL LOSSES	2.00
BEARINGS & SEALS	1.30
L/C PMA	1.57
Hg PMA	0.33
SPEED CONTROL	0.20
LTCA	0.10
CAPACITOR	15.00

DESCRIPTIVE FEATURES
(DEPARTURES FROM EGS-0)

TURBINE AERODYNAMIC EFFICIENCY - 62.5%

TURBINE INLET PRESSURE - 350 PSIA

TURBINE FLOW AREAS ADJUSTED FOR \dot{w} AND INLET PRESSURE

REDUCED ΔP IN PNL AND HRL

NaK PMA's CUSTOM DESIGNED FOR LOOP ΔP AND \dot{w}

NaK PMA's COOLED BY HRL NaK

Hg PMA MOTOR SCAVENGER REMOVED

BOILER SCALED TO HIGHER \dot{w} (9 Hg TUBES)

CONDENSER SCALED TO HIGHER \dot{w} (85 Hg TUBES)

ADVANCED REACTOR

PARASITIC LOAD RESISTOR IN HR LOOP

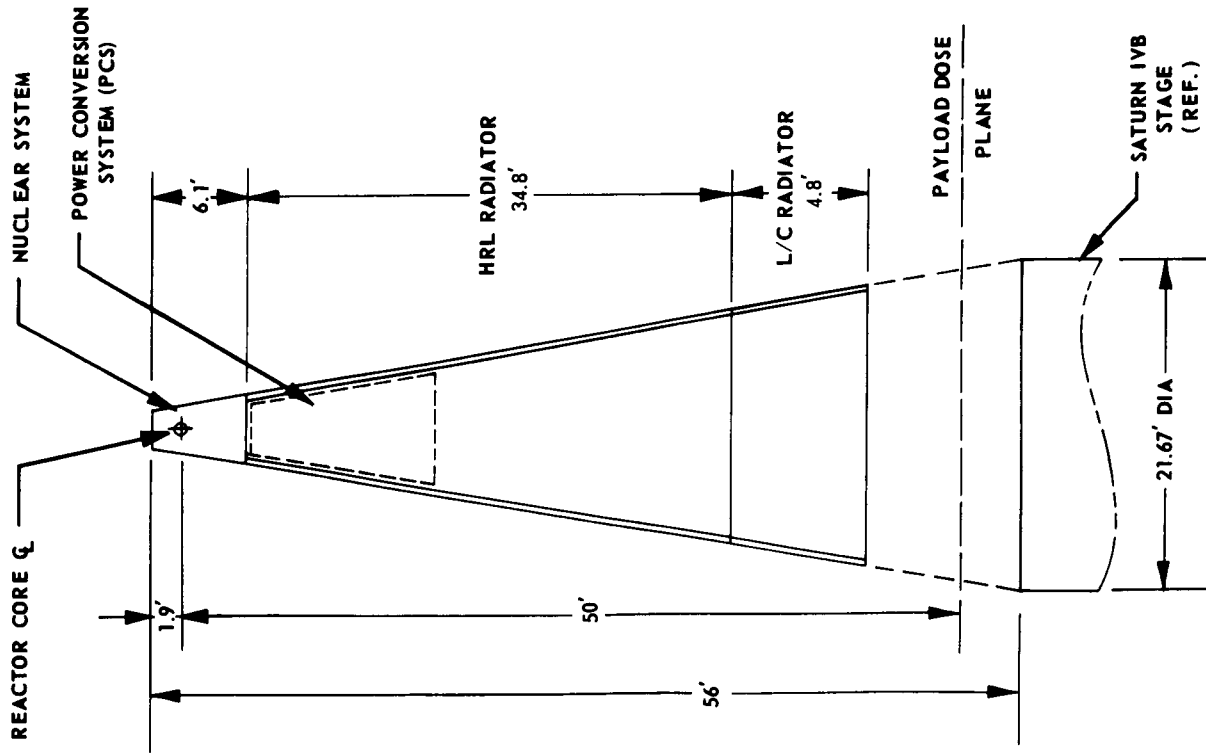
ALTERNATOR POWER FACTOR CORRECTED BY CAPACITORS

SPEED CONTROL - SCR TYPE

RADIATOR NaK $\Delta T = 150^\circ F$

PERFORMANCE SUMMARY

NET REACTOR INPUT TO PCS	600 KWT
NET ELECTRICAL OUTPUT	71.1 KWE
OVERALL SYSTEM EFFICIENCY	11.9 %
EGS WEIGHT	9959 LB
SPECIFIC WEIGHT	140 LB/KWE
HRL RADIATOR AREA	1173 FT ²
HEAT REJECTED	499 KWT
L/C RADIATOR AREA	267 FT ²
HEAT REJECTED	15.0 KWT
TOTAL RADIATOR AREA	1440 FT ²
SPECIFIC RADIATOR AREA	20.2 FT ² /KWE



LEGEND
W = FLOW RATE, LB/HR
T = TEMPERATURE, °F
P = PRESSURE, PSIA

CONE HALF-ANGLE = 9.75°

EGS-6 Summary Performance Chart

TV SATELLITE

267-NF-1330

22,300 MILE ORBIT

$2 \pm .1$ DEG BEAM WIDTH

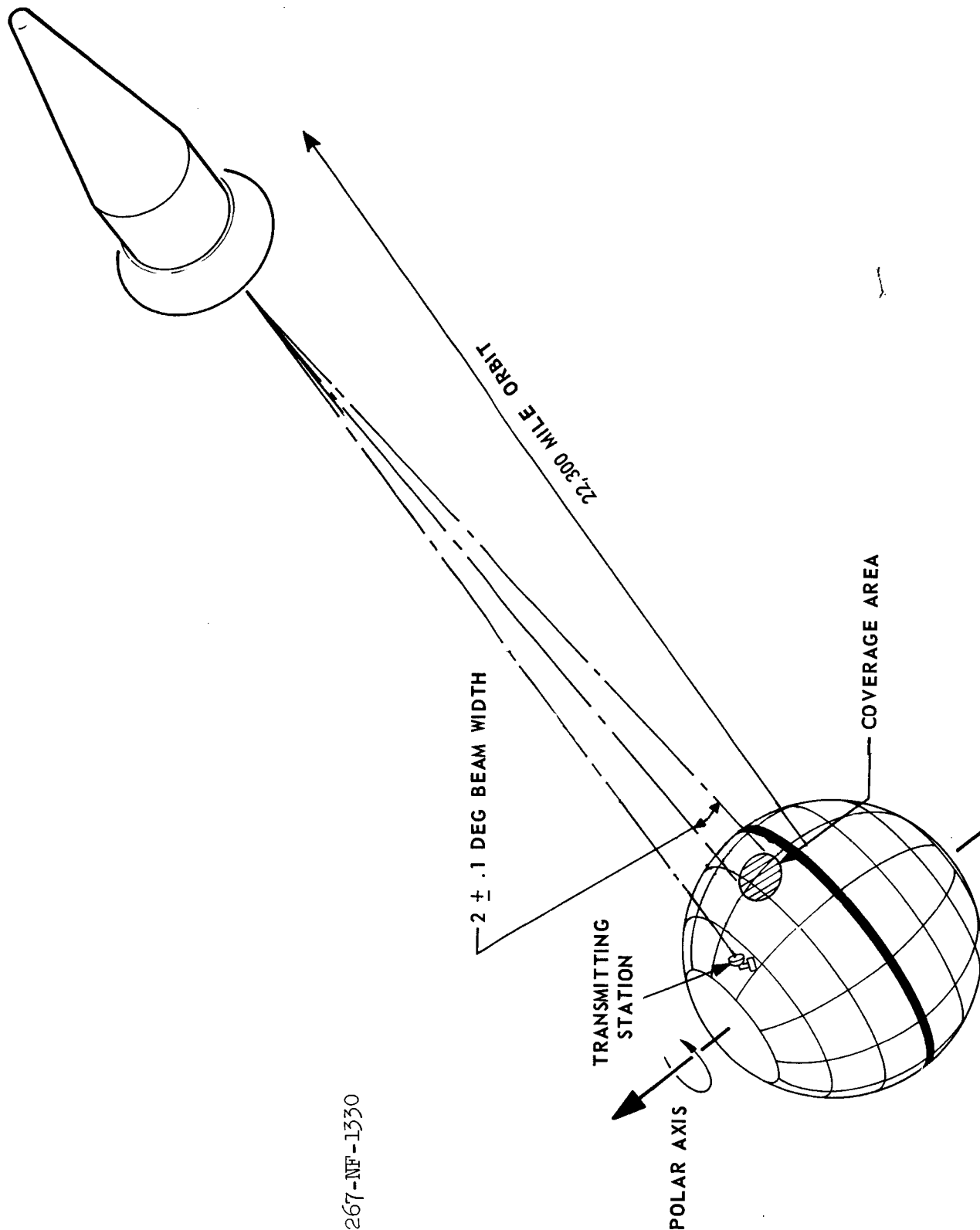
TRANSMITTING
STATION

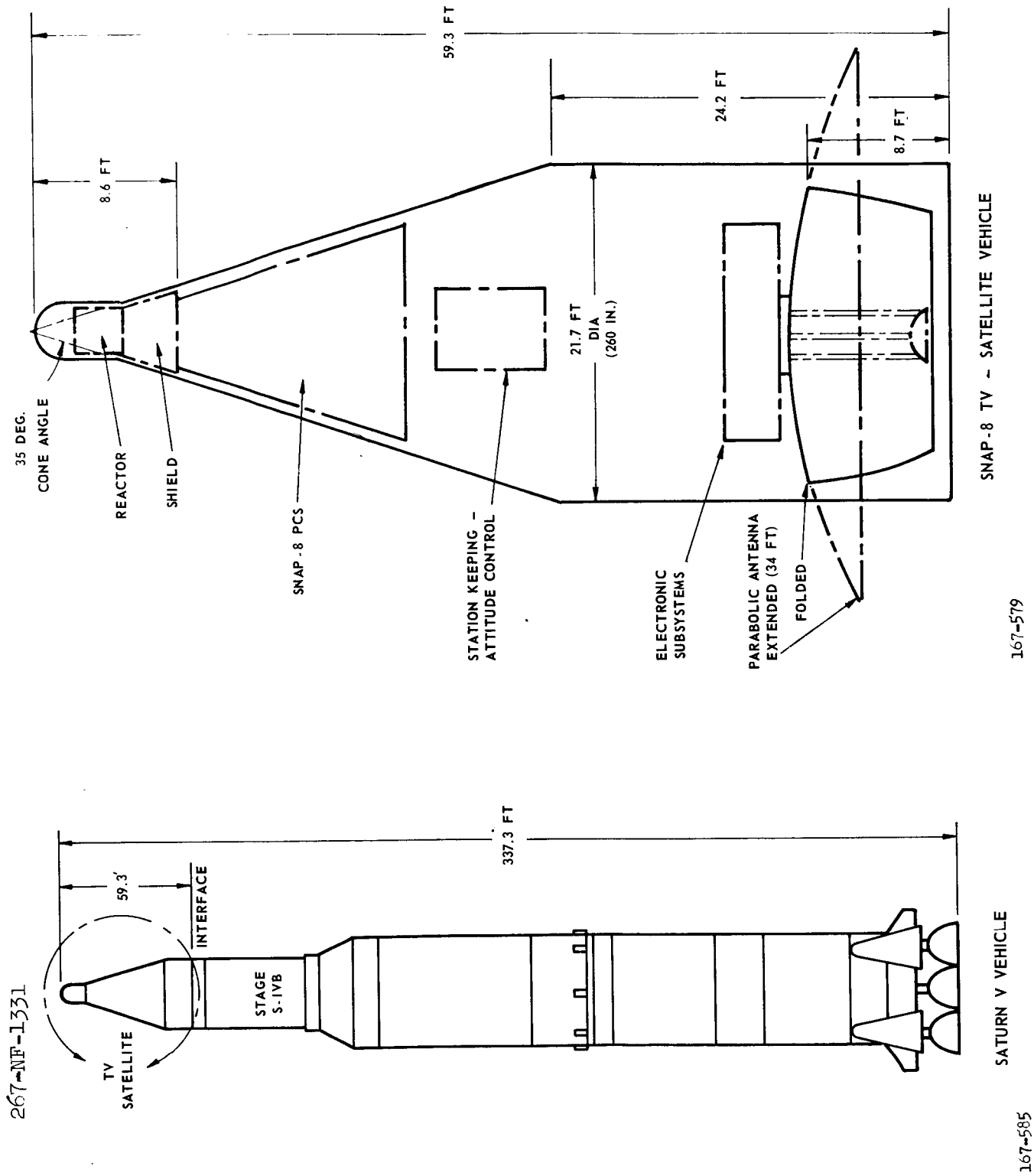
POLAR AXIS

COVERAGE AREA

Diagram of TV Satellite in Synchronous Orbit

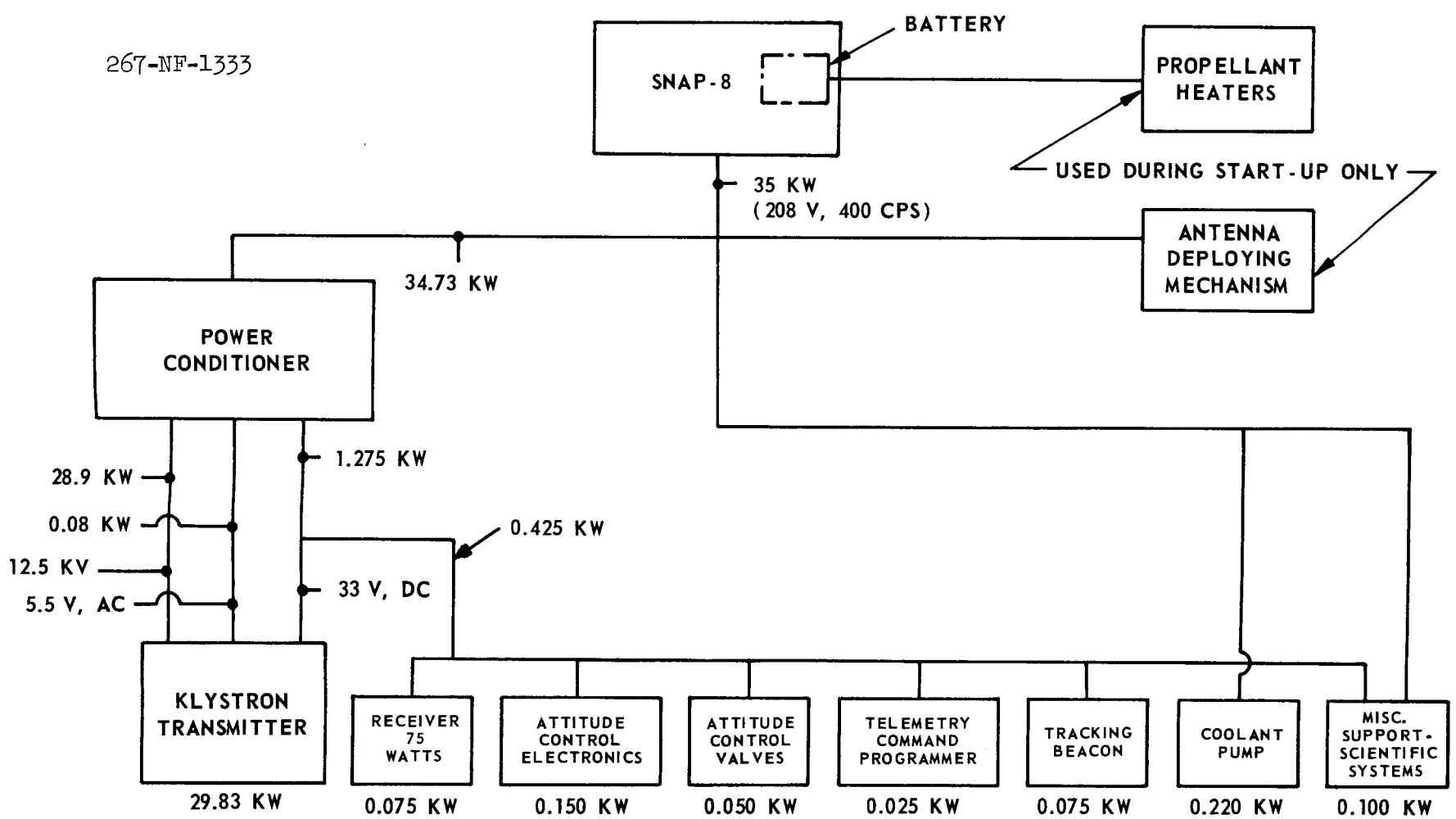
Figure 43



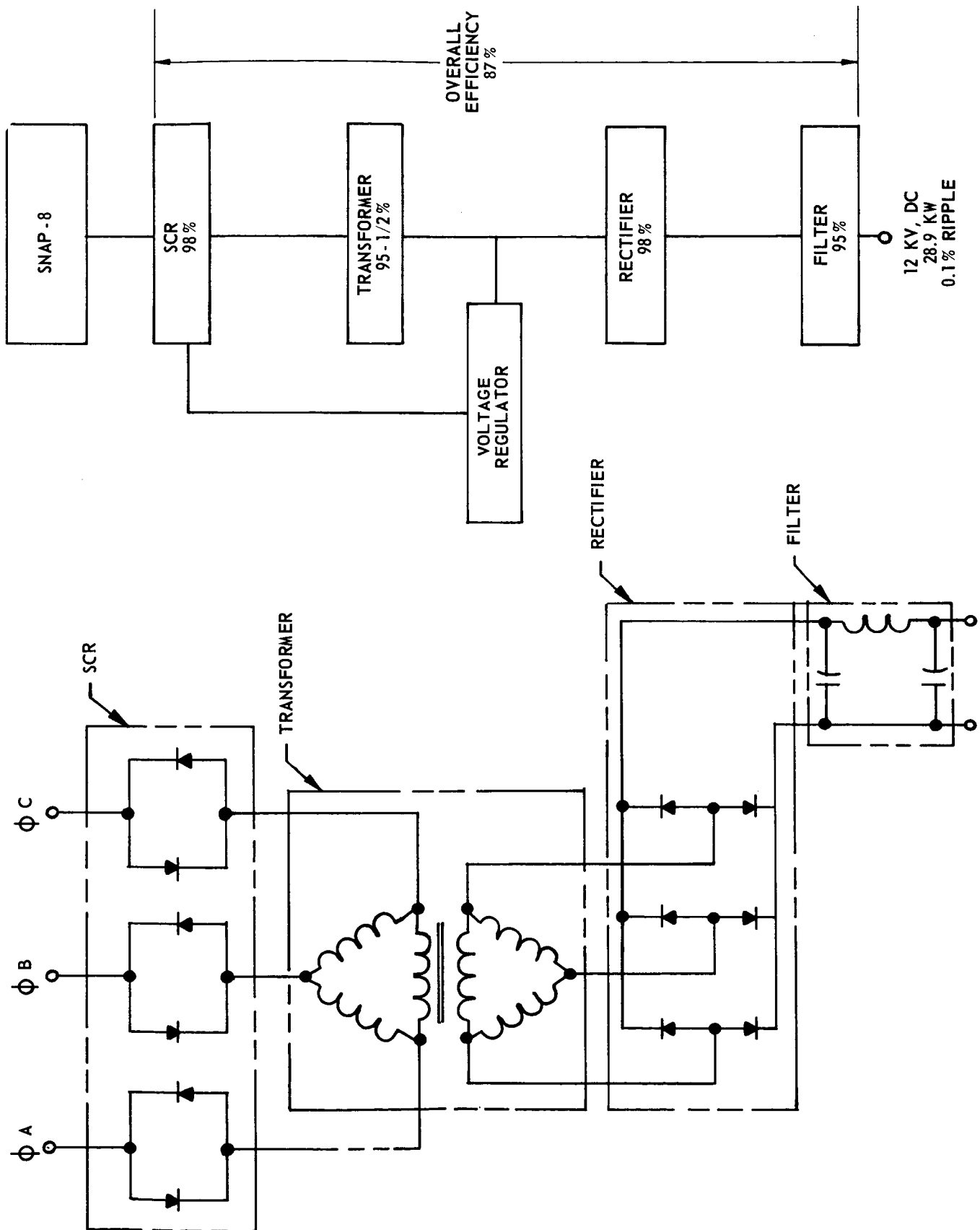


Saturn V Vehicle (Left) and Enlarged
View of SNAP-8 TV-Satellite Vehicle (Right)

Figure 44



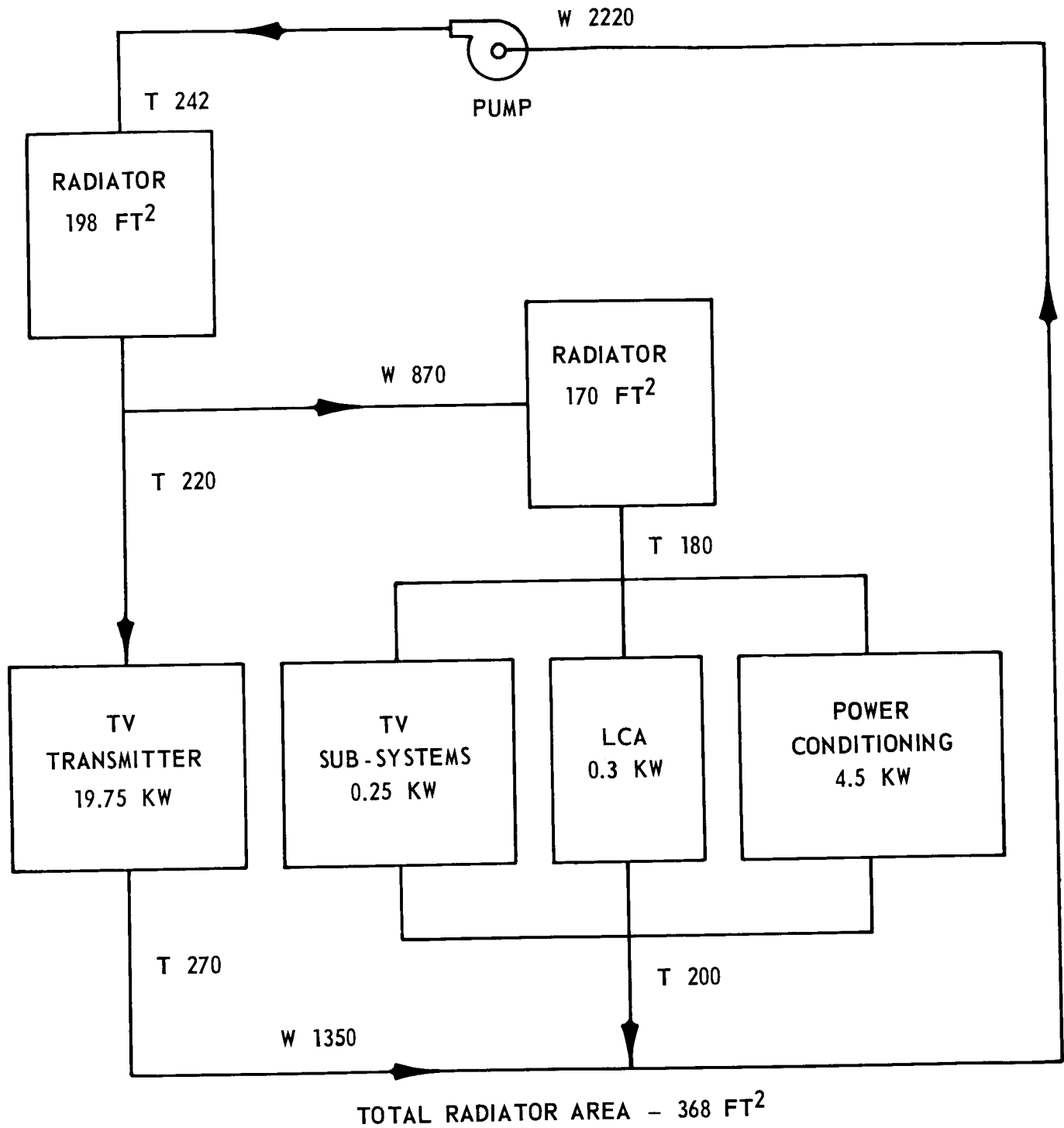
Electrical Power Distribution



Power Conditioning System Diagram

Figure 47

167-586



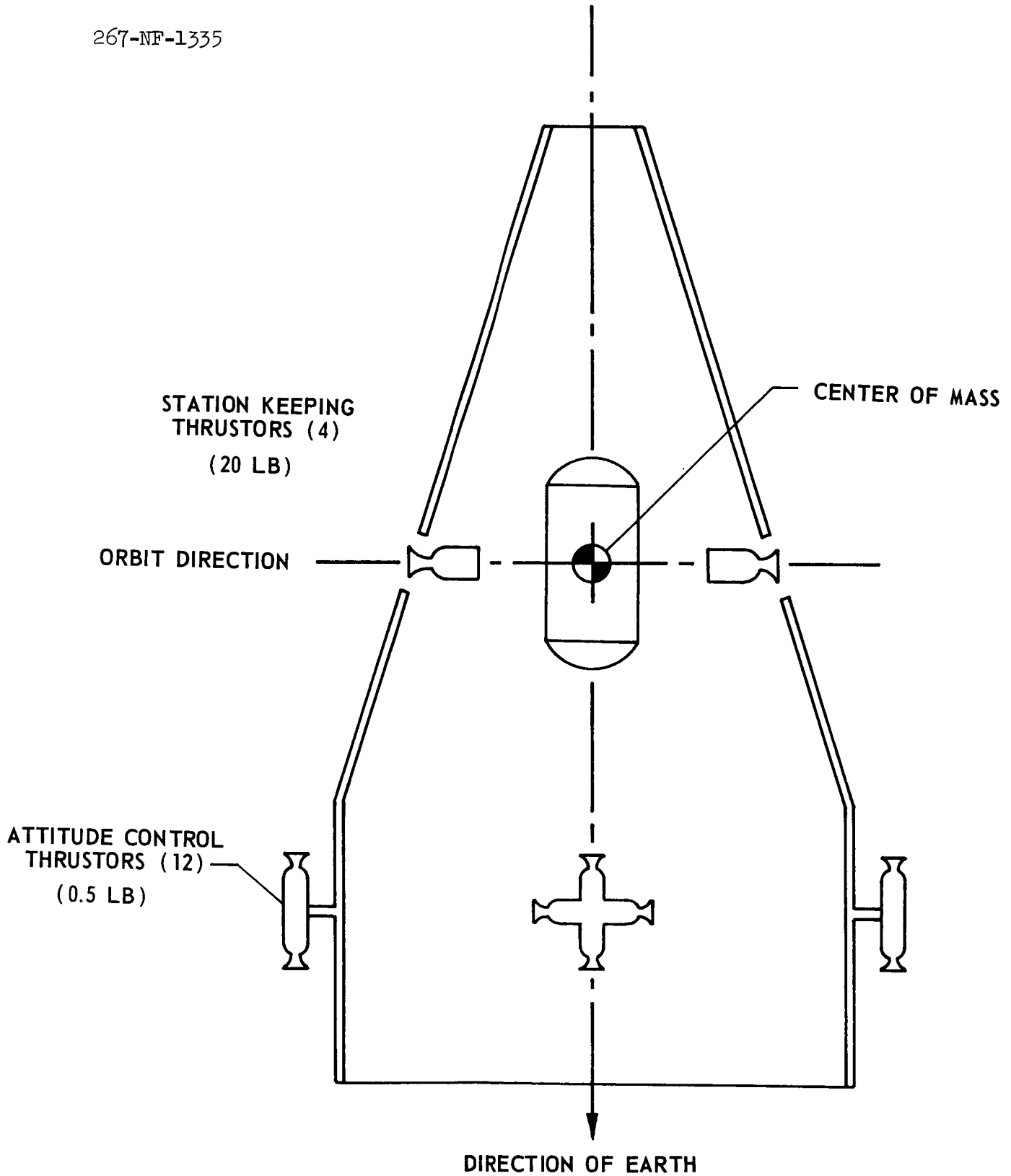
LEGEND

W = FLOW RATE, LB/HR
T = TEMPERATURE, °F

TV Subsystem Water Cooling Circuit

Figure 48

267-NF-1335



Attitude Control System Diagram

APPENDIX A

METEOROID PROTECTION CRITERIA*

The protection of radiators from critical damage due to meteoroid impact is composed of two fields of study. First, the definition of the meteoroid hazard in terms of particle mass, flux, density, and effective velocity, and second, the definition of high velocity impact in terms of damage mechanisms for various target-projectile combinations.

I. METEOROID HAZARD

Analysis of the meteoroid population in terms of the above-mentioned variables has led to the following values to be used for radiator protection purposes:

The cumulative frequency $F>$, is expressed as a function of the meteoroid mass m , by an equation of the form,

$$F> = \alpha m^{-\beta} \quad (1)$$

where α and β are experimentally determined constants. For $F>$ expressed in units of the number of particle impacts per day of mass m or larger, on a target of one square foot of area, the constants α and β are,

$$\alpha = 5.3 \times 10^{-11}$$

$$\beta = 1.34$$

These are the Whipple 1963A values without earth shielding. The value of meteoroid density considered most applicable to this range of the meteoroid population is that given by Verniani as $\rho_p = 0.2 \text{ g/cm}^3$.

*The information in this Appendix is taken from a NASA-Lewis Research Center Memorandum from S. Lieblein, Chief, Flow Analysis Branch, Fluid System Components Division to Charles J. Daye, Space Power Systems Division, same subject, dated August 20, 1965.

Analysis of the available photographic meteor data currently being conducted indicates that the particle velocity in the vicinity of the Earth's orbit has an effective value for penetration calculations of between 17 and 20 km/sec. Until a final value is obtained, 20 km/sec (65,500 ft/sec) is recommended for use.

Comprehensive discussions of the meteoroid population in the photographic meteor range can be found in NASA TN D-2958 by N. Clough and S. Lieblein, and in reports in preparation by C. D. Miller. An analysis of the entire meteoroid population currently is available in a technical note by I. Loeffler and S. Lieblein, currently in editorial committee review.

II. IMPACT DAMAGE

The second area requiring definition, that of high-velocity impact, has been studied experimentally under NASA contract with the aim of generating comparative design information for space radiator meteoroid protection.

Potential damage under space operating conditions has been defined for conventional material radiators as inner surface dimple, spall, and perforation. Extensive investigation into various materials has yielded required thicknesses for prevention of inner surface damage, as well as for the materials correlating coefficient for the penetration relations.

The calculations of required armor thickness for a single material can be obtained from the following equation along with the various constants obtained from the above described program.

$$t_a = \frac{a}{2.54} \gamma \left(\frac{6}{\pi}\right)^{1/3} \rho_p^{-1/3} \left(\frac{62.4 \rho_p}{\rho_t}\right)^{1/2} \left(\frac{V}{C}\right)^{2/3} \left(\frac{\alpha A \tau}{\ln P(0)}\right)^{1/3\beta} \left(\frac{1}{\beta + 1}\right)^{1/3\beta} \quad (2)$$

where

t_a = required armor thickness in inches

a = damage thickness factor

γ = materials correlating coefficient

ρ_p = 0.2 g/cm³

ρ_t = target material density lb/ft³

$$V = 65,500 \text{ fps}$$

$$C = 12 \sqrt{E_t g / \rho_t} \text{ sonic velocity of target material where } E_t \text{ is Young's modulus at operating temperature in lb/in.}^2 \text{ and } g \text{ is } 32.2 \text{ ft/sec}^2$$

$$\alpha = 5.3 \times 10^{-11}$$

$$\beta = 1.34$$

$$A = \text{external surface area of armor (ft}^2\text{)}$$

$$\tau = \text{mission time in days}$$

$$P(o) = \text{design probability of no critical damage}$$

The constants a and γ vary from material to material and with damage mode. Materials coefficients for use in Equation (2) obtained for aluminum at room temperature are summarized in the following tabulation.

<u>Material</u>	<u>γ</u>
7075-T6 Al	1.99
2024-T6 Al	1.86
6061-T6 Al	1.80
356-T51 Al (Cast)	2.27

At a temperature of 700°F, the values of γ tend to increase by about 10 percent.

Equation (2) can also be used for the calculation of armor thickness for lined aluminum tubes with a correct choice of the damage factor a . For cast aluminum armor over 316-stainless steel liners, .028" thick, the inner surface of the liner will not spall. In general, the inner surface integrity is not lost, even at complete closure of the tube. Values of the damage thickness factor as a function of dimple height produced in the liner are given in Figure A-1. A recommended value of a is 1.5, which represents a dimple height of about 20 percent the diameter. In using this value, however, it is implied that the Alfin bonded configuration is comparable to the cast bond configuration of the impact target.

III. FIN-TUBE GEOMETRY

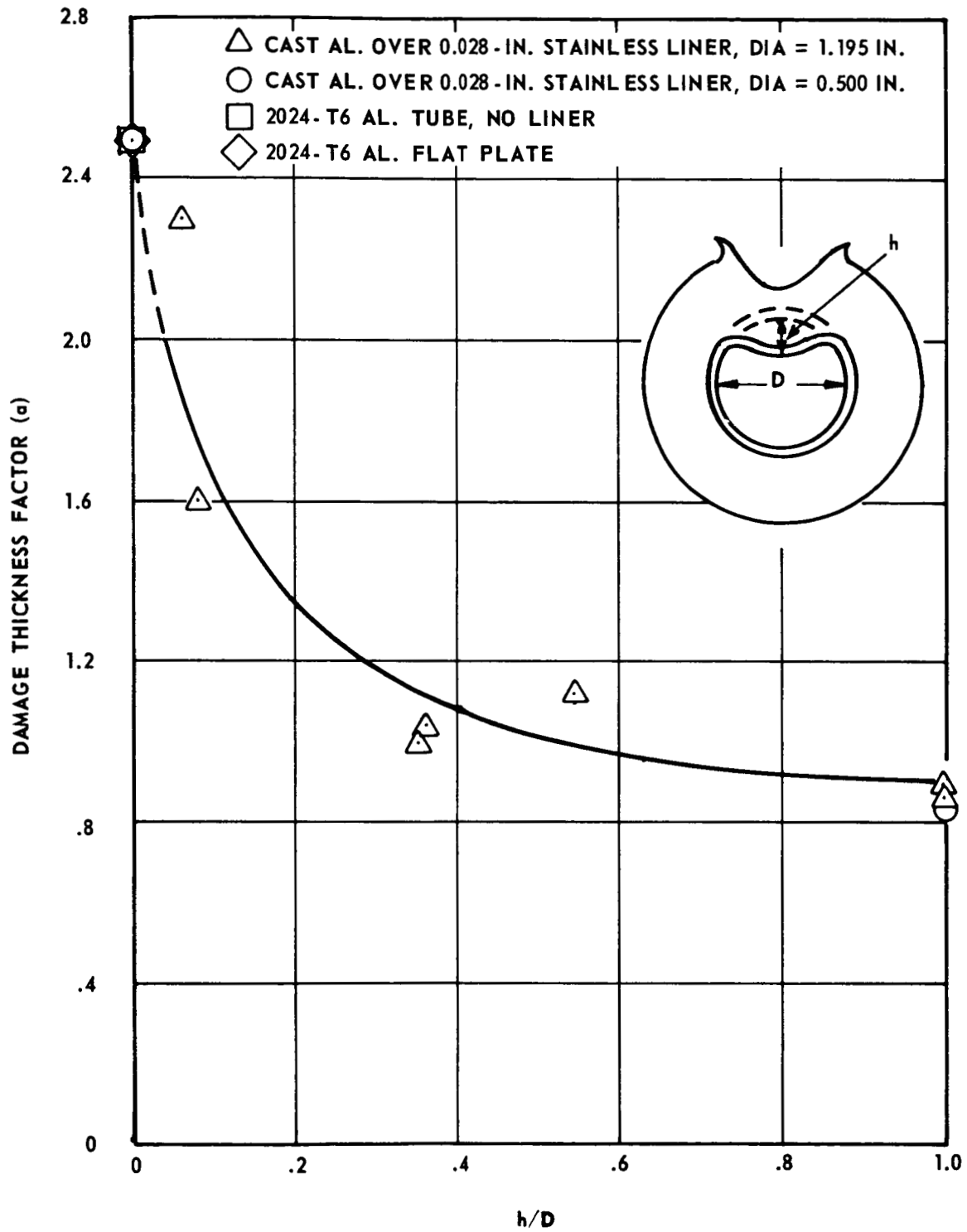
Reproduced in Figure A-2 is the typical SNAP-8 radiator tube and fin element enclosed in your memorandum of August 10, 1965. The thickness calculated from

Equation (2) with the above constants refers to t_a as shown. The side wall surface with armor thickness, t_s , is vulnerable to impacts through the fin only and, therefore, is subject to design as bumpered armor. Preliminary results from impacts into similar stainless steel bumper configurations with a .020" thick fin indicates that t_s can be substantially smaller than t_a . Comparable shots with aluminum are scheduled, but have not yet been fired. It appears, however, that the adoption of the relationship $t_s = 0.25 t_a$ should be adequate for the configuration of Figure A-2.

Since it appears that very little thickness is needed for t_s , it may be well to consider configurations for a tube and fin element as shown in Figures A-3a and A-3b. In these configurations, an increase in liner thickness, t_l , to around .060 inches, will allow the removal of all the side wall armor, t_s , and possibly produce lower weights. For the bumpered configuration, the use of $t_f < t_w < 2t_f$ and $t_a \sim 3/8"$ should be adequate from the meteoroid protection point of view.

Preliminary results of the experimental impact program can be found in NASA TN D-2472 by S. Lieblein, N. Clough, and A. McMillan. The more comprehensive design results from the program are in a series of four technical notes by N. Clough, A. McMillan, and S. Lieblein (in review) and summarized in papers in preparation by N. Clough and J. Diedrich to be presented at the AIAA First Rankine Cycle Space Power Systems Specialists Conference, October 26 - 28, and by S. Lieblein to be presented at the American Nuclear Society Annual Meeting in November 1965.

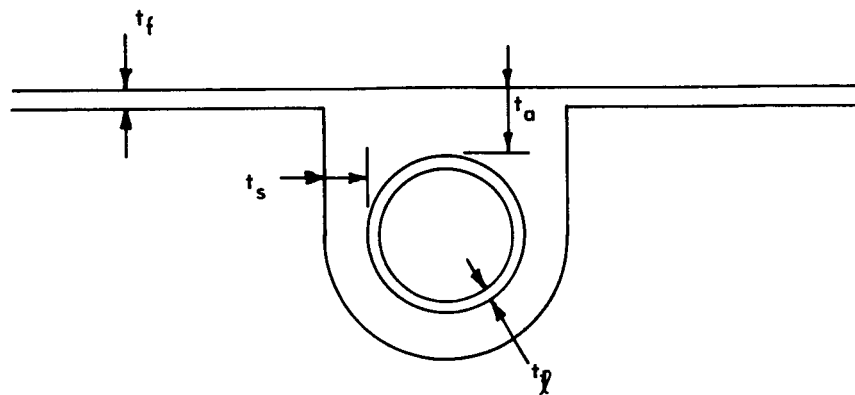
267-NF-1360



Damage Thickness Factor vs Relative Dimple Height

Figure A-1

267-NF-1361



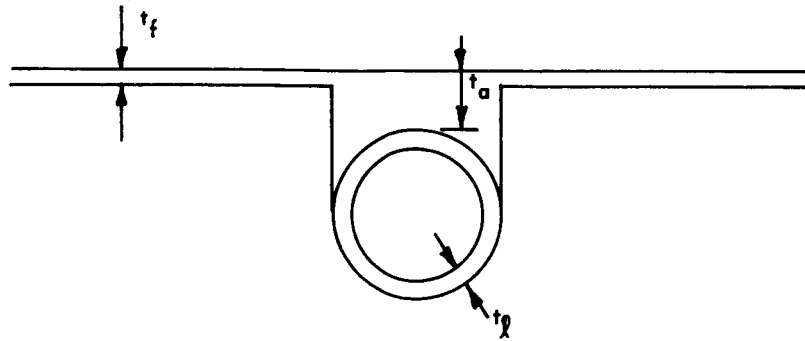
$$t_f = .070'' \text{ (Al.)}$$

$$t_g = .030'' \text{ (S.S.)}$$

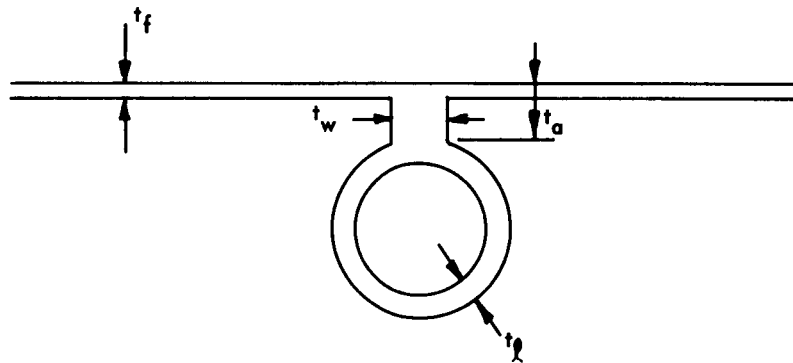
Proposed SNAP-8 Fin-Tube Configuration

Figure A-2

267-NF-1362



A. INTEGRAL ARMOR



B. BUMPER PRINCIPLE

Alternative Fin-Tube Configurations

APPENDIX B

ELECTRICAL GENERATING SYSTEM WEIGHTS

The tables in this appendix present the weights of each EGS studied in the performance potential program. Remarks are given to aid in interpreting the significance of the values listed. The weights for the PCS are grouped by loops as Primary NaK loop, mercury loop, etc. Dry weights, liquid inventories in components, and wet weights are listed. The total fluid inventory of each loop is listed separately at the bottom of the detailed system weight breakdown.

The effect of system improvement and specific component substitution or improvement on overall system weight can be determined by comparing the weight breakdown for the two systems involved in the change. EGS-0, -1, -2, -4, and -5 are to be compared directly since they have a comparable net power output. EGS-3 and -6 both have a reactor input of 600 kw; these systems are directly comparable.

TABLE B-1

EGS-O Weight Breakdown

Subsystem and Component	Dry Weight (lb)	Fluid Inventory Weight (lb)	Wet Weight (lb)	Remarks
I. NUCLEAR SYSTEM				
A. Reactor Assembly	761	29	790	S8DS reactor
B. Shield	1550	--	1550	Sized for selected config. and reactor kw
I. Total	2311	29 (NaK)	2340	
II. POWER CONVERSION SYSTEM				
A. Primary Loop				
1. NaK PMA	225	8	233	M. * measured weight
2. Parasitic load resistor	67	22	89	M.
3. Auxiliary start heat exchanger	20	11	31	C. * detailed calculation
4. NaK expansion reservoir	134	18	152	Loop inventory estimated for 70°F fluid
5. Piping	33	49	82	40' - 2" OD x .035"
6. Thermal insulation	23	--	23	1/2" Min - k F 182
7. Boiler NaK inventory	--	107	--	Included in wet weight of Item B1
A. Subtotal	502	215 (NaK)	610	
B. Mercury Rankine Loop				
1. Boiler	377	17	501	C. Wet weight includes Item A7
2. Turbine alternator assembly	702	--	702	C.
3. Condenser	91	18	142	M. Wet weight includes Item C5
4. Hg PMA	150	--	150	M.
5. Hg injection system	86	58	144	M. Reservoir inventory after injection
6. Valves	13	--	13	C. Flow control and isolation valves
7. Hg piping (vapor)	51	1	52	13' - 1.75" OD x .120"; Turb. exit bellows, 24 lb.
8. Hg piping (liquid)	11	95	106	12' - 1" OD x .035"; 24' - 3/4 OD x .035"
9. Thermal insulation	32	--	32	1/2" Min - k F 182
B. Subtotal	1513	189 (Hg)	1842	
C. Heat Rejection Loop				
1. HRL NaK PMA	225	8	233	M.
2. HRL NaK expansion reservoir	45	25	70	Loop inventory estimated for 70°F fluid
3. Valves	12	--	12	Temp. control and aux. start loop s/o valves
4. Piping	30	34	64	30' - 2" OD x .035"; 18' - 3/4" x .035" (Start Loop)
5. Condenser NaK inventory	--	33	--	Included in wet weight of Item B3
C. Subtotal	312	100 (NaK)	379	
D. Lubricant-Coolant Loop				
1. L/C PMA	28	--	28	
2. L/C expansion reservoir	35	15	50	Loop inventory estimates for 70°F fluid
3. Valves	16	--	16	M. 4 shutoff valves
4. Piping	47	30	77	87' - 1" OD x .035"; 46' - 3/4" OD x .035"
5. Thermal insulation	33	--	33	1/2" Min - k F 182
6. Component L/C inventory	--	10	10	Estimated for components using L/C fluid
D. Subtotal	159	55 (4P3E)	214	
E. Electrical System				
1. Transformer reactor assembly	356	--	356	C.
2. Low-temperature control assembly	209	--	209	M.
3. Inverter assembly	316	--	316	M.
4. Batteries	140	--	140	C.
5. Start programmer	15	--	15	C.
6. Power bus, harness, misc.	190	--	190	Power bus 99 lb; PCS harness 60 lb; Min - k 20 lb.
7. SCR speed control	--	--	--	} Not used in this system
8. Capacitor	--	--	--	} Speed control included in E1 and 2
E. Subtotal	1226	--	1226	
F. PCS Structure				
1. PCS frame	1600	--	1600	Rigid truss type
2. Support brackets	235	--	235	Estimated for components mounted on frame
F. Subtotal	1835	--	1835	
G. Instrumentation	120	--	120	
II. Total	5667	--	6226	
III. FLIGHT RADIATOR ASSEMBLY				
A. HRL Radiator Assembly				
1. Radiator	1099	110	1209	Incl. tubes, manifolds, armor, fins
2. Piping	30	48	78	40' - 2" OD x .035"
A. Subtotal	1129	158 (NaK)	1287	
B. L/C Radiator Assembly				
1. Radiator	281	56	337	Incl. tubes, manifolds, armor, fins
2. Piping	20	12	32	70' - 3/4" OD x .035"
3. Insulation	110	--	110	1/4" Min - k diaphragm at base of HRL rad.
B. Subtotal	411	68 (4P3E)	479	
C. Radiator stringers & rings	670	--	670	Described in Sec. IIID.
III. Total	2210	--	2436	
TOTAL EGS WEIGHT	10188	--	11002	
Fluid Inventory Summary:				
Sodium-Potassium Alloy (NaK)	502			
Mercury (Hg)	189			
Polyphenyl Ether (4P3E)	123			
	814			

Table B-1

TABLE B-2

EGS-1 Weight Breakdown

EGS-1 WEIGHT BREAKDOWN

Subsystem and Component	Dry Weight (lb)	Fluid Inventory Weight (lb)	Wet Weight (lb)	Remarks
I. NUCLEAR SYSTEM				
A. Reactor Assembly	761	29	790	S8DS reactor
B. Shield	1510	--	1510	Adjusted for reactor kw
I. Total	2271	29 (NaK)	2300	
II. POWER CONVERSION SYSTEM				Components lightened as described in Sec. VB
A. Primary Loop				
1. NaK PMA	170	8	178	
2. Parasitic load resistor	67	22	89	
3. Auxiliary start heat exchanger	12	10	22	
4. NaK expansion reservoir	98	13	111	Lightened and sized to loop inventory
5. Piping	33	49	82	
6. Thermal insulation	23	--	23	
7. Boiler NaK inventory	--	56	--	
A. Subtotal	403	158 (NaK)	561	
B. Mercury Rankine Loop				
1. Boiler	258	17	331	Wet weight includes Item A7
2. Turbine alternator assembly	603	--	603	
3. Condenser	91	18	142	Wet weight includes Item C5
4. Hg PMA	85	--	85	
5. Hg injection system	86	58	144	
6. Valves	13	--	13	
7. Hg piping (vapor)	51	1	52	
8. Hg piping (liquid)	11	95	106	
9. Thermal insulation	32	--	32	
B. Subtotal	1230	189 (Hg)	1508	
C. Heat Rejection Loop				
1. HRL NaK PMA	170	8	178	
2. HRL NaK expansion reservoir	45	25	70	
3. Valves	12	--	12	
4. Piping	30	34	64	
5. Condenser NaK inventory	--	33	--	
C. Subtotal	257	100 (NaK)	324	
D. Lubricant-Coolant Loop				
1. L/C PMA	20	--	20	
2. L/C expansion reservoir	35	15	50	
3. Valves	16	--	16	
4. Piping	47	30	77	
5. Thermal insulation	33	--	33	
6. Component L/C inventory	--	10	10	
D. Subtotal	151	55 (4P3E)	206	
E. Electrical System				
1. Transformer reactor assembly	356	--	356	
2. Low-temperature control assembly	209	--	209	
3. Inverter assembly	316	--	316	
4. Batteries	140	--	140	
5. Start programmer	15	--	15	
6. Power bus, harness, misc.	190	--	190	
7. SCR speed control	--	--	--	} Not used in this system; Speed control included in E1 and 2.
8. Capacitor	--	--	--	
E. Subtotal	1226	--	1226	
F. PCS Structure				
1. PCS frame	500	--	500	Tension-member type frame
2. Support brackets	235	--	235	
F. Subtotal	735	--	735	
G. Instrumentation	120	--	120	
II. Total	4122	--	4624	
III. FLIGHT RADIATOR ASSEMBLY				
A. HRL Radiator Assembly				
1. Radiator	993	102	1095	
2. Piping	30	48	78	
A. Subtotal	1023	150 (NaK)	1173	
B. L/C Radiator Assembly				
1. Radiator	281	56	337	70' - 3/4" OD x .035
2. Piping	20	12	32	1/4" Min-k diaphragm at base of HRL rad.
3. Insulation	98	--	98	
B. Subtotal	399	68 (4P3E)	467	
C. Radiator stringers & rings	708	--	708	
III. Total	2130	--	2348	
TOTAL EGS WEIGHT	8523	--	9272	
Fluid Inventory Summary:				
Sodium-Potassium Alloy (NaK)	437			
Mercury (Hg)	189			
Polyphenyl Ether (4P3E)	123			
	749			

Table B-2

TABLE B-3

EGS-2 Weight Breakdown

EGS-2 WEIGHT BREAKDOWN				
Subsystem and Component	Dry Weight (lb)	Fluid Inventory Weight (lb)	Wet Weight (lb)	Remarks
I. NUCLEAR SYSTEM				
A. Reactor Assembly	761	29	790	S8DS reactor
B. Shield	1480	--	1480	Adjusted for reactor kw
I. Total	2241	29 (NaK)	2270	
II. POWER CONVERSION SYSTEM				
A. Primary Loop				
1. NaK PMA	170	8	178	
2. Parasitic load resistor	67	22	89	
3. Auxiliary start heat exchanger	12	10	22	
4. NaK expansion reservoir	98	13	111	
5. Piping	33	49	82	
6. Thermal insulation	23	--	23	
7. Boiler NaK inventory	--	56	--	
A. Subtotal	403	158 (NaK)	561	
B. Mercury Rankine Loop				
1. Boiler	258	17	331	Wet weight includes Item A7
2. Turbine alternator assembly	603	--	603	
3. Condenser	91	18	142	Wet weight includes Item C5
4. Hg PMA	85	--	85	
5. Hg injection system	86	58	144	
6. Valves	13	--	13	
7. Hg piping (vapor)	51	1	52	
8. Hg piping (liquid)	11	95	106	
9. Thermal insulation	32	--	32	
B. Subtotal	1230	189 (Hg)	1508	
C. Heat Rejection Loop				
1. HRL NaK PMA	170	8	178	
2. HRL NaK expansion reservoir	43	24	67	Adjusted to HRL inventory (IIC plus IIAA)
3. Valves	12	--	12	
4. Piping	30	34	64	
5. Condenser NaK inventory	--	33	--	
C. Subtotal	255	99 (NaK)	321	
D. Lubricant-Coolant Loop				
1. L/C PMA	20	--	20	
2. L/C expansion reservoir	35	15	50	
3. Valves	16	--	16	
4. Piping	47	30	77	
5. Thermal insulation	33	--	33	
6. Component L/C inventory	--	10	10	
D. Subtotal	151	55 (4P3E)	206	
E. Electrical System				
1. Transformer reactor assembly	170	--	170	
2. Low-temperature control assembly	209	--	209	
3. Inverter assembly	316	--	316	
4. Batteries	140	--	140	
5. Start programmer	15	--	15	
6. Power bus, harness, misc.	190	--	190	
7. SCR speed control	90	--	90	Includes 50 lb for radiation shield
8. Capacitor	15	--	15	24 KVAR correction
E. Subtotal	1145	--	1145	
F. PCS Structure				
1. PCS frame	500	--	500	
2. Support brackets	235	--	235	
F. Subtotal	735	--	735	
G. Instrumentation	120	--	120	
II. Total	4039	--	4540	
III. FLIGHT RADIATOR ASSEMBLY				
A. HRL Radiator Assembly				
1. Radiator	904	96	1000	
2. Piping	30	48	78	
A. Subtotal	934	144 (NaK)	1078	
B. L/C Radiator Assembly				
1. Radiator	202	50	252	60" - 3/4" OD x .035
2. Piping	17	10	27	1/4" Min-k diaphragm at base of HRL rad.
3. Insulation	88	--	88	
B. Subtotal	307	60 (4P3E)	367	
C. Radiator stringers & rings				
- Subtotal	641	--	641	
III. Total	1882	--	2086	
TOTAL EGS WEIGHT	8162	--	8896	
Fluid Inventory Summary:				
Sodium-Potassium Alloy (NaK)	430			
Mercury (Hg)	189			
Polyphenyl Ether (4P3E)	115			
	734			

Table B-3

TABLE B-4

EGS-3 Weight Breakdown

EGS-3 WEIGHT BREAKDOWN

Subsystem and Component	Dry Weight (lb)	Fluid Inventory Weight (lb)	Wet Weight (lb)	Remarks
I. NUCLEAR SYSTEM				
A. Reactor Assembly	761	29	790	S8DS reactor
B. Shield	1600	--	1600	Adjusted for reactor kwf
1. Total	2361	29 (NaK)	2390	
II. POWER CONVERSION SYSTEM				
A. Primary Loop				
1. NaK PMA	170	8	178	
2. Parasitic load resistor	96	44	140	Adjusted for higher power rating
3. Auxiliary start heat exchanger	12	10	22	
4. NaK expansion reservoir	114	15	129	Adjusted for loop inventory
5. Piping	36	62	98	OD increased to 2.25"
6. Thermal insulation	25	--	25	
7. Boiler NaK inventory	--	72	--	
A. Subtotal	453	211 (NaK)	592	
B. Mercury Rankine Loop				
1. Boiler	343	22	437	Wet weight includes Item A7; 9 tubes
2. Turbine alternator assembly	613	--	613	Adjusted for larger flow passages in TA
3. Condenser	106	21	165	Wet weight includes Item C5; 85 tubes
4. Hg PMA	85	--	85	
5. Hg injection system	88	66	154	Adjusted for increased loop inventory
6. Valves	13	--	13	
7. Hg piping (vapor)	51	1	52	
8. Hg piping (liquid)	11	95	106	
9. Thermal insulation	32	--	32	
B. Subtotal	1342	205 (Hg)	1657	
C. Heat Rejection Loop				
1. HRL NaK PMA	170	8	178	
2. HRL NaK expansion reservoir	53	30	83	Adjusted to HRL inventory (11C plus 111A)
3. Valves	12	--	12	
4. Piping	35	43	78	OD increased to 2.25"
5. Condenser NaK inventory	--	38	--	
C. Subtotal	270	119 (NaK)	351	
D. Lubricant-Coolant Loop				
1. L/C PMA	20	--	20	
2. L/C expansion reservoir	35	15	50	
3. Valves	16	--	16	
4. Piping	47	30	77	
5. Thermal insulation	33	--	33	
6. Component L/C inventory	--	10	10	
D. Subtotal	151	55 (4P3E)	206	
E. Electrical System				
1. Transformer reactor assembly	218	--	218	
2. Low-temperature control assembly	209	--	209	
3. Inverter assembly	316	--	316	
4. Batteries	140	--	140	
5. Start programmer	15	--	15	
6. Power bus, harness, misc.	190	--	190	
7. SCR speed control	100	--	100	Includes 50 lb for radiation shield
8. Capacitor	27	--	27	46 KVAR correction
E. Subtotal	1215	--	1215	
F. PCS Structure				
1. PCS frame	500	--	500	
2. Support brackets	235	--	235	
F. Subtotal	735	--	735	
G. Instrumentation	120	--	120	
II. Total	4286	--	4876	
III. FLIGHT RADIATOR ASSEMBLY				
A. HRL Radiator Assembly				
1. Radiator	1251	122	1373	
2. Piping	34	60	94	40" - 2.25" O.D. x .035
A. Subtotal	1285	182 (NaK)	1467	
B. L/C Radiator Assembly				
1. Radiator	230	60	290	
2. Piping	20	12	32	70" - 3/4" OD x .035
3. Insulation	126	--	126	1/4" Min-k diaphragm at base of HRL rad.
B. Subtotal	376	72 (4P3E)	448	
C. Radiator stringers & rings	792	--	792	
III. Total	2453	--	2707	
TOTAL EGS WEIGHT	9100	--	9973	
Fluid Inventory Summary:				
Sodium-Potassium Alloy (NaK)	541			
Mercury (Hg)	205			
Polyphenyl Ether (4P3E)	127			
	873			

Table B-4

TABLE B-5

EGS-4 Weight Breakdown

EGS-4 WEIGHT BREAKDOWN

Subsystem and Component	Dry Weight (lb)	Fluid Inventory Weight (lb)	Wet Weight (lb)	Remarks
I. NUCLEAR SYSTEM				
A. Reactor Assembly	729	29	758	Advanced reactor
B. Shield	1475	--	1475	Adjusted for reactor kwt
I. Total	2204	29 (NaK)	2233	
II. POWER CONVERSION SYSTEM				
A. Primary Loop				
1. NaK PMA	170	8	178	
2. Parasitic load resistor	67	22	89	
3. Auxiliary start heat exchanger	12	10	22	
4. NaK expansion reservoir	114	15	129	
5. Piping	33	49	82	
6. Thermal insulation	23	--	23	
7. Boiler NaK inventory	--	107	--	Boiler shell dia. increased to reduce ΔP in HRL
A. Subtotal	419	211 (NaK)	523	
B. Mercury Rankine Loop				
1. Boiler	280	17	404	Wet weight includes Item A7
2. Turbine alternator assembly	603	--	603	
3. Condenser	91	18	142	Wet weight includes Item C5
4. Hg PMA	85	--	85	
5. Hg injection system	86	58	144	
6. Valves	13	--	13	
7. Hg piping (vapor)	51	1	52	
8. Hg piping (liquid)	11	95	106	
9. Thermal insulation	32	--	32	
B. Subtotal	1252	189 (Hg)	1581	
C. Heat Rejection Loop				
1. HRL NaK PMA	170	8	178	
2. HRL NaK expansion reservoir	41	24	65	Adjusted to HRL inventory (IIC plus I11A)
3. Valves	12	--	12	
4. Piping	30	34	64	
5. Condenser NaK inventory	--	33	--	
C. Subtotal	253	99 (NaK)	319	
D. Lubricant-Coolant Loop				
1. L/C PMA	20	--	20	
2. L/C expansion reservoir	35	15	50	
3. Valves	16	--	16	
4. Piping	47	30	77	
5. Thermal insulation	33	--	33	
6. Component L/C inventory	--	10	10	
D. Subtotal	151	55 (4P3E)	206	
E. Electrical System				
1. Transformer reactor assembly	170	--	170	
2. Low-temperature control assembly	209	--	209	
3. Inverter assembly	316	--	316	
4. Batteries	140	--	140	
5. Start programmer	15	--	15	
6. Power bus, harness, misc.	190	--	190	
7. SCR speed control	90	--	90	
8. Capacitor	28	--	28	Includes 50 lb for radiator shield 48 KVAR correction
E. Subtotal	1158	--	1158	
F. PCS Structure				
1. PCS frame	500	--	500	
2. Support brackets	235	--	235	
F. Subtotal	735	--	735	
G. Instrumentation	120	--	120	
II. Total	4088	--	4642	
III. FLIGHT RADIATOR ASSEMBLY				
A. HRL Radiator Assembly				
1. Radiator	802	88	890	
2. Piping	30	48	78	
A. Subtotal	832	136 (NaK)	968	
B. L/C Radiator Assembly				
1. Radiator	183	50	233	
2. Piping	16	9	25	55' x 3/4" OD x .035"
3. Insulation	76	--	76	1/4" Min-k diaphragm at base of HRL rad.
B. Subtotal	275	59 (4P3E)	334	
C. Radiator stringers & rings	590	--	590	
III. Total	1697	--	1892	
TOTAL EGS WEIGHT	7989	--	8767	
Fluid Inventory Summary:				
Sodium-Potassium Alloy (NaK)	475			
Mercury (Hg)	189			
Polyphenyl Ether (4P3E)	114			
	778			

Table B-5

TABLE B-6

EGS-5 Weight Breakdown

EGS-5 WEIGHT BREAKDOWN

Subsystem and Component		Dry Weight (lb)	Fluid Inventory Weight (lb)	Wet Weight (lb)	Remarks
I.	NUCLEAR SYSTEM				
A.	Reactor Assembly	729	29	758	Advanced reactor
B.	Shield	1470	--	1470	Adjusted to reactor kwf
	I. Total	2199	29 (NaK)	2228	
II.	POWER CONVERSION SYSTEM				
A.	Primary Loop				
1.	NaK PMA	170	8	178	
2.	Parasitic load resistor	67	22	89	
3.	Auxiliary start heat exchanger	12	10	22	
4.	NaK expansion reservoir	114	15	129	
5.	Piping	33	49	82	
6.	Thermal insulation	23	--	23	
7.	Boiler NaK inventory	--	107	--	
	A. Subtotal	419	211 (NaK)	523	
B.	Mercury Rankine Loop				
1.	Boiler	280	17	404	Wet weight includes Item A7
2.	Turbine alternator assembly	603	--	603	
3.	Condenser	91	18	142	Wet weight includes Item C5
4.	Hg PMA	85	--	85	
5.	Hg injection system	86	58	144	
6.	Valves	13	--	13	
7.	Hg piping (vapor)	51	1	52	
8.	Hg piping (liquid)	11	95	106	
9.	Thermal insulation	32	--	32	
	B. Subtotal	1252	189 (Hg)	1581	
C.	Heat Rejection Loop				
1.	HRL NaK PMA	170	8	178	
2.	HRL NaK expansion reservoir	41	23	64	Adjusted to HRL inventory (11C plus 111A)
3.	Valves	12	--	12	
4.	Piping	30	34	64	
5.	Condenser NaK inventory	--	33	--	
	C. Subtotal	253	98 (NaK)	318	
D.	Lubricant-Coolant Loop				
1.	L/C PMA	20	--	20	
2.	L/C expansion reservoir	35	15	50	
3.	Valves	16	--	16	
4.	Piping	47	30	77	
5.	Thermal insulation	33	--	33	
6.	Component L-C inventory	--	10	10	
	D. Subtotal	151	55 (4P3E)	206	
E.	Electrical System				
1.	Transformer reactor assembly	170	--	170	
2.	Low-temperature control assembly	209	--	209	
3.	Inverter assembly	316	--	316	
4.	Batteries	140	--	140	
5.	Start programmer	15	--	15	
6.	Power bus, harness, misc.	190	--	190	
7.	SCR speed control	90	--	90	Includes 50 lbs for radiation shield
8.	Capacitor	28	--	28	47 KVAR correction
	E. Subtotal	1158	--	1158	
F.	PCS Structure				
1.	PCS frame	500	--	500	
2.	Support brackets	235	--	235	
	F. Subtotal	735	--	735	
G.	Instrumentation	120	--	120	
	II. Total	4088	--	4641	
III.	FLIGHT RADIATOR ASSEMBLY				
A.	HRL Radiator Assembly				
1.	Radiator	762	85	847	
2.	Piping	30	48	78	
	A. Subtotal	792	133 (NaK)	925	
B.	L/C Radiator Assembly				
1.	Radiator	182	50	232	
2.	Piping	16	9	25	
3.	Insulation	73	--	73	1/4" Min-k diaphragm at base of HRL rad.
	B. Subtotal	271	59 (4P3E)	330	
C.	Radiator stringers & rings	575	--	575	
	III. Total	1638	--	1830	
	TOTAL EGS WEIGHT	7925	--	8699	
	Fluid Inventory Summary:				
	Sodium-Potassium Alloy (NaK)	471			
	Mercury (Hg)	189			
	Polyphenyl Ether (4P3E)	114			
		774			

Table B-6

TABLE B-7

EGS-6 Weight Breakdown

EGS-6 WEIGHT BREAKDOWN

Subsystem and Component	Dry Weight (lb)	Fluid Inventory Weight (lb)	Wet Weight (lb)	Remarks
I. NUCLEAR SYSTEM				
A. Reactor Assembly	729	29	758	Advanced reactor
B. Shield	1600	--	1600	Adjusted to reactor kwt
I. Total	2329	29 (NaK)	2358	
II. POWER CONVERSION SYSTEM				
A. Primary Loop				
1. NaK PMA	170	8	178	
2. Parasitic load resistor	96	44	140	Adjusted for higher power rating
3. Auxiliary start heat exchanger	12	10	22	
4. NaK expansion reservoir	138	19	157	Adjusted for larger loop inventory
5. Piping	39	69	108	
6. Thermal insulation	27	--	27	
7. Boiler NaK inventory	--	138	--	Boiler shell dia. increased for low ΔP
A. Subtotal	482	288 (NaK)	632	
B. Mercury Rankine Loop				
1. Boiler	356	22	516	Wet weight includes Item A7: 9 tubes
2. Turbine alternator assembly	613	--	613	
3. Condenser	106	21	165	Wet weight includes Item C5: 85 tubes
4. Hg PMA	85	--	85	
5. Hg injection system	88	66	154	
6. Valves	13	--	13	
7. Hg piping (vapor)	51	1	52	
8. Hg piping (liquid)	11	95	106	
9. Thermal insulation	32	--	32	
B. Subtotal	1355	205 (Hg)	1736	
C. Heat Rejection Loop				
1. HRL NaK PMA	170	8	178	
2. HRL NaK expansion reservoir	52	29	81	Adjusted to HRL inventory (IIC plus I11A)
3. Valves	12	--	12	
4. Piping	35	43	78	
5. Condenser NaK inventory	--	38	--	
C. Subtotal	269	118 (NaK)	349	
D. Lubricant-Coolant Loop				
1. L/C PMA	20	--	20	
2. L/C expansion reservoir	35	15	50	
3. Valves	16	--	16	
4. Piping	47	30	77	
5. Thermal insulation	33	--	33	
6. Component L/C inventory	--	10	10	
D. Subtotal	151	55 (4P3E)	206	
E. Electrical System				
1. Transformer reactor assembly	223	--	223	
2. Low-temperature control assembly	209	--	209	
3. Inverter assembly	316	--	316	
4. Batteries	140	--	140	
5. Start programmer	15	--	15	
6. Power bus, harness, misc.	190	--	190	
7. SCR speed control	100	--	100	Includes 50 lbs for radiation shield
8. Capacitor	42	--	42	71 KVAR correction
E. Subtotal	1235	--	1235	
F. PCS Structure				
1. PCS frame	500	--	500	
2. Support brackets	235	--	235	
F. Subtotal	735	--	735	
G. Instrumentation	120	--	120	
II Total	4347	--	5013	
III. FLIGHT RADIATOR ASSEMBLY				
A. HRL Radiator Assembly				
1. Radiator	1183	115	1298	
2. Piping	34	60	94	40" - 2.25" OD x .035"
A. Subtotal	1217	175 (NaK)	1392	
B. L/C Radiator Assembly				
1. Radiator	218	60	278	
2. Piping	20	12	32	70" - 3/4" O. D. x .035"
3. Insulation	119	--	119	1/4" Min-k diaphragm at base of HRL rad.
B. Subtotal	357	72 (4P3E)	429	
C. Radiator stringers & rings	767	--	767	
III. Total	2341	--	2588	
TOTAL EGS WEIGHT	9017	--	9959	
Fluid Inventory Summary:				
Sodium-Potassium Alloy (NaK)	610			
Mercury (Hg)	205			
Polyphenyl Ether (4P3E)	127			
	942			

Table B-7

APPENDIX CANALYSIS OF TURBINE EFFICIENCY AS AFFECTED
BY PRESSURE RATIO AND NUMBER OF STAGES

The SNAP-8 performance potential study requires analysis of the system performance when the turbine inlet and outlet pressures are changed. In order to obtain more accurate results, it was necessary to evaluate the effect of changing pressures on turbine efficiency.

In order to minimize the turbine modification required, it was assumed that the turbine and wheel pitch diameters are held constant. Thus, only blade profiles, flow areas, and number of pressure stages were considered. The number of pressure stages required is based on the overall pressure ratio, the resulting blade velocity to nozzle exit velocity (u/c) ratio and the nozzle area ratio requirements. The evaluation was based on the equations in AGC TM 394:63-1-112. The overall efficiency is:

$$\eta_T = \frac{\sum \eta_s (\Delta H_{ad})_s}{(\Delta H_{ad})_T}$$

where

η_s = stage efficiency

$(\Delta H_{ad})_s$ = isentropic enthalpy change in stage

$(\Delta H_{ad})_T$ = isentropic enthalpy change for entire turbine pressure ratio

The equation for stage efficiency is:

$$(\eta_s)_n = (\eta_{hi})_n X_{Nn} L_s - (\Delta \eta_s)_b - (\Delta \eta_p)_n - (\Delta \eta_m)_n - (\Delta \eta_d)_n$$

where n refers to stage number

η_{hi} = stage diagram efficiency

X_N = quality of mercury vapor at stage inlet

L_s = seal losses factor

$\Delta \eta_s$ = scavenging loss

$\Delta \eta_p$ = blade pumping loss

$\Delta\eta_m$ = loss due to liquid mercury in vapor

$\Delta\eta_d$ = disk friction loss

The equations defining these terms follow:

$$(\eta_{hi})_n = 2 \left(\frac{u}{C_o} \right)_n \left[1 + (\psi_B)_n (K_L)_n (K_F)_n \right] \left[(\psi_N)_n \cos (\alpha_1)_n - \left(\frac{u}{C_o} \right)_n \right]$$

where

u = blade velocity - ft/sec

C_o = ideal nozzle velocity = $\sqrt{2g(\Delta H_{ad})_s}$ - ft/sec

ψ_B = blade velocity coefficient

K_L = tip leakage correction factor

K_F = filling and emptying loss factor

ψ_N = nozzle velocity coefficient

α_1 = nozzle angle

In this analysis, the following design parameters were held constant:

Wheel pitch diameter	= 5.1 inches
RPM	= 12,000
Radial tip clearance	= 0.040 inch
Blade velocity coef.	= 0.8203 (first stage)
Nozzle velocity coef.	= 0.9459
Nozzle angle cosine	= 0.956
K_L	= 0.7709

Substituting these values into the stage diagram efficiency expression and re-arranging

$$(\eta_{hi})_1 = \left[1 + 0.632 (K_F)_1 \right] \left[\frac{2.166}{(\Delta H_{ad})_s} - \frac{2.86}{(\Delta H_{ad})_s} \right]$$

The value of $(K_F)_1$, to be used in evaluating this expression, is given by:

$$(K_F)_1 = 1 - \frac{t}{2a_N} (np)_1$$

and

$$a_N = \frac{\xi \pi D}{(np)_n}$$

where

t = blade pitch = 0.2025 inch

a_N = arc length for each admission arc

np = number of admission arcs = 2 for 1st stage

D = wheel pitch diameter inches

$\xi = 0.38 \frac{265}{P^4} \times \frac{\dot{w}}{11,200}$ = admission arc fractions

where

0.38 = admission arc fraction for 265 psia turbine inlet pressure and 11,200 lb/hr mercury flow; P^4 is new inlet pressure; and \dot{w} is new flow rate.

Substituting and simplifying

$$(K_F)_1 = 1 - \frac{2.81 P^4}{\dot{w}}$$

The $(\Delta H_{ad})_s$ is $(\Delta H_{ad})_T / N_{ST}$

where N_{ST} is the number of stages. Using these two expressions, the equation for the first stage diagram efficiency becomes:

$$(\eta_{hi})_1 = \left[1.632 - \frac{1.777 P^4}{\dot{w}} \right] \left[\frac{2.166 (N_{ST})^{1/2}}{(\Delta H_{ad})_T^{1/2}} - \frac{2.86 N_{ST}}{(\Delta H_{ad})_T} \right]$$

The pumping losses for the first stage is given by

$$(\Delta\eta_p)_1 = 0.00045 \frac{P_4 N_{ST}}{(\Delta H_{ad})_T} \left(\frac{P_5}{P_4} \right)^{1/N_{ST}} \left(1.383 - 0.01048 \frac{\dot{W}}{P_4} \right)$$

where P5 is the turbine exhaust pressure.

The disc losses are given by:

$$(\Delta\eta_D)_1 = 0.000383 \frac{P_4}{(\Delta H_{ad})_T} \left(\frac{P_5}{P_4} \right)^{1/N_{ST}}$$

With these equations to solve for the values, the equation for the first stage efficiency which follows can be evaluated for different inlet pressures and flow rates.

$$(\eta_s)_1 = (\eta_{hi})_1 \times 0.98 \times 0.98 - \left[0.0332 + (\Delta\eta_p)_1 + 0.001 + (\Delta\eta_D)_1 \frac{11,200}{\dot{W}} \right]$$

The analysis is now carried out for the second stage, using the second stage constants as follows:

$$(\psi_B)_2 = 0.8543$$

$$(K_L)_2 = 0.7655$$

$$(\psi_N)_2 = 0.9375$$

$$\cos(\alpha_1)_2 = 0.956$$

The equation for the second stage diagram efficiency becomes:

$$(\eta_{ni})_2 = \left[1.653 - 1.19 \frac{P_4}{P_4} \right] \left[\frac{2.148 (N_{ST})^{1/2}}{(\Delta H_{ad})_T^{1/2}} - \frac{2.86 N_{ST}}{(\Delta H_{ad})_T} \right]$$

The equation for the change in second stage pumping losses becomes:

$$(\Delta\eta_p)_2 = 0.000873 \frac{P_4 N_{ST}}{(\Delta H_{ad})_T} \left(\frac{P_5}{P_4} \right)^{2/N_{ST}} \left[1.412 - 0.00569 \frac{\dot{W}}{P_4} \left(\frac{P_4}{P_5} \right)^{1/N_{ST}} \right]$$

and the equation for the change in second stage disk losses becomes:

$$(\Delta\eta_D)_2 = 0.000504 \frac{P_4 N_{ST}}{(\Delta H_{ad})_T} \left(\frac{P_5}{P_4} \right)^{2/N_{ST}}$$

The values obtained from these equations can then be substituted into the following equation for the efficiency of the second turbine stage which follows:

$$(\eta_s)_2 = (\eta_{hi})_2 \times 0.98 \times 0.98 - 0.0322 + (\Delta\eta_p)_2 + 0.00518 + (\Delta\eta_D)_2 \frac{11,200}{\dot{W}}$$

The two stage efficiencies can now be substituted into the overall turbine efficiency equation below.

$$\eta_T = \frac{(\eta_s)_1 + (\eta_s)_2 + 0.64 (N_{ST} - 2)}{N_{ST}}$$

Evaluation of these equations for different pressure ratios and number of stages provides the turbine efficiencies required to complete the state-point analysis study.

The results of the evaluation of these equations are presented in Table B-1 in this appendix.

TABLE C-1

TURBINE EFFICIENCY VS PRESSURE RATIO RESULTS

Turbine Efficiency - %						
P5	P4 = 200	250	300	350	400	450
8.5	63.0	63.0	62.5	62.0	61.5	61.0
14.5	63.5	63.5	63.0	62.5	62.0	61.5
20.5	64.0	64.0	63.5	63.0	62.5	62.0
26.5	64.0	64.0	63.5	63.0	62.5	62.0
32.5	64.0	64.0	64.0	63.5	63.0	62.5

P4 = turbine inlet pressure (psia)

P5 = turbine exit pressure (psia)

DISTRIBUTION LIST

	<u>No. of Copies</u>
Mr. C. J. Daye, MS 500-201 NASA-Lewis Research Center SNAP-8 Project Office 21000 Brookpark Road Cleveland, Ohio 44135	6
Mr. Paul R. Miller, Code RNP National Aeronautics and Space Administration Washington, D.C. 20546	5
Lewis Research Center SNAP-8 Field Office P.O. Box 754 Azusa, California 91702 Attn: J. G. Kennard	1
Mr. Leon Dondey NASA, Western Support Office 150 Pico Boulevard Santa Monica, California 90406	1
Mr. R. E. Alexovitch, MS 54-3 NASA-Lewis Research Center 21000 Brookpark Road Cleveland, Ohio 44135	1
Mr. Morris A. Zipkin General Electric Company Missile and Space Division P.O. Box 15132 Cincinnati, Ohio 45215	1
Mr. D. G. Mason Atomic International P.O. Box 309 Canoga Park, California 91304	1
TRW Systems, Inc. 1 Space Park Redondo Beach, Calif 90200 Attn: Tech. Lib. Doc. Acquisitions	1

DISTRIBUTION LIST (cont.)

	<u>No. of Copies</u>
Dr. B. Lubarsky, Chief Space Power Systems Division, MS 500-201 NASA-Lewis Research Center 21000 Brookpark Road Cleveland, Ohio 44135	1
Mr. Henry O. Slone, MS 500-201 Chief, SNAP-8 Project Office NASA-Lewis Research Center 21000 Brookpark Road Cleveland, Ohio 44135	1
Mr. George M. Thur, MS 500-201 Head, SNAP-8 Systems Section NASA-Lewis Research Center 21000 Brookpark Road Cleveland, Ohio 44135	1
NASA-Lewis Research Center 21000 Brookpark Road Cleveland, Ohio 44135 Attn: Library	1
Mr. A. M. Greg Andrus, Code SAC National Aeronautics and Space Administration Washington, D.C. 20546	1
Mr. R. N. Parker, MS 156 NASA-Langley Research Center Langley Station Hampton, Virginia 23365	1
NASA-Flight Research Center P.O. Box 273 Edwards, California 93523 Attn: Library	1
NASA-Goddard Space Flight Center Greenbelt, Maryland 20771 Attn: Library	1
Jet Propulsion Laboratory 4800 Oak Grove Drive Pasadena, California 91103 Attn: Library	1

DISTRIBUTION LIST (cont.)

	<u>No. of Copies</u>
Mr. Jerry P. Davis Jet Propulsion Laboratory 4800 Oak Grove Drive Pasadena, California 91103	1
Mr. Roger Arno Bldg. N202-9 NASA-Ames Research Center Moffett Field, California 94035	1
Mr. R. W. Schaupp NASA-Ames Research Center Mail Stop 202-7 Moffett Field, California 94035	1
Dr. Joseph LaFleur AEC Headquarters Space Nuclear Systems Division Washington, D.C. 20545	1
Mr. Carl Johnson AEC Headquarters Space Nuclear Systems Division Washington, D.C. 20545	1
Mr. Stan R. Stamp U.S. Atomic Energy Commission Canoga Park, California 91304	1
Director of Development Department of the Air Force AFRDD, The Pentagon Washington, D.C. 20301	1
Director of Science and Technology Department of the Air Force AFRST, The Pentagon Washington, D.C. 20301	1
Aero-Propulsion Laboratory Wright Patterson AFB Dayton, Ohio 45433	

DISTRIBUTION LIST (cont.)

	<u>No. of Copies</u>
Cmdr. Marvin C. Demler Research & Technology Division Bolling AFB Washington, D.C. 20332	1
Mr. B. J. Crowe Communications Systems Inc. 5718 Columbia Pike, P.O. Box 530 Falls Church, Virginia 22046	1
Mr. Vern D. Kirkland, Program Manager Power Systems, Advanced Manned Spacecraft Systems Douglas Aircraft Company 5301 Bolsa Avenue Huntington Beach, California 92606	1
Mr. M. H. Greenfield Lockheed Missile and Space Company P.O. Box 504 Sunnyvale, California 94086	1
Mr. Joseph Doss Boeing Company P.O. Box 3707 Seattle, Washington 98124	1
Mr. James Hadley Lawrence Radiation Laboratory University of California Berkeley, California 94720	1
Mr. Robert Thorpe General Electric Company P.O. Box 8555 Philadelphia, Pennsylvania 19101	1
Mr. A. J. Miller Oak Ridge National Laboratory Oak Ridge, Tennessee 37830	1
Mr. Tony Redding, EP5 NASA-Manned Spacecraft Center 2101 Webster Seabrook Road Houston, Texas 77058	1

DISTRIBUTION LIST (cont.)

	<u>No. of Copies</u>
Mr. Gordon Woodcock, R-AS NASA-Marshall Space Flight Center Huntsville, Alabama 35812	1
Mr. Carroll Dailey NASA-Marshall Space Flight Center Huntsville, Alabama 35812	1
NASA-Electronics Research Center 575 Technology Square Cambridge, Massachusetts 02139 Attn: Library	1
NASA-John F. Kennedy Space Center Kennedy Space Center, Florida 32899 Attn: Code ATS-132	1
National Aeronautics and Space Administration Washington, D.C. 20546 Attn: Library Code USS-10	1
National Aeronautics and Space Administration Lewis Research Center 21000 Brookpark Road Cleveland, Ohio 44135 Attn: V. Hlavin, Mail Stop 3-14	1
National Aeronautics and Space Administration Lewis Research Center 21000 Brookpark Road Cleveland, Ohio 44135 Attn: M. Sabala, Mail Stop 3-19	1
National Aeronautics and Space Administration Lewis Research Center 21000 Brookpark Road Cleveland, Ohio 44135 Attn: J. Dilley, Mail Stop 500-309	1
NASA Scientific and Technical Information Facility P.O. Box 33 College Park, Maryland 20740	1
Internal	26